Investigating pluripotency and primordial germ cell development in axolotl with a focus on *axnanog* and *axblimp1*

Catherine Redwood, BSc.
(née Jackson)

Thesis submitted to the University of Nottingham for the degree of Doctor of Philosophy

December 2009

Abstract

The study of pluripotent cells in mouse has revealed a core transcription factor network. Pluripotent cells have not been identified in many non-mammalian organisms, but cells with pluripotent properties are found in axolotl (*Ambystoma mexicanum*) a urodele amphibian. Similarities, between the morphological processes in amniotes and those in urodeles led to the suggestion that amniotes may have arisen from a urodele-like ancestor. Thus, studying the pluripotency network in axolotl may be key to understanding the evolution of mechanisms governing pluripotency in amniotes. This study describes the investigation of two of the core pluripotency trancription factors, Axnanog and Axoct4. Coexpression of *axnanog* and *axoct4* was detected in the undifferentiated tissues of blastula and gastrula stage embryos, suggesting a conserved role in pluripotency/multipotency. Antisense morpholino oligonucleotides were employed to investigate the function of these two molecules. Gastrulation was disrupted in Axnanog morphant embryos. Additionally, they maintained expression of genes associated with pluripotency and early lineage specification, but only expressed low levels of terminal differentiation markers. There are two explanations for this phenotype, a cell migration defect or a developmental block. Axoct4 morphant embryos had a similar phenotype suggesting that Axoct4 may function in a common pathway.

Primordial germ cells (PGCs) are the only cells that retain the ability throughout development to derive all of the tissues of the embryo, upon fertilisation, and these cells express many pluripotency-associated factors. Little is known about PGC development in axolotl. In this study, the roles of Axoct4, Axnanog and Axblimp1 were investigated. Neither Axnanog nor Axoct4 were found to have a role in PGC development. Axblimp1 is unlikely to have a role in PGC specification, as in mouse, but a role in PGC maintenance was not ruled out.

Acknowledgements

Foremost, thanks to the University of Nottingham for allowing me to undertake my PhD and the MRC for funding.

I could not have completed my PhD without the support and advice of many people. Thanks go to past and present members of the AJ, Gering, and Loose labs. For experimental and technical advice thanks go to James ("The Deuce"), Maz, Ramiro, Cinzia, Yuhong and Matt. For excellent technical support my thanks go to Jodie and Dave. Thanks also go to my project students Katie and Matt.

Special thanks go to Dr Gem for her continued support and friendship; I think I will pass on the black sambuca in future though. Extra special thanks go to my husband, Mark, without whom this definitely wouldn't have been possible. He has provided with me with all of the support I could possibly ask for and lots lots more.

Finally, thanks to my family and friends for sticking with me through it all. Particularly, thanks to my Mum who is always there when I need to whinge and have a two-hour phone conversation. Special thanks also go to my nephew, Michael, who has continuely asked me throughout my PhD, "Don't you have your own lab yet?".

Table of Contents

List of Figures

List of Tables

Common Abbreviations

ATG-morphant	embryos injected with translation-blocking morpholino
BLAST	basic local alignment search tool
Blimp1	b-lymphocyte maturation factor 1
CK	cytoskeletal keratin
CT value	cycle threshold value
DNA	deoxyribose nucleic acid
E	embryonic day
ES cell	embryonic stem cell
EST	expression sequence tag
ISH	*in situ* hybridisation
Ncam	neural cell adhesion molecule
NODE	Nanog and Oct4 associated histone deacetylase
NuRD	nucleosome remodelling and histone deacetylase
ODC	ornithine decarboxylase
ORF	open reading frame
PCR	polymerase chain reaction
PCR	polycomb repressor complex
PFA	paraformaldehyde
PGC	primordial germ cell
PR-domain	positive regulatory domain
qRT-PCR	quantitative RT-PCR
RACE	rapid amplification of cDNA ends
RNA	ribose nucleic acid
RT-PCR	reverse transcriptase PCR
S.D.	standard deviation
Splice-morphant	embryos injected with splice-blocking morpholino
UTR	untranslated region
WISH	whole-mount *in situ* hybridisation
ZnF	zinc-finger

Chapter 1. Introduction

1.1 Pluripotency

Pluripotency is defined as the ability of a cell to develop into all of the cells of an embryo including the germline [Smith 2005]. Cells with this potential are found in early mammalian embryos and in cultured mammalian cells, such as embryonic stem (ES) cells. Cells with equivalent potential have not been identified in most non-mammalian model systems. However, axolotl animal cap cells have pluripotent properties being able to develop into derivatives of all three germ layers (ectoderm, mesoderm and endoderm) and primordial germ cells (**Section 1.6**). However, only transplantation experiments can prove that these cells have the ability to contribute to all of the cell lineages of the embryo. The derivation of pluripotent cells during murine development and the factors involved in establishing pluripotency will be discussed along with the pluripotent properties of axolotl animal cap cells.

1.2 Pluripotency in mouse

Pluripotency is first established in the mouse embryo as the inner cell mass (ICM) develops from the inner cells of the morula (**Figure 1.1A**). All the cells of the morula are totipotent, having the ability to derive all the tissues of the embryo and the extra-embryonic tissues, until the 8-cell stage [Tarkowski 1959; Tsunoda and McLaren 1983; Zernicka-Goetz 1998; Ciemerych *et al.* 2000; Johnson and McConnell 2004]. The inner cells of the morula subsequently form the ICM and the outer

cells form the trophoblast [Fleming 1987] (**Figure 1.1B**). The ICM gives rise to all of the tissues of the embryo, whereas the trophoblast forms only extraembryonic tissues that contribute to the placenta [Pedersen *et al.* 1986; Fleming 1987].

At the late-blastocyst stage the ICM gives rise to the epiblast (primitive ectoderm) and the extraembryonic endoderm (primitive endoderm) (**Figure 1.1C**) [Niwa 2007]. The epiblast retains the ability to develop into all of the cells of the embryo, but it does not have the same developmental potential as the ICM, as it cannot give rise to extraembryonic endoderm or trophectoderm (TE) (TE cells can be derived from ICM cells *in vitro*) [Gardner and Rossant 1979]. Thus, the epiblast has restricted development in comparison to the ICM, but retains pluripotency. The epiblast subsequently derives the embryo proper, giving rise to derivatives of all three germ layers and the germ cells (**Figure 1.1D**).

The study of pluripotent cells in mammalian embryos is complicated by placental development. However, the derivation of embryonic stem (ES) cells has enabled more detailed study of pluripotency *in vitro*. ES cells can be derived from the morula [Chung *et al.* 2006 and references therein] and the ICM [Evans and Kaufman 1981]. They can be maintained in an undifferentiated state indefinitely under specific culture conditions and retain the ability to derive all three somatic germ layers including the germ cells both *in vivo* and *in vitro* [Suda *et al.* 1987].

More recently it was shown that cells derived from the epiblast, epiblast stem cells (EpiSCs), can also be maintained in culture in an undifferentiated state [Brons *et al.* 2007; Tesar *et al.* 2007]. EpiSCs can, like ES cells, give rise to derivatives of all three somatic germ layers *in vivo* and *in vitro*, but unlike ES cells they have not been shown to contribute to the germ line in chimeras [Brons *et al.* 2007]. The inability to contribute efficiently to the tissues of chimeras was attributed to a developmental asynchrony between the EpiSCs and the blastocysts into which they were transplanted. Notably, EpiSCs were isolated at E5.75 and PGCs in mouse are specified at E5.5 [Ohinata *et al.* 2005]. Thus, the inability of EpiSCs to contribute to the germ line might also be associated with the developmental capabilities of the epiblast cells at the time of isolation.

Pluripotency is determined by a complex interplay of extrinsic cell signalling and intrinsic transcription factor networks [recent reviews Niwa 2007; Pan and Thomson 2007]. The study of pluripotency in ES cells and embryos has revealed a network of transcription factors that is central to the establishment and maintenance of pluripotency both *in vivo* and *in vitro*. The pluripotency transcription factor network includes three key molecules, Oct4, Sox2 and Nanog.

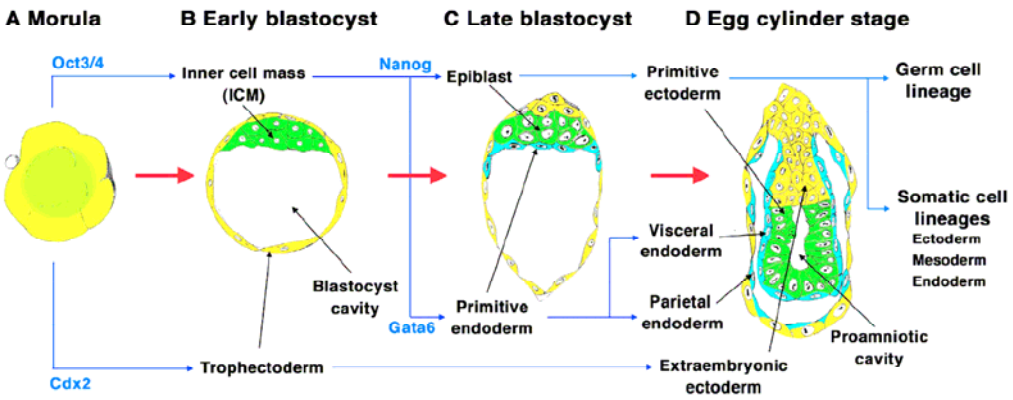

Figure 1.1 Cell lineage development in the early mouse embryo.
Pluripotent cell lineages are shown in green. The inner cells of the morula (**A**) form the inner cell mass (ICM) of the blastocyst (**B**) and the outer cells form the trophectoderm. The ICM gives rise to the epiblast (primitive ectoderm) (**C**) and the primitive endoderm. The primitive ectoderm (**D**) gives rise to all three somatic germ layers and the germ cells. Reciprocal inhibition between Oct4 and Cdx2 are thought to be involved in the establishment of the ICM and trophectoderm lineages. Similarly, reciprocal inhibition between Nanog and Gata6 is thought to be involved in the segregation of the epiblast and the primitive endoderm [Figure adapted from Niwa 2007]

1.3 The core pluripotency transcription factor network in mouse: Oct4, Sox2 and Nanog.

1.3.1 Oct4

Oct4 is a POU-domain transcription factor that can bind to octamer sequence motifs *via* its homeodomain to activate or repress the transcription of target genes [Pesce and Schöler 2001]. Three independent studies identified murine Oct4 (also referred to as Oct3/4) as a pluripotency associated transcription factor [Schöler *et al.* 1989; Okamoto *et al.* 1990; Rosner *et al.* 1990]. Oct4 was identified as a molecule that was specifically expressed in undifferentiated ES cells, undifferentiated embryonal carcinoma (EC) cells, pluripotent cells of the embryo and germ cells. Maternal *oct4* RNA and protein are present in oocytes and persists in early embryos until the 2 cell stage [Rosner *et*

al. 1990; Palmieri *et al.* 1994]. Zygotic transcription commences at the 2 cell stage and RNA initially accumulates in all of the cells of the morula [Rosner *et al.* 1990]. RNA and protein are then progressively restricted to pluripotent cells, first the ICM and then the epiblast [Schöler *et al.* 1989; Rosner *et al.* 1990; Palmieri *et al.* 1994]. Expression progressively decreases in the epiblast during gastrulation in an anterior to posterior direction as the cells begin to differentiate. The only cells that express Oct4 post-gastrulation are the primordial germ cells (PGCs) [Schöler *et al.* 1989].

Functional analyses showed that Oct4 was essential for the formation of pluripotent tissues in mouse embryos. Oct4-null embryos fail to form a pluripotent ICM [Nichols *et al.* 1998]. Blastocyst-like structures form but the putative ICM diverts to the trophectoderm (TE) lineage. In addition, perturbations of Oct4 expression in ES cells cause them to differentiate [Niwa *et al.* 2000; Ivanova *et al.* 2006]. Increased Oct4 expression causes differentiation to primitive endoderm and mesoderm [Niwa *et al.* 2000], whereas a decrease causes differentiation to TE [Niwa *et al.* 2000; Ivanova *et al.* 2006] and extraembryonic endoderm [Hay *et al.* 2004]. Thus, a critical level of Oct4 is required to maintain self-renewal.

1.3.2 Sox2

Sox2 is an SRY-related HMG (High Mobility Group) box transcription factor that is predominantly expressed in pluripotent and multipotent cells of mouse embryos [Avilion *et al.* 2003]. Maternal protein is

present at high levels in mature oocytes and persists in embryos until at least the blastocyst stage. RNA and protein encoded by *sox2* is expressed in the ICM and persists throughout the epiblast. Protein is also detected in the trophoblast where it is mainly cytoplasmic, whereas in the ICM it is mainly nuclear [Avilion *et al.* 2003]. *Sox2* expression is downregulated as epiblast cells differentiate, and persists only in the neuroectoderm. At later stages of development expression is detected in neural tissues (including neural stem cells), branchial arches, gut endoderm and male and female germ cells.

Consistent with expression in pluripotent tissues, Sox2-null mice form an ICM-like structure but fail to survive beyond implantation (late-blastocyst) [Avilion *et al.* 2003]. Furthermore, the ICM-like cells are not pluripotent, differentiating only into TE cells in culture, and less frequently into extraembryonic endoderm [Avilion *et al.* 2003]. Sox2-null embryos resemble Oct4-null embryos, but the phenotype is not quite as severe, perhaps due to the persistence of maternal protein or the presence of functionally redundant Sox genes [Avilion *et al.* 2003]. Perturbations of Sox2 expression in ES cells cause their differentiation. Depletion of Sox2 in ES cells, similar to Oct4 depletion, yields TE cells [Ivanova *et al.* 2006; Li *et al.* 2007] and also multiple epiblast lineages (ectoderm,mesoderm and neural crest) [Ivanova *et al.* 2006]. Slight increases in expression also result in the differentiation of ES cells into multiple lineages [Ivanova *et al.* 2006; Kopp *et al.* 2008]. Together this data indicates that Sox2 is essential for the maintenance

of pluripotency and only slight perturbations in expression cause ES cells to differentiate. Sox2 has additionally been found to have a role in neural development, coinciding with the reported expression in neural tissues [Reviewed in Wegner and Stolt 2005].

1.3.3 Nanog

Nanog is the most recently discovered member of the core pluripotency transcription factor network. It is a homeobox transcription factor closely related to the NK-2 family of homeobox transcription factors, but distinct from the NK-2 family as it does not contain the NK2 or TN (tinman) domain [Mitsui *et al.* 2003]. Two independent groups identified Nanog as a pluripotency associated factor. Mitsui *et al*. (2003) identified Nanog as a molecule that was enriched in undifferentiated ES cells and preimplantation mouse embryos. Chambers *et al*. (2003) identified *nanog* in a screen for genes that could maintain self-renewal of ES cells in the absence of LIF (Leukaemia inhibitory factor), which is normally required [Smith *et al.* 1992]. Nanog RNA is first detected in the interior cells (future ICM) of morula stage embryos [Wang *et al.* 2003]. Expression continues in the ICM and epiblast; and is excluded from extraembryonic tissues [Chambers *et al.* 2003]. By the late blastocyst stage expression decreases in the epiblast but it is later detected in migrating PGCs [Yamaguchi *et al.* 2005]. Expression is maintained in the PGCs until they reach the gonads and differentiate into mature germ cells.

Nanog-null embryos fail to form an epiblast [Mitsui *et al.* 2003]. Presumptive embryonic cells from these embryos divert to extraembryonic endoderm in culture. This implied that Nanog expression was required to prevent differentiation into the primitive endoderm lineage. However, recent investigations using RNA interference (RNAi) showed that depletion of Nanog in ES cells results in differentiation into multiple lineages including trophectoderm and epiblast derived lineages; ectoderm, mesoderm and neural crest [Ivanova *et al.* 2006]. This suggests that Nanog might be a global regulator, repressing multiple programmes of differentiation. Nanog expression in murine ES cells, however, is dispensable for the maintenance of self-renewal [Chambers *et al.* 2007]. Nanog-null ES cells are prone to differentiation but continue to self-renew and express other pluripotency associated factors such as Oct4 and Sox2. They can also contribute to all of the tissues of chimeric embryos including the germ cells, showing that they retain pluripotency. Nanog-null germ cells, however, cannot differentiate into mature germ cells once they reach the genital ridges.

1.3.4 Oct4 and Nanog in the establishment of the trophectoderm and primitive endoderm lineages

The establishment of the ICM and the TE in the early mouse embryo is the first lineage decision in mouse development. There has been debate as to whether the segregation of morula cells into the ICM and trophoblast lineages is a random or programmed event [Zernicka-Goetz 2006]. Niwa *et al* (2005) proposed a reciprocal interaction between

Oct4 and another transcription factor, Cdx2 (Caudal-related homeobox 2) [Niwa *et al.* 2005] Initially, both Cdx2 and Oct4 are expressed in all of the cells of the morula, but Cdx2 expression becomes restricted to the outer cells that will derive the TE and Oct4 to the inner cells that will derive the ICM [Schöler *et al.* 1989; Rosner *et al.* 1990; Beck *et al.* 1995; Niwa *et al.* 2005]. Both Cdx2 and Oct4 can be autoregulated and additionally Oct4 and Cdx2 can form a complex, which may act as a transcriptional repressor complex [Niwa *et al.* 2005]. Based on this it was proposed that once expression of Cdx2 and Oct4 reach threshold levels an asymmetrical distibution of the two molecules might be amplified by reciprocal inhibition. Thus, downregulation of Oct4 results in upregulation of Cdx2, and vice versa. Subsequently, leading to the segregation of the TE and ICM lineages by establishing their mutually exclusive expression [Niwa *et al.* 2005]. Accordingly, overexpression of Cdx2 in ES cells causes differentiation into TE, mimicking the effect of Oct4 depletion [Niwa *et al.* 2005; Tolkunova *et al.* 2006]. In addition, Cdx2-null embryos fail to correctly form trophectoderm, maintaining expression of Oct4 and Nanog in the outer cells of the blastocyst [Strumpf *et al.* 2005]. Recent investigations, however, have shown that Cdx2-mutant cells, which show cell-autonomous expression of Nanog and Oct4 do not preferentially contribute to the inner cell mass [Ralston and Rossant 2008]. Thus, it is likely that Cdx2 expression is not the primary event in this lineage segregation, but a secondary process resulting in functional maturation. Interestingly, cell polarisation events that occur at the 8-cell stage are independent of Cdx2 erxpression

[Ralston and Rossant 2008]. Thus, upstream molecules that regulate this polarisation may regulate Cdx2 expression and lineage segregation. A recent study showed that cells of the 4-cell stage embryo, with increased histone H3 arginine methylation on specific residues, were biased towards the ICM lineage [Torres-Padilla *et al.* 2007]. This histone modification was associated with expression of a histone methyltransferase, Carm1. Overexpression of Carm1 in specific-blastomeres results in increased histone H3 arginine methylation and increased expression of *nanog* and *sox2*. Subsequently, these blastomeres contributed more frequently to the ICM. Carm1 may operate upstream of Cdx2 and Oct4 in this lineage segregation event.

Similar to the proposed interaction between Oct4 and Cdx2, it has been suggested that mutual inhibition between Nanog and Gata6 could be involved in the segregation of primitive endoderm and the epiblast [Niwa 2007]. Cells expressing Nanog and Gata6 are fated to form the epiblast and the extraembryonic endoderm, respectively. The ICM initially develops as a mosaic of Nanog and Gata6 expressing cells, which subsequently sort into two distinct cell layers [Chazaud *et al.* 2006]. Mutual inhibition between Nanog and Gata6 could result in the establishment of this “salt and pepper” appearance. In agreement with this hypothesis, overexpression of Gata6 in ES cells, similarly to depletion of Nanog, causes them to differentiate into extraembryonic endoderm [Fujikura *et al.* 2002]. In addition, depletion of Gata6 in ES

cells or embryos inhibits primitive endoderm differentiation [Morrisey *et al.* 1998; Koutsourakis *et al.* 1999]. However, there is no evidence for a direct interaction between Nanog and Gata6 [Niwa 2007]. FGF signalling and the Grb2-Ras-Mapk signalling pathway have also been implicated in the establishment of these two cell-lineages [Arman *et al.* 1998; Chazaud *et al.* 2006]. Inactivation of Grb2, a component of the Grb2-Ras-Mapk signalling pathway, results in all ICM cells expressing Nanog [Chazaud *et al.* 2006]. Likewise, targeted disruption of the fibroblast growth factor receptor 2 (FGFR2) in mouse embryos results in a failure to form the primitive endoderm [Arman *et al.* 1998]. Much remains to be determined about this lineage segregation event but it is clear that Nanog has a pivotal role in the maintenance of pluripotency at this crucial stage in development.

1.3.5 A central self-organising transcription factor network governing pluripotency

The studies decribed above outline the critical roles that Nanog, Oct4 and Sox2 have in the establishment/maintenance of pluripotent cells, both *in vivo* and *in vitro*. Reprogramming studies have also identified Nanog, Oct4 and Sox2 as critical molecules. Mouse fibroblasts are successfully reprogrammed to a pluripotent state by the introduction of Oct4, Sox2, Klf4 and cMyc, although only Oct4 and Sox2 were absolutely necessary [Takahashi and Yamanaka 2006; Wernig *et al.* 2007]. Furthermore, it has been reported that to reach a fully reprogrammed state both *nanog* and *oct4* must also be transcriptionally activated [Brambrink *et al.* 2008]. This data, along with several other

recent studies, led to the suggestion that there is a central self-organising transcription factor network governing pluripotency in mouse ES cells, in which Nanog, Oct4 and Sox2 have pivotal roles.

Loh *et al* (2006) carried out a large-scale study that identified binding sites for Nanog, Oct4 and Sox2. They were found to have many common targets (44.5% of genes were found to have binding sites for both Nanog and Oct4 and the majority of Oct4 bound genes also had binding sites for Sox2.), amongst which were the genes encoding each of the three molecules. This led to the suggestion that these three molecules might not only coordinately regulate the expression of their targets, but also their own expression levels, thus stably maintaining pluripotency. RNAi experiments demonstrated that Nanog could regulate the expression of Oct4 and Sox2, supporting this suggestion.

Ivanova *et al* (2006) used an integrated functional genomics approach to identify genetic mechanisms controlling mouse ES cell self-renewal. They identified Nanog, Oct4, Sox2, Esrrb, Tbx3 and Tcl1. Downregulation of each of these genes resulted in differentiation towards specific lineages. Interestingly, overexpression of Nanog was shown to compensate for the loss of Esrrb, Tbx3 and Tcl1, leading to the suggestion that these molecules are part of an interconnected network governing pluripotency where the loss of one molecule might sometimes be compensated for by upregulation of another. The relatively late embryonic stages at which Esrrb, Tbx3 and Tcl1

knockouts exhibit a phenotype could be explained by the presence of a stablising interconnected network of transcription factors.

Some studies, however, have challenged the pivotal roles that Oct4, Nanog and Sox2 have in the pluripotency network. Given the similarity of Oct4 and Sox2 knockout phenotypes [Nichols *et al.* 1998; Avilion *et al.* 2003] and the identification of Oct4 and Sox2 binding sites in close proximity within the regulatory regions of many genes [Loh *et al.* 2006], it has long been considered that Oct4 and Sox2 could cooperate in the regulation of target genes. Oct4 and Sox2 are able to heterodimerize and moderate the expression of multiple genes in mouse ES cells [Yuan *et al.* 1995; Botquin *et al.* 1998; Nishimoto *et al.* 1999]. However, it was recently reported that although Sox2 was indispensable for the self-renewal of ES cells, it was not required for the activation of Oct-Sox enhancers [Masui *et al.* 2007]. The regulatory regions of many key pluripotency factors, including *oct4* and *nanog* contain Oct-Sox binding sites [Loh *et al.* 2006]. The expression of many of these factors including *oct4* was reduced following the depletion of Sox2 in ES cells [Masui *et al.* 2007]. The authors proposed that a reduction of Oct4 expression could have caused the resulting phenotype. Given that Oct-Sox enhancers remained active, it was suggested that Sox2 might indirectly affect Oct4 expression in ES cells by regulating upstream molecules. To support this hypothesis, Oct4 overexpression was able to rescue the Sox2-null ES cells. This data suggests Sox2 and Oct4 may not coordinately regulate targets in the central self-organising

network proposed by Loh *et al*. (2006) and also that Sox2 may not directly regulate Oct4 expression.

Chambers *et al* (2007) challenged the pivotal role of Nanog in a central self-organising network governing pluripotency. They showed that Nanog-null ES cells could continue to self-renew and maintain the expression of Oct4 and Sox2, although these cells were prone to differentiation and could not form mature germ cells *in vivo*. These findings highlight how much remains to be discovered about the establishment and maintenance of pluripotency both *in vivo* and *in vitro*, even in the context of these three highly studied transcription factors.

1.4 Interactions of Oct4 and Nanog with epigenetic regulators

Recent observations by Chambers *et al*. (2007) suggest that Nanog is not required for the maintenance of pluripotency (**Section 1.3.5**). At both time-points when Nanog function is required, establishment of the epiblast, as determined by gene deletion [Mitsui *et al.* 2003], and differentiation of PGCs into mature germ cells [Chambers *et al.* 2007], are associated with genome-wide epigenetic changes [Surani *et al.* 2007]. Based on these observations, Chambers *et al* (2007) proposed that Nanog might have a role in the establishment of the epigenetically erased states in pluripotent cells and germ cells. In agreement with this, Nanog expression is first detected in the inner cells of the morula [Wang *et al.* 2003], preceding the establishment of the epigenetic modifications that distinguish the ICM and the TE in mouse [Surani *et*

al. 2007]. In addition, a Nanog protein-protein interaction study has identified multiple interactions with epigenetic modifiers, including polycomb group repressor complex 2 (PRC2), SWI/SNF complex, and the NuRD (Nucleosome Remodelling and histone Deacetylase) complex [Wang *et al.* 2006]. Each of these complexes has an essential role in early murine development [Reviewed in Surani *et al.* 2007] and components of each are necessary for ES cell maintenance [Kaji *et al.* 2006; Rajasekhar and Begemann 2007; Gao *et al.* 2008]. For example, MBD3, a component of the NuRD complex is required for development of the epiblast [Kaji *et al.* 2007]. Gene deletion of MBD3 is embryonic lethal. These embryos develop an ICM, which subsequently fails to derive mature epiblast cells. In addition, pluripotency is disrupted in $MBD3^{-/-}$ ES cells [Kaji *et al.* 2006]. MBD3-null ES cells fail to respond to differentiation signals and they maintain expression of pluripotency genes. Thus, it could be the absence of the correct epigenetic modifications in Nanog-null embryos that results in failure to derive epiblast cells from the ICM [Mitsui *et al.* 2003].

In addition to Nanog interactions with the aforementioned complexes, a recent study identified interactions of both Nanog and Oct4 with a modified NuRD complex in mES cells, named NODE (Nanog and Oct4 associated Deacetylase) [Liang *et al.* 2008]. Depletion of NODE in mES cells resulted in increased expression of Nanog and Oct4 target genes, normally repressed in ES cells, and subsequently, differentiation of the ES cells. This suggests that both Nanog and Oct4 may have key

roles in the establishment of epigenetically erased states during development.

1.5 Conserved roles for Oct4, Sox2 and Nanog

1.5.1 Human

Human ES (hES) cells differ from mouse ES (mES) in many ways including their response to growth factors, regulation of pathways involved in senescence signalling, cell surface antigen expression, rate of proliferation and sensitivity to differentiation factors [Daheron *et al.* 2004; Amit and Itskovitz-Eldor 2006; Fong *et al.* 2008]. Nevertheless, the three transcription factors, Oct4, Sox2 and Nanog, have roles in the maintenance of pluripotency in hES cells (**Table 1.1**), and Oct4 expression has also been detected in the ICM of early human blastocysts [Hansis *et al.* 2000]. Furthermore, the reprogramming of human somatic cells to pluripotency has been achieved using the same conditions that reprogram mouse cells (Oct4, Sox2, Klf4 and cMyc) [Takahashi *et al.* 2007]. This indicates that the pluripotency network is conserved in mammals. Surveys of Oct4 and Nanog binding sites in hES cells and mES cells however, has revealed only limited conservation of targets (9.1% of Oct4 bound genes and 13% of Nanog bound genes), this may indicate that there are differences in the transcription factor circuitry in the two types of cells [Boyer *et al.* 2005; Loh *et al.* 2006]. However, it is also possible that this limited overlap is due to the differing methods used to survey the binding sites in the two studies. For example, Boyer *et al* (2005) only surveyed 6% of the human genome, whereas Loh *et al* (2006) carried out an unbiased

survey of the entire mouse genome. Similarly to mouse, it is also thought that Sox2 has a function in neural development in adults [Fantes *et al.* 2003; Ragge *et al.* 2005].

Table 1.1 Comparison of phenotypes in mESCs and hESCs.
Knock-down and overexpression phenotypes for each of the three core transcription factors, Oct4, Sox2 and Nanog are described in mouse embryonic stem (mES) cells and human embryonic stem (hES) cells

	Overexpression in HESCs	**Overexpression in mESCS**	**Knock-down in hESCs**	**Knock-down in mESCs**
Oct4	Not Known.	A small increase (less than 2-fold) causes differentiation into primitive endoderm and mesoderm as determined by increased expression of Gata4 and Brachyury, respectively [Niwa *et al.* 2000]. A critical amount is required to maintain self-renewal, up or down regulation induces divergent developmental programmes.	Hay *et al* (2004) found that knock-down by transfecting siRNAs (small interfering RNAs) induces epithelial-like differentiation and expression of genes associated with endoderm differentiation, and restricted induction of trophoblastic markers. Whereas, Zaehres *et al* (2005) with the use of retroviral and lentiviral vectors to deliver siRNAs found that knock-down results in upregulation of trophoblastic markers [Hay *et al.* 2004; Zaehres *et al.* 2005].	Niwa *et al* (2000) and Ivanova *et al* (2006) reported loss of pluripotency and increased expression of trophectodermal markers, suggesting dedifferentiation towards the trophectoderm lineage (mESC cannot normally contribute to the trophectoderm lineage) [Niwa *et al.* 2000]. Hay *et al* (2004), however, additionally reported induction of markers of extraembryonic endoderm, suggesting differentiation towards both trophectoderm and extraembryonic endoderm lineages.

	Overexpression in HESCs	**Overexpression in mESCS**	**Knock-down in hESCs**	**Knock-down in mESCs**
Sox2	Not known	Zhao *et al* 2004 reported that overexpression does not impair the propogation of ES cells, but on removal of LIF these cells differentiate exclusively into neural phenotypes [Zhao *et al.* 2004]. Contrastingly, Kopp *et al* 2008 reported that small increases (2-fold or less) reduce self-renewal coincident with reduced Nanog expression and trigger differentiation into multiple lineages including neuroectoderm, mesoderm, and trophectoderm, but not endoderm. There is a bias towards differentiation into neuroectoderm lineages. Additionally, 4-fold or higher levels of overexpression induces significant cell death, in agreement with previously published data [Mitsui *et al.* 2003].	Loss of stem cell identity, coincident with reduced expression of stem cell markers including *nanog* and *oct4* and increased expression of trophectodermal markers [Fong *et al.* 2008].	Loss of pluripotency and induction of markers of trophectoderm and epiblast-derived lineages (mesoderm, ectoderm and neural crest), suggesting differentiation towards multiple lineages [Ivanova *et al.* 2006].

	Overexpression in HESCs	Overexpression in mESCS	Knock-down in hESCs	Knock-down in mESCs
Nanog	Maintenance of pluripotency in the absence of conditioned media [Normally required for the maintenance of pluripotency in HESCs; Xu *et al.* 2001] but growth is slowed, suggesting that Nanog cannot substitute for all of the components of the conditioned media [Darr *et al.* 2006]. Additionally, the gene expression profile is altered from one characteristic of ICM to that characteristic of primitive ectoderm (as judged by comparison to known expression profiles in murine cells as human primitive ectoderm cells have not been isolated in culture).	Pluripotency and self-renewal is maintained in the absence of LIF and ES cells have enhanced resistance to some differentiation signals [Chambers *et al.* 2003; Mitsui *et al.* 2003].	Loss of stem cell identity, downregulation of *oct4*, and upregulation of markers of trophectoderm and extraembryonic endoderm, suggesting differentiation toward extraembryonic lineages [Hyslop *et al.* 2005; Zaehres *et al.* 2005].	Cells can continue to self-renew and remain pluripotent (as determined by integration into the tissues of chimeras), but renewal efficiency is reduced and cells are prone to differentiation [Chambers *et al.* 2007]. Original studies reported that depleted cells differentiate towards the extraembryonic endoderm lineages [Mitsui *et al.* 2003], but more recent studies reported that cells differentiate towards multiple lineages including trophectoderm and epiblast-derived lineages (mesoderm, ectoderm and neural crest) [Ivanova *et al.* 2006].

.

1.5.2 Chicken

Homologues of Oct4 and Nanog have been identified in chicken and similar to their murine counterparts are predominantly expressed in pluripotent tissues and germ cells [Lavial *et al.* 2007]. Functional analyses confirmed roles for cOct4 and cNanog in the maintenance of chicken ES (cES) cells [Lavial *et al.* 2007]. Similar to observations with mES cells, overexpression of cNanog in cES cells promotes feeder-free growth, and knock-down of cOct4 (PouV) induces the expression of trophectoderm and endoderm markers, Cdx2 and Gata4/6 respectively. Conversly, depletion of cOct4 or cNanog leads to the loss of proliferation and induction of differentiation, marked by increased expression of Gata6. Furthermore, cOct4 can partially rescue Oct4-null mES cells, and cNanog can completely rescue Nanog-null mES cells. Collectively, this data indicates that the function of cNanog and cOct4 is conserved.

Chicken Sox2 (cSox2) is expressed in the primitive ectoderm (epiblast) of pre-streak stage embryos [Streit and Stern 1999], suggesting that it may have a role in pluripotency. However, a role in pluripotency is yet to be identified. cSox2 is also widely expressed in neural tissues, similarly to the mouse homologue [Streit *et al.* 1997], and has a conserved role in neural development [Bylund *et al.* 2003; Graham *et al.* 2003]. Future analyses may identify a role in pluripotency.

1.5.3 Xenopus

Three *oct4* homologues have been identified in *Xenopus laevis*, *xlpou91*, *xlpou60* and *xlpou25*, which have overlapping expression patterns [Hinkley *et al.* 1992; Morrison and Brickman 2006]. *Xlpou60* expression is detected in oocytes, where it is mainly localised to the animal hemisphere [Whitfield *et al.* 1993; Morrison and Brickman 2006]. mRNA and protein encoded by *xlpou60* is maternally inherited by the embryo [Hinkley *et al.* 1992]. The mRNA persists in the animal pole and marginal zone (presumptive mesodermal cells) of the embryo until late-blastula and is undetectable by early gastrulation [Hinkley *et al.* 1992; Whitfield *et al.* 1993; Morrison and Brickman 2006]. *Xlpou25* mRNA is also detected at low levels in oocytes and early embryos [Hinkley *et al.* 1992]. However, protein is not detected until gastrulation when transcription is dramatically upregulated [Hinkley *et al.* 1992; Morrison and Brickman 2006]. Similar to *xlpou60*, *xlpou25* expression is localised to the animal pole and marginal zone of embryos [Cao *et al.* 2004; Morrison and Brickman 2006]. Transcription of the third homologue, *xlpou91*, is not activated until after the onset of zygotic transcription (mid-blastula transition (MBT) [Hinkley *et al.* 1992; Morrison and Brickman 2006]. The highest level of expression is detected at late-gastrula. *Xlpou91* expression, like *xlpou60* and *xlpou25*, is also localised to the animal pole and the marginal zone of embryos [Morrison and Brickman 2006]. Later in development *xlpou25* and *xlpou91* are also expressed in the neuroectoderm, [Cao *et al.* 2004; Morrison and Brickman 2006]. The composite expression pattern of the

three *Xenopus* homologues during blastula and gastrula stages has been proposed to resemble the expression of murine *oct4* [Morrison and Brickman 2006]. The three homologues are expressed throughout blastula and gastrula stages in multipotent tissues that will derive differentiated ectodermal and mesodermal tissues. Expression is only detected in marginal zone cells that have not started to ingress during gastrulation. Similar to murine *oct4,* expression of all three homologues is reduced post-gastrulation.

Antisense morpholino oligonucleotides targeted to disrupt expression of each of the three *Xenopus oct4* homologues were used in functional analyses [Morrison and Brickman 2006]. Morpholinos targeted to *xlpou60* or *xlpou25* had no discernable effect, which was attributed to functional redundancy between the three homologues. Morphant embryos injected with *xlpou91* morpholino (mo) alone, *xlpou91* and *xlpou25* mos or a combination of all three mos, had posterior truncation and anterior neural defects. The depletion of all three molecules produced the most severe phenotype. Analysis of gene expression in gastrula-stage morphant embryos showed reduced expression of genes associated with multipotent marginal zone cells, and increased expression of genes associated with more mature cell states. Similar to the mouse *oct4* knockout [Nichols *et al.* 1998] depletion of the three Xlpou molecules also resulted in the ectopic expression of *xcad3*, a *cdx2* homologue. It was therefore proposed that the Xlpou molecules have a conserved function, suppressing differentiation and maintaining

a multipotent population of cells. Accordingly, Xlpou91, Xlpo60 and Xlpou25 were shown to partially rescue Oct4-null mES cells. The most effective rescue was achieved with Xlpou91. Additionally, overexpression of Xlpou25, Xlpou60 or Xlpou91 was shown to inhibit mesendoderm differentiation [Cao *et al.* 2004; Cao *et al.* 2006]. Xlpou25 and Xlpou91 also have a role in anterior and posterior neural development coincident with the anterior neural defects observed in morphant embryos [Morrison and Brickman 2006]. Furthermore, overexpression of Xlpou25 in presumptive ectoderm has been shown to promote a neuroectoderm fate whilst suppressing terminal differentiation of neurons [Cao *et al.* 2006].

The *Xenopus* Sox2 homologue has a role in neural induction [Mizuseki *et al.* 1998]. It is widely expressed in the dorsal ectoderm during early gastrula, stages when neural induction first takes place. Expression persists in neural tissues throughout embryonic development, including the central nervous system (CNS), neural crest, placodes and lateral line. *Xenopus* Sox2 is essential for neuroectoderm formation and functions as a neural competence factor [Kishi *et al.* 2000]. A role in pluripotency/multipotency, however, has not been identified.

1.5.4 Zebrafish

An *oct4* homologue, *pou2*, was identified in zebrafish [Takeda *et al.* 1994; Hauptmann and Gerster 1995]. *Pou2* is initially uniformly expressed in oocytes and is subsequently restricted to the animal

oocyte region [Howley and Ho 2000]. After fertilisation *pou2* is ubiquitously expressed in all blastomeres until MBT and is then restricted to the epiblast during gastrulation [Takeda *et al.* 1994; Hauptmann and Gerster 1995; Reim *et al.* 2004]. Towards the end of gastrulation expression is confined to the neural plate, predominantly in the prospective hindbrain and spinal cord [Hauptmann and Gerster 1995].

Depletion of Pou2 in Zebrafish mutants or through the use of antisense morpholino oligonucleotides has revealed multiple functions during development [Belting *et al.* 2001; Burgess *et al.* 2002; Reim and Brand 2002; Lunde *et al.* 2004; Reim *et al.* 2004; Reim and Brand 2006]. Embryos depleted of both maternal and zygotic Pou2 exhibit extreme dorsal-ventral (D-V) patterning defects and independently, a blastoderm specific arrest of epiboly [Reim and Brand 2006]. Analysis of maternal-zygotic mutants additionally revealed a function in endoderm development [Lunde *et al.* 2004; Reim *et al.* 2004]. The D-V patterning defect and the defect in endoderm development are considered independent as the D-V defect occurs shortly after MBT, whereas the disruption in endoderm development occurs from the beginning of gastrulation onwards [Reim and Brand 2002]. Later in development Pou2 was shown to have a role in the establishment of the midbrain-hindbrain organiser [Belting *et al.* 2001; Burgess *et al.* 2002; Reim and Brand 2002]. A role for Pou2 in the establishment/maintenance of pluripotency or the maintenance of

primordial germ cells during development has not been identified [Lunde *et al.* 2004; Reim and Brand 2006]. Pou2 cannot rescue Oct4-null ES cells, also suggesting that it does not have a conserved function in pluripotency [Morrison and Brickman 2006]. However, the function of Pou2 shares some similarities with *Xenopus* homologues, Xlpou25 and Xlpou91, which have also been shown to have a role in neural development [Cao *et al.* 2006; Morrison and Brickman 2006].

Similarly, to other vertebrate homologues, the Zebrafish *sox2* homologue is expressed predominantly in neural tissues [Okuda *et al.* 2006]. Zebrafish *sox2* is initially uniformly expressed in the presumptive ectoderm and then becomes restricted to the neuroectoderm. Subsequently, strong expression is detected in the presumptive forebrain and weak expression is detected in the presumptive spinal cord. Thus, Zebrafish Sox2 is likely to have a conserved role in neural development and is unlikely to have a role in pluripotency.

1.5.5 Axolotl

A homologue of *oct4*, *axoct4*, was identified in axolotls. *Axoct4* expression was detected in the animal pole of blastula stage embryos and in the ectoderm and presumptive mesodermal cells (marginal zone cells) of gastrula stage embryos [Bachvarova *et al.* 2004; **Chapter 3**]. Interestingly, this expression pattern closely resembles the combined expression of the three *Xenopus* homologues suggesting as in mouse that there is only one *oct4* homologue [Bachvarova *et al.* 2004;

Morrison and Brickman 2006]. The role of Axoct4 in embryonic development has yet to be determined. However, Axoct4 has been shown to partially rescue Oct4 deficient mES cells and *Xenopus* embryos depleted of all three homologues, suggesting that it may have a conserved function [Morrison and Brickman 2006]. Thus, preliminary evidence indicates that Axoct4 may also have a function in the maintenance of pluripotency/multipotency.

1.5.6 Summary of conserved roles

Early indications suggest that Nanog, Sox2 and Oct4 have conserved roles in the maintenance of pluripotency in amniotes, and Oct4 may have a conserved role in the maintenance of pluripotency/multipotency in anamniotes. Sox2 has a conserved role in neural development in vertebrates [Reviewed in Wegner and Stolt 2005] but a role in pluripotency has not been identified in non-mammalian organisms. Although it is possible that other Sox family transcription factors [Soullier *et al.* 1999] may have a role in pluripotency in the absence of Sox2 function. The study of these molecules in other organisms is necessary to uncover their ancestral roles during embryonic development.

1.6 Pluripotency in axolotls

Cells with pluripotent properties were first identified in axolotl (*Ambystoma mexicanum*), a urodele amphibian. A series of *in vitro* experiments showed that axolotl animal cap cells, from which ectoderm normally derives during development, could be induced to make mesoderm and endoderm [Nieuwkoop 1969]. For example, Grunz (1968) induced mesoderm and endoderm in axolotl animal caps in response to Li ions. He showed that axolotl animal caps are first competent to respond to mesoderm and endoderm inducing signals at late-cleavage stages of development, with competence peaking at the mid-late blastula stage and terminating at early gastrula. Subsequently, Nieuwkoop (1969) carried out a series of transplantation experiments to determine the origin of mesoderm *in vivo*, and showed that *in vivo* signals also induced mesoderm in axolotl animal caps. Importantly, he showed that the entire mesoderm was derived from the animal cap. Blastula (stage 8-9) embryos were divided into four zones (**Figure 1.2A**). Each of the four zones was cultured in isolation (**Figure1.2C**) and various different combinations of the four zones were cultured as recombinates (**Figure 1.2B**). During normal development, zone I develops into neuroectoderm, zone II develops predominantly into neuroectoderm and some mesoderm, zone III develops into mesoderm and endoderm derivatives and zone IV is comprised mainly of nutritive yolk that is absorbed by the embryo during development. Cultured in isolation zones I and II develop only into undifferentiated ectoderm, zone III is comprised of ectoderm, mesoderm and endoderm, and zone

IV develops only into undifferentiated endoderm (**Figure 1.2C**). By combining the different zones of the embryo, Nieuwkoop showed that mesoderm and endoderm could be induced in the ectodermal animal cap (zones I and II) in response to signals from the underlying endoderm. The most striking result was observed when zones I and II were combined with zone IV, causing the induction of mesoderm, ectoderm and endoderm derivatives in zones I and II (**Figure 1.2B**). Thus, derivatives of all three somatic germ layers can be induced in the animal cap cells of blastula stage axolotl embryos.

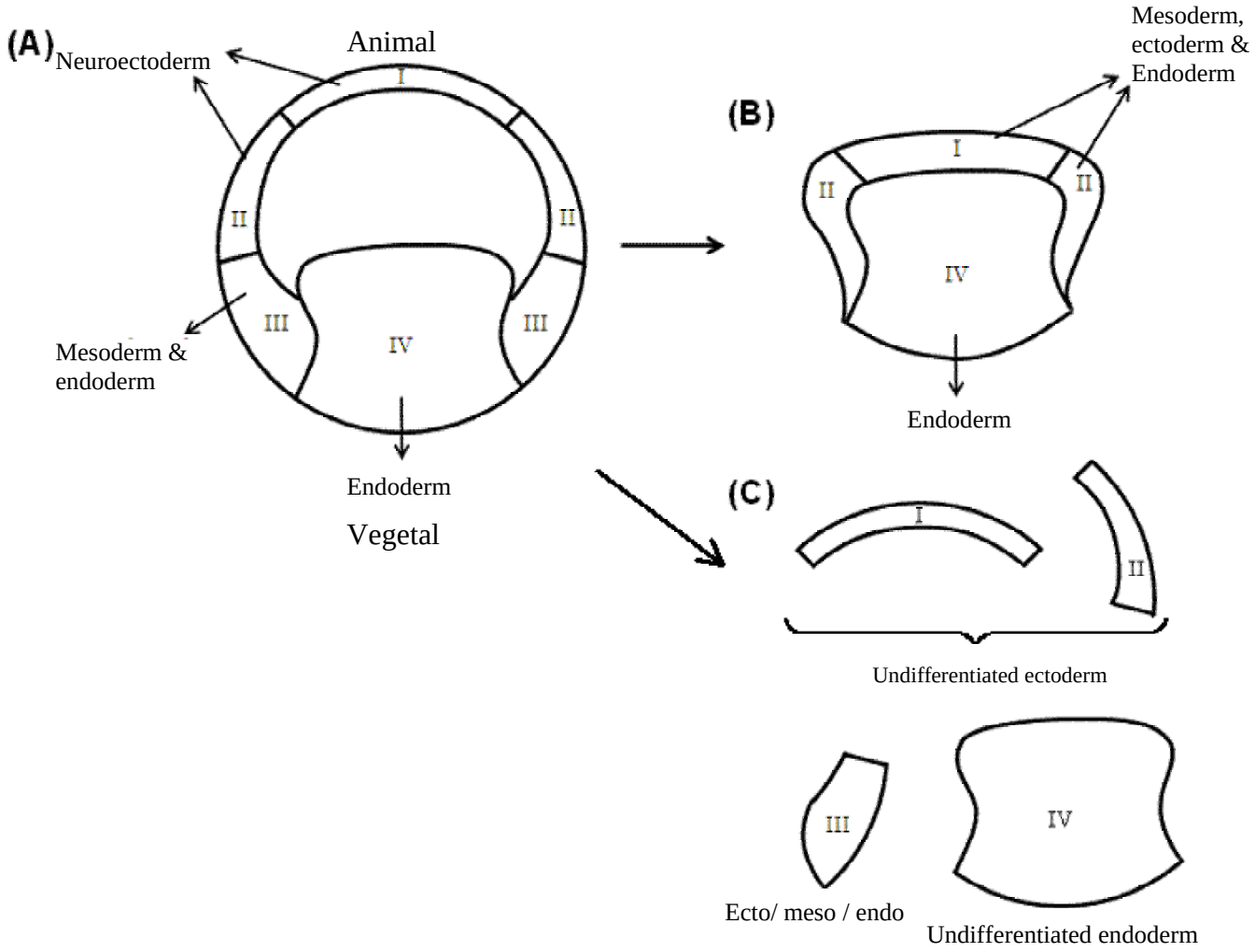

Figure 1.2 A schematic demonstrating Nieuwkoop's transplantation experiments. Blastula (stage 8/9) embryos were divided into four zones (**A**). The four zones were cultured as recombinates (**B**) or isolates (**C**). When zones I and II were cultured with zone IV (**B**), mesoderm, ectoderm and endoderm derivatives were induced in zones I and II. In contrast, in isolation, zones I and II only develop into undifferentiated ectoderm, and zone IV develops only into undifferentiated endoderm.

It had previously been shown that primordial germ cells (PGCs), the precursor cells of eggs and sperm, develop in the lateral plate mesoderm of mid-gastrula stage axolotl embryos [Humphrey 1925a; Nieuwkoop 1947]. The complete derivation of mesoderm from presumptive-ectoderm in the animal cap (zones I and II) would, therefore, be expected to include PGCs. PGCs can be distinguished from other mesodermal cells by their distinct morphology; they retain the size and yolk content of an early embryonic cell [Humphrey 1925b]. Additionally, the chromatin is less highly packaged resulting in the nucleus in PGCs having a spherical appearance, which is distinct from the flattened nuclei of other mesodermal cells. In similar transplantation experiments to those described above, Boterenbrood and Nieuwkoop (1973) showed that the PGCs were a characteristic component of the ventral mesoderm when it was induced in animal caps in response to signals from the ventral endoderm [Boterenbrood and Nieuwkoop 1973] This suggested that PGCs could be induced in the presumptive-ectoderm in response to signals from the ventral vegetative yolk mass. However, the presumptive-ectodermal origin of the PGCs could not be proven without lineage tracing. A series of xenoplastic and homoplastic transplantation experiments carried out by Sutasurja and Nieuwkoop (1974) confirmed that PGCs were derived from the animal cap. In the xenoplastic transplantation experiments, animal caps from one urodele amphibian (including axolotl) were transplanted onto the vegetative yolk mass of another urodele species [Sutasurja and Nieuwkoop 1974]. Differences in pigmentation and yolk

platelet size were used to discern the origin of the PGCs. The PGCs were always derived from the species that had furnished the animal cap. Homoplastic transplantation experiments carried out with axolotl yielded the same result. In these experiments, either the animal cap or the vegetal endoderm was radioactively labelled with methyl-tritiated thymidine (^{3}H) and combined with unlabelled halves. The origin of the PGCs was traced by the presence or absence of radioactive label. In further experiments different regions of axolotl animal caps were combined with different regions of the endoderm [Sutasurja and Nieuwkoop 1974]. The results showed that the entire animal cap was competent to form PGCs. Thus, all of the animal cap cells in blastula stage axolotl embryos can give rise to derivatives of all three germ layers, including the PGCs.

The derivation of PGCs from axolotl animal cap cells was confirmed more recently in animal cap explant experiments (**Figure 1.3**). Axolotl embryos were injected at the 1-2 cell stage with *Xenopus* BMP4 RNA and eFGF RNA to induce PGCs [Johnson *et al.* 2003b; O'Reilley et al. unpublished]. In *Xenopus* embryos FGF is known to induce posterior mesoderm [Amaya *et al.* 1991], and a high level of BMP is known to induce ventral mesoderm [Jones and Smith 1998]. Co-injection of the two RNAs was predicted to induce posterior ventral mesoderm, the tissue from which axolotl PGCs are derived [Nieuwkoop 1947]. Animal caps were isolated from injected embryos at late-blastula (stage 9) and cultured until stage 42. At stage 42 PGC induction was determined by

the expression of RNA binding proteins *axdazl* and *axvasa,* which are PGC specific genes [Johnson *et al.* 2001; Bachvarova *et al.* 2004].

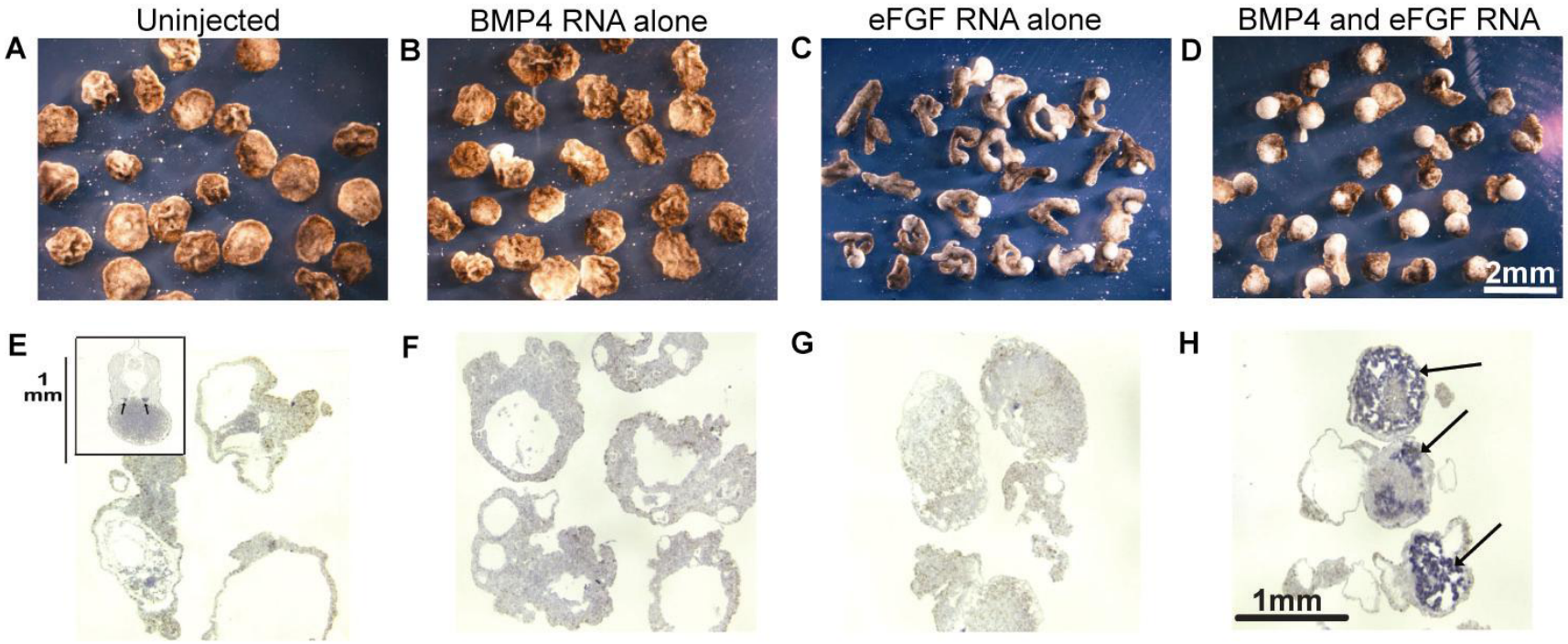

Figure 1.3 Animal caps induced to make PGCs (PGC-induced caps) and expression of *axdazl* in PGC-induced caps.
[Johnson *et al* unpublished]. Embryos were injected at the 1-2 cell stage with BMP4 RNA alone or eFGF RNA alone or BMP4 and eFGF RNA. Animal caps were cut at stage 9 (late-blastula). Panels A–D show the phenotypes of animal caps at stage 16 (mid-neurula). Panel **A** shows uninjected caps. Panel **B** shows caps injected with 5 ng *Xenopus* BMP4 RNA. Panel **C** shows caps injected with 5 pg *Xenopus* eFGF RNA. Panel **D** shows PGC-induced caps (injected with 5 ng *Xenopus* BMP4 RNA and 20 pg eFGF RNA). The scale bar in panel D applies to panels A-D. Panels **E-H** show ISH for *axdazl* expression on 15 µm sections of animal caps at stage 42. *Axdazl* expression is only visible in PGC-induced caps, panel **H,** indicated by arrows and uninjected whole embryos (inset panel **E**). The scale bar in panel H applies to panels E-H.

Additionally, similar to murine pluripotent cells, axolotl animal cap cells express *axoct4* (**Section 1.5.5 and Chapter 3**), a pluripotency associated transcription factor. Evidence suggests that Axoct4 has a conserved function in the maintenance of pluripotency (**Section 1.5.5**). Thus, axolotl animal cap cells have pluripotent properties, similar to pluripotent cells in mammals, having the ability to derive all three somatic germ layers and the PGCs, and additionally express markers of pluripotency.

1.7 Focus of this study

In order to understand the evolution of mechanisms governing pluripotency it is necessary to study them in a wider variety of organisms. This study describes the investigation of Axnanog, the first Nanog homologue to be identified in an anamniote model organism, and Axoct4 during axolotl embryonic development (**Chapter 4**). There are a number of similarities between the morphological processes in axolotl development and those in amniotes (outlined in **Chapter 3**). Based on these it has been proposed that amniotes may have arisen from a urodele-like ancestor. Thus, studying the function of these molecules in axolotl might be informative with regards to the evolution of the mechanisms governing pluripotency in amniotes. Unfortunately, genomic sequence is unavailable for axolotl. Therefore, it was necessary to clone and characterise multiple genes for use in this study (**Chapter 3**).

Primordial germ cells (PGCs) are the embryonic precursors of the gametes, sperm or oocytes. These cells have restricted developmental potential. Yet, paradoxically they are the only cells that can contribute to the next generation, retaining the ability to derive all of the cells of the embryo upon fertilisation. Additionally, pluripotent cells, embryonic germ (EG) cells, can be derived from PGCs in culture [McLaren and Durcova-Hills 2001]. Thus, understanding how PGCs retain this ability throughout embryonic development might be valuable in understanding the mechanisms governing pluripotency and totipotency. How the germline is segregated from the somatic cells during development is a fundemental question in developmental biology. Little is known about PGC development in axolotls; hence it forms a focus of this study (**Chapter 5**).

Chapter 2. Materials and Methods

2.1 Solutions and buffers

Agarose plates	2% agarose in dH_2O + 0.1% Tris-HCl pH8
Antibiotics (1000x)	10 mg/ml penicillin/streptomycin; 10 mg/ml fungizone; 10 mg/ml kanamycin
Bleaching solution	5% formamide; 1x SSC pH 4.5; 3 - 5% H_2O_2
Blocking Reagent	MAB containing 2% (w/v) Blocking reagent (Roche)
Bouins fixative	25% formaldehyde; 5% glacial acetic acid; 5% methanol; 1% picric acid. dH_2O to final volume
Collagenase/Dispase (4x)	80 mg collagenase type II (Sigma), 48 mg dispase II, dissolved in 10 ml of 1x MBS. Store at –20^{o}C in 5 ml aliquots and dilute to 1x solution with 1x MBS before use.
Denaturing solution	1.5 M NaCl; 0.5 M NaOH
DNA-gel loading dye	0.1% Bromophenol blue, 0.1% Xylene Cyanol FF, 30% glycerol
Electrophoresis Buffer – aka Laemmli electrolyte buffer	25 mM Tris-HCl; 192 mM Glycine; 0.1% w/v SDS; H_20 to volume; pH to 8.3 using Glycine
High Phosphate Buffer (HPB)	0.5 M NaCl; 0.1 M $Na_2HPO_4/7H_2O$; 5 mM EDTA
Homogenisation buffer	50 mM NaCl; 5 ml dH_20; 300 µl protease inhibitor cocktail (Sigma); 0.5 M PMSF (phenylmethylsulfonylflouride);
Hybridisation mix for ISH	50% (v/v) formamide (Sigma); 4x SSC (pH 4.5); 5 mM EDTA; 0.05 mg/ml tRNA (Sigma); 0.1 mg/ml heparin (Sigma); 1% SDS
LB Agar	LB Broth containing 15 g Bacto Agar/litre
Luria Broth (LB)	10 g Bacto Tryptone, 5 g Bactoyeast, 10 g NaCl in 1 litre distilled water. To pH 7.0 with NaOH. Autoclave
Maleic acid buffer (MAB)	0.1 M Maleic Acid; 0.15 M NaCl adjusted to pH 7.5 with NaOH
Marc's Modified Ringers (MMR) (10 x)	1 M NaCl, 20 mM KCl, 20 mM $CaCl_2$ 10mM $MgCl_2$, 50 mM Hepes to pH 7.5
Modified Barth's Saline (MBS)	88 mM NaCl; 1 mM KCl, 2.4 mM $NaHCO_3$; 15 mM Hepes; 0.3 mM $CaNO_3$; 0.41 mM $CaCl_2$; 0.82 mM $MgSO_4$. pH 7.8 with NaOH and autoclave
Neutralising solution	1 M Tris-HCl (pH 7.5) 1.5 M NaCl
NTMT	0.08 M NaCl; 0.1 M Tris-HCl (pH 9.5); 0.05 M $MgCl_2$; 1% (v/v) Tween

NZY Agar	NZY Broth with 1.5% (w/v) Bacto Agar
NZY Broth	5 g NaCl, 2 g $MgSO_4 \cdot 7H_2O$, 5 g yeast extract, 10 g NZ amine (casein hydrolysate). Made up to 1 litre with dH_2O, to pH 7.5 with NaOH. Autoclave.
NZY Top Agar	NZY Broth with 0.7% (w/v) Bacto Agar
Phosphate buffered saline (PBS) (10 x)	27 mM Potassium Chloride; 14.7 mM Potassium Phosphate monobasic; 1.38 M NaCl; 80.6 mM Sodium Phosphate dibasic (Invitrogen)
PBS-Tween	1x PBS; 0.1% Tween
Paraformaldehyde (PFA) (4%)	4% paraformaldehyde in 1x PBS
Resolving Gel (10%) pH 8.8	375 mM Tris-HCl pH 8.8; 10% acrylamide (from 30%:0.8% acrylamide:bisacrylamide stock (Protogel – BioRad); 0.1% SDS; 375 mM. Immediately before pouring add to 10 ml gel; 100 µl 10% Ammonium persulphate; 10 µl TEMED
RNA-gel loading dye	95% formamide; 0.025% xylene cyanol; 0.025% bromophenol blue; 18 mM EDTA; 0.025% SDS
Sodium dodecyl sulfate (SDS) gel-loading buffer (2 x)	100 mM Tris-Cl (pH 6.8); 4% w/v SDS; 0.2% w/v bromophenol blue; 20% glycerol; 200 mM Dithiothreitol (DTT)
SDS-PAGE running buffer	0.1% SDS; 0.25 M glycine; 25 mM Tris-HCl pH 8.3
SET buffer (20 x)	3 M NaCl; 1 M Tris-HCl pH8; 0.02 mM EDTA
SM buffer	100 mM NaCl; 8 mM $MgSO_4.7H_2O$; 0.05 M Tris-HCl (pH7.5); 0.01% (w/v) gelatine
SOC	20 g Bacto Tryptone; 5 g Bacto Yeast; 10 mM NaCl; 2.5 mM KCl; 10 mM $MgCl_2$; 10 mM $MgSO_4$; 20 mM Glucose
SSC (20 x):	3 M NaCl; 0.3 M sodium citrate. pH to 7 (blotting) or 4.5 (ISH) with NaOH
Stacking Gel (4%) pH 6.8	125 mM Tris-HCl pH 6.8; 4% acrylamide (from 30%: 0.8% acrylamide:bisacrylamide stock (Protogel – BioRad); 0.1% SDS. Immediately before pouring add to 5 ml gel: 50 µl 10% Ammonium persulphate; 5 µl TEMED
Tris-acetate-EDTA (TAE) buffer (50 x)	2 M Tris-acetate; 0.05M EDTA
Tris-EDTA (TE) buffer	10 mM Tris-HCl (pH 7.5); 1 mM EDTA
Wet Transfer Buffer	25% Methanol; 24 mM Tris-HCl; 153 mM Glycine

2.2 Extraction of protein, DNA and RNA

2.2.1 RNA extraction from embryos and oocytes

RNA was extracted from embryos/ oocytes using TRI reagent® (Sigma) following the standard protocol (T9424). Staged embryos/ oocytes were homogenised on ice in TRI reagent® until completely suspended. Large embryo debris was removed from the homogenate by centrifugation (12,000 g, 5 min) and the supernatant was then transferred to a fresh tube. 200 µl of chloroform was added per ml of TRI reagent® before the mixture was vortexed and separated by centrifugation (12,000 g, 10 min). The upper aqueous phase was removed and 500 µl of isopropanol was added per ml of TRI reagent®. RNA was precipitated for 20 min at -20°C. The RNA was then pelleted at room temperature by centrifugation (12,000 g 10 min). The pellet was resuspended in non-DEPC treated nuclease free water (Ambion) and an equal volume of 8 M LiCl was added. Precipitation of the RNA was then carried out at 4°C for 1-2 days. This further precipitation ensured the removal of contaminating genomic DNA. The RNA was pelleted at room temperature by centrifugation (12,000 g, 10 min). The pellet was resuspended in an appropriate volume of nuclease free water and the RNA was then treated with DNAseI (Ambion) for 30-40 min at 37°C to remove remaining genomic contamination. Quality was checked by gel electrophoresis (1.5% agarose as described in **Section 2.3.6**) and by measurement of concentration (**Section 2.3.3**). Purified RNA was stored at –80°C until use.

2.2.2 Poly-A^+ RNA extraction

Poly-A^+ RNA was isolated from total RNA extracted from embryos and oocytes using an Oligotex mRNA Mini Kit (Qiagen) according to the manufacturer's guidelines. The integrity of the poly-A^+ RNA was checked on a 2% (w/v) agarose gel (**Section 2.3.6**) and it was quantified (**Section 2.3.3**) prior to storage at –80^{o}C.

2.2.3 Protein extraction from oocytes

Protein extractions were carried out according to the method described by [Johnson *et al.* 1990]. Oocytes were homogenised in 50 mM NaCl containing 0.5 M phenylmethylsululfonyl fluoride (PMSF) and protease inhibitor cocktail (Sigma). Homogenates were separated by centrifugation (12,000 g, 5 min) into three phases; the top phase contained fat, the supernatant contained non-membrane bound proteins and the pellet contained membrane bound proteins. The supernatant was removed and precipitated with 4 volumes of acetone for 15 min at -20^{o}C. Precipitated protein was resuspended in 1 x SDS gel loading buffer and stored at –20^{o}C until use.

2.2.4 Extraction of genomic DNA from erythrocytes

An axolotl was sacrificed by administering MS-222 (Tricaine methane sulfonate; 0.5-2 g/l; pH 7.0). Blood was extracted and mixed immediately with 1 x SET solution. The mixture was separated by centrifugation (6000 g, 3 min) and the pelleted red blood cells were resuspended in 1 x SET solution. Proteinase K was added to a

concentration of 200 µg/ml and SDS or SDS buffer was added to 0.5% (w/v). The red blood cells were then incubated at 37°C overnight.

The following day genomic DNA was purified by two phenol:chloroform extractions (**Section 2.3.7**) and an ethanol precipitation (**Section 2.3.8**). The pelleted DNA was resuspended in TE buffer, quantified (**Section 2.3.3**) and stored at –20°C until use.

2.3 Preparation and manipulation of DNA

2.3.1 Minipreps

Plasmid DNA was prepared using QIAprep® Spin Miniprep Kit, (Qiagen) according to the manufacturer's protocol.

2.3.2 cDNA synthesis

cDNA was synthesised using SuperScript™ reverse transcriptase III (Invitrogen) according to the manufacturer's guidelines. A maximum of 4 µl of RNA was added to each reaction and 200 ng of random hexamer primers were used. Reactions were carried out in a Techne thermal cycler (TC-312) using standard reaction conditions (Invitrogen). Reaction volumes were typically made up to 50 µl with non-DEPC treated nuclease free water (Ambion), aliquoted and stored at -20°C until use.

2.3.3 Determination of DNA and RNA concentration

DNA and RNA preparations were quantified using a Nanodrop 1000 spectrophotometer. Absorbance ratios of 260/280 and 260/230 nm were used to confirm product purity.

2.3.4 Amplification of DNA by polymerase chain reaction (PCR)

All PCR [Saiki *et al.* 1985] reactions were carried out in Techne thermal cyclers (TC-312).

RT-PCR

PCRs were carried out in a final volume of 20 µl and consisted of: 1 x REDTaq® Ready Mix™ PCR mix (Sigma), 5 µl dH_20, typically <100 ng (1µl) DNA and 2 µl each of forward and reverse primer at 1 mM final concentration. DNA was amplified according to the following program: 94°C for 2 min followed by 20-30 cycles; 94°C for 45 sec; Tm-5 for 45 sec; 72°C for 1 min. This was followed by a final extension at 72°C for 2 min.

	Forward	**Reverse**
axnanog	GTTCCAGAACCGAAGGATGA	CGAAGGGTACTGCAGAGGAG
***axnanog* ORF**	ATGCCCGCCCACTGCATGAC	ACATGCCCTGCGTGCTCTGA
axodc	TGCGTTGGTTTAAAGCTCTC	ACATGGAAGCTCACACCAAT
axck	AACGAGCGCCTGGCCTCCTAC	CATGGCGCCAAATTAAACTGAAC

Table 2.1 RT-PCR primer sequences
Sequence is given 5' to 3'.

Degenerate PCR

Primers were designed in conserved regions identified from the alignment of amino acid sequences from human, mouse, *Xenopus* and zebrafish. Alignments of the corresponding nucleotide sequences were utilised to reduce the degeneracy of the primers; degenerate nucleotides were replaced with single nucleotides at positions where all of the aligned sequences showed usage of the same nucleotide.

PCRs were carried out in a final volume of 20 µl and consisted of 1 x Extensor Hi-Fidelity PCR Master Mix with Buffer 1 (Abgene), 7 µl dH_20, typically <100 ng (1 µl) DNA and 1 µl each of forward and reverse primers at 2.5 mM final concentration. DNA was amplified using the following program: 94^oC for 2 min followed by 45 cycles: 94^oC 45 sec, 45^oC for 45 sec, 68^oC for 1 min per kb. This was followed by a final extension at 68^oC for 2 min.

	Forward	**Reverse**
axblimp1	ACTGGATGGGCTAYGTIAAY	YTTRTGRCAIACCTGRCAYTC
axcarm1	ATCGGIGACGCIAAYGGIGAI	CTGRTCCACYTGIGCIACAAT
axncam	GGMATYAARAARACAGATGARGGI	RCTTGCTTGRACMAGIATGAAYTC

Table 2.2 Degenerate PCR primer sequences
Sequence is given 5' to 3'. Base codes: I = inosine; R = A + G, Y = C + T, M = A + C, K = G + T, H = A + T +C, D = G + A + T.

Semi-degenerate PCR

PCRs were carried out by the same method as degenerate PCRs except that only one degenerate primer was used at a final concentration of 2.5 mM and a specific primer, designed to the

sequence obtained by degenerate PCR, was used at a final concentration of 1 mM.

	Degenerate Primer	Specific Primer
***axblimp1* 5'**	ATGAARATGGAYATGGARGA	GAGTTCTCCCGAGGAAGGGTAGTTC
***axcarm1* 3'**	RCTCCCRTARTGCATTGTGTTGGT	TCTCGGGGACTGTCCTCCTTATAG
***axncam* 5'**	ATGCTGCARAYTCAGGARCTCATC	CACAACCACTTGGATATCCCTGAAG
***axncam* 3'**	TGCYTTGCTCTCATTCTCRTTTGT	ACTGCACAGCAGTCAACCGCATTG

Table 2.3 Semi-degenerate PCR primer sequences
Sequence is given 5' to 3'. Base codes: R = A + G, Y = C + T.

Identification of introns by PCR

Exon-exon boundary sequences were identified in order to amplify intron sequences from genomic DNA. Boundary sequences were predicted from known boundaries in human homologues and by the alignment of the axolotl nucleotide sequences with homologues from human, mouse, *Xenopus* and zebrafish. Primers were then designed 50, 80, and 100 bp (where possible) upstream and downstream of the predicted boundaries.

PCRs were carried out in a final volume of 20 µl and consisted of 1 x Extensor Hi-Fidelity PCR Master Mix with Buffer 1 (Abgene), 5 µl dH_20, 150–200 ng genomic DNA and 2 µl each of forward and reverse primers at 1 mM final concentration. DNA was amplified according to the following program; 94°C for 2 min, followed by 40 cycles: 94°C for 45 sec, annealing temperature (Tm-5) for 45 sec, 68°C typically for 2-5 min (extension times were estimated according to the length of human introns; 1 min/kb). This was followed by a final extension at 68°C for 2 min.

	Forward primers	Reverse primers
axnanog **intron 1**	50bp CGTGTGCTGTGGCGGCGAAC 80bp GCCTACCCGGAACTGAACCAAC 100bp CGCAAATGAGGGTGCCAGGATAC	50bp CTGGTGGCTGAGTCGGGGGAAG 80bp TCCGGGGCACACTGGGCGAAC
axnanog **intron 2**	50bp AAGCAGCATTACATGAACCCAATG 80bp CTCGTGGCCCTGCACCGAATG 100bp GACGAAGGCCCAGGCGAGAAAG	50bp TGTCCAGCCACACTGAGTCCTTC
axoct4 **intron 1**	50bp AGCAGCGCCAGCCCGGACCTG 80bp GTCCGATGACAGCCCGCACAG 100bp GCCAGGTCGCCTGCGTCCGTG	50bp CCACGGACGCAGGCGACCTG 80bp CCTGCGTAAAGCCCAGCGTGATG
axoct4 **intron 2**	50bp AAGCGCATCACGCTGGGCTTTAC 80bp GAACAGTTTGCCAAGGAGCTGAAG	50bp ACACATGTTCTTGAAGCTCAGTTG 80bp CTGGAGCAGGGGTCTCAGTTTAC 100bp CCTCGACCAGCCAGCGCTG
axoct4 **intron 3**	50bp GTAAACTGAGACCCCTGCTCCAG 100bp CGAGGCCCTGCAACTGAGCTTC	50bp GACGCTGTTCTCGATGCTGGTTC 100bp ATGGGTGGGCTTCGGACACTTC
axoct4 **intron 4**	50bp AAGTGTCCGAAGCCCACCCATC – 100bp CGGAAGAGGAAAAGAACCAGCATC	50bp CAAATGCTGCGCTTCCCCTTCTG 100bp CCCGGCTGCATCCCTGGGTAC
axblimp1 **intron 4**	50bp CGGGACTTTGCAGATAGGCTGAAC 80bp CATTCCCGCCAACCAGGAGCTAC 100bp GGACATCTACTTCTACACCATCAAG	50bp GGCACTTTTGTGGTGAAGCACCTC 80bp AAGAATCTCCTTCATGCTGTGTTC 100bp TGCCTTTGGATTGGCTTACAGAAG
axblimp1 **intron 5**	50bp CAAGAAGCAGAACGGGAAGATTAAG 80bp GACTGGTTACAAAACGCTTCCATATC 100bp GCCAGCAACGAAGAAGCAATGAATC	50bp TGGGCCAGCTGCGTGAATCCTTTG 80bp TACAAGGTAGTGCTTCTGCAGATG 100bp GTGTGGCTTTTCTCCCGTGTGTAC
axcarm1 **intron 2**	50bp GAGTCGGCAAGCAGTCTTTTATTG 80bp AAGTGTTCGGTGTCCCGTGAAAC 100bp TGTGTGCGTATTTAAGTGTTC	50bp TGAAGACGGACCGCTCAGAGTTG 80bp AATACTGAACAGCTGACGACTCCTC 100bp CCATAGAACTGGAAATACTGAAC

Table 2.4 Intron PCR primer sequences
Sequence is given 5' to 3'. Values indicate locations relative to the exon:exon boundary.

2.3.5 Restriction enzyme digest

DNA was digested using restriction enzymes (NEB) according to manufacturer's guidelines. Digested DNA was analysed on 1.2-2% (w/v) agarose gels.

2.3.6 Agarose gel electrophoresis

Agarose gels were prepared with 1 x TAE buffer and electrophoresis was carried out in 1 x TAE buffer. Ethidium bromide was added to cooled molten gels, to enable visualisation of nucleic acids, at a final concentration of 1 µg/ml. RNA preparations were analysed on 1.5-2% (w/v) agarose gels. DNA preparations were analysed on 1.2-2% (w/v) agarose gels. Prior to electrophoresis DNA and RNA samples were mixed with the appropriate loading buffers (**Section 2.1**) and RNA samples were heated to 60-80°C for denaturation and quenched on ice to prevent renaturation. Care was taken to prevent RNAse contamination when handling RNA preparations. 100 bp and 1 kb DNA ladders (NEB) were utilised for size estimation. Gels were visualised in a MultiMage™ light cabinet and photographed using an Alpha-Imager™ 1220 Documentation & Analysis System (Alpha Innotech Corporation).

2.3.7 Phenol:chloroform extraction

Phenol:chloroform:isoamylalcohol (25:24:1; pH 8.0) (Fluka) was equilibrated to room temperature and then mixed in a 1:1 ratio with the DNA/RNA samples. Samples were vortexed before separating by centrifugation (5-10 min, maximum speed). The aqueous phase

containing DNA/RNA was transferred to a clean tube and an equal volume of chloroform:isoamylalcohol (24:1) was added and mixed by vortexing before separating by centrifugation (as previous). The aqueous phase was removed to a new tube.

2.3.8 Ethanol precipitation of DNA

DNA and RNA samples were precipitated with 1/10th volume (final concentration 0.3 M) 10 M ammonium acetate (pH 5.2) and 2.5 x volume 100% ethanol. For low concentration samples 1 µl glycogen (Roche) was added as a carrier and to aid pellet visualisation. Samples were mixed by vortexing and incubated at –20°C for 15 min. After incubation samples were separated by centrifugation (10-15 min, maximum speed). The supernatant was removed with care and the pellet was resuspended in an appropriate volume of dH_2O.

2.3.9 Purification of DNA from agarose gels

DNA was separated by electrophoresis on a 1.2% (w/v) agarose gel. Separated DNA was then visualised using a low intensity UV transilluminator and excised from the gel using a scalpel. Excised DNA fragments were purified from the agarose gel using spin columns from a QIAquick gel extraction Kit (Qiagen) or a MinElute kit (Qiagen) according to manufacturer's guidelines.

2.3.10 Ligation of DNA fragments

Insert and vector were mixed at a ratio of approximately 10:1, respectively. Ligations were typically carried out with 50-100 ng of

vector. 1 µl of T4 DNA ligase (NEB) was added to reactions and the provided buffer was added to 1 x concentration. Reactions were incubated at room temperature for 2-16 hours.

Calculating Vector Insert Ratio:

$$x\ ng\ insert = \frac{ng\ \ vector\ \times\ insert\ size\ (kb)}{vector\ size\ (kb)} \times \frac{10}{1}$$

2.3.11 Transformations

Chemically competent *E. coli* strain XL1-Blue Mrf- were thawed slowly on ice. Half the volume of a ligation reaction or 50-100 ng of plasmid DNA was added to 150 µl of competent cells and incubated on ice for 30 min. The cells were then heat-shocked in a 42°C water bath for 90 sec and cooled on ice for 90 sec. Following cooling, 250 µl of SOC media was added and the cells were incubated in a 37°C shaking incubator for 45 min. 20 µl and 200 µl of the transformation were spread onto LB agar plates containing the appropriate antibiotic. The plates were then incubated overnight at 37°C. For blue/white selection, 40 µl of 20 mg/ml X-GAL and 15 µl of 100 mM IPTG were spread onto the agar prior to plating.

2.3.12 DNA sequencing

DNA sequencing reactions were performed using 100 ng plasmid DNA, 1 µl Big Dye sequencing buffer (Applied Biosystems), 1 µl Big Dye mix (Applied Biosystems), 0.5 µl Primer (10 µM) (primer varied according to the template), and 5.5 µl dH_2O to make up the reaction volume to 10 µl.

The DNA was amplified according to the following PCR program: 25 cycles at 96°C for 30 sec, 50°C for 15 sec and 60°C for 4 min. Following the PCR, the reactions were precipitated with 2 µl 3 M sodium acetate (pH 5.6) and 100 µl 100% ethanol at room temperature for 15 min. The DNA was pelleted by centrifugation (maximum speed, 15 min) before washing with 150 µl 80% ethanol and air-drying. Air-dried pellets were sent to Geneservice (Nottingham, UK) for analysis.

2.3.13 Sequence analysis and comparison

Sequence comparisons were carried out using NCBI Basic Local Alignment Tool (BLAST) (version 2.2.18). All alignments were performed using the Clustal W feature [Thompson *et al.* 1994] of the Bioedit sequence alignment program [Hall 1999].

2.4 Treatment and preparation of embryos and oocytes

2.4.1 Axolotl matings

Male and female axolotls were housed in separate water systems until mating. A male and a female animal were selected randomly from a database and placed together in a chilled mating tank containing gravel and stones in darkness overnight. The next day the tank was checked for the presence of spermatophores and the male was removed. The female remained covered to minimise disturbance. If the female began to lay embryos on the same day, she was chilled to 16°C overnight in order to obtain 1-2 cell stage embryos the following day.

2.4.2 Culture of axolotl embryos

Embryos obtained from fertilisations were de-jellied manually at the 1-2 cell stage or stage 8 (for ISH) and placed in 0.1 x MBS with added antibiotics and fungizone. Embryos for microinjection were placed in 1 x MBS plus 4% ficoll$_{400}$ (Sigma) and antibiotics before use in order to shrink the pre-vitelline space, whereas embryos for ISH were cultured in 0.1 x MBS at 16-22°C. Staging was according to [Bordzilovskaya *et al.* 1989].

2.4.3 Preparation of oocytes for microinjection

A mature *Xenopus tropicalis* female was sacrificed by administering a lethal dose of MS-222 (Tricaine methane sulfonate; 0.5-2 g/l; pH 7.0) and ovary tissue was removed surgically and placed directly into 1 x MBS to preserve the oocytes. In order to liberate the oocytes, ovary tissue was placed into a solution of type II collagenase (Sigma) and dispase (Gibco BRL) on a rocking platform at room temperature. Oocytes were collected and washed with 1 x MBS to remove traces of collagenase and then stored in a petri dish containing 1 x MBS plus 4% Ficoll$_{400}$ (Sigma) until injection.

2.4.4 *In vitro* transcription of mRNA for microinjection

Plasmid DNA templates were linearised with an appropriate restriction enzyme and purified by phenol:chloroform extraction (**Section 2.3.7**) and a subsequent ethanol precipitation (**Section 2.3.8**). mRNA was

reverse transcribed from linearised templates using the appropriate Message Machine kit (Ambion). All reactions were carried out for 2 hours to achieve the maximum yield. Unincorporated nucleotides were removed by two phenol:chloroform extractions and isopropanol precipitations according to the manufacturer's guidelines. RNA was resuspended in 20 µl of non-DEPC treated nuclease free water (Ambion) and the concentration was determined (**Section 2.3.3**) prior to aliquoting for storage at –80°C. Aliquots were thawed on ice before dilution for microinjection.

	Vector	**Linearise**	**Transcribe**	**Reference**
***axnanog* full-length**	pBut3HA	SfiI	T3	This work
***axnanog* ORF (-5'UTR)**	pBut3HA	SfiI	T3	This work
GFP	pCSGFP2	EcoRI	Sp6	A.D. Johnson
***Xenopus* BMP4**	pSP64T	EcoRI	Sp6	[Dale *et al.* 1992]
***Xenopus* eFGF**	pSP64T	SacI	Sp6	[Isaacs *et al.* 1994]

Table 2.6 Vectors for RNA synthesis.

2.4.5 Preparation of morpholinos

Morpholinos were designed and supplied by Genetools (www.genetools.com). They were rehydrated in non-DEPC treated nuclease free water (Ambion) to a stock concentration of 40 ng/nl. Repeated vortexing and heating to 65°C ensured complete suspension. Stock solutions were stored at 4°C. Prior to use stock solutions were again heated to 65°C and diluted aliquots were incubated at 37°C until injection.

Morpholino	Sequence
Axnanog translation-blocking	GGTCAATCCAAAAGCTCCTCCTAAG
Axnanog mismatch control	GGTGAATGCAAAACCTCGTCGTAAG
Axnanog splice-blocking (intron-exon)	GGCAGGACTGAAACAAAACGAAGAC
Axnanog splice-blocking (exon-intron)	GGATTTCAAGGTTGTTTACCTGCCG
Axoct4 translation-blocking	TCTCCTGTCCCAAATGCCCAGCCAT

Table 2.7 Morpholino sequences
Sequence is given 5' to 3'.

2.4.6 Microinjection of embryos and oocytes

Embryos

Axolotl embryos were placed in a specially designed injection dish containing 1 x MBS plus 4% ficoll$_{400}$ (Sigma). Glass needles pulled on a micropipette puller (Flaming/Brown Model P-9) were calibrated to inject 4 nl using a graticule and 1-2 cell stage embryos were injected twice with 4 nl of RNA or morpholino using a PL1-100 (Harvard Apparatus Medical Systems Research Products) microinjector. Injected embryos were cultured in 1 x MBS plus 4% ficoll$_{400}$ and antibiotics until stage 8 (mid-blastula) when they were transferred to 0.1 x MBS with antibiotics and cultured until they reached appropriate stages. For "capping experiments", animal caps were disected from stage 9

(late-blastula) embryos immersed in 0.5 x MMR plus antibiotics. Caps were then cultured on agarose plates in 0.5 x MMR plus antibiotics. The staging of cultured caps was determined using untreated sibling embryos.

Oocytes

Xenopus tropicalis oocytes were injected in the same way as axolotl embryos but with 2 nl of RNA or morpholino, and cultured in 1 x MBS plus 4% ficoll$_{400}$ at 18°C.

2.5 *In situ* hybridisation (ISH)

2.5.1 Preparation of axolotl embryos for ISH

Staged embryos were placed in 4% paraformaldehyde (PFA) in round-bottomed 2 ml tubes (no more than 5 embryos per tube). Embryos were fixed for 5-7 days at 4°C, before being dehydrated in 100% methanol and stored at –20°C until use. The 100% methanol was changed once during storage to ensure complete dehydration.

2.5.2 Embedding embryos for sectioning

Embryos stored as above were washed twice in xylene for 45 min. Xylene was replaced with a pre-warmed 50:50 solution of xylene:wax and embryos were incubated at 65°C for 45 min. Subsequently, they were incubated in 100% wax 3 times for 45 min each at 65°C. For the final incubation embryos were transferred to embedding moulds. They were orientated in the final wax change using heated forceps and a light microscope. Tailbud stage embryos could be orientated by eye. Embedded embryos were stored at 4°C.

2.5.3 Sectioning

Embryos were removed from embedding moulds and orientated on mounting blocks for sectioning. Ribbons of 15 µM sections were generated on a Leica microtome (RM2265) and were then floated briefly in a 42°C water bath and mounted onto SuperFrost™ Plus slides (VWR). Sections were stored for up to 1 month before use in ISH experiments.

2.5.4 Hemisectioning

Embryos were hemisectioned following a modification of the protocol described for *Xenopus laevis* [Lee *et al.* 2001]. Embryos stored as described above (**Section 2.5.1**) were rehydrated through a methanol series to PBST; 100% methanol, 75% methanol, 50% methanol, 25% methanol and 100% PBST each for 5 mins. Following rehydration they were washed 3 times for 1 hour in PBS plus 0.3 M sucrose. They were then visualised by light microscopy and embedded and orientated in 4% (w/v) low melting point agarose (Promega) made up with PBS plus 0.3 M sucrose. Once the embryos had set in the agarose it was covered with PBS plus 0.3M sucrose and the embryos were bisected using a scalpel. Hemisectioned embryos were transferred to 100% methanol in 2 ml tubes and stored at –20°C until use. ISH was carried out on hemisections according to the whole-mount protocol (**Section 2.5.6**).

2.5.5 Preparation of dioxigenin (DIG) labelled RNA probes

Plasmids containing probe sequences were linearised at the 5' end of the inserted sequence to produce antisense probes and at the 3' end to produce sense probes using an appropriate restriction enzyme. Linearisation was checked on an agarose gel. Impurities were removed from linearised templates by phenol:chloroform extraction (**Section 2.2.7**) followed by an ethanol precipitation (**Section 2.2.8**). Linearised template was then resuspended in non-DEPC treated nuclease free water (Ambion).

In vitro transcription reactions were performed using 1 µg linearised template, 2 µl of 2 x DIG-UTP NTP mix (Roche), 4 µl of 5 x transcription buffer (Promega), 20 units of RNase Out (Invitrogen) and 1-2 units of the appropriate RNA polymerase (Promega). The reaction was made up to a total volume of 20 µl using non-DEPC treated nuclease free water (Ambion) and incubated at 37°C for two hours. Following RNA synthesis 1 µl of DNaseI (Ambion) was added and the reaction was incubated at 37°C for 15 min to degrade the DNA template. Reaction volumes were made up to 50 µl with nuclease free water and purified from unincorporated nucleotides using a $G\text{-}_{50}$ spin column (GE Healthcare) according to manufacturer's guidelines. The synthesised probe was quantified (**Section 2.3.3**) and the integrity was checked on an agarose gel (**Section 2.3.6**). Synthesised probes were then stored at -80°C until use.

	Sequence	Vector	Linearise	Transcribe	Reference
axnanog	Full-length	pGemT easy (Promega)	SpeI	T7	J. Dixon (Unpublished)
axoct4	Full-length	pBS-SK+	EcoRI	Sp6	A. D.Johnson (AY542376)
axmix	Full-length	pBS-SK+	Hind III	T3	G. Swiers (Unpublished)
axbrachyury	Full-length	pBS-SK+	XhoI	T3	G. Swiers (AF308870)
axblimp1	Degenerate fragment*	pGemT easy (Promega)	NcoI	Sp6	This work
axncam	Degenerate fragment*	pGemT easy (Promega)	ApaI	Sp6	This work
axck	Full-fragment cloned	pGemT easy (Promega)	NcoI	Sp6	This work
axcarm1	Degenerate fragment*	pBS-SK+	Sac II	Sp6	This work
axdazl sense	Full-length	pBS-SK+	Hind III	T3	A.D. Johnson (AF308872)

Table 2.8 Vectors for ISH probe synthesis
* See **Appendix 8.1** for probe sequences

2.5.6 Whole-mount *in situ* hybridisation (WISH)

Whole-mount and hemisection *in situ* hybridisations were performed using a method adapted from the Harland laboratory protocol (http://tropicalis.berkeley.edu/home/gene_expression/in-situ/insitu.html; accessed June 2008). ISH was carried out in glass vials for whole embryos or 2 ml round-bottomed microfuge tubes for hemisections. Embryos, stored at –20°C in 100% methanol, were first rehydrated to PBST through a methanol series; as in **Section 2.5.4**. Following rehydration they were refixed in 4% PFA for 15-20 min and were then washed 3-5 times with PBST to remove all traces of PFA. Following fixation embryos were equilibrated for 5 min in 50:50 hybridisation mix:PBST at 60°C which was then replaced with fresh hybridisation mix.

They were then incubated in hybridisation buffer (6 hour, 60°C). After 6 hours hybridisation buffer was recovered for later use and replaced with hybridisation buffer containing DIG-UTP (roche) labelled RNA probe (0.5 ng/µl). Embryos were incubated with probes in a 60°C waterbath overnight.

The next day, the hybridisation buffer containing the DIG labelled probe was recovered and stored at –20°C for reuse. The embryos were washed for 2 min with recovered pre-warmed hybridisation buffer and in pre-warmed 2 x SSC (pH 4.5) at 60°C 3 times for 20-30 min, followed by two washes in 0.2 x SSC (pH 4.5) for 20-30 min at 60°C. They were subsequently washed twice in MABT for 10-15 min at room temperature before incubation in MAB plus 2% Blocking reagent (Roche) for 5 hours at room temperature. This solution was replaced with MAB plus 2% Blocking reagent containing a 1:3000 dilution of anti-DIG antibodies conjugated with alkaline phosphatase (Roche) and the embryos were incubated at 4°C overnight.

Following antibody incubation embryos were washed once for 5 min in MABT followed by at least 4 washes in MABT over a 4-hour period. They were then washed three times for 5 min in NTMT. NTMT was replaced with BM purple (Roche) and they were incubated in darkness at room temperature to allow colour development for 1–5 days. Incubation times varied according to the probe. After colour

development embryos were washed briefly in MAB and fixed in Bouin's fixative overnight at room temperature.

Yellow staining, resulting from incubation in Bouin's fixative, was removed by a number of washes in buffered 70% ethanol (70% ethanol:30% PBST) at room temperature. Embryos were then rehydrated through an ethanol series to 1 x SSC (pH 7.0). To remove pigment and facilitate visualisation of staining, bleaching was performed on a light box in 2-5% bleaching solution. Once adequate bleaching was achieved embryos were washed twice in 1 x SSC and once in 100% methanol before transferring to 80% glycerol for storage at 4°C and photography.

2.5.7 *In situ* hybridisation (ISH) on sections

All room temperature steps were carried out in glass coplin jars or modified food storage containers (where stated) and plastic coplin jars were used for incubations in the 37°C waterbath. Sections were dewaxed by washing the slides three times in 100% histoclear (VWR). Slides were then washed once in 100% ethanol and once in 100% methanol for 5 min each followed by rehydration to PBST through a methanol series, as described in **Section 2.5.4**. After rehydration slides were incubated in pre-warmed PBST containing proteinase K (Roche) (3 µg/ml) at 37°C for 10 min. Following this incubation slides were washed briefly in PBST and then refixed in 4% PFA for 20 min at room temperature. Slides were washed 2-3 times in PBST for 5 min each at room temperature to remove any remaining PFA. They were then

rinsed with 300 µl of hybridisation buffer and hybri wells (Stratech) covered with 300 µl of hybridisation buffer containing the appropriate DIG UTP (Roche) labelled RNA probe (5 ng/µl) were applied to the slides. They were then laid flat in a specially modified food storage container lined with wet paper towel. The air-tight lid was replaced and the container was incubated overnight at 60°C in a hybridisation oven. Care was taken to select food storage containers having a tight seal to prevent the slides from drying during incubation.

The next day, the hybri wells were removed with care to avoid damage to the sections and where possible the probe solution was recovered and stored at –20°C. Slides were washed briefly in pre-warmed solution 1 (4 x SSC; 50 % formamide; 0.1% SDS (w/v)) at 60°C. They were then washed in solution 1 for 20 min at 60°C, followed by a single wash in solution 2 (2xSSC; 50% formamide; 0.1% SDS (w/v)) for 20 min at 60°C. This was followed by two washes in MAB for 10-15 min at room temperature. Subsequently, the slides were laid flat in a food storage container and covered with approximately 300 µl of MAB plus 2% Blocking reagent (Roche) which was then overlaid with a piece of parafilm. Care was taken to ensure that hybridisation boxes were cleaned thoroughly between each use. Incubation in the blocking solution was carried out for 1 hour. The blocking solution was replaced with MAB plus 2% Blocking reagent containing a 1:5000 dilution of anti-DIG antibodies conjugated with alkaline phosphatase (Roche) and incubated for 2 hours at room temperature. Excess antibody was

removed by two 20 min washes in MABT. Slides were then washed three times in NTMT for 5 min each. BM purple (Roche) was equilibrated to room temperature. Next, slides were placed flat in the hybridisation boxes and covered with 300 µl of BM purple and overlaid with parafilm. The lid of the box was replaced and the box was stored at room temperature in darkness until appropriate colour development was achieved. Colour development typically took 1-7 days; during long incubations the BM purple solution was replaced several times.

When the appropriate colour development had been achieved the parafilm was floated off in PBST. The slides were then washed twice in PBST for 5 min and fixed in 4% PFA for 20 min. Post-fixation they were washed twice in PBST for 5 min each. Sections were then mounted in 80% glycerol and coverslips were sealed with clear nail-varnish.

2.5.8 Microscopy and photography

Embryos were visualised with Nikon SMZ 1500 microscopes and sections were visualised with a Nikon Eclipse 80i. Embryos were photographed on agarose plates. Photographs of embryos and sections were taken using a Nikon DXM 1200F utilising Nikon ACT-1 software (version 2.70) and a Nikon Digital Sight 5Mc utilising Nikon ACT-2U software (version 1.40.85.221).

2.6 Real-time PCR (qRT-PCR)

For relative quantification of gene expression 25 µl reactions were performed in triplicate for each sample on 96 well Fast plates (Applied Biosystems). Reactions consisted of 1 µl cDNA, 1 x Absolute^{TM} qPCR ROX mix (ABgene), 200 nM (final concentration) of both forward and reverse primers and 5 pmol of probe. Reactions volumes were made up to 25 µl with non-DEPC treated nuclease free water (Ambion). Plates were sealed with optical adhesive film (Applied Biosystems) and air bubbles were removed by brief centrifugation. They were then run on an AB 7500 sequence detection system using a standard program: 50°C for 2 min, 94°C for 15 min followed by 40 cycles of 94°C for 15 sec and 60°C for 1 min. Each plate had an endogenous control (*axodc*) for each sample and controls lacking reverse-transcriptase in the cDNA synthesis reaction were included for each gene.

2.6.1 Primer and probe design

Primer Express software (version 3.0) was used for the design of all probes and primers for qRT-PCR according to manufacturer's guidelines using standard parameters. Where possible primer-probe sets were selected so that either a primer or probe spanned a known or predicted exon-exon boundary. Primers and dual-labelled fluorogenic probes (5'FAM; 3'TAMRA) were supplied by Sigma, all primers were desalted and all probes were HPLC purified. Primers and probes were suspended to 100 µM, aliquoted and stored at –80°C until use; probes

were aliquoted into brown tubes to prevent photodegradation. Primers and probes diluted for use were stored at -20°C.

2.6.2 Data analysis

qRT-PCR data was analysed according to the comparative CT method ($2^{-\Delta\Delta C}t$) [Livak and Schmittgen 2001]. The efficiency of primer and probe pairs was validated on a 4-fold dilution series of cDNAs from 1 to 1/256 to ensure the PCR efficiencies of the target and endogenous reference (*axodc*) were approximately equal. Threshold values were set manually and data was exported to Microsoft Excel for analysis.

	Forward primer	Reverse Primer	Probe
axnanog	TCACATACAAGCAGGTGAAGAACTG	CTCTTGTCCAGCCACACTGAGT	TTCCAGAACCGAAGGATGAAGCACAAAC
axnanog UTR	ACTTTACCAAAAAGCGTGACACTAGA	ACAGAGCACCCAATTTTCCAA	TGCGCCGAATAAAAACAAACCCTACTGA
axoct4	GCGGACCTTGAACAGTTTGC	ACATCCGCCTGCGTAAAGC	AGCTGAAGCAGAAGCGCATCACGCT
axbrachyury	CATTGACCACATGTACCAATTGC	GATCAAGGGTCAATCGTGAGTTC	TACCCATAGTTCTTTTGTGCAGCATCCACG
axmix	AGCTTGGCACGAGCATCTCT	TGGTCATTGAGCAGATGGAAGA	GCGCTACCCTTTTTTCATGCACCCATATT
axsox17	TGGATACGACGCTCCACAGA	CTCCCTGTAGTGGCCGATGT	CATGAGCAGCAGTTCCAGCAGGACAAC
axblimp1	CGATGGTGACTCCGAAACAGA	GGCACTTTTGTGGTGAAGCA	AACCCAAAGCAACAGCACACTGAAAAGG
axcarm1	CGAAGCGGCGCTCATC	ACGGGACACCGAACACTTAAA	CTCTCTACAGCCACGAAGATGTGTGCGT
axdazl	CAGTTTCGTAGAAGTAAAGCTGTGTTC	ATAATCTACTTCTTGGAAGGCTTTGG	AACTGTGCCAAACTGAAGTCTGTGGTAAA
axvasa	GATCGAATGCTTGATATGGGTTT	TGTTTGCCGTTCTTCTTTGGT	AAGACGTTAGTCACCAGTCCAGGAATGCC
axmbd3	GGGCAAACCGGACTTGAATA	TGACTGGCTGTTTGAAGATGGA	TGCACTCCCCGTCAGACAAACTGC
ax-α-actin	GGTCATCCAGGCTGTGTTGTC	CATCACCAGAGTCCAAGACGATAC	CTACGCTTCCGGCCGCACCA
axodc	ATGCCCGTCATGAGTAGTACCA	CCCGGACCCAGGTTACG	TGACAGTTCCAAGGTTTCATTCAATTGCTG
axncam	TGAATGTCGTTCAACGTGAGAGA	AAGAAAAGACTCTGGATGGACGTATC	AGACCCTGGCGTGACTGCTCACCA
axck	AACCACCAAGAGGAATTGCAA	GGAGCCGCGTCCATCTC	CGTTTCATCCAGTGCTGCCGGC

Table 2.9 qRT-PCR primer and probe sequences.
Sequence is given 5' to 3'.

2.7 Handling and manipulating protein

2.7.1 SDS-Polyacrylamide gel electrophoresis (SDS-PAGE)

Proteins were separated by SDS-PAGE. Resolving gels (typically 10-15%) were poured between two glass plates, which had previously been cleaned using 100% ethanol. The resolving gel was overlaid with isopropanol to aid polymerisation and the formation of a level surface. Once the resolving gel had set, the isopropanol was removed and the stacking gel was poured on the top. A gel comb was inserted to form loading wells in the stacking gel.

Gels were immersed in electrophoresis buffer in the electrophoresis tank prior to loading. Protein samples were mixed with 2 x SDS-loading buffer in a 1:1 ratio and boiled for 5 min. They were then quenched on ice and carefully loaded into the wells of the gel. Protein Rainbow ladder (GE Healthcare) was used for size estimation. Electrophoresis was performed at 120 V for approximately 90 min.

2.8 Detection of tagged proteins by Western blot and ECL

Following SDS-PAGE electrophoresis the gel was removed carefully from the glass plates and placed in transfer buffer. A piece of Immun-Blot® PVDF membrane (Biorad) was cut to the size of the gel, equilibrated in methanol for a few seconds and then incubated in transfer buffer for at least 5 min. Pieces of 3 mm Whatmann paper were cut to a size slightly larger than the membrane and also incubated

in transfer buffer. A stack was then assembled on a semi-dry blotter (Ancos). First three pieces of 3 mm paper were placed on the blotter, followed by the PVDF membrane, the gel, and finally three more pieces of 3 mm paper. Care was taken to remove air bubbles from the stack. The lid of the blotter was carefully placed on top of the stack and transfer was then carried out for 40 min at 20 V.

Following transfer, the membrane was washed in PBST 2 times for 5 min each, and then incubated in PBST plus 2% non-fat dried milk for 120 min at room temperature or overnight at 4°C. For hemagluttanin (HA)-antibody detection the primary antibody (Anti-HA High affinity Rat monoclonal (Roche)) was diluted 1:3000 in PBST. Incubation with the primary antibody was carried out for 90 min at room temperature on a rocking platform. The primary antibody was removed and saved for re-use at 4°C. The membrane was then washed twice in PBST for 5 min each to remove excess primary antibody. Incubation with the secondary antibody (Goat anti-Rat IgG peroxidise conjugate (Calibiochem)), which was diluted 1:5000 in PBST, was carried out subsequently for 90 min at room temperature on a rocking platform. After this incubation the membrane was again washed twice in PBST for 5 min each to remove excess antibody. Antibody detection was carried out using ECL plus (GE Healthcare) and Amersham Hyperfilm™ ECL (GE Healthcare) according to manufacturer's guidelines. The film was developed automatically using an SRX-201 Xograph.

MAPK detection was carried out by the same method using the primary antibody ERK2 (C-14; Santa Cruz Biotechnologies) at a 1:3000 dilution and the secondary antibody polyclonal swine anti-rabbit IgG peroxidase conjugate (Dako Cytomation) at 1:5000 dilution.

Chapter 3 Development of the axolotl as a model organism

3.1 Amphibians as model organisms

Amphibians are often described as organisms that have a dual existence on land and water. However this is not true of all amphibians. More accurately, amphibians can be defined as organisms that develop from a mesolethical (moderately yolky) egg that undergoes holoblastic cleavage (cleavage furrows completely bisect the egg) [Callery 2006]. There are three living orders of amphibians, the anurans, urodeles and caecilians. Anurans are tailless amphibians such as the frog *Xenopus laevis*. Urodeles have a tail and two sets of limbs, for example axolotls. Caecilians are limbless amphibians with a snake-like form.

The qualities looked for in a model organism are wide-ranging hence, no model organism will fulfil all the requirements [Krebs 1975; The Krogh Principle]. They have generally been selected because of their convenience to researchers. Features that are often considered important include rapid development, short generation time, developmental homogeneity and ease of handling. Amphibians are good model organisms for studying embryology because they have large externally developing embryos and rapid development. The large cells in the embryos can be easily manipulated in transplantation experiments. Historically axolotls and other species of salamander were the amphibian model of choice because they could be induced to

lay eggs when the temperature of the tank water was reduced [Nieuwkoop 2006]. This meant that embryos could be obtained for experiments all year round, whereas embryos could only be obtained from other model amphibians during their mating seasons. Subsequently, however, it was discovered that the frog *Xenopus laevis* could be induced to ovulate by injecting urine from pregnant women due to the presence of chorionic gonadotrophin hormone [Nieuwkoop 2006]. The use of *Xenopus laevis* was adopted as a standard method for pregnancy testing in the 1950s. This meant that *Xenopus laevis* was widely available and chorionic gonadotrophin hormone could be used to induce the production of embryos at any time of year, making *Xenopus* the amphibian model of choice [Nieuwkoop 2006].

Both salamanders and frogs initially fell out of favour in the early days of developmental genetics because of their long generation times (1-2 years) [Gilbert 2000a]. However the advent of techniques such as *in situ* hybridisation, antisense oligonucleotides and dominant negative proteins has since allowed the study of developmental genetics in these organisms. The difficulty with using *Xenopus laevis* in genetic studies is that it has four copies of each chromosome [Gilbert 2000a]. An alternative to *Xenopus laevis* is *Xenopus tropicalis,* which has a faster generation time (6 months) and is diploid, making genetic studies easier. However, it is now becoming evident that *tropicalis* also has multiple copies of some genes that are present only as a single copy in mammals [e.g. Mix genes; D'Souza *et al.* 2003]. Contrastingly,

evidence is now beginning to suggest that gene copy number in axolotls is similar to that in amniotes [Swiers 2008; Smith *et al.* 2009], with 86% of genes between humans and axolotls predicted to be 1:1 orthologs [Smith *et al.* 2009]. Additionally, many of the morphological processes in axolotl development are more similar to those in amniotes than are the processes in *Xenopus* [Shook and Keller 2008a; **Figure 3.1**], suggesting that axolotl may be a good model organism for understanding the evolution of developmental mechanisms in amniotes.

3.2 Axolotl gastrulation

Gastrulation describes the process through which the tissues of the blastula embryo are rearranged to form the three primary germ layers: ectoderm, mesoderm and endoderm. It is a complex process requiring highly coordinated cell and tissue movements. The cells that will form the mesoderm and endoderm are brought inside the embryo whilst the cells that will form the ectoderm spread over the outside surface resulting in the formation of a multilayered organism. The process of gastrulation varies widely amongst different organisms but generally involves four kinds of cell movement; invagination – the bending inwards of cells, involution – the rolling inward movement of an expanding outer layer so that it spreads over the internal surface of the remaining external cells, ingression – the migration of individual cells from the surface layer after detachment from an epithelium into the interior of the embryo, delamination – separation into layers and epiboly

– the movement of epithelial sheets (usually of ectodermal cells) that spread to enclose the deeper layers of the embryo. - [Gilbert 2000b].

During urodele gastrulation a multi-layered epiblast progressively becomes a pseudo-stratified (single-layered) epiblast [Shook *et al.* 2002; Figure 3.1A]. A large proportion of the presumptive mesoderm in urodeles must move from the superficial cell layer into the deep layer. The mesodermal epithelium first involutes through the blastopore to line the wall of the gastrocoel, later known as the archenteron, and is then internalised to become part of the middle layer [Shook *et al.* 2002]. The mechanism through which the mesodermal epithelium is internalised into the deep layer is termed subduction. The urodele blastopore is regarded as “dorsally restricted” or “closed” as involution takes place solely at the dorsal blastopore lip and ingression *via* subduction occurs laterally and ventrally [Shook *et al.* 2002; **Figure3.1Ai and ii**].

The gastrulation mechanisms in urodeles are similar to those in amniotes [Shook *et al.* 2002; Shook and Keller 2008a; **Figure 3.1B**]. The subduction process closely resembles the ingression of the presumptive mesoderm through the primitive streak during chick and mouse development [Shook *et al.* 2002; **Figure 3.1B**]. Thus, the lateral and ventral urodele blastopore lips are considered to be bilateral equivalents of the primitive streak in amniotes [Shook *et al.* 2002]. It has been suggested that the urodele blastopore may represent an intermediate in the evolution of the amniote primitive streak and that

amniotes may have arisen from a urodele-like anamniote ancestor [Shook and Keller 2008a]. Therefore, the study of early developmental processes in urodeles may be insightful in understanding the evolution of mechanisms in amniotes. Notably, anurans do not share these similarities with amniotes [Discussed in Shook and Keller 2008a].

Figure 3.1 Urodele gastrulation
A) Gastrulation movements in urodeles [Taken from Shook and Keller 2008a]. Urodeles begin gastrulation with most of the presumptive mesoderm in the superficial layer (i). Most of the mesoderm ingresses during gastrulation (ii and iii; bottle shaped cells), just after involution (ii, arrow) through the dorsally restricted blastopore (iii). The presumptive notochord remains superficial until the end of neurulation (ii and iii). Dorsal is to the right in i and ii and up in iii. Anterior is up in ii. **B)** A comparison of gastrulation movements in urodele amphibians vs birds and mammals [Taken from Shook and Keller 2008b]. In urodeles ingression occurs through a bilateral primitive streak running around the lateral, and in some cases, ventral sides of the blastopore (dark band). Cells move towards the primitive streak and ingress (dashed arrows in upper box) adjacent to the endoderm, at the base of the blastoporal cleft. In birds or mammals ingression occurs through a single primitive streak running down the centre of the posterior side of the embryo (dark line). Cells move towards the primitive streak and ingress through its centre (dashed arrows in lower box). **LV = Lateral ventral mesoderm; Sub-BP = Sub-blastoporal**

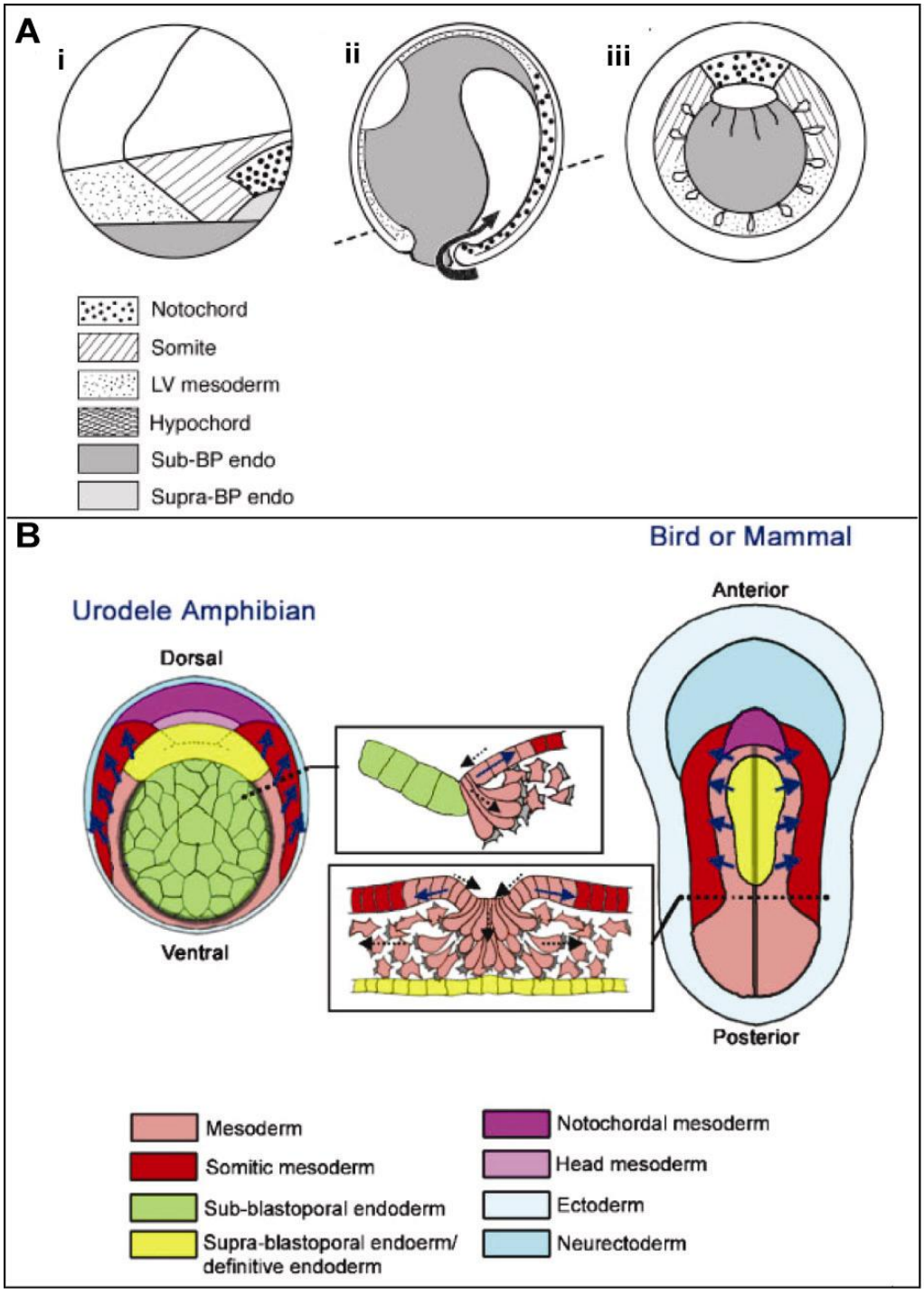
A
i
ii
iii
Notochord
Somite
LV mesoderm
Hypochord
Sub-BP endo
Supra-BP endo
B
Bird or Mammal
Urodele Amphibian
Dorsal
Ventral
Anterior
Posterior
Mesoderm
Somitic mesoderm
Sub-blastoporal endoderm
Supra-blastoporal endoerm/ definitive endoderm
Notochordal mesoderm
Head mesoderm
Ectoderm
Neurectoderm

3.3 The molecular control of gastrulation in axolotl; Axmix and Axbrachyury.

A complex interplay of molecular signals regulates tissue specification during gastrulation. Nieuwkoop discovered that signals emanating from the vegetal hemisphere of amphibian embryos could induce the overlying tissue to become mesoderm [Nieuwkoop 1969; **Section 1.6**]. Mesoderm in vertebrates is induced and subsequently patterned by morphogen gradients; the morphogen originates from a defined point and acts in a concentration-dependent fashion to instruct gene regulation and, hence, cell fate [Ashe and Briscoe 2006]. The ectoderm differentiates into two tissue types, epidermis and neural tissue, in response to mesodermal patterning signals [Reviewed in Stern 2006]. Spemann and Mangold (1923) first demonstrated the ability of dorsal mesoderm to induce neural tissue in the overlying ectoderm [Hemmati-Brivanlou and Melton 1997; Spemann and Mangold 2001]. Understanding of the molecular signals governing gastrulation and early tissue specification during axolotl development is in its infancy. Recent investigations have examined the roles of Axmix and Axbrachyury.

In all organisms examined so far homologues of Mix have been shown to have roles in mesoderm and endoderm specification [Henry and Melton 1998; Lemaire *et al.* 1998; Latinkic and Smith 1999; Hart *et al.* 2002; Kofron *et al.* 2004; Izumi *et al.* 2007]. The expression pattern of *axmix* is consistent with a role in mesoderm and endoderm specification [Swiers 2008]. *Axmix* is expressed from stage 9 until stage 25 (**Figure 3.2A**). Expression is detected in the presumptive endoderm and in the

marginal zone with stronger dorsal than ventral expression, and persists in the deep endoderm until early neurula (**Figure 3.2B**). This expression pattern is similar to the combined expression pattern of the seven *Xenopus mix* homologues [Ecochard *et al.* 1998; Henry and Melton 1998; Lemaire *et al.* 1998; Mead *et al.* 1998; Tada *et al.* 1998; Swiers 2008]. Only genome sequence could provide definitive evidence of gene copy number. However, this data along with Southern blotting and knock-down data (described below) suggests that there is only a single *mix* gene in axolotls. In amniotes, chicken, mouse and human, only a single *mix* gene has been identified [Peale *et al.* 1998; Stein *et al.* 1998; Pearce and Evans 1999; Robb *et al.* 2000; Guo *et al.* 2002], consistent with the suggestion that amniotes may have arisen from a urodele-like ancestor [Shook *et al.* 2002]. Swiers (2008) suggested that multiple copies of *mix* in Zebrafish and *Xenopus* may have arisen after divergence from axolotls in order to facilitate more rapid early development [Swiers 2008]. *Axmix* expression persists for longer than the *Xenopus* homologues, similarly to murine *mix*. The author suggests two explanations for this. The first is that *Xenopus* may express '*mix*' for a shorter more intense period of time than the slower developing axolotl, which may require extended expression for the same patterning events. Alternatively, it has recently been suggested that the late expression of murine *mix* is attributable to a role in blood specification [Willey *et al.* 2006]. In support of this, a region of cells co-expressing *axmix* and blood/ endothelial marker *axflk-1* was identified at stage 12 (late-gastrula) [Swiers 2008].

Preliminary functional data supports a role for Axmix in endoderm and mesoderm specification. Similarly to *Xenopus* homologues, Axmix overexpression in *Xenopus* animal cap explant experiments induces expression of mesodermal and endodermal genes [Swiers 2008]. The response was most similar to that induced by overexpression of *Xenopus* Mixer. In knock-down experiments gastrulation was severely disrupted and *axbrachyury* expression was reduced suggesting that there was a disruption to mesodermal induction [Swiers 2008]. However, examination of a greater array of marker genes is required to fully define the morphant phenotype. The Axmix morphant phenotype was notably far more severe than any one of the reported single *Xenopus* mix gene knock-downs [Henry and Melton 1998; Lemaire *et al.* 1998; Latinkic and Smith 1999; Kofron *et al.* 2004], further supporting the suggestion that there is a single mix gene in axolotl. The knock-down phenotype is most similar to the *Xenopus laevis* mixer knock-down [Kofron *et al.* 2004] and is inconsistent with the mouse knock-down phenotype [Hart *et al.* 2002] where the region of *brachyury* expression is expanded [Swiers 2008].

Brachyury is a T-box transcription factor that has been shown to have a role in posterior mesoderm and notochord differentiation in mouse, zebrafish and *Xenopus* [Herrmann 1991; Smith *et al.* 1991; Schulte-Merker *et al.* 1994; Conlon *et al.* 1996]. *Axbrachyury* is expressed from stage 10.5 (mid-gastrula) through to stage 40, with peak expression at

stage 12 (late-gastrula) (**Figure 3.2A**; This differs slightly from previously published data [Johnson *et al.* 2003b] which suggests a slightly earlier onset of expression; stage 10). Consistent with expression in other vertebrates, *axbrachyury* is expressed in nascent mesoderm (**Figure 3.2B**) and subsequently in the notochord [Herrmann 1991; Smith *et al.* 1991; Johnson *et al.* 2003b; Swiers 2008]. In *Xenopus* '*mix*' and *brachyury* are first co-expressed in the dorsal mesoderm and '*mix*' expression is progressively excluded from the dorsal mesoderm [Lemaire *et al.* 1998]. This is thought to be the result of a negative regulatory loop between the two genes. *Axbrachyury* and *axmix* are not co-expressed in the dorsal mesoderm (**Figure 3.2B**). However, Swiers (2008) suggests that there may still be a negative regulatory loop between Axbrachyury and Axmix to maintain the mutually exclusive expression. It is notable that *axbrachyury* is not expressed early in the dorsal mesoderm as in other vertebrates [Herrmann 1991; Smith *et al.* 1991; Schulte-Merker *et al.* 1994; Swiers 2008]. However, the predominant role of Brachyury orthologues has been shown to be in posterior mesoderm and notochord formation [Herrmann 1991; Halpern *et al.* 1993; Technau 2001]. Swiers (2008) suggests that although other vertebrate orthologues are expressed in the dorsal mesoderm that this expression may not be required for the formation of dorsal mesodermal structures. Thus, the function of Axbrachyury in posterior mesoderm and notochord formation may be conserved. Functional assays are required to further investigate the role of Axbrachyury.

Figure 3.2 Temporal and spatial expression of *axmix* and *axbrachyury*
A) Temporal expression of *axbrachyury* (top) and *axmix* (bottom) determined by real-time PCR. Primary data was analysed using the $2^{-\Delta\Delta C}T$ method [Livak and Schmittgen 2001] and was calibrated to expression level at stage 12 (late-gastrula). The graphs on the left show expression from the 2-cell stage to late-tailbud (stage 40). The graphs on the right show expression through gastrulation (stage 10.5-12) and-early neurulation (stage 13-15) at high resolution. Developmental stages exhibiting background levels of expression are labelled with an asterisk (*****) . (Data obtained by author). **B)** Spatial expression of axbrachyury and axmix as determined by *in situ* hybridisation on hemisectioned embryos (note one half of each embryo was hybridised to *axbrachyury* and the other to *axmix* to determine regions of overlap.) [Taken from Swiers 2008]. Axmix expression was first detected in the blastoporal dorsal mesoderm (i and ii; red arrows) at stage 10 (early-gastrula). Expression was maintained in the dorsal mesoderm and in dorsal cells that had not yet gastrulated (iii and v; green arrows) at stage 10.5 (mid-gastrula). At stage 10.75 (late-gastrula) expression was restricted to the anterior dorsal mesoderm (vi and vii; pink arrows) and expression was also detected in the presumptive ventral mesoderm and endoderm (vi; green arrow). Expression was maintained in the endodermal yolk plug and ventral mesoderm (ix; green arrow) and was no longer expressed in the dorsal mesoderm (ix and xi; pink arrows) at stage 12 (late-gastrula). Expression was maintained in the posterior ventral mesoderm at stage 14 (xii; pink arrow). Axbrachyury expression was first detected in the posterior dorsal mesoderm (vii and viii; pink arrows) and presumptive ventral mesoderm (vii and viii; green arrows) at stage 10.75 (late-gastrula). Expression persisted in the dorsal (x; pink arrow) and ventral posterior mesoderm (x; green arrow) at stage 12 (late-gastrula) and was additionally detected in aring around the blastopore (xi). Expression was restricted to the dorsal mesoderm (xiii; pink arrow) at stage 14. The last panel in each row shows the two halves of each embryo put together with vegetal facing up so that the two expression patterns can be compared.

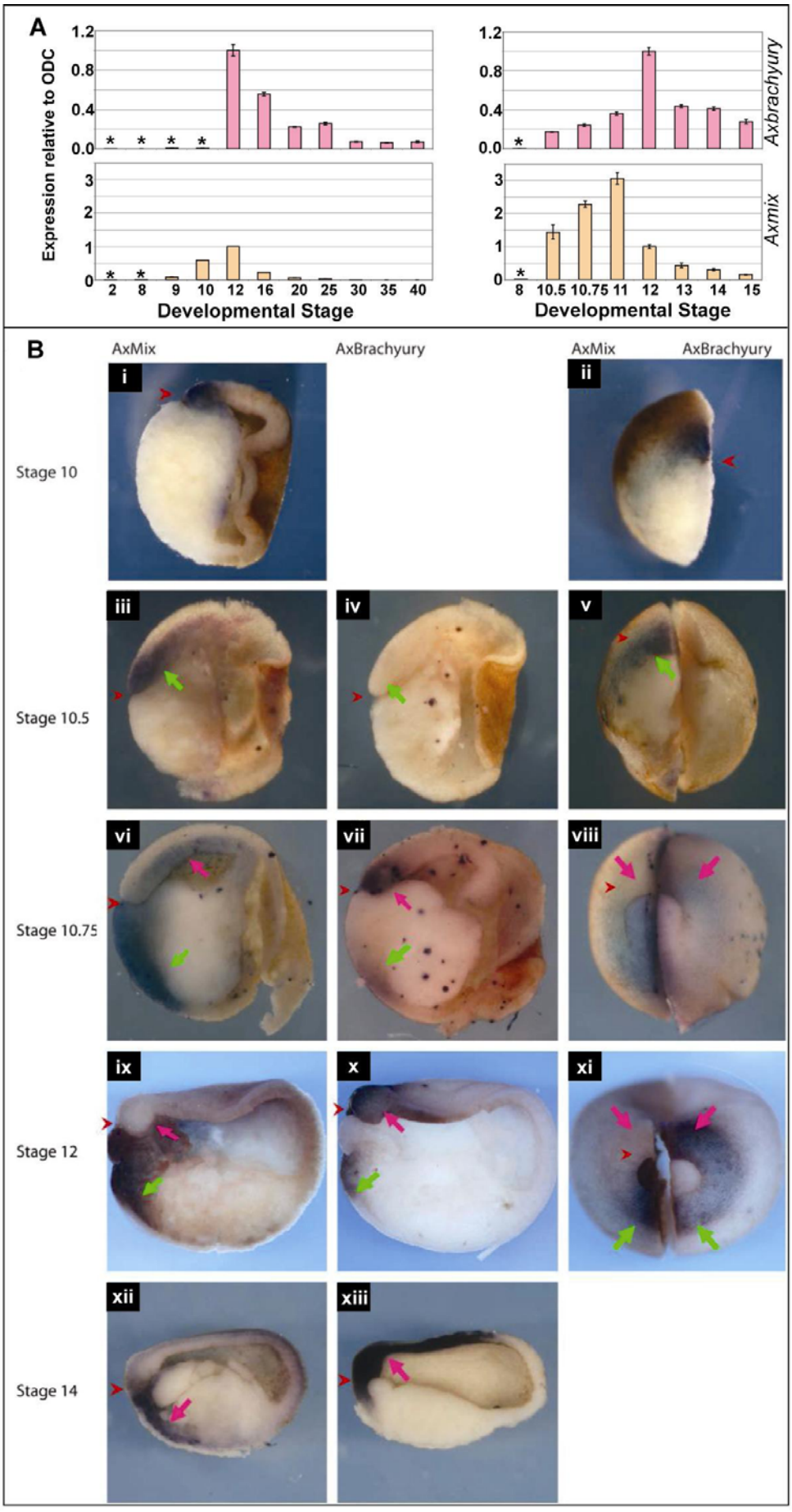
A
Expression relative to ODC
1.2
0.8
0.4
0.0
3
2
1
0
2 8 9 10 12 16 20 25 30 35 40
Developmental Stage
Axbrachyury
Axmix
8 10.5 10.75 11 12 13 14 15
Developmental Stage
B
AxMix
AxBrachyury
AxMix
AxBrachyury
Stage 10
Stage 10.5
Stage 10.75
Stage 12
Stage 14
i
ii
iii
iv
v
vi
vii
viii
ix
x
xi
xii
xiii

3.4 Cloning and characterising genes for the further development of the axolotl as a model organism

In the absence of axolotl genomic sequence it is necessary to clone and characterise genes prior to carrying out any investigations. In this chapter the cloning and characterisation of a pluripotency gene (*axnanog*), ectodermal marker genes (*axck and axncam*), a putative PGC gene (*axblimp1*) and a gene encoding an epigenetic modifier (*axcarm1*) are described.

3.5 Pluripotency genes

3.5.1 Identification of an axolotl *nanog* homologue (*axnanog*)

During amphibian development zygotic transcription does not commence until the mid-blastula transition (MBT; stage 8). Early development is governed entirely by maternally inherited molecules [Newport and Kirschner 1982]. Nieuwkoop's experiments (**Section 1.6**) showed that the animal cap cells of MBT stage axolotl embryos are pluripotent. Based on these observations Johnson *et al.* (2008 unpublished) proposed that pluripotency in axolotls is maternally inherited. In support of this the transfer of pluripotency from axolotl oocytes to primary cells from foetal mice and adult humans was demonstrated [Alberio *et al*. unpublished]. Permeabilised primary cells were transplanted into the germinal vesicles (GVs) of axolotl oocytes. Subsequently, expression of *oct4* and *nanog* was detected in the mammalian cells. Axolotl oocytes were shown previously to express the pluripotency associated transcription factor, *axoct4* [Bachvarova *et al.* 2004; Johnson and McConnell 2004]. However, equivalent oocyte

transplantation experiments carried out with *Xenopus* oocytes, which express the *oct4* homologue, *xlpou60*, also activated *oct4* expression but not *nanog* expression. It was therefore considered that additional molecules must be present in axolotl oocytes that can activate the expression of *nanog*. Subsequently, an axolotl *nanog* homologue, *axnanog*, was cloned from oocytes by degenerate PCR [J. Dixon, unpublished].

Axnanog has two conserved domains (**Figure 3.3**), the divergent homeodomain (underlined in red) and a second region upstream of the homeodomain (underlined in blue). [J. Dixon, unpublished]. *Axnanog* is the first homologue to be identified in an anamniote model organism. Nanog has not been identified in the genomes of frogs (*Xenopus*) or teleost fish (*Danio rerio; Fugu rubripes*).

Axnanog shares only small regions of homology with other homologues. However, intronic sequences have provided further evidence to support the identification of an axolotl *nanog* homologue (**Figure 3.4**). The distance in base pairs from the ATG start site to the first splice junction is identical in human, mouse and axolotl sequences and all identified splice junctions show a high degree of sequence conservation. The ATG start site of chicken nanog is shifted 3 bases upstream in comparison to the other homologues. In protein BLAST searches the closest *Xenopus* molecule is Xvent2, however, alignments of *xvent2*

nucleotide sequence with *axnanog* showed that the first splice junction was in a dissimilar position (not shown).

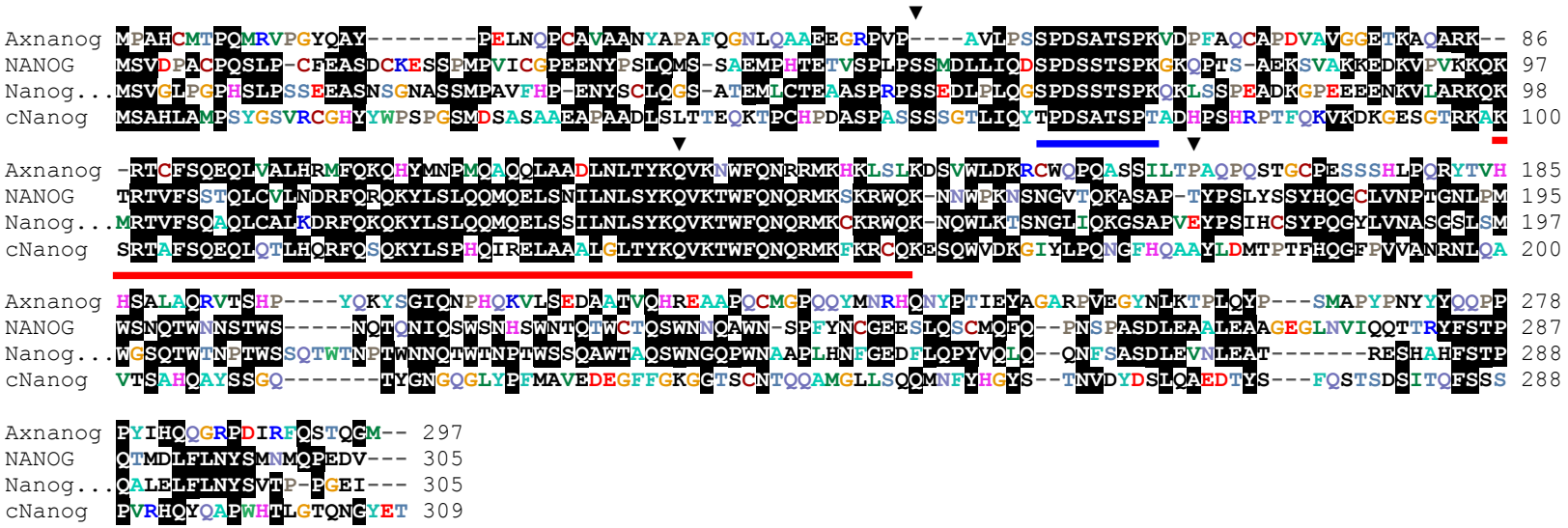

Figure 3.3 An alignment of artificially translated Axnanog and Nanog homologues from other vertebrates.
Axnanog alignment with homologs from Human (NANOG) (NP_079141), mouse (nanog) (NP_082292), and chicken (cNanog) (ABK27429). Conserved amino acids are shaded. Conserved domains are underlined. The homeodomain is underlined in red and another short conserved domain is underlined in blue. Known intron junctions (third junction is predicted) in the Axnanog sequence are indicated by ▼.

Figure 3.4 Alignment of *axnanog* intron boundaries with intron boundaries from other vertebrate *nanog* homologues.
Axnanog sequence has been aligned with homologous sequences from Human (NANOG) (ENST00000229307), mouse (Nanog) (ENSMUST00000012540), and chicken (cNanog) (ENSGALT00000023143**).** Conserved nucleotides are shaded. Exon:Intron and Intron:Exon boundaries are shown for introns 1 and 2 (underlined in blue). *Axnanog* intron 3 sequence has not been obtained. For each boundary 20 bp of exon and 20bp of intron sequence is shown, gaps are indicated by dashes. Exon 1 sequence is shown from the ATG start codon for each sequence in order to show the conservation of the positioning of intron 1.

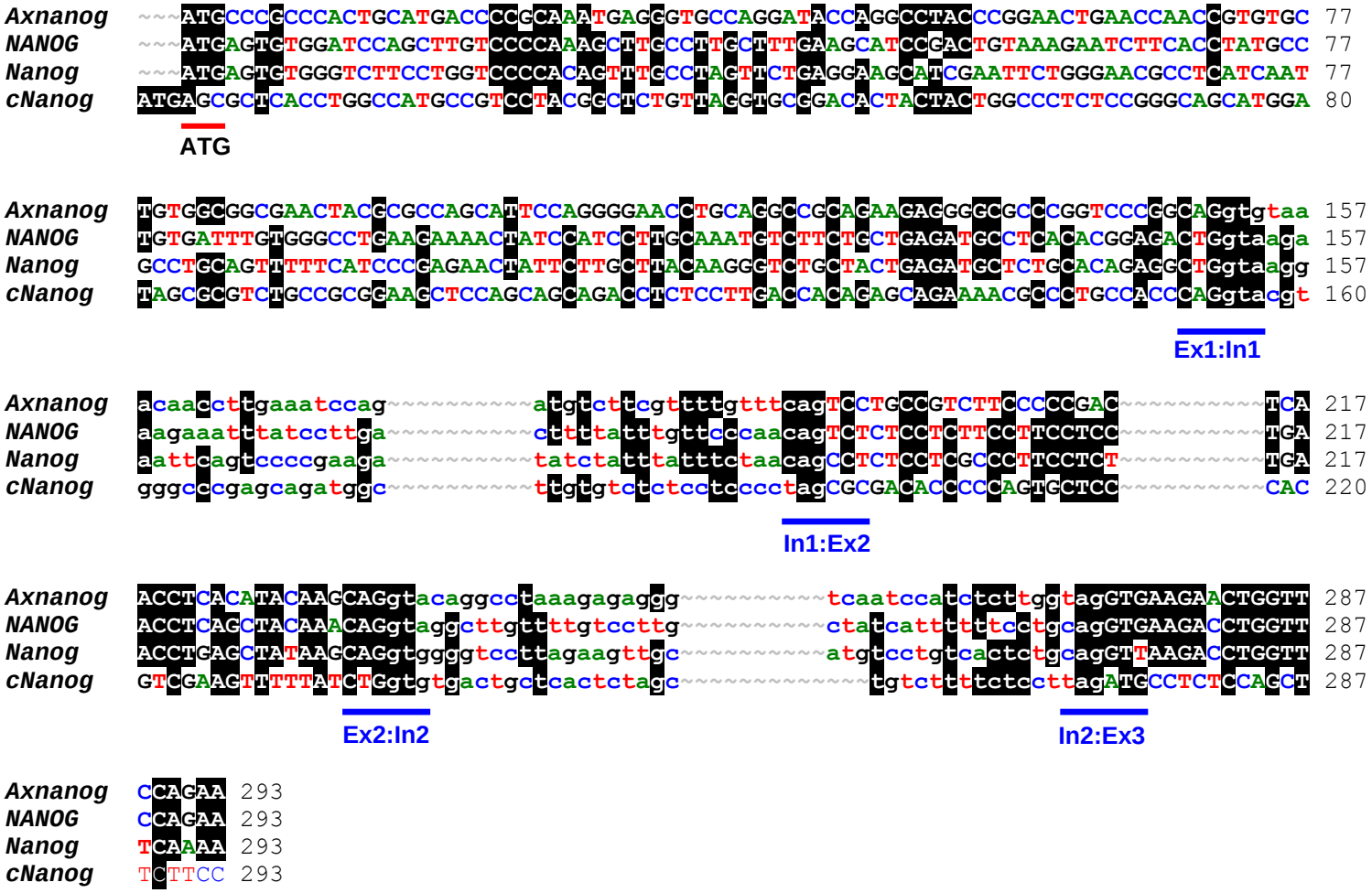
Axnanog
NANOG
Nanog
cNanog
ATG
Ex1:In1
In1:Ex2
Ex2:In2
In2:Ex3

3.5.2 Temporal and spatial co-expression of *axnanog* and *axoct4*

Temporal expression of *axnanog* and *axoct4* was analysed by qRT-PCR from early-cleavage (stage 2) to late-tailbud (stage 40), with special focus on gastrulation to detect any rapid transcriptional changes, coincident with the onset of zygotic transcription (mid-blastula transition, stage 8) [Newport and Kirschner 1982; Figure 3.5A]. *Axoct4* expression was previously reported [Bachvarova *et al.* 2004]. Given the closely intertwined roles of amniote homologues of Oct4 and Nanog [Loh *et al.* 2006; Loh *et al.* 2008] in the maintenance of pluripotency, *axoct4* expression was reanalysed for comparison to *axnanog* on the same cDNA series. The temporal expression of *axoct4* was in agreement with published data. Maternal expression was detected at stage 2 and expression was maintained at an equivalent level following the onset of zygotic transcription (stage 8) until mid-neurula (stage 16). Expression was significantly reduced at stage 16 and undetectable by mid-tailbud (stage 25). Analysis on the focussed cDNA series also revealed a relatively constant level of expression. Similarly to *axoct4*, maternal *axnanog* expression was detected at stage 2 and zygotic expression was maintained from stage 8 until late-gastrula (stage 12). However, contrasting to the relatively constant levels of *axoct4* expression, *axnanog* expression levels changed significantly over time. Low levels of maternal expression were detected at early-cleavage (stage 2) and mid-blastula (stage 8) followed by a rapid increase at late-blastula (stage 9). Expression peaked at early-gastrula (stage 10 to 10.5) followed by a considerable decrease at late-gastrula (stage 12).

Post-gastrulation to late-tailbud (stage 40) only low or background expression was detected. Examination of expression on the focussed cDNA series revealed peak expression at stage 10.5 with expression beginning to decline rapidly from stage 10.75. The temporal expression patterns of *axoct4* and *axnanog* suggested that as in other vertebrates they might function together in the establishment and maintenance of pluripotency. Furthermore, the rapid changes in *axnanog* expression during gastrulation suggest that it may play a key functional role during these developmental stages. Notably, peak *axnanog* expression coincides with the timepoint that axolotl animal caps were previously shown to be most responsive to mesoderm and endoderm inducing signals [Nieuwkoop 1969].

To investigate the spatial co-expression of *axoct4* and *axnanog, in situ* hybridisations were carried out on hemisectioned blastulae and gastrulae using a technique adapted from *Xenopus* for bisecting embryos in order to stain the two halves with two different probes [Lee *et al.* 2001; Figure 3.5D and E]. *Axoct4* expression was equivalent to previously published data of *in situ* hybridisations on sections [Bachvarova *et al.* 2004]. Maternal expression of *axoct4* was detected in the animal hemisphere (presumptive ectoderm) at stage 7 (early-blastula; **Figure 3.5Ei**). In blastula and early gastrula stage embryos zygotic expression was maintained in the presumptive ectoderm (**Figure 3.5 Eii-vii**). At the onset of gastrulation (stage 10) expression was also detected in the presumptive mesoderm extending

vegetally (**Figure 3.5Eiv**). Expression was maintained in the presumptive ectoderm and presumptive mesoderm throughout gastrulation. At stage 10.75 (late-gastula) expression in the presumptive mesoderm extended dorsally to the edge of the blastopore, but expression was not detected in ingressed dorsal mesoderm as reported previously [Bachvarova *et al.* 2004; **Figure 3.5Evi**]. *Axnanog* expression was very similar to *axoct4* (**Figure 3.5D**), differing only in that expression was not detected until stage 8 (mid-blastula; **Figure 3.5Di**), much weaker than that of *axoct4* and was undetectable at stage 12 (late-gastrula; **Figure 3.5Dvi**). In murine development *nanog* and *oct4* expression is downregulated as cells differentiate [Mitsui *et al.* 2003]. The spatial co-expression of *axoct4* and *axnanog* in undifferentiated tissues (the presumptive ectoderm and mesoderm) suggests that they may have conserved roles, functioning together to maintain pluripotency/ multipotency, as suggested in mouse [Loh *et al.* 2006; Loh *et al.* 2008].

Figure 3.5 Temporal and spatial expression of *axnanog* and *axoct4*
A) Temporal expression of *axnanog* (top) and *axoct4* (bottom) determined by real-time PCR. Primary data was analysed using the $2^{-\Delta\Delta C}T$ method [Livak and Schmittgen 2001] and was calibrated to expression level at stage 12 (late-gastrula). The graphs on the left show expression from the 2-cell stage to late-tailbud (stage 40). The graphs on the right show expression through gastrulation (stage 10.5-12) and-early neurulation (stage 13-15) at high resolution. Developmental stages exhibiting background levels of expression are labelled with an asterisk (*****). **B)** Fate-maps for stage 10 (early-gastrulation) and stage 12.5 (late-gastrulation) urodele amphibians (taken from Shook *et al.,* 2002). Presumptive ectoderm is highlighted in light blue (epidermis) or dark blue (neural). Presumptive mesoderm is shown as magenta (notochordal), red (somatic) or orange (head, lateral and ventral mesoderm). Endodermal fate is indicated as yellow–green (supra-blastoporal endoderm) or lime green (sub-blastoporal endoderm). The stage 10 fate map shows only the superficial view. In general, the presumptive fates continue radially toward the blastocoel, except that the presumptive head mesoderm continues vegetally under the superficial layer of the supra-blastoporal endoderm. The stage 12.5 fate map shows a sagittal section of an embryo, such that the stippled tissues are at the face of the cut, while the surface of the gastrocoel cavity curves into the page. **C)** Schematic representation of axolotl embryos in various developmental stages as indicated (i –vii) to show how embryos in panels D and E were hemisectioned prior to the *in situ* hybridisations. **D)** Spatial expression of *axnanog* as determined by *in situ* hybridisations on hemisectioned embryos. Weak expression was detected throughout presumptive ectoderm at stage 8 (early-blastula; i) and persisted in the presumptive ectoderm at stage 9 (late-blastula; ii) and stage 10 (early gastrula; iii). In addition *axnanog* expression was detected in the presumptive mesoderm extending vegetally at stage 10 (early-gastrula; iii). This pattern of expression persisted in stage 10.5 (iv) and 10.75 embryos (mid-gastrula; v).. Expression was no longer detected at stage 12 (late-gastrula; vi). **E)** Spatial expression of *axoct4* as determined by *in situ* hybridisation on hemisectioned embryos. Expression was detected in the presumptive ectoderm at stage 7 (64 cells; i) as well as stages 8 (ii), 9 and 10 (iii)). Expression was also evident in the presumptive mesoderm at stage 10 (early-gastrula; iv) and this pattern of expression persisted in stages 10.5 (v), 10.75 (vi) and 12 (late-gastrula; vii). **A = Anterior; P = Posterior; V = Ventral; D = Dorsal; black triangles indicate the dorsal lip.**

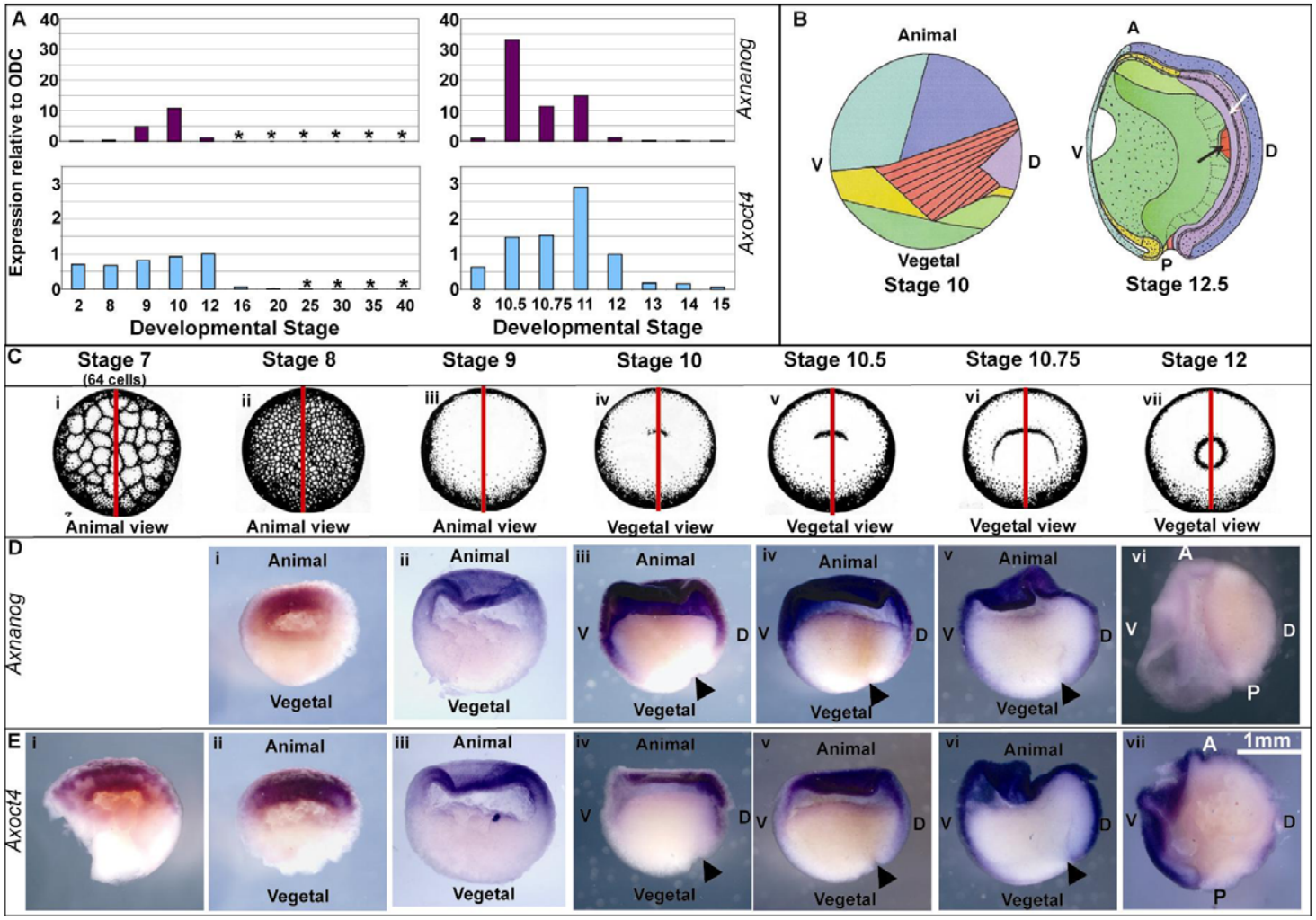
A
Expression relative to ODC
Axnanog
Axoct4
Developmental Stage
Developmental Stage
B
Animal
Vegetal
Stage 10
Stage 12.5
C
Stage 7
(64 cells)
Stage 8
Stage 9
Stage 10
Stage 10.5
Stage 10.75
Stage 12
Animal view
Vegetal view
D
Axnanog
Animal
Vegetal
E
Axoct4
1mm

3.6 Ectodermal genes

In order to study the formation of ectodermal tissues in my investigations it was first necessary to clone molecular markers of both epidermis and neural tissue. Neural cell adhesion molecule (Ncam) was selected as a marker of neural tissue, and cytoskeletal keratin (CK) was selected as a marker of epidermis.

3.6.1 Formation of neural and epidermal tissue

Ectoderm gives rise to two main derivatives during embryogenesis; the surface ectoderm (or epidermis) and the nervous tissue. Neural induction converts a portion of the dorsal ectoderm into neural ectoderm in response to signals from the underlying mesoderm [Bouwmeester 2001; Spemann and Mangold 2001 translated from original paper 1923]. The neural ectoderm gives rise to all derivatives of the central and peripheral nervous system. During neurulation the neural-ectoderm first forms the neural plate which will then fold and fuse to form the neural tube [Moury and Jacobson 1989; Schoenwolf and Smith 1990; Jacobson and Moury 1995; Schoenwolf and Smith 2000; Colas and Schoenwolf 2001]. The neural tube separates from the surface ectoderm and gives rise to the central nervous system. Neural crest cells develop from the crest of the neural tube [Moury and Jacobson 1990]; these cells generate all of the cells of the peripheral nervous system. The ectodermal cells surrounding the embryo at the end of neurulation form the presumptive epidermis [Colas and Schoenwolf 2001].

3.6.2 Neural Cell Adhesion Molecule (Ncam)

Neural Cell Adhesion Molecule (Ncam) is a member of the immunoglobulin superfamily [Hemperly *et al.* 1986; Barthels *et al.* 1987]. Amongst the cell adhesion molecules, members of the immunoglobulin superfamily are the most diverse in structure, expression and function [Brummendorf and Rathjen 1994, 1995]. Ncam is characteristic of the immunoglobulin superfamily as multiple isoforms are generated by alternative splicing of pre-mRNA; at least 20-30 distinct forms are generated by alternative splicing and post-translational modifications from a single copy gene of human Ncam [Goridis and Brunet 1992]. Murine Ncam has three main isoforms named Ncam-180, Ncam-140, and Ncam-120 in reference to their molecular weight [Barthels *et al.* 1987]. Ncam-180 and Ncam-140 differ only in their cytoplasmic domain [Barthels *et al.* 1988], whereas Ncam-120 lacks the transmembrane domain and cytoplasmic domain [Barthels *et al.* 1988; Edelman and Crossin 1991]. Binding of Ncam-120 to the cell-surface membrane is mediated *via* glycosylphosphatidylinositol (GPI) [Barthels *et al.* 1988; Edelman and Crossin 1991]. These three isoforms are developmentally regulated and differentially expressed [Barthels *et al.* 1988]. In addition to alternative splicing, Ncam structure and function can also be regulated by the addition or removal of polysialic acid [Bonfanti 2006].

Ncam expression in vertebrate embryos is induced in the neural-ectoderm during early neurulation and continues in the

neuroepithelium, neural plate and neural tube of later embryos [Boucaut *et al.* 1985; Jacobson and Rutishauser 1986; Kintner and Melton 1987; Levi *et al.* 1987; Saint-Jeannet *et al.* 1989b; Ballycuif *et al.* 1993; Mizuno *et al.* 2001]. In adult *Xenopus* and mouse, Ncam expression is predominantly detected in neural tissues [Levi *et al.* 1987; Cremer *et al.* 1994].

3.6.3 Cytoskeletal keratin

Cytoskeletal keratins (*CKs*) are the largest group of genes from the intermediate filament multigene family [Magin *et al.* 2007]. The *CK* genes are expressed in epithelial cells in spatially and temporally specific patterns during development, and are highly abundant in epidermal tissue [Miyatani *et al.* 1986; Jamrich *et al.* 1987; Watanabe *et al.* 2001; Magin *et al.* 2007]. Keratins can be subdivided into two groups, type I (acidic) and type II (basic) keratins. Heterodimers of type I and II keratins form a dynamic network of 10-12nm filaments in the cytoplasm of cells [Magin *et al.* 2007].

It is widely accepted that keratins function to provide protection from mechanical stresses to cells [Gu and Coulombe 2007]. However, it is now known that the function of keratins within cells is much more diverse and complex. Additional roles include cell-size determination, translation control, proliferation, organelle transport, and responses to stress [Gu and Coulombe 2007; Magin *et al.* 2007].

CK molecules in *Xenopus laevis* are among the earliest tissue specific markers to be expressed [Jamrich *et al.* 1987]. A group of type I cytokeratins including XK81 are expressed from the mid-blastula transition (stage 9) in the bipotential ectoderm which gives rise to both epidermis and neural tissues [Jamrich *et al.* 1987]. During neurulation these CKs become progressively restricted to epidermal tissues and are excluded from neural tissues [Jamrich *et al.* 1987]. *CK* genes in *Xenopus laevis* are expressed in a stage-specific manner, with different keratins expressed in oocytes, embryos and larva [Jonas *et al.* 1985; Winkles *et al.* 1985; Franz and Franke 1986; Miyatani *et al.* 1986]. The same is not true of murine *CK*s, murine CKs found in embryonic or foetal tissues are also synthesised in several tissues of the adult.

3.6.4 Identification of *axncam*

A 900 bp fragment of *axncam* was cloned by degenerate PCR (**Methods 2.3.4**) from stage 25 (early-tailbud) cDNA. Further 5' and 3' coding sequence was obtained by semi-degenerate PCR from the same cDNA. BLAST searches confirmed the identity of the sequence obtained. The most robust alignments were obtained with *Cynops pyrrhogaster ncam* (D85084.1). *Cynops pyrrhogaster ncam* has two splice forms. The sequence obtained for *axncam* most closely resembled the short *Cynops* splice form, Ncam-140 (91% sequence identity; **Figure 3.6**).

In the cloning of *axncam*, a splice form containing a VASE element [Small *et al.* 1987; Santoni *et al.* 1989; Mizuno *et al.* 2001] was also identified (**Figure 3.6**).

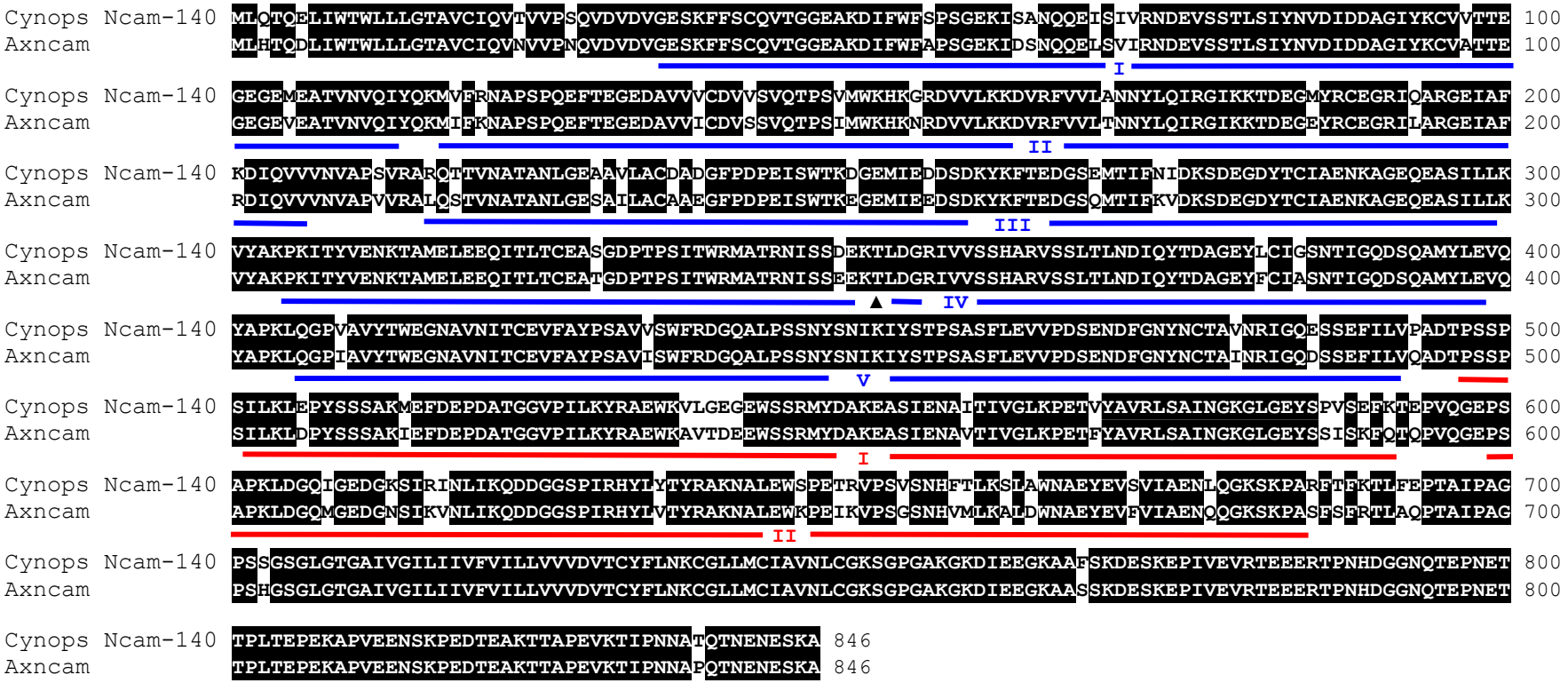

Figure 3.6 Alignment of *axncam* with *Cynops pyrrhogaster ncam-140*
Shading shows identical residues. Immunoglobulin (Ig) – like domains are underlined in blue. Fibronectin III (FN3) – like domains are underlined in red. ▲ indicates the position of an identified VASE element (ASWTRSEKQK) [Mizuno *et al.* 2001]. The overall sequence identity is 91%.

3.6.5 *Axncam* temporal and spatial expression

Axncam temporal expression was analysed by qRT-PCR (**Figure 3.7A**). Expression was first detected at stage 13 (early-neurula) coincident with the specification of neural tissue. Expression continued to increase throughout neurulation, reaching peak expression at mid-tailbud (stage 30). This level of expression was maintained through late-tailbud stages.

Axncam spatial expression was examined on whole-mounts, hemisectioned embryos and sections by *in situ* hybridisation (**Figures 3.7 and 3.8)**. In other vertebrates, including *Pleurodeles waltl,* another urodele amphibian*, ncam* homologues are expressed predominantly in neural tissues but expression is also detected in non-neural tissues [Boucaut *et al.* 1985; Jacobson and Rutishauser 1986; Kintner and Melton 1987; Levi *et al.* 1987; Saint-Jeannet *et al.* 1989a; Ballycuif *et al.* 1993; Cremer *et al.* 1994]. Taking this into account, the careful examination of *axncam* spatial expression was critical in order to ensure that it was a suitable marker of neural tissue. Weak expression was first detected in the neural plate of mid-neurula (stage 16) embryos (**Figure 3.7C**). Notably, expression was not detected in early-neurula (stage 14) embryos (**Figure 3.7B**). Expression persisted in the neural tube of late-neurula (stage 20) embryos (**Figure 3.7D**) and tail-bud (stage 25-38) embryos (**Figure 3.8A-D**). Additionally, expression was detected in the brain, optic vesicles, otic vesicles, and cranial nerves of mid-tailbud (stage 30 and 35) embryos (**Figure 3.8B and C**). Close

examination of expression on sections of a late-tailbud (stage 38; **Figure 3.8D**) embryo showed that *axncam* was expressed throughout all regions of the brain, optic vesicles, otic vesicles, and neural tube. Examination of the sections provided evidence of restricted neural expression. Thus, this data provides robust evidence that *axncam* is a reliable marker of neural tissue.

Figure 3.7 Temporal expression of *axncam* and spatial expression of *axncam* in neurula embryos

A) Temporal expression of *axncam* determined by real-time PCR. Primary data was analysed using the $2^{-\Delta\Delta C}T$ method [Livak and Schmittgen 2001] and was calibrated to expression level at stage 12 (late-gastrula). The graphs on the left show expression from the 2-cell stage to late-tailbud (stage 40). The graphs on the right show expression through gastrulation (stage 10.5-12) and-early neurulation (stage 13-15) at high resolution. Developmental stages exhibiting background levels of expression are labelled with an asterisk (*****). Spatial expression of *axncam* in neurula embryos as determined by *in situ* hybridisations on hemisectioned embryos (B-D). Upper panels B-D i) Schematic representation of axolotl embryos at stages 14-20, to show how embryos in panels ii were hemisectioned prior to the *in situ* hybridisation. **B)** Expression was not detected at stage 14 (early-neurula; ii and iii). The other half of the embryo was stained with an axblimp1 probe to show expression in the presumptive neural folds (bottom half; iii) **C)** Expression was detected in the neural plate (arrows; NP) at stage 16 (mid-neurula; ii and iii). **D)** Expression was detected in the neural tube (arrow; NT) at stage 20 (late-neurula;ii). **A = Anterior; P = Posterior; V = Ventral; D = Dorsal; NF = Neural fold; NP = Neural plate; NT = Neural tube; PA = Pharyngeal arches**

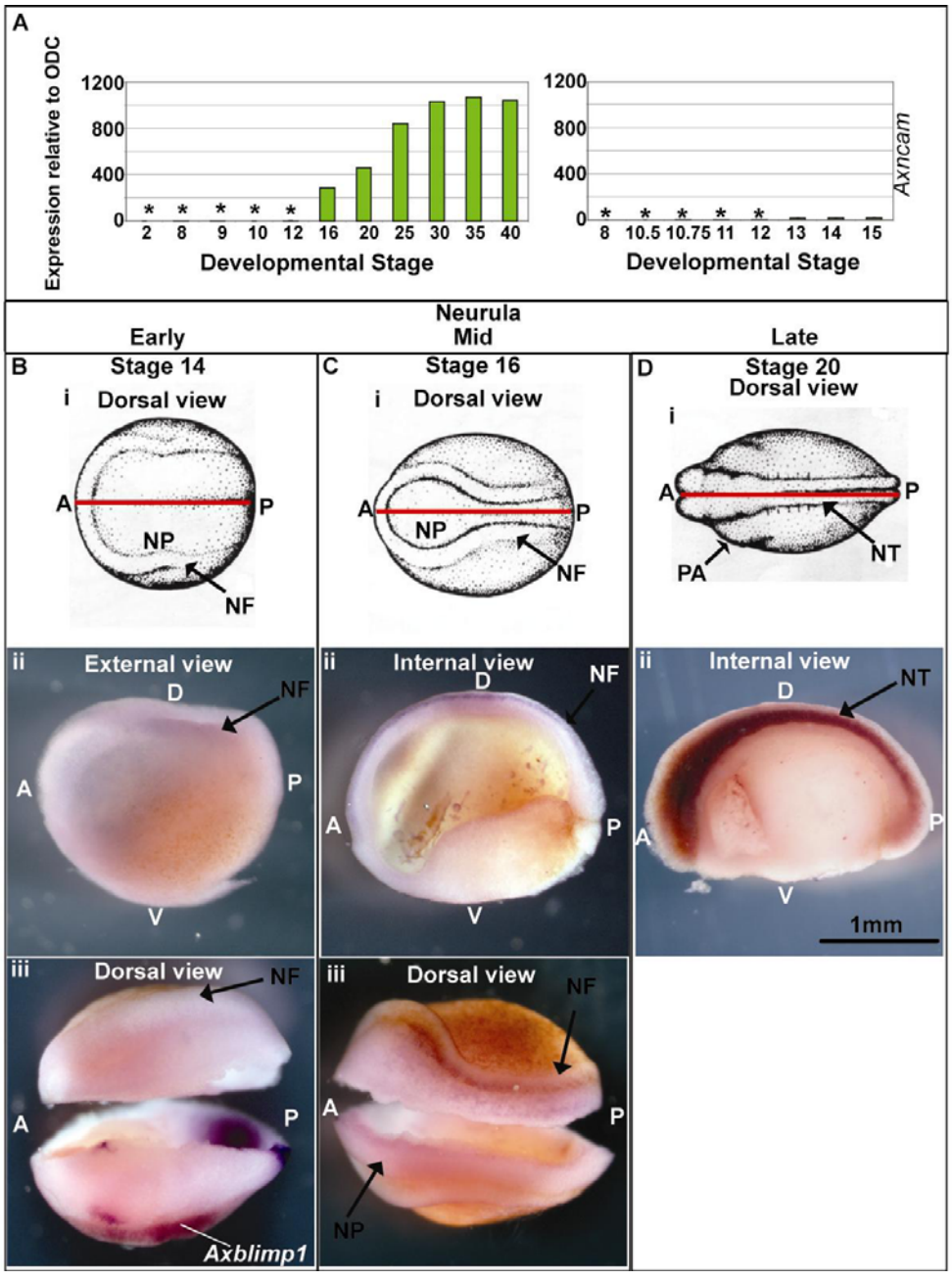
A
Expression relative to ODC
1200
800
400
0
2 8 9 10 12 16 20 25 30 35 40
Developmental Stage
1200
800
400
0
8 10.5 10.75 11 12 13 14 15
Developmental Stage
Axncam
Neurula
Early
Mid
Late
B Stage 14
i Dorsal view
A
P
NP
NF
C Stage 16
i Dorsal view
A
P
NP
NF
D Stage 20
Dorsal view
i
A
P
NT
PA
ii External view
D
NF
A
P
V
ii Internal view
D
NF
A
P
V
ii Internal view
D
NT
A
P
V
1mm
iii Dorsal view
NF
A
P
Axblimp1
iii Dorsal view
NF
A
P
NP

Figure 3.8 Spatial expression of *axncam* in tailbud stage embryos.
Upper panels A-D(i) Schematic representation of axolotl embryos to show how embryos in panel ii were hemisectioned or sectioned prior to the *in situ* hybridisation. **A)** Expression was detected in the neural tube (arrow; NT) at stage 25 (early-tailbud; ii). iii). Schematic of an axolotl embryo showing the neural tube. **B)** Expression was detected in the neural tube (ii;arrow; NT) and in the brain, optic vesicles, otic vesicles and cranial nerves (ii-iii) at stage 30 (mid-tailbud). **C)** Expression was maintained in the neural tube (ii; arrow; NT) and the brain, optic vesicles, otic vesicles and cranial nerves (iii) at stage 35. **D)** Expression was maintained throughout the brain, in the procencephalon (ii), diancephalon (iii), infindibulum (iii), and the rhombencephalon (iv) at stage 38 (late-tailbud). Expression also persisted throughout the optic vesicles (iii, OpV), otic vesicles (iv; OV) and the neural tube (v-vi; NT). **NT = Neural tube; B = brain; OpV = Optic vesicles; OV = Otic vesicles; Pro = Procencephalon; D = Diancephalon; I = Infindibulum; R = rhombencephalon.**

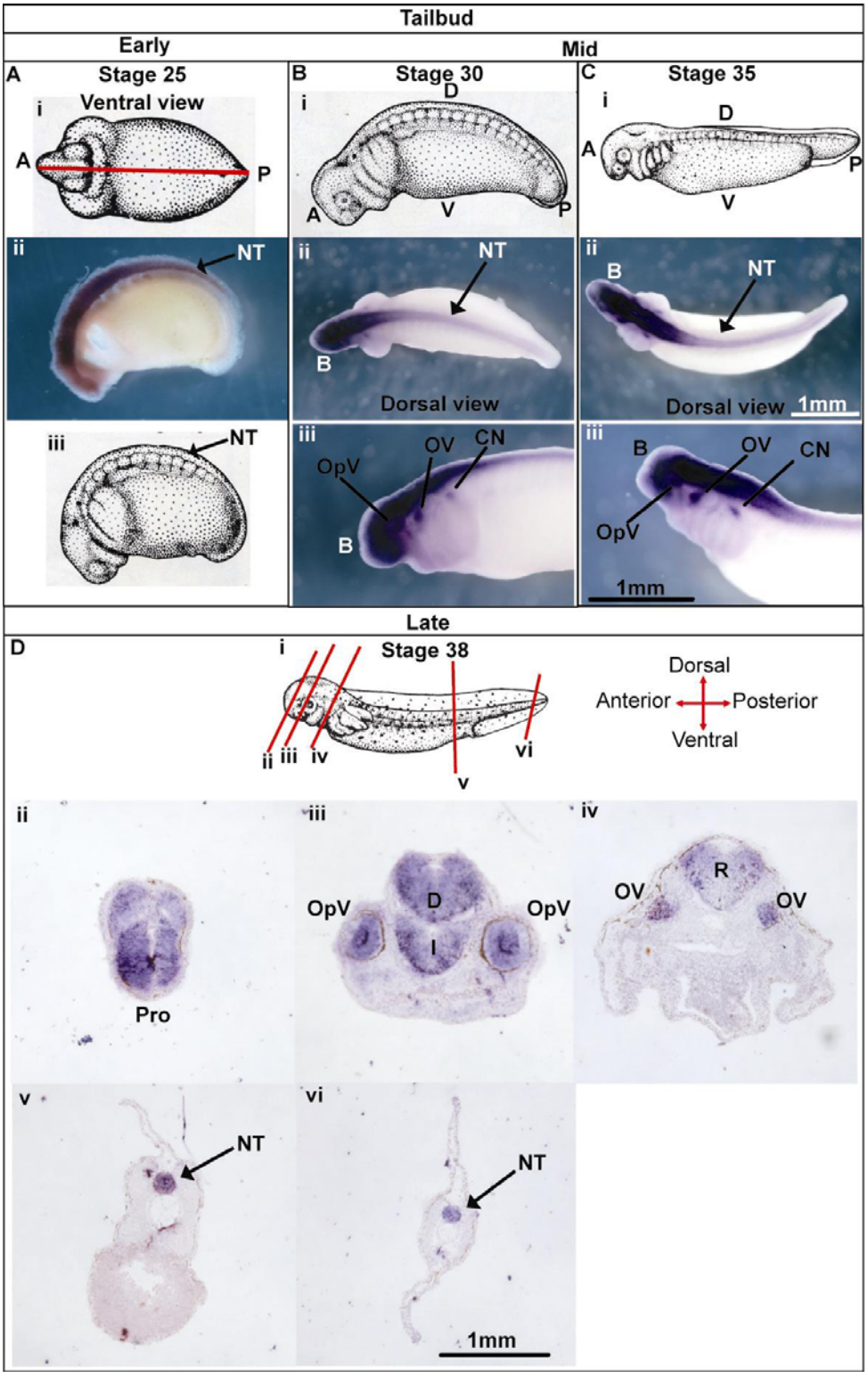
Tailbud
Early
Mid
A
Stage 25
Ventral view
i
A
P
ii
NT
iii
NT
B
Stage 30
i
D
A
V
P
ii
NT
B
Dorsal view
iii
OV
CN
OpV
B
C
Stage 35
i
D
A
P
V
ii
B
NT
Dorsal view
1mm
iii
B
OV
CN
OpV
1mm
Late
D
i
Stage 38
ii iii iv
v
vi
Dorsal
Anterior
Posterior
Ventral
ii
Pro
iii
OpV
D
OpV
I
iv
R
OV
OV
v
NT
vi
NT
1mm

3.6.6 Identification of *axck*

Axolotl cytoskeletal keratin (*axck*) was identified in the *Ambystoma mexicanum* EST database (http://salamander.uky.edu; Mex_NM_000223_Contig_11). Primers were designed to obtain a 1.2 kb fragment of *axck* encoding the majority of the ORF. PCR was carried out on cDNA synthesised from stage 30 (mid-tailbud) embryos. The fragment obtained was then used to synthesise an ISH probe to characterise *axck* expression through embryonic development.

3.6.7 Temporal and spatial expression of *axck*

Axck temporal expression was analysed by qRT-PCR (**Figure 3.9A**). Expression was detected from the onset of zygotic transcription (stage 8). Expression levels continued to rise until early-tailbud (stage 25) and were maintained at this level throughout the tailbud stages.

Spatial expression was examined by *in situ* hybridisation on hemisectioned and sectioned embryos (**Figure 3.9B-H**). Expression was first detected in the presumptive-epidermis of late-gastrula (stage 12) embryos (**Figure 3.9B**). Expression was maintained in the epidermis of neurula (stage 13-20; **Figure 3.9C-E**) and tailbud (stage 25 –36; **Figure3.9F-H**) embryos. Close examination of expression in sections of tailbud (stage 30 and stage 36; **Figure 3.9G and H**) embryos showed that expression was restricted to the epidermis. Thus, *axck* is a robust marker for epidermis.

Figure 3.9 Temporal and spatial expression of *axck*
A) Temporal expression of *axck* determined by real-time PCR. Primary data was analysed using the $2^{-\Delta\Delta C}$T method (Ref) and was calibrated to expression level at stage 12 (late-gastrula). The graphs on the left show expression from the 2-cell stage to late-tailbud (stage 40). The graphs on the right show expression through gastrulation (stage 10.5-12) and-early neurulation (stage 13-15) at high resolution. Developmental stages exhibiting background levels of expression are labelled with an asterisk (*****). **B-H** upper panels (i) Schematic representation of axolotl embryos to show how embryos in panel ii were hemisectioned or sectioned prior to the *in situ* hybridisation. **B)** Expression was detected throughout the presumptive epidermis at stage 12 (late-gastrula; ii and iii). Expression was maintained throughout the epidermis at stage 13 (early-neurula; **C**ii and iii), stage 16 (mid-neurula; **D**ii and iii), stage 20 (late-neurula; **E**ii and iii), stage 25 (early tailbud; **F**ii and iii), stage 30 (Mid-tailbud; **G**ii and iii) and stage 36 (**H**ii and iii).

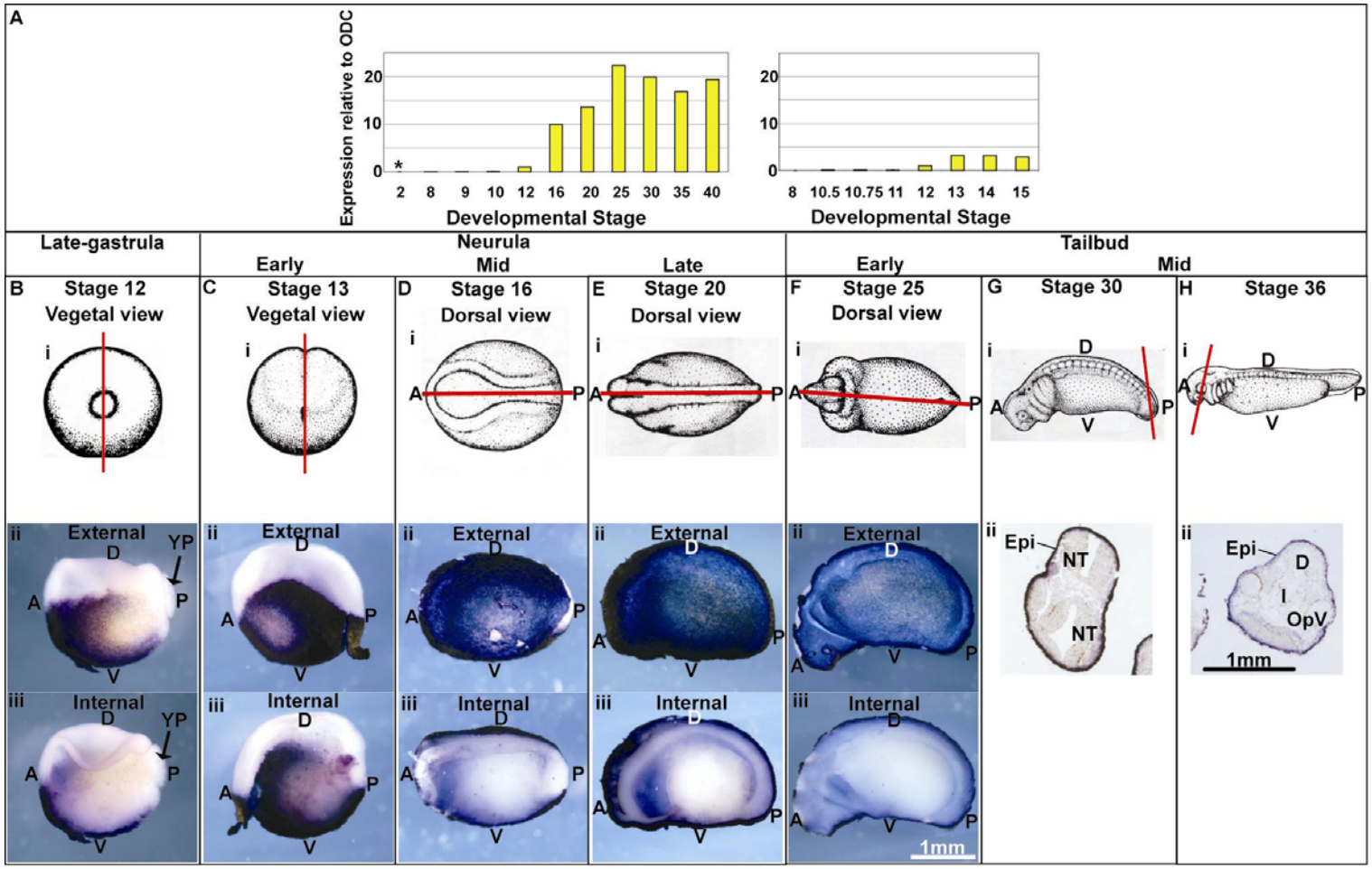
A
Expression relative to ODC
20
10
0
*
2 8 9 10 12 16 20 25 30 35 40
Developmental Stage
20
10
0
8 10.5 10.75 11 12 13 14 15
Developmental Stage
Late-gastrula
Neurula
Early
Mid
Late
Tailbud
Early
Mid
B Stage 12
Vegetal view
C Stage 13
Vegetal view
D Stage 16
Dorsal view
E Stage 20
Dorsal view
F Stage 25
Dorsal view
G Stage 30
H Stage 36
i
ii External
iii Internal
D
A
P
V
YP
Epi
NT
I
OpV
1mm

3.7 Putative PGC gene

3.7.1 Blimp1

Blimp1 plays a critical role in PGC development in mouse and there is also some indication that Blimp1 may be expressed in chicken PGCs [Vincent *et al.* 2005; Motono *et al.* 2008]. Based on the similarities between axolotl and mouse PGC specification it was considered that a homologous molecule might have a role in axolotl PGC development (**Chapter 5**).

3.7.2 Previously identified roles for Blimp1

Blimp1 (Prdm1) was first identified in mouse for its role in B-cell differentiation [Shapiro-Shelef *et al.* 2003; Kallies *et al.* 2004; Shaffer *et al.* 2004; Kallies *et al.* 2006; Kallies and Nutt 2007]. It acts as a master regulator of B-cell differentiation, restricting cells to a plasma cell fate and eliminating partially activated B cells [Kallies *et al.* 2006; Kallies and Nutt 2007]. Blimp1 (PRDMI-BF1) was discovered in humans as a silencer of β-interferon gene expression, but it also has a role in B-cell differentiation [Keller and Maniatis 1991; Turner *et al.* 1994].

Homologues of Blimp1 have been identified in organisms from *C. elegans* to human [Tunyaplin *et al.* 2000]. Vertebrate *blimp1* homologues are expressed in a wide range of tissues throughout embryonic development and expression in many regions is conserved [de Souza *et al.* 1999; Chang *et al.* 2002; Wilm and Solnica-Krezel

2005]. A general paradigm is that *Blimp1* is expressed in tissues as they begin to differentiate and is down-regulated once the tissue is fully formed [de Souza *et al.* 1999; Chang *et al.* 2002; Ha and Riddle 2003; Baxendale *et al.* 2004; Roy and Ng 2004; Wilm and Solnica-Krezel 2005]. For example, zebrafish neural crest cells, a population of multipotent cells that can develop into a variety of neural cell types, activate Blimp1 expression as they differentiate towards a sensory neuron fate [Roy and Ng 2004]. Blimp1 is thought to regulate terminal differentiation through the recruitment of epigenetic modifiers, for example Groucho proteins [Ren *et al.* 1999], which then silence target genes.

A major role for Blimp1 in zebrafish and *Xenopus* was identified in the formation of anterior endomesoderm [de Souza *et al.* 1999; Wilm and Solnica-Krezel 2005]. Experiments to disrupt Blimp1 function in zebrafish and *Xenopus*, through the use of morpholinos and dominant negative constructs respectively, result in the loss of anterior endomesodermal structures and conversely overexpression of Blimp1 in both organisms also disrupts the antero-posterior axis [de Souza *et al.* 1999; Wilm and Solnica-Krezel 2005]. Contrastingly, a homozygous *blimp1* knockout in mouse (Blimp1$^{-/-}$) does not affect early axis formation or anterior patterning [Vincent *et al.* 2005]. In Blimp1$^{-/-}$ mouse embryos morphogenesis of the caudal branchial arches is disrupted, and the labrinythe layer of the placenta fails to form correctly. There is also widespread tissue apoptosis and PGCs are entirely absent

[Vincent *et al.* 2005]. It is possible that the antero-posterior axis is unaffected in the Blimp1 mouse knockout because of functionally redundant PR (positive regulatory) domain-containing proteins as more than 15 PR domain-containing proteins have been identified in mouse [Hoyt *et al.* 1997].

Robertson *et al* (2007) used a conditional knockout of Blimp1 in the mouse epiblast to avoid the embryonic lethality caused by the placental defects [Vincent *et al.* 2005; Robertson *et al.* 2007]. As a result defects were observed in the forelimb, heart, pharyngeal arches and sensory vibrissae, and PGCs were again absent. Interestingly, another non-embryonic lethal Blimp1 mutant producing a C-terminal truncated Blimp1 had a similar profile of defects, but the sensory vibrissae were unaffected [Robertson *et al.* 2007].

Given the differing severity of defects in Blimp1 mouse knockouts, it was considered that Blimp1 may be acting in a dose-dependent manner [Robertson *et al.* 2007]. The Blimp1 mutant expressing C-terminal truncated Blimp1 was shown to have leaky expression of the full-length molecule which could explain the less severe phenotype when compared to the conditional knockout [Robertson *et al.* 2007]. Thus, PGCs require the highest level of Blimp1 expression, demonstrated by the loss of PGCs in all of the Blimp1 knockouts [Vincent *et al.* 2005; Robertson *et al.* 2007], and extra-embryonic tissues require the lowest levels, demonstrated by their loss only in the full Blimp1 knockout

[Vincent *et al.* 2005; Robertson *et al.* 2007]. Vincent *et al.* (2005) also observed a dose-dependent requirement for Blimp1 in PGCs. It was observed that PGCs were reduced in heterozygotes, and completely absent in homozygotes [Vincent *et al.* 2005].

The identification and characterisation of an axolotl *blimp1* homologue, *axblimp1* is described below. The function of Axblimp1 in PGC development is explored in **Chapter 5**.

3.7.3 Identification of ax*blimp1*

A 1.4kb fragment of *axblimp1* was cloned by degenerate PCR (**Methods 2.3.4**) from stage 9 (late-blastula) embryos. A further 400 bp of 5' coding sequence was obtained from stage 40 (late-tailbud) embryos by semi-degenerate PCR. BLAST searches were used to confirm the identity of the 1.8 kb sequence obtained. The most robust alignments obtained were with human, mouse and *Xenopus laevis*. Across the entire sequence the artificially translated Axblimp1 fragment showed 74% sequence identity to the human sequence (**Figure 3.10**).

Blimp1 has several important functional domains. The largest functional domain is the PR domain. The function of the PR domain in Blimp1 is not known, however, PR domains are closely related to SET domains in sequence, which are found in protein lysine methyl transferases and are thought to be involved in protein-protein interactions [Huang *et al.* 1998; Huang 2002; Gyory *et al.* 2004]. The

ZnF region in human Blimp1, containing five zinc-fingers (ZnF), is thought to be multifunctional [Gyory *et al.* 2004]. Deletion of the first two ZnFs does not prevent DNA binding, but inhibits localisation to the nucleus and deletion of all five entirely prevents nuclear localisation [Gyory *et al.* 2004]. There are two acidic domains, one in the N-terminal region and one in the C-terminal region. In addition, two proline-rich domains are found in the N-terminal. Deletion of these domains results in loss of histone deacetylase (HDAC) activity which is thought to be due to a loss in the ability to recruit co-repressors [Ren *et al.* 1999; Yu *et al.* 2000; Gyory *et al.* 2004]. The sequence identity of the functional domains of Axblimp1 that were cloned in full was calculated in comparison to the human sequence (**Figure 3.10**). All functional domains were found to share a high degree of homology; the PR domain shows 81% identity, the first proline-rich region shows 79% identity, the second proline-rich region shows 69% identity, the first ZnF shows 90% identity and the second ZnF shows 100% identity. (Blimp1 contains five ZnFs, only the first two ZnFs of Axblimp1 were cloned in full.) Thus, the Axblimp1 sequence is highly conserved, with particularly high conservation of the first two ZnFs providing robust evidence for the identification of a Blimp1 homologue.

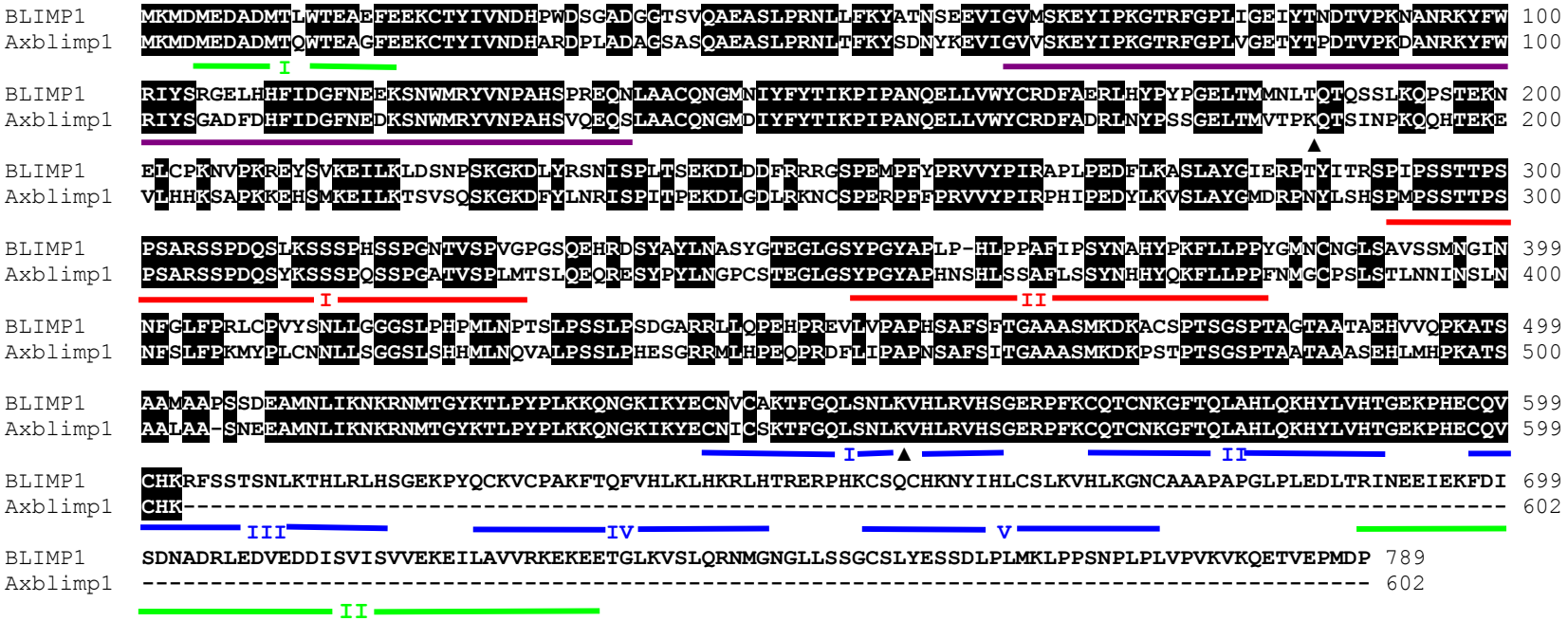

Figure 3.10 Alignment of Human Blimp1 (PRDM1) and Axblimp1 amino acid sequence.
Human Blimp1(NP_001189) (top). Axblimp1 (bottom). Shading shows identical residues. Acidic domains are underlined in green; the PR domain is underlined in purple; proline rich regions are underlined in red; and ZnFs are underlined in blue. The overall identity between the two sequences is 74%. The functional domains show a high level of sequence identity; PR domain 81% identity, first proline rich region 79% identity, second proline rich region 69% identity, first ZnF 90% identity and the second ZnF 100% identity. ▲ indicates the position of exon-exon boundaries in Axblimp1.

3.7.4 Temporal and spatial expression of *axblimp1*

Axblimp1 temporal expression was analysed by qRT-PCR (**Figure 3.11B**). The expression of *axvasa* and *axdazl*, two known markers of axolotl PGCs, was also examined on the same cDNA series for comparison (**Figure 3.11A**). The expression of *axdazl* and *axvasa* was previously determined by RT-PCR [Johnson *et al.* 2001; Bachvarova *et al.* 2004]. *Axdazl* and *axvasa* exhibited very similar patterns of expression. They were expressed maternally (stage 2) at a high level. This level of expression was maintained after the onset of zygotic transcription (stage 8) and throughout the early stages of gastrulation (stage 9-10.5). Expression decreased towards the end of gastrulation (stage 12) and the reduced level of expression was then maintained to late-tailbud (stage 40). Contrastingly, *axblimp1* expression was relatively constant throughout development, from stage 2 right through to stage 40. This suggests that Axblimp1 may not function in the same pathways as Axdazl and Axvasa during PGC development, but it does not rule out a role for Axblimp1 in PGC development. The relatively constant level of expression may reflect a core role for Axblimp1 in the regulation of multiple developmental pathways, as has been suggested for other Blimp1 homologues [Vincent *et al.* 2005]. The maternal expression of *axblimp1* may reflect a novel function as it is much earlier than any expression that has been detected in other vertebrates; *Xenopus* blimp1 is first expressed at the mid-blastula transition (stage 8.5) [de Souza *et al.* 1999] whereas in zebrafish and mouse expression

begins at early-gastrula [Chang *et al.* 2002; Wilm and Solnica-Krezel 2005].

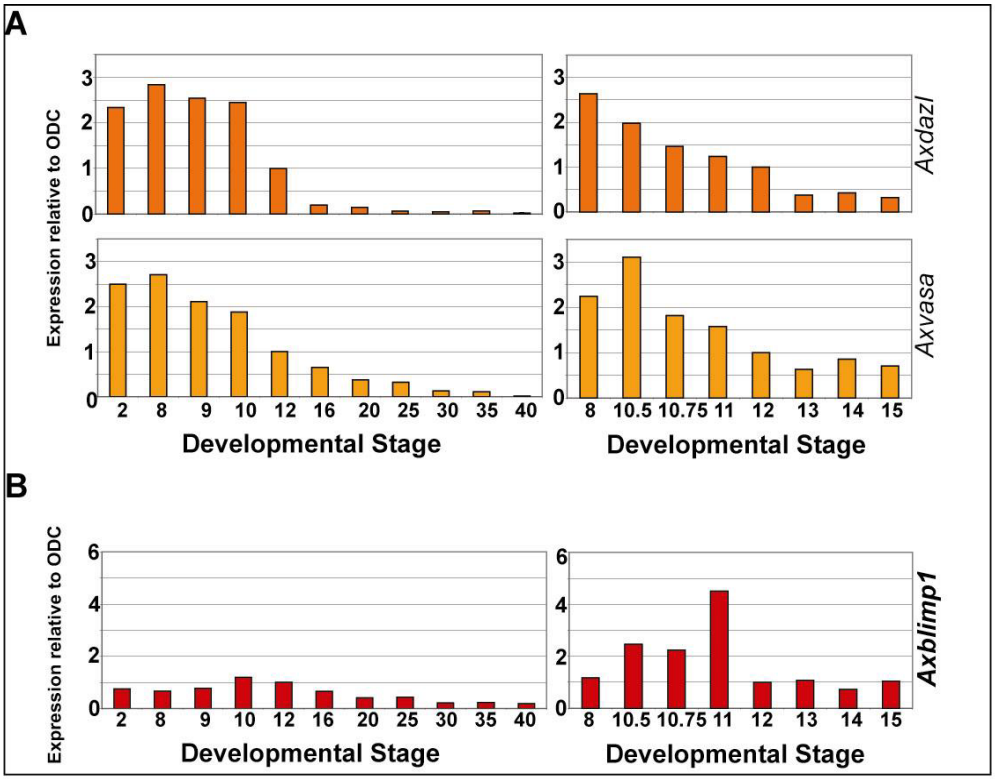

Figure 3.11 Temporal expression of *axdazl*, *axvasa* and *axblimp1*.
Temporal expression determined by real-time PCR. Primary data was analysed using the $2^{-\Delta\Delta C}T$ method [Livak and Schmittgen 2001] and was calibrated to expression level at stage 12 (late-gastrula). The graphs on the left show expression from the 2-cell stage to late-tailbud (stage 40). The graphs on the right show expression through gastrulation (stage 10.5-12) and-early neurulation (stage 13-15) at high resolution. **A)** Temporal expression of PGC genes *Axdazl and axvasa*. **B)** Temporal expression of *Axblimp1*.

A thorough examination of *Axblimp1* spatial expression was carried out by *in situ* hybridisation on whole-mounts, hemisectioned embryos and sections in order to determine if *axblimp1* is expressed in PGCs (**Figure 3.12 and 3.13**). Expression was first detected in the presumptive neural folds and prechordal plate at stage 12 (late-gastrula; **Figure 3.12A**). The prechordal plate is also one of the earliest *blimp1* expressing tissues in *Xenopus*, mouse and Zebrafish [de Souza *et al.* 1999; Chang *et al.* 2002; Wilm and Solnica-Krezel 2005]. However, the expression of vertebrate *blimp1* homologues has not previously been identified in the presumptive neural folds [de Souza *et al.* 1999; Chang *et al.* 2002; Wilm and Solnica-Krezel 2005]. Given the expression of *axblimp1* in the prechordal plate it is possible that, as in *Xenopus* [de Souza *et al.* 1999] and Zebrafish, [Wilm and Solnica-Krezel 2005] *axblimp1* may have a major role in the formation of anterior endomesodermal structures.

Consistent with the expression pattern of other vertebrate *blimp1* homologues studied [de Souza *et al.* 1999; Chang *et al.* 2002; Wilm and Solnica-Krezel 2005], expression was subsequently detected in a wide array of tissues throughout neurula (**Figure 3.12B-E**) and tailbud stages (**Figure 3.13**). Expression was detected in the pharyngeal arches, somites, tail, otic vesicles, optic vesicles, hypophysis, gut and a stripe bisecting the neural folds which have all been identified as Blimp1 expressing region in at least one other vertebrate model organism [de Souza *et al.* 1999; Chang *et al.* 2002; Wilm and Solnica-Krezel 2005].

The widespread expression of *axblimp1* suggests that, as in other vertebrates, *axblimp1* may have a role during the terminal differentiation of multiple tissue types [de Souza *et al.* 1999; Chang *et al.* 2002; Ha and Riddle 2003; Baxendale *et al.* 2004; Roy and Ng 2004; Wilm and Solnica-Krezel 2005]. The progressive expression of *axblimp1* in somites, coinciding with somite formation from anterior to posterior, is in agreement with a role in terminal differentiation. Notably, expression was not detected in PGCs.

Figure 3.12 *Axblimp1* expression in late-gastrula and neurula stage embryos
A) Expression of *axblimp1* as determined by *in situ* hybridisation on whole-mount stage 12 embryos. i) Fate-map for stage 12.5 (late-gasrula) (taken from Shook 2002). Saggital section, stippled tissues are at the surface of the cut, while the surface of the gastrocoel curves into the page. Presumptive ectoderm is highlighted in light blue (epidermis) and dark blue (neural). Presumptive mesoderm is shown as magenta (notochordal), red (somatic) or orange (head, lateral and ventral mesoderm). Endodermal fate is indicated as yellow–green (supra-blastoporal endoderm) or lime green (sub-blastoporal endoderm). Expression was detected in the presumptive neural folds (NF; arrows) and the prechordal plate (PCP; arrow) at stage 12 (late-gastrula; ii-iv). **B- E** upper panels (i) Schematic representation of axolotl embryos to show how embryos in panels ii and iii were hemisectioned prior to the *in situ* hybridisation. **B)** Expression was maintained in the neural folds (NF; arrow) and prechordal plate (PCP; arrow) and was also detected in a block of paraxial mesoderm (P mes; arrow) at stage 14 (early-neurula; ii-iii). **C)** Expression was detected in the pharyngeal arches (PA; arrow, ii) and the somites (S; arrow; iii) at stage 15 (mid-neurula). **D)** Expression was maintained in the pharyngeal arches (ii) and somites (i and ii) at stage 17 (mid-neurula). **E)** Expression persisted in the pharyngeal arches and somites, and was additionally detected in a stripe bisecting the neural folds (ii and iii) at stage 20 (late-neurula). **A = Anterior; P = Posterior; D= Dorsal; V = Ventral; NP = Neural plate; NF = Neural fold; PCP = Prechordal plate; P mes = Paraxial mesoderm; YP = Yolk plug; PA = Pharyngeal arches; S = Somite; NF = Neural fold; NT = Neural tube**

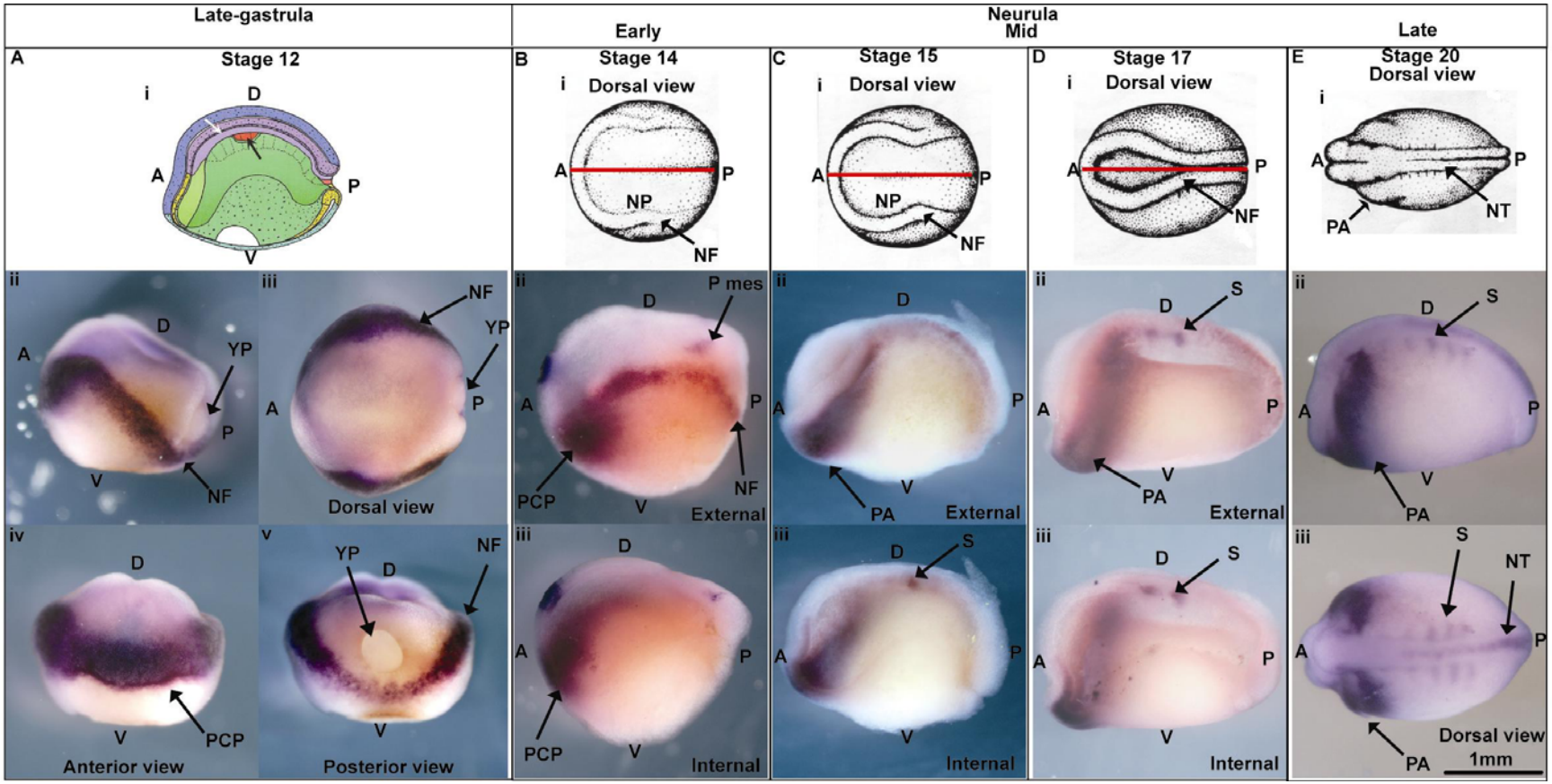
Late-gastrula
Neurula
Early
Mid
Late
A
Stage 12
i
D
A
P
V
ii
D
A
YP
P
V
NF
iii
NF
YP
A
P
Dorsal view
iv
D
V
PCP
Anterior view
v
YP
D
NF
V
Posterior view
B
Stage 14
i
Dorsal view
A
P
NP
NF
ii
D
P mes
A
P
PCP
V
NF
External
iii
D
A
P
PCP
V
Internal
C
Stage 15
i
Dorsal view
A
P
NP
NF
ii
D
A
P
V
PA
External
iii
D
S
A
P
V
Internal
D
Stage 17
i
Dorsal view
A
P
NF
ii
D
S
A
P
V
PA
External
iii
D
S
A
P
V
Internal
E
Stage 20
Dorsal view
i
A
P
PA
NT
ii
D
S
A
P
V
PA
iii
S
NT
A
P
PA
Dorsal view
1mm

Figure 3.13 Expression of *axblimp1* in tailbud embryos
A) Whole-mount *in situ* hybridisations for axblimp1 in tailbud stage embryos. Expression was detected in the pharyngeal arches (PA; arrow), otic vesicles (OV; arrow), somites (S; arrow), hypophysis (H; arrow) and tip of the tail (T; arrow) at stage 25 (early-tailbud; i and ii). Expression persisted in the otic vesicles, pharyngeal arches and tailfin (TF; arrow) at stage 30 (mid-tailbud; iii) and 35 (mid-tailbud, iv) and was additionally detected in the optic vesicles. These regions of expression were maintained at stage 38 (late-tailbud;v), although only the posterior somites maintained expression. vi-x) Schematic representation of axolotl embryos in the developmental stages indicated to show how embryos in panels B-F were sectioned prior to *in situ* hybridisation. **B)** Expression in the pharyngeal arches and gills. Expression was concentrated in the mesoderm and neural crest (the central core) of the pharyngeal arches at stage 30 (mid-tailbud; i). Expression was strongest in the mesodermal layer of the gills at stage 38 (late-tailbud; ii). **C)** Expression was localised to the dermamyotome portion of the somite at stage 30 (mid-tailbud). **D)** Expression in the optic vesicles and facial glands. Expression was detected throughout the optic vesicle at stage 35 (i), but became more restricted to the cilliary marginal zone (CMZ) at stage 43 (late-tailbud; ii) and was only detected in the lens (L) at larval stages (iii). Expression was also detected in the facial glands (Gl) at stage 43. **E)** Expression was also detected in the gall bladder (Gb, i) and the lining of the large intestine (ii) at larval stages. **F)** Expression was restricted to the mesodermal layer of the tail at stage 25 (i) and the tip of the tail at stage 38 (ii). **PA = Pharangeal arches; OV = Otic vesicle; S = Somite(s); H = Hypophysis; OpV = Optic vesicle; G = Gills; TF = Tailfin; T= tail**.

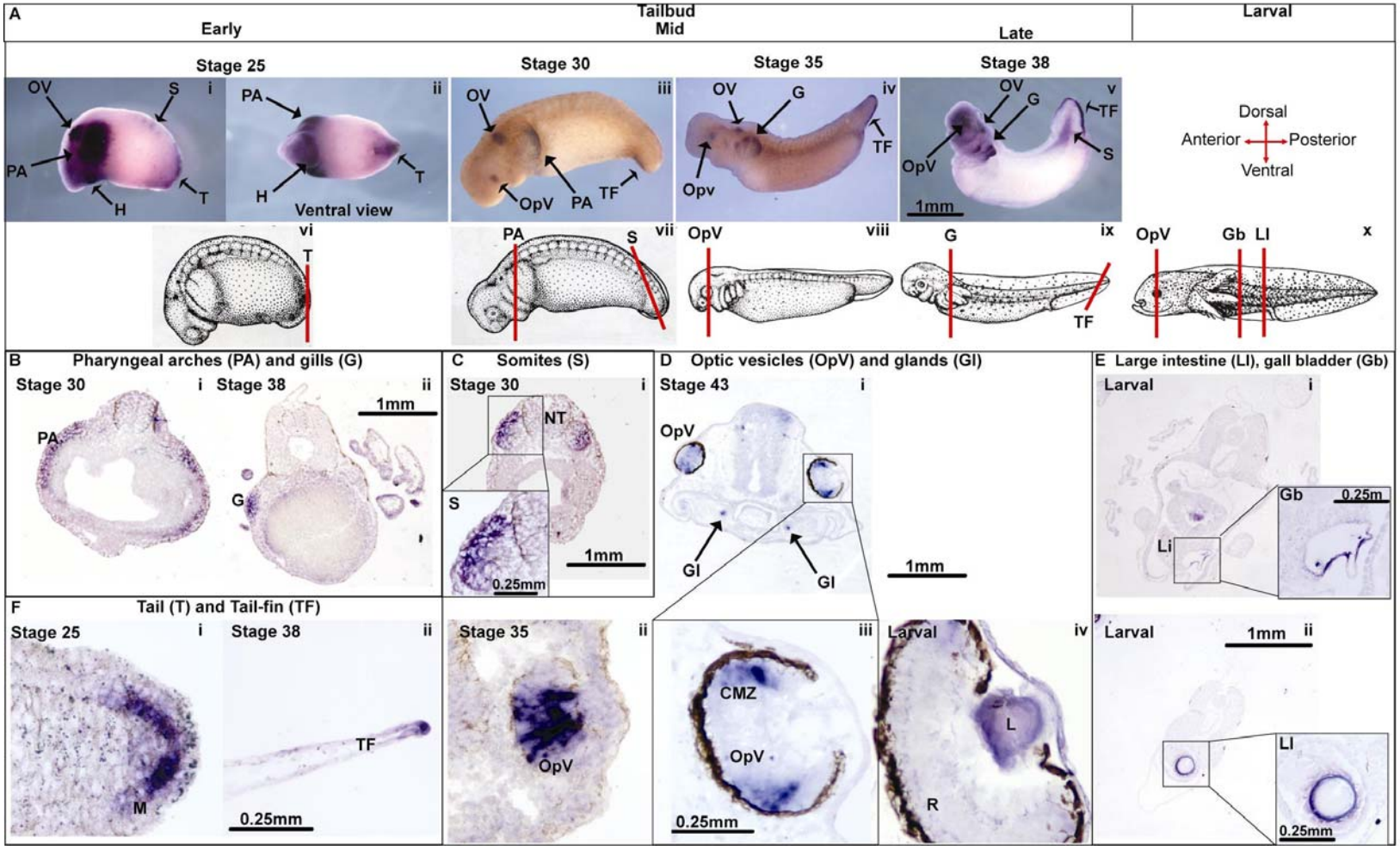
A
Early
Tailbud
Mid
Late
Larval
Stage 25
Stage 30
Stage 35
Stage 38
OV
S
PA
T
H
Ventral view
OpV
TF
G
Opv
1mm
Dorsal
Anterior
Posterior
Ventral
vi
vii
viii
ix
x
Gb
LI
B Pharyngeal arches (PA) and gills (G)
Stage 30
Stage 38
C Somites (S)
NT
0.25mm
D Optic vesicles (OpV) and glands (GI)
Stage 43
GI
E Large intestine (LI), gall bladder (Gb)
Larval
Li
0.25m
F Tail (T) and Tail-fin (TF)
M
CMZ
L
R

3.8 Epigenetic markers

3.8.1 Carm1

Carm1 (Coactivator-associated-protein-arginine-methyltransferase 1) is a coactivator of transcription [Chen *et al.* 2002; Lee *et al.* 2005]. It is recruited to transcriptional promoters which results in methylation of both histone H3 at arginine 17 and histone acetyltransferases p300/CBP, resulting in the activation of targets [Chen *et al.* 2002; Lee *et al.* 2005]. Investigations in mouse have shown that overexpression of histone methyltransferase, Carm1, in specific blastomeres of four-cell stage embryos results in increased expression of *nanog* and *sox2* and those blastomeres contribute more frequently to the ICM [Torres-Padilla *et al.* 2007]. *Axcarm1* was, therefore, cloned in order to investigate if it has a role in axolotl pluripotency. Expression of Axcarm1 in Axnanog morphant embryos is examined in **Chapter 4**.

3.8.2 Identification of an axolotl *carm1* homologue (*axcarm1*)

Degenerate PCR (described in methods **2.3.4**) was carried out on cDNA synthesised from stage 9 embryos to clone a fragment of *axcarm1*. A further 200 bp of *axcarm1* 3' coding sequence was obtained by performing semi-degenerate PCR on cDNA synthesised from stage 35 embryos. Basic Local Alignment Search Tool (BLAST) searches were carried out to confirm the identity of the sequence and the most robust alignments were obtained with human, mouse, and rat homologues of *carm1.* The artificially translated *axcarm1* fragment

shares 92% sequence identity with the human Carm1 homologue (**Figure 3.14**).

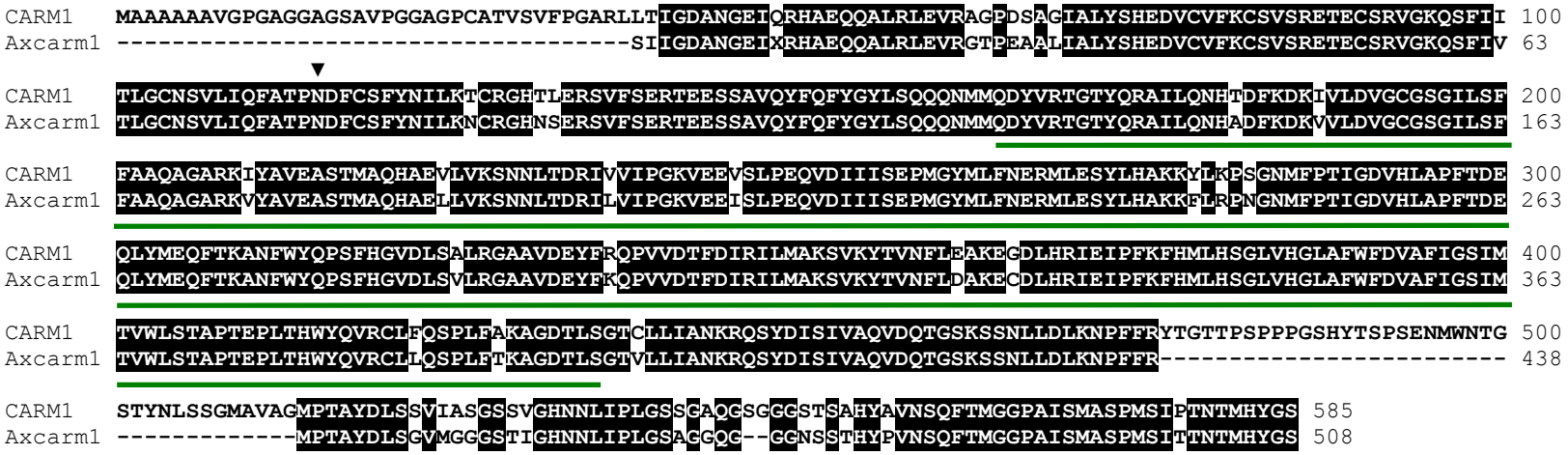

Figure 3.14 An alignment of the artificially translated Axcarm1 sequence with *Homo sapiens* Carm1.
Homo sapiens Carm1 (NP_954592) is shown at the top and the artificially translated Axcarm1 sequence is shown underneath. Shading indicates conserved amino acids. The region underlined in green is the methyltransferase domain. The artificially translated Axcarm1 fragment shares 92% sequence identity with the human Carm1 homologue. Known intron junctions in the Axcarm1 sequence are indicated by ▼.

3.8.3 Temporal and spatial expression of *axcarm1*

Temporal expression of *axcarm1* was determined by RT-PCR (**Figure 3.15A**). Expression was detected at a relatively constant level throughout all stages examined. This might be expected as *axcarm1* is an epigenetic regulator and these molecules often have multiple roles throughout development and are regulated *via* localisation rather than transcription [e.g. NODE Liang *et al.* 2008].

Spatial expression was examined by *in situ* hybridisation on hemisectioned embryos (**Figure 3.15D**). Interestingly, the expression pattern observed was strikingly similar to that reported for *axnanog* and *axoct4* (**Section 3.5.2**). In blastula stage embryos expression was detected in the presumptive ectoderm (**Figure 3.15Di-ii**). This expression persisted in gastrulae stage embryos and expression was additionally detected in the presumptive mesoderm, extending vegetally towards the blastopore (**Figure 3.15Diii-iv**). Notably, expression appeared to become ventrally restricted towards the end of gastrulation (stage 12; **Figure 3.15Dvi**). This data provides compelling evidence to suggest as in mouse, *axcarm1* may have a role in the establishment or maintenance of pluripotency and it is possible, given the similarity between the expression patterns, that *axcarm1* regulates *axnanog* and *axoct4* expression as in mouse [Torres-Padilla *et al.* 2007].

Figure 3.15 Temporal and spatial expression of *axcarm1*
A) Temporal expression of *axcarm1* determined by real-time PCR. Primary data was analysed using the $2^{-\Delta\Delta C}$T method [Livak and Schmittgen 2001] and was calibrated to expression level at stage 12 (late-gastrula). The graphs on the left show expression from the 2-cell stage to late-tailbud (stage 40). The graphs on the right show expression through gastrulation (stage 10.5-12) and-early neurulation (stage 13-15) at high resolution**.** **B)** Fate-maps for stage 10 (early-gastrulation) and stage 12.5 (late-gastrulation) urodele amphibians (taken from Shook *et al.,* 2002). Presumptive ectoderm is highlighted in light blue (epidermis) or dark blue (neural). Presumptive mesoderm is shown as magenta (notochordal), red (somatic) or orange (head, lateral and ventral mesoderm). Endodermal fate is indicated as yellow–green (supra-blastoporal endoderm) or lime green (sub-blastoporal endoderm). The stage 10 fate map shows only the superficial view. In general, the presumptive fates continue radially toward the blastocoel, except that the presumptive head mesoderm continues vegetally under the superficial layer of the supra-blastoporal endoderm. The stage 12.5 fate map shows a sagittal section of an embryo, such that the stippled tissues are at the face of the cut, while the surface of the gastrocoel cavity curves into the page. **C)** Schematic representation of axolotl embryos in various developmental stages as indicated (i –vi) to show how embryos in panels D were hemisectioned prior to the *in situ* hybridisations. **D)** Expression was detected in the animal hemisphere (presumptive ectoderm) at stage 7 (early-blastula; i) and persisted in the presumptive ectoderm at stage 8 (mid-blastula;ii) and stage 10 (early-gastrula; iii). In addition expression was detected in the presumptive mesoderm, extending vegetally towards the blastopore at stage 10 (iii). This pattern of expression persisted at stage 10.5 (mid-gastrula; iv) and stage 10.75 (late-gastrula; v). At stage 12 (late-gastrula; vi), the expression appeared to become more ventrally restricted in the presumptive ectoderm and mesoderm.

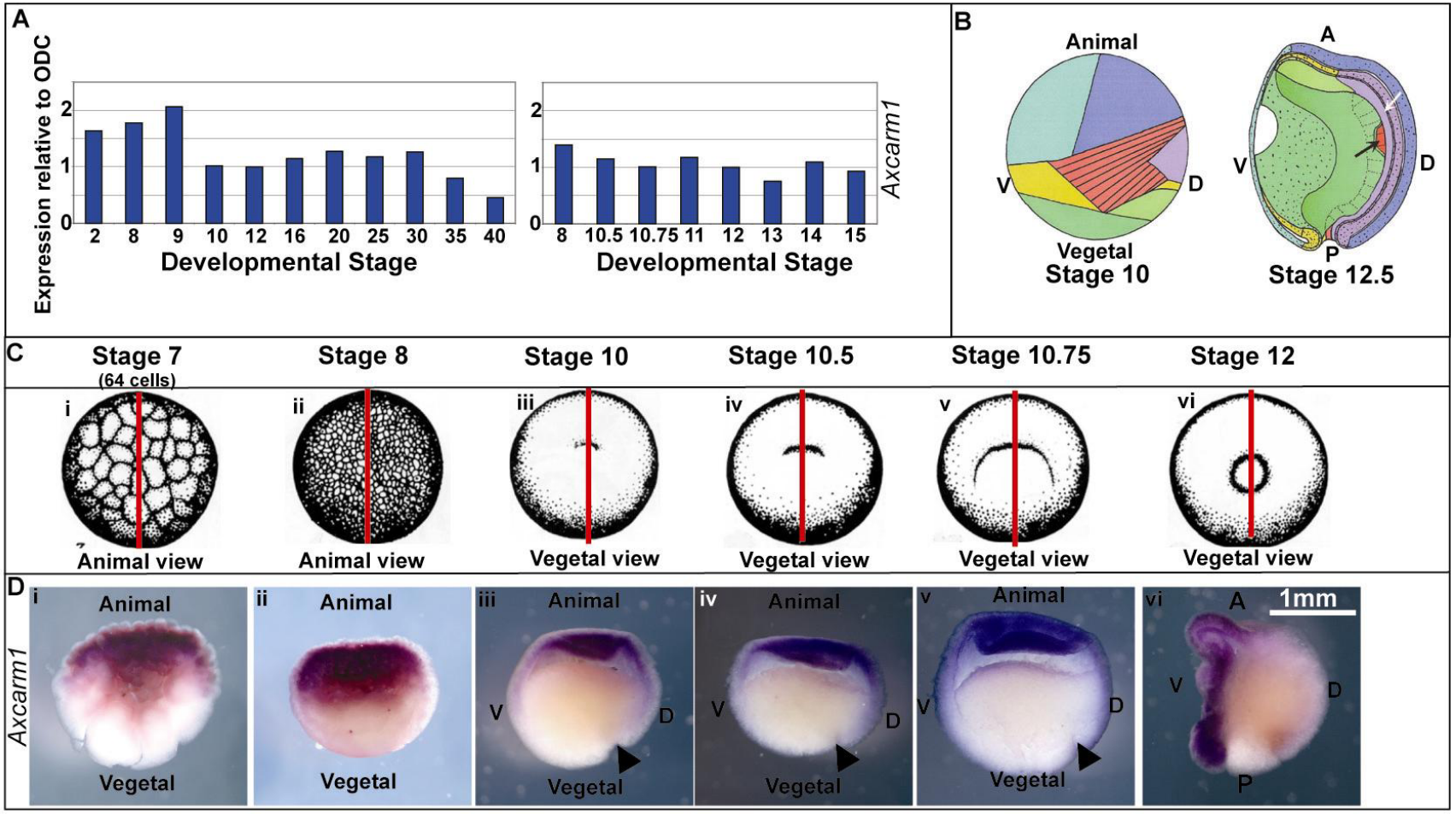
A
Expression relative to ODC
2
1
0
2 8 9 10 12 16 20 25 30 35 40
Developmental Stage
2
1
0
8 10.5 10.75 11 12 13 14 15
Developmental Stage
Axcarm1
B
Animal
V
D
Vegetal
Stage 10
A
V
D
P
Stage 12.5
C
Stage 7
(64 cells)
Stage 8
Stage 10
Stage 10.5
Stage 10.75
Stage 12
i
ii
iii
iv
v
vi
Animal view
Animal view
Vegetal view
Vegetal view
Vegetal view
Vegetal view
D
Axcarm1
i Animal
Vegetal
ii Animal
Vegetal
iii Animal
V
D
Vegetal
iv Animal
V
D
Vegetal
v Animal
V
D
Vegetal
vi
A
1mm
V
D
P

3.9 Discussion

Axolotls are convenient model organisms for studying embryology given their large, externally developing embryos. Additionally, gene copy number (predicted) and similarities between the developmental mechanisms in axolotl and amniotes make them ideal for studying the evolution of developmental processes. Unfortunately, genomic sequence is unavailable; therefore, this chapter has described the cloning and characterisation of multiple genes for use in the investigations reported in **Chapters 4 and 5**.

Interestingly, **Section 3.5** described the cloning and characterisation of the first anamniote homologue of *nanog*, *axnanog*. *In situ* hybridisations revealed that *axnanog* is co-expressed with *axoct4* during early development in undifferentiated tissues of the embryo. Thus, Axnanog and Axoct4 may prove to have conserved roles in the maintenance of multipotency/pluripotency. The roles of Axnanog and Axoct4 in pluripotency are explored further in **Chapter 4** and their roles in PGC development are explored in **Chapter 5**. Furthermore, it was shown that *axcarm1* was also expressed in equivalent regions to *axoct4* and *axnanog* during early development, suggesting that it may also have a conserved role in establishing and/or maintaining pluripotency. The expression of *axcarm1* in Axnanog morphant embryos is described in **Chapter 4**. The role of Axcarm1 in relation to pluripotency was not explored directly. The identification of these molecules could be key to

understanding the evolution of the mechanisms governing pluripotency in amniotes.

Very little is known about the specification of PGCs in axolotl. Given that there are a number of similarities between axolotl and mouse PGC development, it was considered that homologous molecules might be involved (**Chapter 3**). Thus, a homologue of Blimp1, *axblimp1*, was cloned. The temporal expression pattern of *axblimp1* differed from that of other PGC-specific genes, *axdazl* and *axvasa*, suggesting that it does not operate in the same pathways, but this does not rule out a role in PGC development. Initial analyses of expression by *in situ* hybridisation revealed a conserved pattern of expression, but expression was not detected in PGCs. However, this may be attributable to assay sensitivity. For most of the gene expression analyses described in this chapter, including those carried out by Swiers (2008), expression was detected by real-time PCR at stages when expression was not detected by *in situ* hybridisation, highlighting a lack of sensitivity in the *in situ* hybridisation assay. Future work should include method development aiming to increase the sensitivity of *in situ* hybridisation. The role of Axblimp1 in PGC development is explored further in **Chapter 5**.

Robust markers of neural tissue, *axncam*, and epidermal tissue, *axck*, were also cloned. These markers were used to determine the effect of

Axnanog depletion on the development of ectodermally derived tissues (**Chapter 4**).

It is important to consider that the selection of model organisms for their convenience, the size of embryos, availability, speed of development etc. may bias our understanding of development. This chapter has highlighted the importance of studying developmental processes in the axolotl model system for furthering our understanding of the evolution of developmental mechanisms in amniotes. However, only the study of these processes in a vast array of organisms is likely to reveal the full picture. It has been argued that different model organisms should be used, as unique adaptations are as important as conserved features [Jenner 2006; Jenner and Wills 2007]. The discussion of PGC development in **Chapter 5** highlights this issue, and describes how the inclusion of a wider variety of organisms changed the prominent view of PGC development.

3.9.1 Summary

1. Developmental processes in urodeles are similar to those in amniotes and it is, therefore, thought that amniotes might have evolved from a urodele-like ancestor. Thus, studying the processes of development in axolotl could be key to understanding the evolution of developmental mechanisms in amniotes.

2. The first anamniote homologue of *nanog*, *axnanog*, was identified and temporal and spatial expression patterns suggest it may have a conserved role in the establishment and/or maintenance of pluripotency perhaps in conjunction with Axoct4 (given the regions of co-expression). **Chapter 4** explores this further. The roles of Axoct4 and Axnanog in PGC development are explored, in **Chapter 5**.

3. A homologue of *blimp1*, *axblimp1*, was identified in order to investigate its role in PGC development but initial analyses did not detect expression in the PGCs. However, this may be due to the sensitivity of the assay. The role of Axblimp1 in PGC development is explored further in **Chapter 5**.

4. *Axncam* and *axck* were cloned as markers of neural and epidermis respectively. Expression analyses revealed them to be robust markers of these tissues.

5. A homologue of *carm1*, *axcarm1*, was cloned and its expression in early embryos suggests that it may have a conserved role in the establishment/ maintenance of pluripotency. Expression in Axnanog morphant embryos is described in **Chapter 4**.

Chapter 4. Investigating the function of *axnanog* and *axoct4* using antisense morpholino oligonucleotides

4.1 Introduction

Axnanog is the first *nanog* homologue to be identified in an anamniote. This chapter describes the use of translation and splice-blocking morpholinos to investigate Axnanog function. Preliminary knock-down data is also presented for Axoct4.

4.2 Confirmation of the activity of *axnanog* translation-blocking and splice-blocking morpholinos

Morpholinos were designed for the investigation of Axnanog function. Morphlinos are 25 bp antisense oligonucleotide molecules with a modified backbone that is resistant to nuclease activity and they are therefore stable in cells [Gene-Tools 2008]. Two types of morpholino can be used to disrupt protein expression. Translation-blocking morpholinos (ATG-morpholinos) bind to the AUG start site or the 5'UTR and block translation of the target transcript in the cytosol by blocking ribosome binding. Splice-blocking morpholinos (splice-morpholinos) bind to splice junctions of target pre-mRNAs in the nucleus and prevent the production of a mature mRNA by disrupting splicing through blocking the binding of splicing machinery. Both an ATG-morpholino and a splice-morpholino were designed to target Axnanog.

ATG-morpholinos have the advantage of targeting both maternal and zygotic transcripts, which was a valuable property in this study as *axnanog* is maternally expressed. The specificity and activity of the

axnanog ATG-morpholino was initially determined by *in vivo* tests in *Xenopus tropicalis* oocytes (**Figure 4.1A**). Oocytes were first injected with 80 ng of the ATG-morpholino or a mismatch control morpholino containing five base mismatches (sequences given in **Section 2.4.5**). The oocytes were cultured overnight and then injected with 500 pg of artificially transcribed full-length hemagluttanin (HA)-tagged *axnanog* mRNA or HA-tagged *axnanog* mRNA lacking the 5'UTR. After a further overnight incubation protein was extracted from the oocytes and was analysed on a western blot (**Figure 4.1A**). The *axnanog* ATG-morpholino caused a complete block to the translation of HA-tagged *axnanog* mRNA, whereas no blocking occurred in the absence of the 5'UTR, to which the morpholino was targeted entirely. The mismatch control morpholino did not affect the translation of HA-tagged *axnanog* RNA. The ATG-morpholino was, therefore, shown to specifically and efficiently inhibit the translation of *axnanog* mRNA.

The disadvantage of using a translation-blocking morpholino is that its activity in embryos can only be confirmed by using an antibody specific to the target protein. In the absence of an Axnanog antibody, splice-morpholinos were also designed. The function of a splice-morpholino can be more easily confirmed using RT-PCR to check for the presence of normal transcripts. Two splice-morpholinos were designed and they were injected into embryos to test their activity. Embryos were injected with 160 ng of a splice-morpholino targeted either to the exon-intron boundary or to the intron-exon boundary of

intron 1. Only the morpholino targeted to the intron-exon boundary produced a phenotype. In order to examine splicing defects by RT-PCR, embryos were collected at mid- to late-gastrula (stage 10.5-11). RT-PCR was carried out on cDNA synthesised from the embryos using primers designed to the coding region (**Figure 4.1B**).

In embryos injected with the morpholino targeted to the intron-exon boundary only low levels of normal transcript were detected (**Figure 4.1B**). In addition, three aberrant products were detected at higher levels than the normal product. These products were cloned and sequenced. The largest of the products (1134 kb) contained an insertion of intron 1 sequence, presumably as a result of a cryptic splice site within intron 1. The other two aberrant transcripts were shorter than the full-length *axnanog* coding region; the 667 bp product obtained lacked exon 2, and the 555 bp product lacked both exon 2 and exon 3 (intron 3 junction predicted). All splice variants were shown to encode truncated proteins lacking both the homeodomain and the short region of conservation upstream of the homeodomain (**Appendix 8.3**), thus, all splice-variants are expected to be non-functional. Only normal *axnanog* transcript was detected in embryos injected with the morpholino targeted to the exon-intron junction. In conclusion, as suggested by the observed phenotypes, the splice-morpholino targeted to the intron-exon boundary efficiently disrupted the production of normal *axnanog* transcript, whereas the splice-morpholino targeted to the exon-intron

boundary was ineffective. The non-functional morpholino was employed as a control in subsequent experiments.

Both the functional splice-morpholino (targeted to the intron-exon boundary of intron 1) and the ATG-morpholino were used to investigate the function of Axnanog. It is recommended to use both a splice-morpholino and a translation-blocking morpholino to investigate the function of a protein in order to control for off-target effects [Eisen and Smith 2008]. If the two morpholinos produce a similar phenotype one can be more confident that the phenotype is indicative of the target's function. Carrying out this control in axolotl studies is particularly important as genome sequence is unavailable, and so the potential binding of the morpholino to similar sequences cannot be ruled out. The Axnanog ATG-morpholino and splice-morpholino might be expected to give at least partially differing phenotypes because the ATG-morpholino targets both maternal and zygotic transcripts, whereas the splice-morpholino can target only zygotic transcripts.

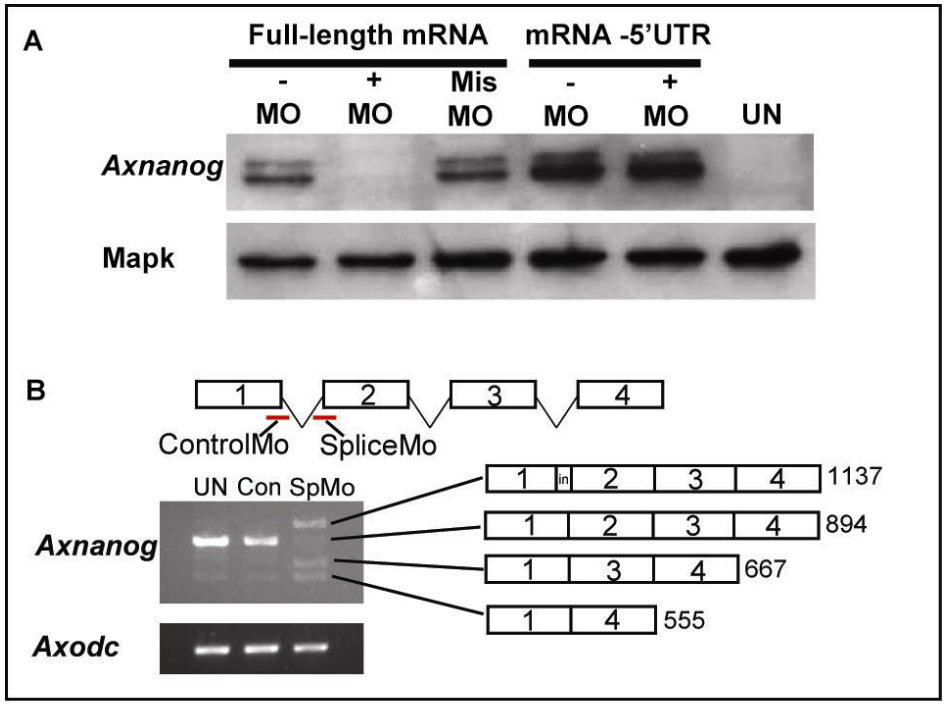

Figure 4.1 Confirmation of activity of *A*xnanog translation-blocking and splice blocking morpholinos

A) Western blots to detect hemagluttanin (HA) tagged Axnanog protein (top) and Mapk protein (bottom). MapK is a loading control. *Xenopus tropicalis* oocytes were injected with 80 ng *axnanog* ATG-morpholino or a mismatch control morpholino with 5 base pair mismatches. After overnight incubation they were then injected with full-length HA-tagged *axnanog* mRNA or HA tagged mRNA lacking the 5'UTR. Protein was extracted after a further overnight incubation. Each lane of the western blot was loaded with protein equivalent to that in 5 oocytes. **-MO** = mRNA injected alone; **+MO** = mRNA and morpholino injected; **Mis MO** = mRNA and mismatch control morpholino injected; **UN** = uninjected. **B)** RT-PCR to detect the effect of Axnanog splice-morpholinos on the production of normal *axnanog* transcript. Embryos were injected at the 1-cell stage with 160 ng of splice-morpholino targeted to the exon-intron (ControlMo) or intron-exon (SpliceMo) boundary of *axnanog* intron 1. Embryos were collected on day 2 after injection. Uninjected embryos were approximately at stage 10.5-11 (mid- to late-gastrula). RT-PCR was carried out on cDNA synthesised from the embryos using primers designed to the coding region. The schematic at the top represents the coding region of *axnanog*. Red lines indicate sites targeted by morpholinos; the boxes 1-4 represent exons. The splice-morpholino targeted to the intron-exon junction effectively blocked normal splicing; only a low level of normal product was detected. Three aberrant splice products were detected; the 1137 bp product had an insertion of intron 1, the 667 bp product lacked exon 2 and the 555 bp product lacked exons 2 and 3. All alternatively spliced products were sequenced and are predicted to produce non-functional proteins (**Appendix 8.3**). The alternatively spliced products persisted on day 3 after injection (not shown). Only normal product was detected in embryos injected with the splice-morpholino targeted to the exon-intron junction (ControlMo), this was subsequently employed as a control. *Axodc* is a loading control.

4.3 Depletion of *Axnanog* disrupts gastrulation

Embryos were injected at the 1-cell stage with 160 ng of translation-blocking or splice-blocking morpholino. The splice-morpholino and the ATG-morpholino produced similar phenotypes (**Figure 4.2A and B**).

On day 2 after injection, when uninjected and control-morpholino injected embryos had reached late-gastrula stages (stage 10.75-12; **Figure 4.2Ai-ii and Bi**), there was no dorsal-lip visible in the vegetal region of Axnanog morphant embryos and they resembled late-blastula (stage 9) embryos (**Figure 4.2Aiii and Bii**). Morphant embryos underwent epiboly, but the ectoderm subsequently receded. Dorsal lip-like structures were sometimes visible in the vegetal pole of morphant embryos (19%), but the ectoderm in these embryos receded as in morphant embryos lacking these structures (not shown). All morphant embryos exhibiting a phenotype failed to complete gastrulation, but ISH data suggests that some morphant embryos had started to gastrulate (**Figure 4.4Diii**).

On day 3 after injection, when uninjected embryos and control-morpholino injected embryos had reached late-neurula to mid-tailbud stages (stage 19-28; **Figure 4.2Aiv-v and Biii**), morphant embryos most frequently (80%) resembled undifferentiated tissue, a ball of ectoderm-like tissue attached to a ball of yolky-endoderm with an equatorial indentation (**Figure4.2Avi and Biv**). The equatorial

indentation could be the formation of a circumferential blastopore and a site of involution. Less frequently (18%), neural-fold like structures formed in the animal region of morphant embryos (**Figure 4.2Avii**). Embryos injected with 160 ng of either of the control morpholinos developed normally, although a slight delay in development was often observed (**Figure 4.2Av**).

In conclusion, Axnanog knock-down severely disrupted gastrulation. The splice-morpholino and the ATG-morpholino produced similar phenotypes, therefore, the phenotype can be attributed confidently to disrupted Axnanog expression. The high degree of similarity between the ATG-morphant and splice-morphant phenotype suggests that the role of the maternal transcript during development is minimal.

Figure 4.2 Axnanog morphant phenotype
Embryos were injected at the 1-2 cell stage with 160 ng of Axnanog splice-morpholino, Axnanog ATG-morpholino or a splice-control morpholino. Embryos are shown on day 2 and day 3 after injection. **A)** Phenotype of morphant embryos injected with splice-morpholino. Uninjected (i) and control-morpholino injected embryos (ii) developed normally and on day 2 after injection were approximately stage 10.75 (mid-gastrula). Arrows indicate the dorsal lip. The splice-morphant embryos (iii) however failed to gastrulate and a dorsal lip was not visible. On day 3 after injection the uninjected embryos (iv) had reached approximately stage 23 (early-tailbud) and control morpholino injected embryos (v) were slightly delayed having reached approximately stage 20 (early-tailbud). Splice-morpholino injected embryos underwent epiboly but the presumptive epidermis subsequently receded (vi). The majority of the splice-morphant embryos consisted of a ball of ectoderm-like tissue attached to ball of endoderm (vi), a slight indentation was visible suggesting that some involution may have occurred. A small proportion of the embryos developed neural-fold like structures in the ectoderm-like portion of the embryo (vii). **B)** Phenotype of morphant embryos injected with ATG-morpholino. On day 2 after injection the uninjected embryos (i) were approximately stage 12 (late-gastrula). However, similarly to splice-morphant embryos a dorsal lip was not visible in the vegetal portion of the morphant embryos (ii). On day 3 after injection the uninjected embryos (iii) reached approximately stage 25 (early-tailbud) and the morphant embryos (iv) exhibited a similar phenotype to splice-morphant embryos. The blastocoel cavity in the animal region of morphant embryos sometimes collapsed, giving the presumptive ectoderm a 'wrinkly' appearance because of the convoluted tissue (iv). **A = Anterior; P = Posterior; D = Dorsal; V = Ventral.**

Summary of morpholino phenotype occurrence (7 experiments)					
Morphant embryos on day 2 (%)			**Morphant embryos on day 3 (%)**		
No visible dorsal lip	**Slightly visible dorsal lip**	**Normal**	**Severe phenotype**	**Neural fold-like structures visible**	**Normal**
80	19	1	80	18	2

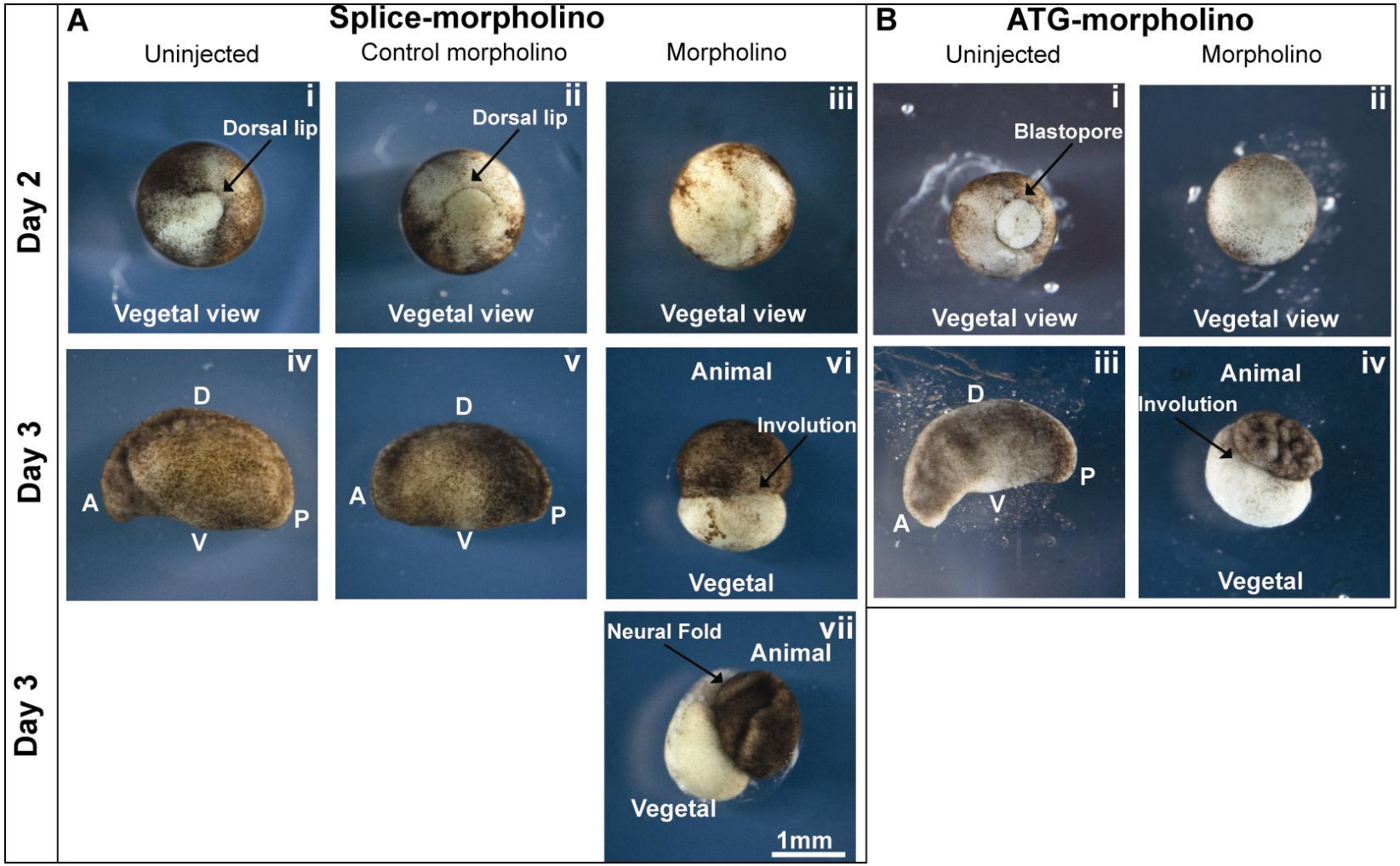
A
Splice-morpholino
Uninjected
Control morpholino
Morpholino
B
ATG-morpholino
Uninjected
Morpholino
Day 2
Day 3
Day 3
i
Dorsal lip
Vegetal view
ii
Dorsal lip
Vegetal view
iii
Vegetal view
i
Blastopore
Vegetal view
ii
Vegetal view
iv
D
A
P
V
v
D
A
P
V
Animal
vi
Involution
Vegetal
iii
D
P
V
A
Animal
iv
Involution
Vegetal
Neural Fold
vii
Animal
Vegetal
1mm

4.3.1 The transcription profile of *axnanog* morphant embryos

qRT-PCR was used to analyse the expression of molecular markers in *axnanog* morphant embryos on day 2 and day 3 after injection. Expression was analysed in splice-morphant embryos and in ATG-morphant embryos. Spatial expression of some markers was also analysed by ISH on hemisectioned embryos.

Expression of pluripotency genes was maintained in morphant embryos

In order to examine the effect of Axnanog depletion on the expression of the core pluripotency network, the expression of *axnanog* and *axoct4* was examined (**Figure 4.3C**). There were no marked differences in expression on day 2 after injection. However, on day 3 after injection a*xnanog* and *axoct4* expression was maintained in morphant embryos, whereas only background levels were detected in uninjected and control morpholino injected embryos (consistent with developmental series data; **Figure 3.5**). The level of expression in morphant embryos was similar to that in late-gastrula (stage 10.75-11) uninjected embryos.

Expression of *axnanog* and *axoct4* was also analysed in hemisectioned morphant embryos collected on day 3 after injection by *ISH* (**Figure 4.3D**). Expression of both genes was detected in the ectodermal-like tissue of morphant embryos and was undetectable in control morpholino injected and uninjected embryos, as expected. The pattern of expression was similar to that in uninjected gastrula stage embryos where expression of both genes can be detected throughout the

ectoderm and presumptive mesoderm (**Figure 3.5**). This is consistent with the qRT-PCR data.

This data indicates that the depletion of Axnanog inhibits development and thus the down-regulation of pluripotency genes that accompanies normal development (**Chapter 3)**.

Figure 4.3 Expression of pluripotency genes in morphant embryos
A) Schematic showing temporal *axoct4* and *axnanog* expression during normal development from the 2-cell stage to stage 40 (late-tailbud). The blue line indicates the stage at which morphant embryos are thought to have halted development. **B)** Schematic showing the overlapping expression (yellow-green shading) of *axoct4* and *axnanog* at stage 10.75 (late-gastrula). *Axoct4* and *axnanog* are co-expressed in the presumptive ectoderm and presumptive mesoderm extending vegetally towards the blastopore. Morphant embryos are thought to have halted development close to this stage. **C)** Relative expression of *axnanog* (top) and *axoct4* (bottom) in splice-morphant and ATG-morphant embryos on days 2 and 3 after injection as determined by qRT-PCR analysis. Data was analysed using the $2^{-\Delta\Delta C}$T method [Livak and Schmittgen 2001] and was calibrated to expression in the uninjected samples on day 2 after injection. In the splice-morpholino experiment uninjected embryos were approximately stage 10.5-11 (mid-late gastrula) on day 2 and approximately stage 19-22 (late-neurula to early-tailbud) on day 3. Control morpholino injected embryos were slightly delayed by comparison, stage 10-10.75 (early-late gastrula) on day 2 and stage 17-18 (early-neurula) on day 3. In the ATG-morpholino experiment uninjected embryos were approximately stage 10.75-11.5 (late-gastrula) on day 2 and stage 26-30 (early to mid-tailbud) on day 3. Perturbations in expression were not observed on day 2 after injection. Differences between the expression in control and uninjected samples can be explained by the observed delay in development. In both experiments the expression of *axoct4* and *axnanog* was maintained on day 3 after injection whereas it was undetectable in the uninjected and control samples. **D)** Spatial expression of *axnanog* and *axoct4* in morphant embryos. Embryos were collected on day 3 after injection. *In situ* hybridisations were then carried out on hemisectioned embryos. The schematics at the top indicate how the embryos on panel iii were hemisectioned; i) uninjected and control morpholino injected embryos, ii) morphant embryo. *Axnanog* expression was not detected in uninjected and control morpholino injected embryos but was detected in the ectoderm-like tissue of morphant embryosm (iii). Similarly, *axoct4* expression was not detected in uninjected and control morpholino injected embryos but was detected in the ectoderm-like tissue of morphant embryos (iv).

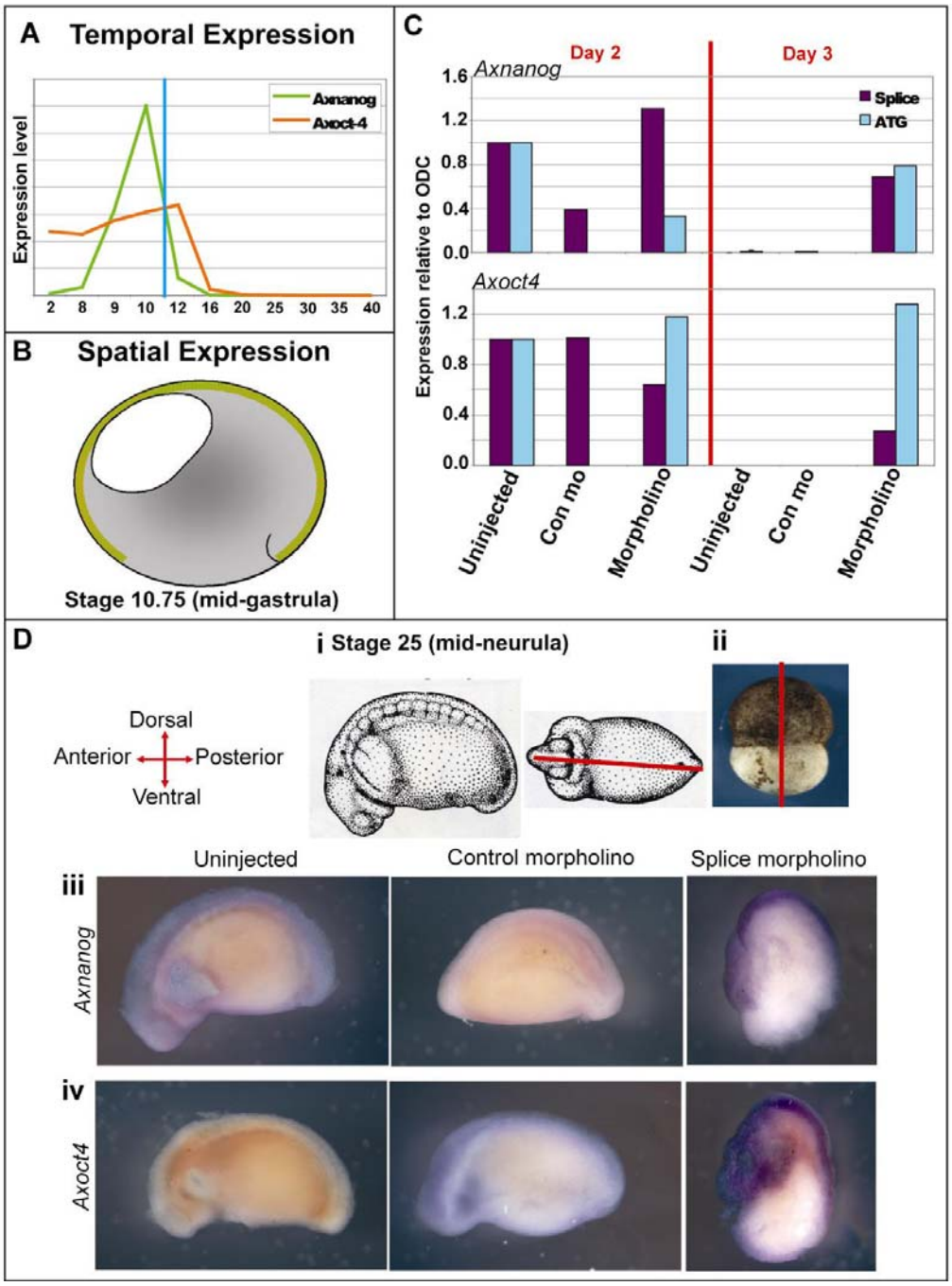
A Temporal Expression
Axnanog
Axoct-4
Expression level
2 8 9 10 12 16 20 25 30 35 40
B Spatial Expression
Stage 10.75 (mid-gastrula)
C
Day 2
Day 3
Axnanog
Splice
ATG
Axoct4
Expression relative to ODC
1.6
1.2
0.8
0.4
0.0
Uninjected
Con mo
Morpholino
Uninjected
Con mo
Morpholino
D
i Stage 25 (mid-neurula)
ii
Dorsal
Anterior
Posterior
Ventral
Uninjected
Control morpholino
Splice morpholino
iii
Axnanog
iv
Axoct4

Expression of early mesodermal and endodermal genes was maintained at a high level in morphant embryos

To examine the effect of Axnanog depletion on the differentiation of mesoderm and endoderm the expression of *axbrachyury, axmix* and *axsox17* was examined by qRT-PCR (**Figure 4.4C**). Axbrachyury is normally expressed in developing mesoderm and in later embryos expression is restricted to the notochord (**Chapter 3**). *Axmix* is expressed in developing mesoderm and endoderm (**Chapter 3**). *Axsox17* is expressed in developing endoderm [Yi Hsien unpublished; not shown].

On day 2 after injection slight perturbations in expression of all three genes were observed in morphant embryos in comparison to the uninjected sample (**Figure 4.4C**). However, where the levels of expression differed significantly from the uninjected sample they were similar to those in the control sample, suggesting these perturbations may be the result of a delay in development similar to that observed in the control sample.

On day 3 after injection, similar to the pluripotency genes, expression of *axbrachyury*, *axmix* and *axsox17* was maintained at a high level in morphant embryos, whereas expression decreased as expected in uninjected and control morpholino injected embryos. The level of expression in morphant embryos was similar to levels in uninjected embryos on day 2 after injection (late-gastrula).

The spatial expression of *axbrachyury* was examined in hemisectioned embryos collected on day 3 after injection by ISH (**Figure 4.4D**). In uninjected and control morpholino injected embryos expression was detected in the notochord, as expected [Johnson *et al.* 2003b]. In morphant embryos expression was detected in a small region of ectodermal-like tissue adjacent to the endoderm and in a stripe of involuted tissue, resembling a notochord. This suggests that some morphant embryos began gastrulation, forming early mesodermal tissue, but failed to complete it.

These results indicate that morphant embryos were unable to progress beyond an early stage of lineage specification maintaining high levels of *axbrachyury*, *axmix* and *axsox17* similar to a late-gastrula embryo (stage 10.75-12; **Figure 4.4**).

Figure 4.4 Expression of early mesodermal and endodermal genes in morphant embryos

A) Schematic showing temporal expression of *axbrachyury* (mesoderm), *axmix* (endomesoderm) and *axsox17* (endoderm) expression during normal development from the 2-cell stage to stage 40 (late-tailbud). The blue line indicates the stage at which morphant embryos are thought to have halted development. **B)** Schematic showing the expression of *axbrachyury* (pink shading) and *axmix* (yellow shading) at stage 10.75 (late-gastrula). *Axbrachyury* and *axmix* are co-expressed in a region of the ventral mesoderm and expression partially overlaps in the dorsal mesoderm. Morphant embryos are thought to have halted development close to this stage. **C)** Relative expression of *axbrachyury* (top), *axmix* (middle) and *axsox17* (bottom) in splice-morphant and ATG-morphant embryos on day 2 and day 3 after injection as determined by qRT-PCR analysis. Data was analysed using the $2^{-\Delta\Delta C}$T method [Livak and Schmittgen 2001] and was calibrated to expression in the uninjected samples on day 2 after injection. In the splice-morpholino experiment uninjected embryos were approximately stage 10.5-11 (mid-late gastrula) on day 2 and approximately stage 19-22 (late-neurula to early-tailbud) on day 3. Control morpholino injected embryos were slightly delayed by comparison, stage 10-10.75 (early-late gastrula) on day 2 and stage 17-18 (early-neurula) on day 3. In the ATG-morpholino experiment uninjected embryos were approximately stage 10.75-11.5 (late-gastrula) on day 2 and stage 26-30 (early to mid-tailbud) on day 3. Slight perturbations in expression were observed for all three genes on day 2 after injection. In both experiments the expression of *axbrachyury*, *axmix* and *axsox17* was maintained on day 3 after injection whereas it was undetectable in the uninjected and control samples. Differences between the expression in control and uninjected samples can be explained by the observed delay in development. **D)** Spatial expression of *axbrachyury* in morphant embryos. Embryos were collected on day 3 after injection. *In situ* hybridisations were then carried out on hemisectioned embryos. The schematics at the top indicate how the embryos were hemisectioned prior to the *in situ* hybridisation; i) uninjected and control morpholino injected embryos**,** ii) morphant embryo. *Axbrachyury* expression was detected in the notochord of uninjected and control morpholino injected embryos, as expected [Johnson *et al.* 2003b]**.** In morphant embryos expression was detected in a portion of the ectoderm-like tissue adjacent to the endoderm and in a stripe of involuted tissue, which resembled a notochord. Thus, some morphant embryos appear to have commenced gastrulation, but have failed to complete it. **N = Notochord; PN = Presumptive notochord**

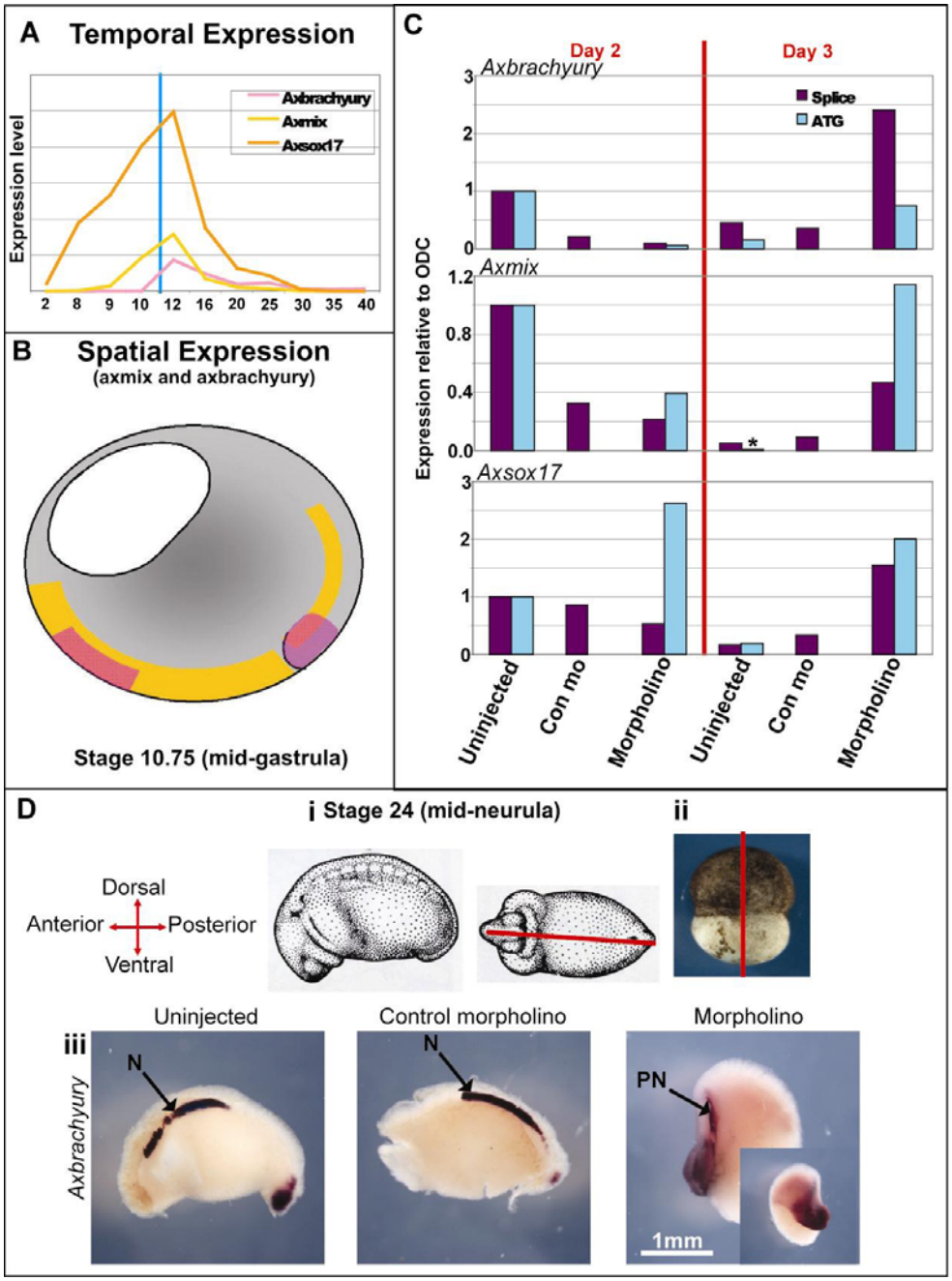
A Temporal Expression
Expression level
Axbrachyury
Axmix
Axsox17
2 8 9 10 12 16 20 25 30 35 40
B Spatial Expression
(axmix and axbrachyury)
Stage 10.75 (mid-gastrula)
C
Day 2
Day 3
Axbrachyury
Axmix
Axsox17
Splice
ATG
Expression relative to ODC
Uninjected
Con mo
Morpholino
Uninjected
Con mo
Morpholino
D
i Stage 24 (mid-neurula)
ii
Dorsal
Anterior
Posterior
Ventral
Uninjected
Control morpholino
Morpholino
iii
Axbrachyury
N
N
PN
1mm

Expression of late mesodermal genes was not activated in morphant embryos

The maintenance of high levels of early mesodermal genes in late-neurula and mid-tailbud morphant embryos suggested that morphant embryos were unable to progress beyond an early stage of lineage-specification. In order to examine the effect of Axnanog depletion on the terminal differentiation of mesoderm, the expression of *ax-α-actin* and *axglobin*, terminal differentiation markers of somitic mesoderm and blood, respectively, was examined by qRT-PCR [Masi *et al.* 2000 ; Johnson *et al*. unpublished; Figure 4.5B].

On day 2 after injection there were no significant differences in expression levels.

On day 3 after injection expression of both genes increased significantly in uninjected embryos, as expected, but only low levels of expression were detected in morphant embryos. Thus, morphant embryos failed to activate the normal developmental program for mesodermal differentiation, having expression levels more similar to late-gastrula uninjected embryos (day 2 after injection). Thus, morphant embryos seem to be unable to progress beyond an early stage of lineage specification.

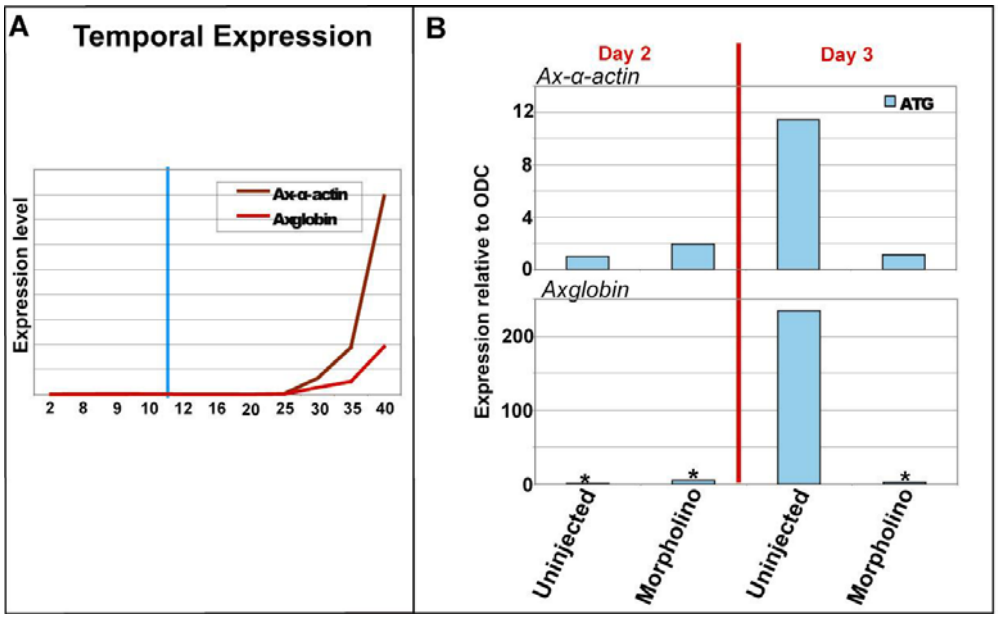

Figure 4.5 Expression of late mesodermal genes in morphant embryos
A) Schematic showing temporal expression of *ax-α-actin,* a marker of somatic mesoderm and *axglobin,* a blood marker, during normal development from the 2-cell stage to stage 40 (late-tailbud). The blue line indicates the stage at which morphant embryos are thought to have halted development. **B)** Relative expression of *ax-α-actin* (top) and *axglobin* (bottom) in ATG-morphant embryos on day 2 and day 3 after injection as determined by qRT-PCR analysis. Data was analysed using the $2^{-\Delta\Delta C}$T method [Livak and Schmittgen 2001] and was calibrated to expression in the uninjected samples on day 2 after injection. Uninjected embryos were approximately stage 10.75-11.5 (late-gastrula) on day 2 and stage 26-30 (early to mid-tailbud) on day 3. Perturbations in expression were not observed on day 2 after injection. On day 3 after injection both genes were expressed at a high level in uninjected embryos but were only expressed at low or background levels in morphant embryos. Thus, morphant embryos failed to activate the normal developmental program for mesodermal differentiation. Background levels of expression are indicated by an asterisk (*).

Expression of late-ectodermal genes was not activated in morphant embryos

In order to determine the effect of Axnanog depletion on the terminal differentiation of ectoderm the expression of *axcytoskeletal keratin* (*axck*), a marker of epidermis, and *axncam*, a marker of neural tissue, was examined by qRT-PCR (**Figure 4.6B**).

On day 2 after injection there were no perturbations in expression.

On day 3 after injection only low or background levels of *axck* and *axncam* were detected in morphant embryos, contrasting with high levels of expression in uninjected and control samples. Expression levels were more similar to those of uninjected embryos on day 2 after injection (late-gastrula). This data lends further support to the proposal that Axnanog depletion inhibits the terminal differentiation of morphant embryos and that they are unable to progress beyond an early stage of lineage specification maintaining an expression profile similar to a late-gastrula embryo (stage 10.75-11).

Spatial expression of *axncam* and *axck* was examined by ISH on hemisectioned embryos collected on day 3 after injection (**Figure 4.6C**). *Axncam* expression was detected throughout the neural tube in uninjected and control morpholino injected embryos, as expected (**Chapter 3**). *Axncam* expression was examined in a morphant embryo both with and without (not shown) neural-fold like structures.

Expression was detected along the edge of the ectodermal-like tissue in the embryo with neural-fold like structures but was not detected in the embryo lacking these structures. This suggests that a small proportion of morphant embryos (18%) were able to form differentiated neural tissue. *Axck* expression was detected throughout the epidermis of uninjected and morphant embryos. Thus, the low levels of expression in morphant embryos may represent a failure to expand the population of *axck* expressing cells rather than a failure to form epidermis, or these cells may represent presumptive epidermis rather than differentiated tissue. The analysis of further epidermal markers is required to distinguish between these two possibilities.

Summary

Axnanog morphant embryos halted at an early stage of development and failed to express the normal developmental program of genes. The expression profile of morphant embryos on day 3 after injection, when uninjected embryos had reached early-mid tailbud stages, was similar to that of late-gastrula uninjected embryos. Morphant embryos maintained high levels of pluripotency genes and genes associated with early lineage-specification, but failed to express mesodermal and ectodermal terminal differentiation markers.

Figure 4.6 Expression of late ectodermal genes in morphant embryos
A) Schematic showing *axncam* (neural) and *axck* (epidermis) temporal expression during normal development from the 2-cell stage to stage 40 (late-tailbud). The blue line indicates the stage at which morphant embryos are thought to have halted development. **B)** Relative expression of *axncam* (top) and *axck* (bottom) in splice-morphant and ATG-morphant embryos on day 2 and day 3 after injection as determined by qRT-PCR analysis. Data was analysed using the $2^{-\Delta\Delta C}$T method [Livak and Schmittgen 2001] and was calibrated to expression in the uninjected samples on day 2 after injection. In the splice-morpholino experiment uninjected embryos were approximately stage 10.5-11 (mid-late gastrula) on day 2 and approximately stage 19-22 (late-neurula to early-tailbud) on day 3. Control morpholino injected embryos were slightly delayed by comparison, stage 10-10.75 (early-late gastrula) on day 2 and stage 17-18 (early-neurula) on day 3. In the ATG-morpholino experiment uninjected embryos were approximately stage 10.75-11.5 (late-gastrula) on day 2 and stage 26-30 (early to mid-tailbud) on day 3. Perturbations in expression were not observed on day 2 after injection. On day 3 after injection in both experiments the two genes were expressed at a high level in uninjected and control samples, but only low levels of expression were detected in morphant embryos. Differences between the expression in control and uninjected samples can be explained by the observed delay in development. **C)** Spatial expression of *axncam* and *axck* in morphant embryos. Embryos were collected on day 3 after injection. *In situ* hybridisations were carried out on hemisectioned embryos. The schematics at the top indicate how the embryos were hemisectioned prior to the *in situ* hybridisations; i) uninjected and control morpholino injected embryos, ii) morphant embryo. *Axncam* Expression (iii) was detected throughout the neural tube of uninjected and control morpholino injected embryos**.** Expression was detected along the edge of the ectodermal-like tissue of a morphant embryo with neural fold-like structures. *Axncam* expression was not detected in embryos lacking neural-fold like structures (not shown). *Axck* expression (iv) was detected throughout the epidermis of uninjected and morphant embryos. **NT=Neural tube; NF = Neural fold; Ect = ectoderm**

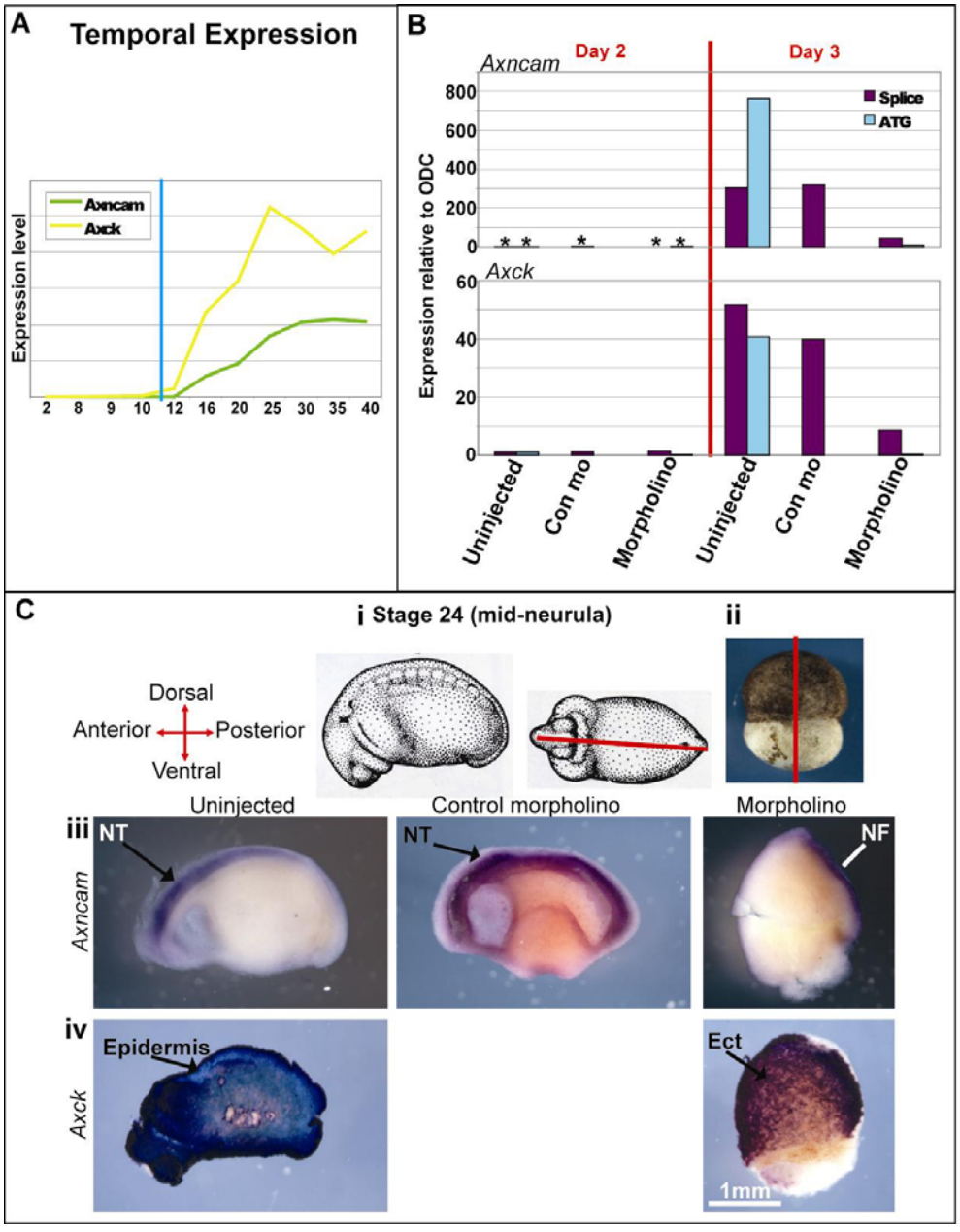
A
Temporal Expression
Axncam
Axck
Expression level
2 8 9 10 12 16 20 25 30 35 40
B
Day 2
Day 3
Axncam
Splice
ATG
Expression relative to ODC
800
600
400
200
0
Axck
60
40
20
0
Uninjected
Con mo
Morpholino
Uninjected
Con mo
Morpholino
C
i Stage 24 (mid-neurula)
ii
Dorsal
Anterior
Posterior
Ventral
Uninjected
Control morpholino
Morpholino
iii
Axncam
NT
NT
NF
iv
Axck
Epidermis
Ect
1mm

4.5 Confirmation of Axoct4 translation-blocking morpholino activity

Preliminary tests were carried out *in vivo* in *Xenopus tropicalis* oocytes to test the activity of an Axoct4 translation-blocking morpholino (**Figure 4.7**). Oocytes were first injected with Axoct4 translation-blocking morpholino or Axmix translation-blocking moroholino. After an overnight incubation they were then injected with full-length HA-tagged Axoct4 mRNA or full-length HA-tagged Axmix mRNA. Oocytes were collected after a further overnight incubation and protein was extracted. A western blot was then carried out to detect the HA-tagged proteins (**Figure 4.7**). The Axoct4 ATG-morpholino caused a complete block to the translation of HA-tagged *axoct4* mRNA but appeared to have no effect on the translation of *axmix* mRNA. The Axmix ATG-morpholino had no effect on the translation of *axoct4* mRNA. This data suggests that the Axoct4 ATG-morpholino specifically targets Axoct4. Further experimentation would be required to confirm these results.

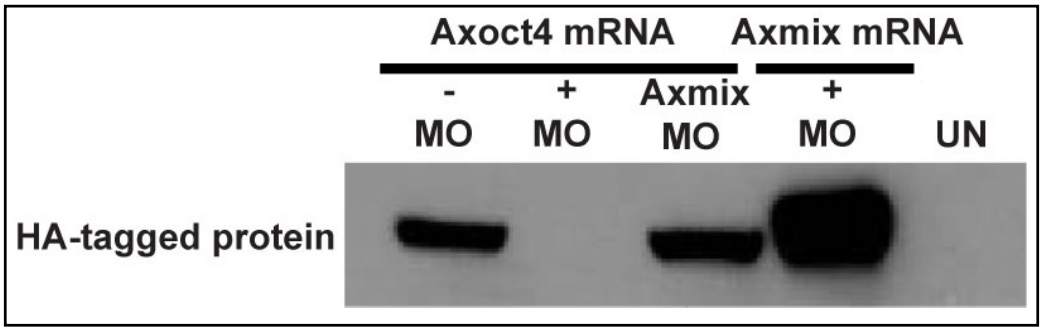

Figure 4.7 Confirmation of activity of Axoct4 translation-blocking morpholino
Western blots to detect hemagluttanin (HA) tagged Axoct4 protein and Axmix protein. *Xenopus tropicalis* oocytes were injected with 80 ng Axoct4 ATG-morpholino or Axmix ATG-morpholino. After overnight incubation they were then injected with full-length HA-tagged *axoct4* mRNA or full-length HA-tagged *axmix* mRNA. Protein was extracted after a further overnight incubation. Each lane of the western blot was loaded with protein equivalent to that in 5 oocytes. **-MO** = mRNA injected alone; **+MO** = mRNA and morpholino injected; **Axmix MO** = Axmix ATG-morpholino and *axoct4* mRNA injected; **UN** = uninjected. The Axoct4 ATG-morpholino effectively blocked the translation of full-length *axoct4* mRNA but had no noticeable effect on the translation of *axmix* mRNA. The Axmix ATG-morpholino did not block the translation of *axoct4* mRNA.

4.6 Axoct4 depletion severely disrupts gastrulation

Embryos were injected at the 1-2 cell stage with 80 or 160 ng of Axoct4 ATG-morpholino. Preliminary data suggests, similarly to Axnanog morphant embryos, Axoct4 depletion severely disrupts gastrulation (**Figure 4.8**). Embryos injected with 80 ng of morpholino gastrulated, but failed to progress beyond early-neurulation. Neural-fold like structures were visible. This phenotype differed from that of Axnanog morphant embryos. However, embryos injected with 160 ng of morpholino exhibited a similar phenotype to Axnanog morphant embryos. Embryos underwent epiboly but failed to form a dorsal lip and the ectoderm subsequently receded so that on day 3 after injection embryos resembled a ball of undifferentiated ectoderm attached to a ball of yolky-endoderm (**Figure 4.8**). This data suggests that Axoct4

and Axnanog may function in the same pathway during early development.

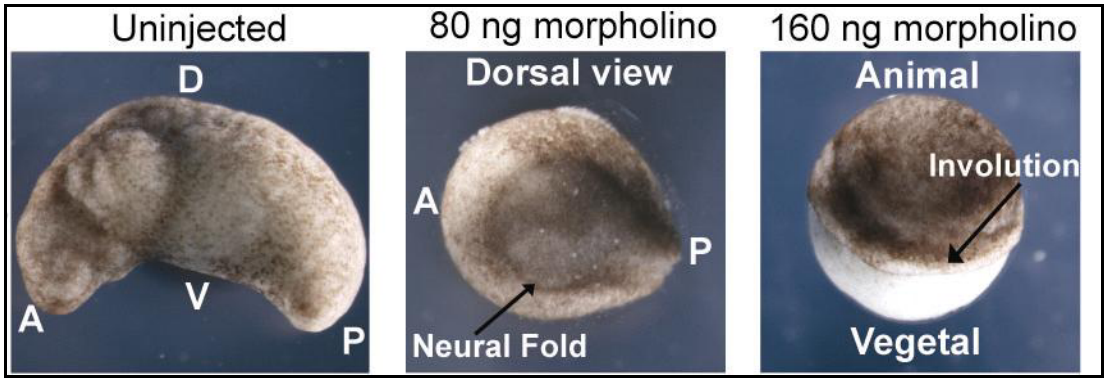

Figure 4.8 Phenotype of embryos injected with Axoct4 ATG-morpholino
Embryos were injected at the 1-2 cell stage with 80 or 160 ng of Axoct4 ATG-morpholino. The images show embryos on day 3 after injection. Uninjected embryos were approximately stage 28 (mid-tailbud). Morphant embryos injected with 80 ng of morpholino exhibited a distinctive phenotype, they gastrulated, but failed to progress beyond an early stage of neurulation. Faint neural-folds are visible. Embryos injected with 160 ng of morpholino exhibited a phenotype similar to Axnanog morphant embryos. The embryos underwent epiboly but failed to form a dorsal-lip. The presumptive ectoderm tissue subsequently receded and similarly to Axnanog morphant embryos they resembled a ball of undifferentiated ectoderm-like tissue attached to a ball of yolky-endoderm. There was an indentation between the ectoderm-like portion and endoderm portion suggesting that similarly to Axnanog morphant embryos some involution had occurred and morphant embryos had started to gastrulate but failed to complete it. **A = Anterior; P = Posterior; D = Dorsal; V = Ventral.**

4.7 Discussion

The role of Nanog in murine embryos and ES cells is well established [Chambers *et al.* 2003; Chambers 2004; Chambers *et al.* 2007]. Nanog has been shown to have a key role in the maintenance of pluripotent cells both *in vivo* and *in vitro*. In Nanog-null mice the pluripotent ICM fails to form and cells adopt an extraembryonic endoderm fate [Mitsui *et al.* 2003]. Nanog homologues have also been shown to have a conserved role in the maintenance of human and chicken pluripotent cells [Hyslop *et al.* 2005; Zaehres *et al.* 2005; Lavial *et al.* 2007]. The identification of Axnanog offered the first opportunity to study the role of Nanog in an anamniote. The expression of *axoct4* and *axnanog* in the undifferentiated tissues of early embryos (**Chapter 3**) suggested that these molecules might have conserved roles in the maintenance of pluripotent/multipotent tissue. In this chapter the function of Axnanog and Axoct4 was investigated using morpholino knock-downs.

Gastrulation was severely disrupted in morphant embryos and they failed to progress beyond an early stage of development; resembling a ball of undifferentiated ectoderm attached to a ball of undifferentiated endoderm with an equatorial region of indentation. The same phenotype was observed with both a splice-morpholino and an ATG-morpholino, providing convincing evidence that the phenotype results from Axnanog depletion rather than off-target effects, although, only a rescue experiment would provide definitive evidence. Expression analysis revealed that pluripotency genes and markers of

early-lineage specification were maintained at high levels in morphant embryos, similar to levels in a late-gastrula embryo, whereas, markers of terminal differentiation were expressed only at low levels. This differs from mouse, where loss of Nanog results in the downregulation of pluripotency markers and the upregulation of differentiation markers, coincident with a failure to maintain the pluripotent cells [Mitsui *et al.* 2003]. Interestingly, neural-fold like structures formed in the animal region of morphant embryos and *axncam* expression confirmed the induction of neural tissue in these embryos. This phenotype occurred more frequently at lower doses, suggesting a dose-dependent effect (not shown). It is notable that *axnanog* expression is downregulated before neural induction during normal development (**Chapter 3**). Thus, neural induction may only require a low level of *axnanog* expression. Additionally, neural crest cells are one of the lineages specified when Nanog is downregulated in mES cells [Ivanova *et al.* 2006].

One explanation for the observed phenotype is that depletion of Axnanog results in cell migration defects that, in effect, disrupt gastrulation. Gastrulation in axolotls begins with much of the presumptive mesoderm in the outer superficial layer, all of which must migrate into the deep layers (**Chapter 3**). Disruption of these cell migration mechanisms may have prevented the formation of terminally differentiated tissues in Axnanog morphant embryos. In support of this hypothesis, a similar phenotype is observed when fibronectin (FN) dependent mesoderm migration is disrupted in Axolotl and *P. waltl*

embryos [Boucaut *et al.* 1985; Darribere and Schwarzbauer 2000]. A FN matrix coats the inner surface of the blastocoel roof from early blastula to late-gastrula [Boucaut *et al.* 1985]. Migrating mesodermal cells interact with this matrix during gastrulation. Disruption of this matrix by injecting a synthetic peptide containing the cell binding sequence of FN or the injection of mutant forms inhibits mesodermal cell migration and disrupts gastrulation [Boucaut *et al.* 1985; Darribere and Schwarzbauer 2000]. The embryos resemble Axnanog morphant embryos, having a non-involuted endodermal mass segregated in the vegetal region, beneath a blastopore-like structure found around the circumference of the embryo, and the blastocoel roof is highly convoluted with deep ectodermal furrows. Furthermore, in some of the Axnanog morphant embryos a bulge of *axbrachyury* expressing cells was visible on the exterior of the embryo (**Figure 4.4iii**), these may be presumptive mesodermal cells that failed to migrate. Depletion of fibroblast growth factors (FGFs) in both *Xenopus* and mouse causes cell migration defects, which in turn disrupts gastrulation and cellular differentiation [Reviewed in Heisenberg and Solnica-Krezel 2008]. In FGF8-null mice a bulge of presumptive mesoderm cells forms where they have failed to migrate through the primitive streak, similarly to those seen in Axnanog morphant embryos [Sun *et al.* 1999]. However, there cannot have been a complete failure in cell migration as some internal Axbrachyury expressing cells were detected (**Figure 4.4iii**) suggesting that some involution had occurred, forming a partial notochord.

An alternative explanation is that in the absence of Axnanog, cells are unable to respond to inducing signals and therefore retain the expression profile of a pluripotent or early differentiating cell. The phenotype and transcription profile of *axnanog* morphant embryos closely resembles that of murine ES cells lacking a component of the NuRD (Nucleosome Remodeling and Histone Deacetylation) co-repressor complex, MBD3 [Kaji *et al.* 2006]. The NuRD complex is an abundant co-repressor complex that is involved in cell-fate decisions in many organisms one example being haematopoietic development in mammals [Ahringer 2000]. MBD3 is a core component of the NuRD complex [Zhang *et al.* 1999]. $MBD3^{-/-}$ ES cells continue to express the pluripotency marker *oct4*, and fail to differentiate in the absence of LIF, a cytokine required for ES cell self-renewal [Kaji *et al.* 2006]. $MBD3^{-/-}$ ES cells, however, are able to form neural tissues in response to retinoic acid, and *brachyury* expression was detected in some cells. In this respect, also, they are similar to *axnanog* morphant embryos [Kaji *et al.* 2006]. Given the similarity between these phenotypes, I propose that during normal embryonic development Axnanog may interact with components of the NuRD complex or other epigenetic modifiers thus regulating epigenetic modifications. Hence, in morphant embryos disruption of this regulation may have rendered Axnanog depleted cells incapable of responding to inducing signals.

The expression of two epigenetic modifiers *axcarm1* and *axmbd3*, was analysed in *axnanog* morphant embryos (not shown). However, the expression of these molecules varied very little in comparison to the uninjected sample. This data suggests that Axnanog does not influence the transcriptional regulation of these maternally expressed epigenetic modifiers but it does not rule out the possibility that it regulates their localisation. Epigenetic modifiers have multiple roles during development and to allow rapid changes in epigenetic modifications, are often regulated by localisation rather than by transcriptional changes [e.g. NODE, Liang *et al.* 2008]. Thus, the localisation of these molecules could be disrupted in morphant embryos.

Interestingly, Chambers *et al*. (2007) proposed that the function of murine Nanog might be to establish epigenetically erased states in pluripotent cells. This was based on the observation that there are genome-wide epigenetic modifications at both time-points when Nanog function is required, establishment of the epiblast [Mitsui *et al.* 2003], and the differentiation of PGCs into mature germ cells [Chambers *et al.* 2007]. Accordingly, gene deletion of epigenetic modifiers typically disrupts the formation of the epiblast [Surani *et al.* 2007]. Interactions have been identified between murine Nanog and multiple epigenetic modifiers, including the NuRD complex and polycomb group factors [Wang *et al.* 2006]. In *C. elegans* development a homologue of the NuRD complex is required for somatic differentiation; in the absence of NuRD, all cells are germline competent, but they cannot form somatic

tissues [Shin and Mello 2003], suggesting that chromatin remodelling by NuRD creates a condition permissive for somatic differentiation. Conversely, polycomb group molecules, another group of chromatin remodelling molecules, are thought to maintain a suitable chromatin configuration in a subset of cells for germline development by modifying the chromatin regulatory regions of targets such as the Hox genes [Shin and Mello 2003]. The germ plasm specific molecule, PIE-1 is thought to interact with the NuRD complex and polycomb group molecules, and thus coordinate the segregation of the somatic cells and germline competent cells. The observed surge of *axnanog* transcription at late-blastula (stage 9) may be required to establish chromatin modifications that ensure somatic differentiation can proceed during gastrulation whilst a subset of cells remain germline competent, similar to the role of PIE-1 in *C. elegans*. Further investigation is required to determine if the underlying cause of the morphant phenotype is a cell migration defect or a block to differentiation. Examining the expression of a greater array of genes in morphant embryos would help to clarify the phenotype. It would also be interesting to test the ability of epigenetic modifiers to rescue the morphant phenotype.

Nanog has not been identified in other anamniotes. However, in prominent model organisms the germline is segregated early in development by the inheritance of maternal molecules (germ plasm) [Extravour and Akam 2003; Johnson *et al.* 2003b]. The inheritance of germ plasm into specific cells results in their segregation into the

germline, whereas in mouse and axolotl PGCs are specified by inductive signals from pluripotent tissues [Sutasurja and Nieuwkoop 1974; McLaren 2003]. It is likely that germ plasm-specific molecules coordinate the epigenetic events that are required to segregate the germline and the soma in these organisms (as in *C. elegans*). In such a context Nanog may become expendable. It is notable that Oct4 function in the maintenance of pluripotent/multipotent cells may also be dispensible in these organisms as evidenced by the divergent role of Pou2 in Zebrafish development [Belting *et al.* 2001; Burgess *et al.* 2002; Reim and Brand 2002; Lunde *et al.* 2004; Reim *et al.* 2004; Reim and Brand 2006].

Preliminary data showed that Axoct4 depletion (160 ng morpholino) severely disrupts gastrulation similarly to that observed in Axnanog morphant embryos. This suggests that Axnanog and Axoct4 might function in the same pathways during early development. The recent identification of the NODE (Nanog and Oct4 associated histone deacetylase) complex in mES cells suggests that Nanog and Oct4 might coordinately regulate epigenetic modifiers [Liang *et al.* 2008]. Thus, I propose that Axnanog and Axoct4 might cooperate in the regulation of epigenetic modifiers during embryonic development. The identification of common targets in mouse and human ES cells supports this hypothesis [Boyer *et al.* 2005; Loh *et al.* 2006]. A*xoct4* introns have been cloned and splice-blocking morpholinos have been designed,

thus, these could be employed in future analyses to confirm the Axoct4 morphant phenotype (**Appendix 8.2**).

Research presented here will provide a good foundation for further investigations into the pluripotency network in axolotls. Future work should focus on developing greater understanding of the Axnanog morphant phenotype. This should include the analysis of the expression of a greater array of marker genes, a demonstration that the phenotype can be rescued and also trying to distinguish between the two possible causes of the gastrulation defect, a cell migration defect or a developmental block.

In order to demonstrate a rescue of the morphant phenotype, Axnanog mRNA, which cannot be bound by the morpholino, must be coinjected with the morpholino. However, all attempts to inject *axnanog* RNA into either axolotl or *Xenopus* embryos (doses ranging from 125 pg to 1 ng) have been lethal (Data not shown); embryos typically survived until MBT. In one of the experiments to test the effect of *axnanog* RNA on *Xenopus laevis* development, *xvent2* (a closely related *Xenopus* homeobox gene) RNA, was also injected at the same doses. Embryos injected with *xvent2* survived and exhibited the expected phenotype [Onichtchouk *et al.* 1998]. This suggests that the fatality in response to *axnanog* RNA is a specific effect. The critical role shown for Axnanog during development could indicate that even small perturbations in expression levels can have a lethal effect. Lower doses of RNA could

be investigated. An alternative to carrying out the rescue in whole embryos, to avoid the lethal effects, would be to attempt the rescue in an animal cap assay (described below).

In order to distinguish between a cell migration defect and a developmental block it is necessary to test the developmental capabilities of cells depleted of Axnanog. Conveniently, mesoderm and endoderm can be induced in axolotl animal caps in response to differing levels of activin mRNA [Johnson *et al.,* unpublished]. The coinjection of the Axnanog morpholino into animal caps would test the ability of Axnanog depleted cells to differentiate into mesoderm and endoderm. This assay could also be extended to test the ability of Axnanog depleted cells to differentiate into other tissue types. For example, PGCs can be induced in animal caps in response to the injection of *Xenopus* eFGF and BMP4 RNA. If the Axnanog depleted caps are able to respond to the inducing signals and form differentiated tissues then the defect is more likely to be the result of a migration defect than a developmental block. If the animal cap assays were to reveal a developmental block, a rescue of this phenotype could then be attempted by coinjecting *axnanog* mRNA, avoiding the lethality of a whole embryo experiment.

An alternative way to test the developmental capabilities of Axnanog depleted cells would be to take cells marked with a lineage tracer from morphant embryos and transplant them into the blastocoel of another

embryo [Technique described in Wylie *et al.* 1985]. The ability of those cells to contribute to the various tissues of the embryo would then be revealed.

4.7.1 Summary

1. *Axnanog* is the first *nanog* homologue to be identified in an anamniote model organism. Its coexpression with *axoct4* in the undifferentiated tissues of early embryos suggested that it along with Axoct4 could have conserved roles in the maintenance of pluripotent/ multipotent tissue.

2. Depletion of Axnanog with antisense morpholino oligonucleotides disrupted gastrulation. The expression of pluripotency genes and markers of early differentiation was maintained whilst terminal differentiation markers were only expressed at low levels. There are two explanations for this, a cell migration defect or a developmental block. Future analyses are required to distinguish between these two possibilities.

3. I proposed that a developmental block could be caused by disruption of epigenetic modifications. Murine Nanog has been shown to interact with multiple epigenetic modifiers. Thus, if Axnanog regulates epigenetic modifications through equivalent interactions, misregulation in Axnanog depleted embryos could result in a developmental block.

To test this theory it would be interesting to try and rescue the morphant phenotype through the injection of RNA encoding epigenetic modifiers.

4. Primary Axoct4 knock-down data revealed a similar morphant phenotype to that that caused by Axnanog depletion. Thus, Axoct4 may function in the same pathway, as suggested in mouse, to coordinately maintain pluripotent/ multipotent tissues.

Chapter 5 Investigating PGC development in axolotl

Primordial germ cells (PGCs) are the precursor cells from which sperm or eggs are derived. It is essential that all sexually reproducing organisms produce germ cells, for without them the enduring genetic link between generations would be lost. How germline fated cells become segregated from somatic cells during development is a fundamental question. In some species, germ cells are specified very early in development by the localisation of maternally inherited determinants, either before or immediately after fertilisation (Preformation; **Figure 5.1A**). In others, germ cells are specified later in development by inductive signals from surrounding tissues (epigenesis; **Figure 5.1B**) [Reviewed in Extravour and Akam 2003]. These two modes of PGC specification are discussed in detail below.

5.1 Preformation

In many species, including the model organisms *Drosophila*, *C. elegans, Xenopus,* zebrafish and chicken, PGCs are specified cell-autonomously by the inheritance of maternal molecules in the form of germ plasm [Houston and King 2000]. Germ plasm is a specific type of cytoplasm, which contains ribosomes, mitochondria, germinal granules and maternally inherited mRNAs and proteins. Early in the development of these organisms germ plasm is segregated into specific cells which will form the PGCs [Houston and King 2000].

Drosophila germ cell specification is perhaps one of the most extensively studied (**Figure 5.1A**). Early in Drosophila development cells initially exist in a cell syncitium i.e. nuclei are not enclosed by cell membranes [Gilbert 2000c]. During the ninth cell division cycle, five nuclei migrate to the posterior pole where they become surrounded by pole plasm (germ plasm). The pole plasm is assembled at the posterior pole of the oocyte before fertilisation [Reviewed in Mahowald 2001]. These nuclei then become enclosed by cell membranes and the pole plasm is segregated into the separate cells [Gilbert 2000c]. The resulting cells, the pole cells, give rise to the PGCs. If the pole plasm is UV irradiated, the pole cells are eradicated [Aboim 1945; Togashi and Okada 1986]. Transplantation of pole plasm to irradiated embryos restores fertility [Okada *et al.* 1974] and transplantation to ectopic sites results in the formation of ectopic PGCs [Illmensee and Mahowald 1974]. Thus, the pole plasm is essential for the formation of the PGCs. Many of the molecular factors contained within Drosophila pole plasm have now been identified and their roles elucidated [Reviewed in Wylie 1999; Jin and Xie 2006].

In *C. elegans* PGCs are specified by maternally inherited electron dense granules termed P-granules, the equivalent of Drosophila pole plasm [Gilbert 2000c]. Unlike Drosophila, the P-granules are scattered throughout the cytoplasm before and just after fertilisation, and then move to the posterior of the embryo during pronuclear fusion [Hird *et al.* 1996]. The germ lineage is progressively segregated from the somatic

lineages through a series of four asymmetric divisions, which segregate the P-granules into the germline blastomeres [Krieg *et al.* 1978; Wolf *et al.* 1983]. At the 16-24 cell stage the P-granules are segregated into the P4 blastomere, the germline precursor [Deppe *et al.* 1978; Strome and Wood 1982]. Many of the molecular regulators of germline development contained within the P-granules have now been identified [Reviewed in Strome and Lehmann 2007].

Anurans were the first vertebrate model organism in which germ plasm was identified [Bounoure 1939]. Maternal determinants are localised during *Xenopus laevis* oogenesis, the germ plasm begins to assemble in stage 2 oocytes at the mitochondrial cloud (Balbiani body) in the vegetal cortex [Reviewed in Kloc *et al.* 2001]. The germ plasm is also localised to the vegetal pole of stage IV and V oocytes and unfertilised eggs. Following fertilisation, the germ plasm forms patchy aggregates in the vegetal hemisphere, which is eventually segregated into the vegetal cells that will become the PGCs [Houston and King 2000; Kloc *et al.* 2001]. As in *C. elegans* the germ plasm is initially segregated asymmetrically into a select few germline blastomeres. At the end of cleavage the 2-6 cells containing germ plasm are the founder cells of the germ line. Ablation of germ plasm in *Xenopus,* by excision or UV irradiation, results in the complete absence of germ cells [Zust and Dixon 1975; Ikenishi and Nieuwkoop 1978]. However, the germ plasm in *Xenopus* appears to be permissive for germ cell fate, and not instructive (as in *Drosophila*). Transplantation of *Drosophila* pole plasm

to an ectopic site, results in the production of PGCs at the site, whereas transplanted germ-lineage blastomeres from *Xenopus* can contribute to all three germ layers. This suggests that *Xenopus* PGCs are not lineage restricted in the same way as *Drosophila* germ cells. [Houston and King 2000].

Germ plasm was first identified in Zebrafish when the localisation of *vasa* mRNA, a germ-line specific molecule, was observed. Prior to this, the origin of zebrafish PGCs was unknown [Olsen *et al.* 1997; Yoon *et al.* 1997]. *Vasa* mRNA is synthesised during oogenesis and localises to the cleavage furrows during the first cleavages [Yoon *et al.* 1997]. The mRNA appears to form clumps, thought to be the germ plasm, which are segregated into four cells at the 32-cell stage. These cells go on to form the PGCs [Yoon *et al.* 1997]. It has since been shown that other germline-specific mRNAs also localise to the cleavage furrows of the 4-cell stage embryo [Koprunner *et al.* 2001; Weidinger *et al.* 2003; Blaser *et al.* 2005; Hashimoto *et al.* 2006; Mishima *et al.* 2006] and some of these genes have been shown to be essential for the normal development of Zebrafish PGCs [Koprunner *et al.* 2001; Weidinger *et al.* 2003]. More recently the localisation of some of the germline determinants has also been observed during oogenesis [Kosaka *et al.* 2007]. Similarly to *Xenopus*, the germline specific mRNAs co-localise with a mitochondrial cloud and are then transported to the vegetal cortex during early oogenesis. Additionally, electron microscopy has identified germinal granule-like structures localised to the cleavage

furrows of 4-cell stage embryos [Knaut *et al.* 2000] and ablation of the cytoplasm at these sites results in the loss of PGCs [Hashimoto *et al.* 2006].

In chicken, as in Zebrafish, potential germ plasm was identified through the analysis of the localisation of a Vasa homologue [Tsunekawa *et al.* 2000]. Chicken Vasa Homolog (CVH) was found to be localised at cleavage furrows at early-cleavage stages, and to a region in oocytes, which also contained material resembling other germ plasm components e.g. the mitochondrial cloud. These observations suggest that chickens have germ plasm [Tsunekawa *et al.* 2000]. However, transplantation experiments are required to prove that this material is responsible for specifying PGCs.

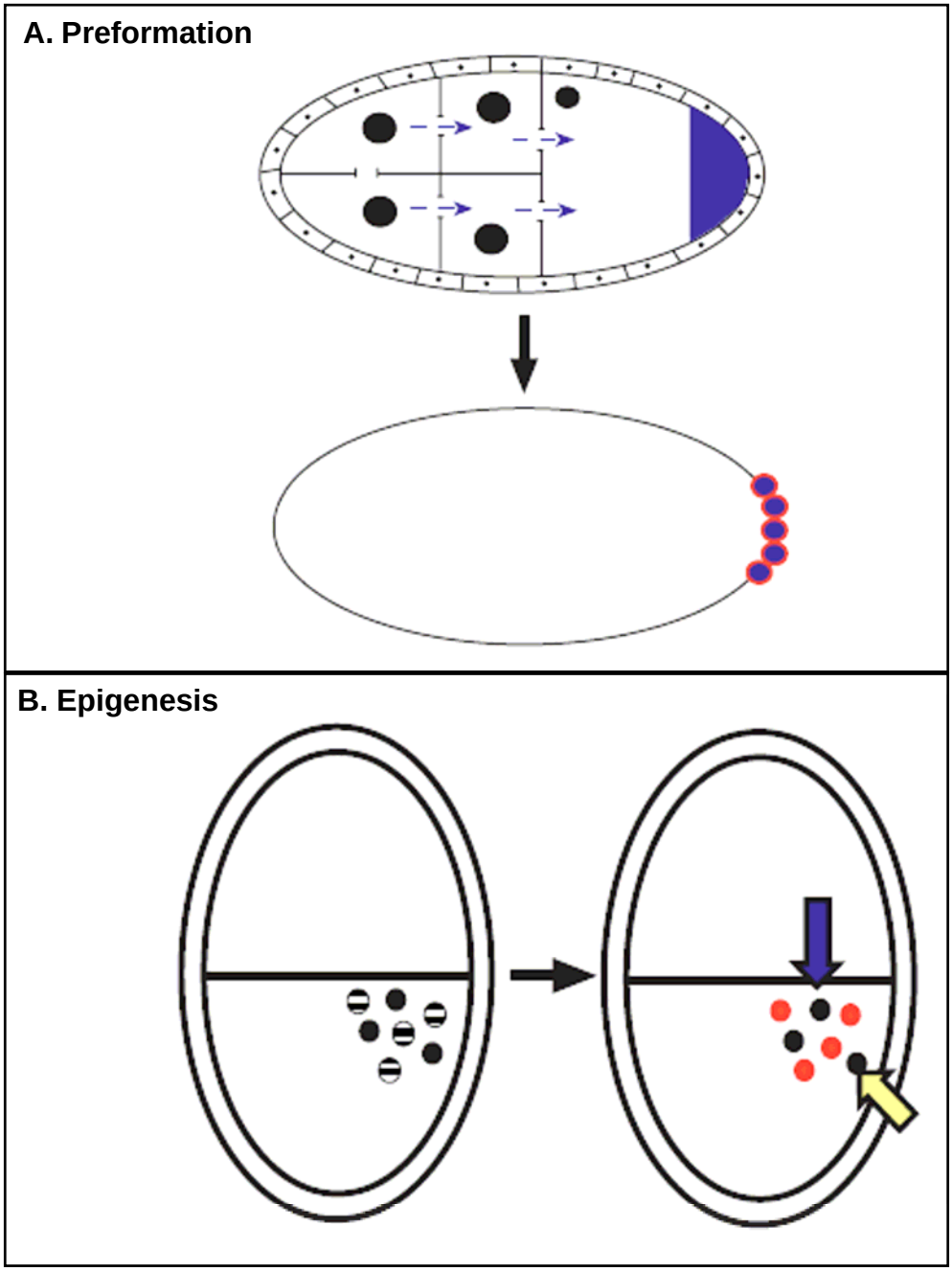

Figure 5.1 Modes of germ cell specification: Preformation and Epigenesis

[Taken from Extravour and Akam 2003] **A)** Schematic representation of preformation in Drosophila. Nurse cells synthesise RNAs and proteins that are transported through cytoplasmic bridges (blue arrows) to the oocyte. They are localised to the posterior of the oocyte forming the germ plasm. During early development, the cells that inherit the germ plasm become the primordial germ cells (PGCs; red). **B)** Schematic representation of epigenesis in mouse. A subpopulation of proximal epiblast cells express 'germ line competence genes' (striped). These cells respond to inductive signals from the neighbouring extraembryonic ectoderm (blue arrow) and extraembryonic endoderm (yellow arrow) and differentiate into PGCs (red).

5.2 Epigenesis

It was once thought that all organisms might specify germ cells *via* preformation. However, germ plasm could not be found within the oocytes or early embryos of mouse and urodeles prior to PGC specification [Eddy 1974, 1975; Ikenishi and Nieuwkoop 1978; Johnson *et al.* 2001]. It has since been shown that these organisms do not contain germ plasm, and instead specify germ cells *via* epigenesis [Watson and Tam 2001; Johnson *et al.* 2003a]. It is now thought that epigenesis may be the most common way in which PGCs are specified and it has been suggested it may be the ancestral mode of PGC specification with many of the basal metazoan organisms appearing to produce PGCs in this way [Extravour and Akam 2003].

In mouse embryos PGCs develop from pluripotent proximal epiblast cells in response to TGF-β (BMP) signals [McLaren 2003; **Figure 5.1B**]. Gene deletion studies have shown that BMP4 and BMP8b signalling from the extra-embryonic ectoderm and BMP2 signalling from the primitive endoderm are all required for the specification of PGCs in mouse [Lawson and Hage 1994; Ying *et al.* 2003]. BMP4 or BMP8b-null embryos lack PGCs, and BMP2-null embryos exhibit a reduction in the number of PGCs [Lawson and Hage 1994; Ying *et al.* 2003]. BMP4 heterozygotes exhibit a haploinsufficiency, with reduced numbers of PGCs, while BMP2 heterozygotes have normal numbers of PGCs. Embryos that are heterozygote mutants for both BMP4 and BMP2 ($BMP4^{+/-}$; $BMP2^{+/-}$) show a greater reduction in PGCs than

heterozygotes with the individual mutations showing that the two molecules have an additive effect on PGC induction [Ying *et al.* 2003]. In addition, it was shown that both BMP4 and BMP8b are required to induce PGCs in cultured epiblast cells [Ying *et al.* 2003]. It is therefore considered that the coordinated action of all three molecules, BMP4, BMP8b and BMP2, is required for PGC induction. Knockouts of the smad genes, smad 1, 4 and 5, downstream components of the TGF-β signalling pathway, also result in a reduction in PGCs [Tremblay *et al.* 2001; Chu *et al.* 2004]. It has been suggested that the BMP molecules may trigger the expression of these smads in the epiblast *via* the type I receptor Alk2 [Brons *et al.* 2007]. Alk2 null-embryos lack PGCs and constitutively active ALK2 can rescue BMP4 null embryos [Brons *et al.* 2007].

Urodele amphibians, including axolotls, are also thought to specify their germ cells *via* epigenesis based on the observation that PGCs can be induced ectopically in animal cap cells [Sutasurja and Nieuwkoop 1974; Johnson *et al.* 2003b]. (The ectopic induction of PGCs in animal caps was described in detail in **Section 1.6**.) However, little is known about the signalling that induces PGCs during normal development.

5.3 Maintenance of PGCs

Following the specification of PGCs, they must be maintained and prevented from responding to somatic inducing signals. In organisms that specify their germ cells *via* preformation, this is achieved by the

early segregation of PGCs, prior to gastrulation *via* the inheritance of maternal molecules in the form of germ plasm. Amongst the germ plasm molecules are transcriptional and translational repressors that prevent the PGCs from responding to somatic inducing signals, thus restricting their developmental potential to the germ cell lineage [Reviewed in Nakamura and Seydoux 2008]. For example, PIE1, an mRNA binding protein, is a maternally inherited molecule that is localised to the germ plasm in *C. elegans* [Mello *et al.* 1996]. Mutations in PIE-1 result in the germ cells assuming a somatic cell fate [Mello *et al.* 1992; Seydoux *et al.* 1996]. PIE-1 mediates the repression of somatic gene expression through several mechanisms. It can bind to mRNA, preventing elongation, or by interfering with other RNA processing events, thus preventing the formation of mature transcripts [Seydoux *et al.* 1996; Seydoux and Strome 1999]. Also, it has been shown to repress somatic gene expression through interactions with epigenetic modifiers [Shin and Mello 2003]. Furthermore, PIE-1 has been shown to promote the expression of other molecules required for maintaining the germline, e.g. nos-2 [Tenenhaus *et al.* 2001].

Similar to PGCs that are specified *via* germ plasm, transcriptional and translational repressors also play a major role in ensuring the maintenance of the germ line in mice [Reviewed in Nakamura and Seydoux 2008]. An essential factor for the maintenance of murine PGCs is the transcriptional regulator named Blimp1 (B-lymphocyte maturation factor I, also known as PRDM1). Blimp1-null embryos lack

PGCs, reflecting a critical role in the development of the PGCs [Vincent *et al.* 2005]. PGCs begin to express Blimp1 as early as E6.25, soon after they are specified and expression continues during migration from the proximal epiblast to the genital ridges, when it is downregulated [Ohinata *et al.* 2005]. PGC-like cells that form in Blimp1-null embryos continue to express Hoxb1 similar to the surrounding mesodermal cells [Ancelin *et al.* 2006]. Thus, it was proposed that Blimp1 functions to maintain the PGCs by repressing somatic gene expression.

Recently, a quantitative single-cell gene expression profiling study was carried out to analyse the transcriptional changes that occur during murine PGC specification [Kurimoto *et al.* 2008]. PGC precursor cells, identified by their expression of *blimp1*, *oct4* and *brachyury,* initially expressed mesodermal genes similarly to neighbouring cells. Subsequently, the expression of the mesodermal genes and many other somatic genes including cell-cycle regulators and epigenetic modifiers was repressed in the PGCs. In addition, PGC-specific genes such as *stella* [Saitou *et al.* 2002]*,* and the pluripotency associated transcription factors *nanog* and *sox2* were upregulated. In order to determine how Blimp1 was involved in modifying transcription in PGCs, expression was also examined in Blimp1-null PGC-like cells. In the absence of Blimp1 the majority of the somatic genes remained active, and there was reduced activation of some PGC specific genes. Thus, Blimp1 appears to be an essential coordinator of the transcriptional changes that occur during PGC specification in mouse, similar to the

role of PIE-1 in *C. elegans* [Tenenhaus *et al.* 2001; Shin and Mello 2003], mediating both repression of somatic gene expression and promoting the expression of PGC specific genes. Blimp1 is thought to mediate repression of target genes by binding to a consensus sequence and recruiting epigenetic modifiers [Kuo and Calame 2004]. Interactions have been identified with multiple epigenetic modifiers, including Groucho [McLaren 1999], HDAC2 [Yu *et al.* 2000], G9a [Gyory *et al.* 2004] and Prmt5 [Vincent *et al.* 2005].

Nanog and Oct4 have also been implicated in the maintenance of murine PGCs post-specification. The only cells that express Oct4 and Nanog after the differentiation of the epiblast are the PGCs [Schöler *et al.* 1989; Yamaguchi *et al.* 2005]. Nanog is expressed in the PGCs from the moment they begin to migrate through the gut, and expression is extinguished once they reach the gonads and begin to differentiate, at the onset of meiosis in females and at the onset of mitotic arrest in males [Yamaguchi *et al.* 2005]. Oct4 is also expressed in PGCs as they proliferate and migrate through the gut [Schöler *et al.* 1989; Yeom *et al.* 1996]. Expression in female PGCs is repressed by the onset of meiosis and is then re-activated after birth, coinciding with the growth phase of oocytes. In male embryos expression persists in germ cells throughout foetal development and is maintained in gonocytes, pro-spermatogonia, and undifferentiated spermatogonia [Pesce *et al.* 1998]. Oct4 depleted ES cells cannot form PGCs in chimeric embryos [Okamura *et al.* 2008]. In addition, gene targeting experiments showed

that Oct4-null PGCs cannot be maintained and consequently undergo apoptosis [Kehler *et al.* 2004]. Nanog however, is required only for the differentiation of PGCs into mature germ cells, once they reach the gonads [Chambers *et al.* 2007].

Axolotl PGC specification shares several similarities with mouse. In both organisms PGCs are mesodermally derived and are specified in response to inductive signals [Sutasurja and Nieuwkoop 1974; McLaren 2003]. However, only two PGC specific molecules have been identified, namely *axdazl* and *axvasa*, which are expressed late in axolotl PGC specification, similarly to mouse [Bachvarova *et al.* 2004]. Molecules that regulate the specification and maintenance of PGCs early in development have not been identified. Based on the similarities between axolotl and mouse PGC specification it was considered that homologous molecules might have a role in the development of axolotl PGCs. In this chapter the roles of *axblimp1, axoct4* and *axnanog* in PGC development are explored through the analysis of expression in oocytes and in animal caps induced to make PGCs (PGC-induced caps).

5.4 Maternal inheritance of pluripotency genes and germ line marker genes

It was shown previously that the pluripotency gene *axoct4* and germline marker gene *axdazl* are maternally inherited and expressed in oocytes [Bachvarova *et al.* 2004]. Temporal and spatial expression data from early embryos suggested that *axblimp1* and *axnanog* were similarly maternally inherited (**Chapter 3; Figures 3.5 and 3.11-13**). To confirm the maternal inheritance of these genes expression was analysed on sections of ovary tissue by *in situ* hybridisation (**Figure 5.2**). Similarly, to *axdazl* and *axoct4*, non-localised expression was detected in the cytoplasm of small oocytes (stage I-II) but was not detected in larger oocytes (IV). Lack of detection in the larger oocytes could be due to the sensitivity of the assay and the dilution of the transcripts in the larger volume of the cytoplasm. The maternal inheritance of *axnanog*, *axoct4* and *axblimp1* suggests that they may have key roles during early development.

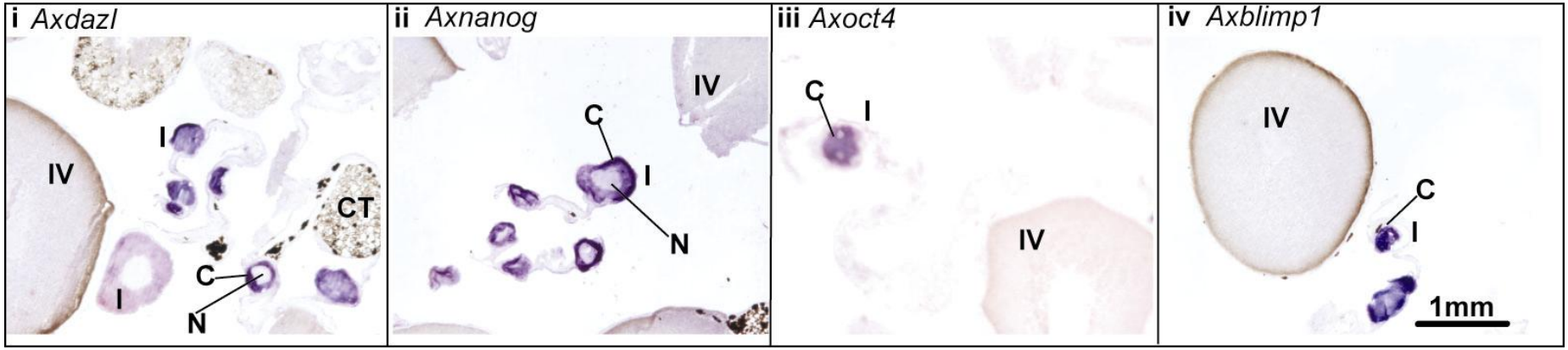

Figure 5.2 Expression of germline and PGC markers in axolotl ovary tissue.
Panels show *in situ hybridisation*s on sections of ovary tissue. Expression of *axdazl* (i), *axnanog* (ii), *axoct4* and *axblimp1* was detected in the cytoplasm of stage I oocytes but was not detected in stage IV oocytes. **N = nucleus; C = Cytoplasm; CT = Connective tissue, I = stage I oocyte, IV = stage IV oocyte**

5.5 The expression of *axoct4*, *axnanog* and *axblimp1* in PGC-induced caps

Axolotl animal caps were injected with *Xenopus* BMP4 and eFGF RNA to induce PGCs (**Section 1.6; Figure 1.3**). Animal caps were collected at stage 11.5 (late-gastrula), stage 28 (mid-tailbud) and stage 42 (late-tailbud). Axolotl PGCs are thought to be specified at late-gastrula during normal development [Sutasurja and Nieuwkoop 1974]. Thus, if *axoct4*, *axnanog* or *axblimp1* were to have a role in PGC specification, an increase in expression levels would be expected in stage 11.5 PGC-induced caps, whereas if they have a role in PGC maintenance an increase in expression might be expected in stage 28 and stage 42 PGC-induced caps.

Increased expression of PGC marker genes, *axdazl* and *axvasa* [Johnson *et al.* 2001; Bachvarova *et al.* 2004] indicated PGC induction in stage 28 and stage 42 PGC-induced caps (**Figure 5.3i and ii**). Additionally, increased expression of *axmix* and *axbrachyury* indicated the induction of PGC precursor tissue, lateral-plate mesoderm, at stages 11.5 and 28 (**Figure 5.3v and vi**). Increased expression of *axdazl* in caps injected with BMP4 alone might be due to mesodermal contamination during cap cutting.

The expression of *axoct4* and *axnanog* in presumptive lateral-plate mesoderm (**Chapter 3**) suggested that they might have roles in PGC specification. However, analysis of expression at stage 11.5 in PGC-induced caps did not reveal a marked increase in the expression

of either gene (**Figure 5.3iii and iv**). Expression of neither gene was detected at stage 28 and stage 42, in agreement with temporal expression data in embryos (**Chapter 3**). Thus, it is unlikely that they have a role in the post-specification maintenance of PGCs, highlighting a difference from murine PGC development in which homologues both have a role in post-specification PGC maintenance.

Axblimp1 expression was not detected in PGCs by *in situ* hybridisation (**Chapter 3**), perhaps due to insufficient assay sensitivity. Analysis of expression in PGC-induced caps revealed a slight increase at stage 28 and stage 42 (**Figure 5.3viii**). These increases may be associated with PGC induction, but it is also possible that they are attributable to the induction of other mesodermal tissues and neural tissues. Coincident with this, there was an almost equivalent increase in stage 42 caps injected with eFGF alone as in the stage 42 PGC-induced caps. Expression of mesodermal markers, *axbrachyury* and *ax-α-actin*, was similarly increased in stage 28 and 42 PGC-induced caps and in stage 42 caps injected with eFGF alone (**Figure 5.3v and vii**). It is notable that *ax-α-actin* is expressed in somites during normal development [Masi *et al.* 2000], a tissue in which *axblimp1* expression was also detected (**Chapter 3**). Expression of *axncam*, a marker of neural tissue (**Chapter 3**), was also increased in stage 28 and 42 PGC-induced caps and in stage 42 caps injected with eFGF alone (**Figure 5.3ix**). Furthermore, extensive expression of *axblimp1* was detected in neural tissues by *in situ* hybridisation. This data does not rule out a role for

axblimp1 in post-specification PGC maintenance but it is unlikely that *axblimp1* has a role at the onset of PGC specification.

In summary, the expression of *axoct4*, *axnanog* and *axblimp1* in PGC-induced caps indicates that they do not have a role in PGC specification but does not rule out a role for *axblimp1* in the post-specification maintenance of PGCs.

Figure 5.3 Analysis of gene expression in PGC-induced animal caps
Panels i-ix show the expression levels of 9 different genes, identified to the right of each chart i) *Axdazl* expression, ii) *Axvasa* expression, iii), *Axnanog* expression, iv) *Axoct4* expression, v) *Axbrachyury* expression vi) *Axmix* expression, vii) *Ax-α-actin* expression, viii) *Axblimp1* expression, ix) *Axncam* expression. Axolotl embryos were injected with 5 ng *Xenopus* BMP4 RNA and 20 pg *Xenopus* eFGF RNA at the 1-2 cell stage to induce PGCs and animal caps were cut at stage 9 (late-blastula). Caps were collected at stage 11.5 (late-gastrula), stage 28 (mid-tailbud) and stage 42 (late-tailbud) (indicated by numbers in red). Uninjected caps were collected at each stage. In addition, at stage 42, caps injected with BMP4 or eFGF were collected. Primary data was analysed using the $2^{-\Delta\Delta C}T$ method [Livak and Schmittgen 2001] and was calibrated to the expression level in uninjected caps at each stage, except for *ax-α-actin* which was calibrated to the expression level in stage 28 uninjected caps as there was no measurable background expression at stage 11.5 in either sample or in uninjected caps at stage 42. Samples exhibiting background levels of expression are indicated with an asterisk (*). (Animal cap processing was carried out by O'Reilly *et al* and expression analysis by the author.)

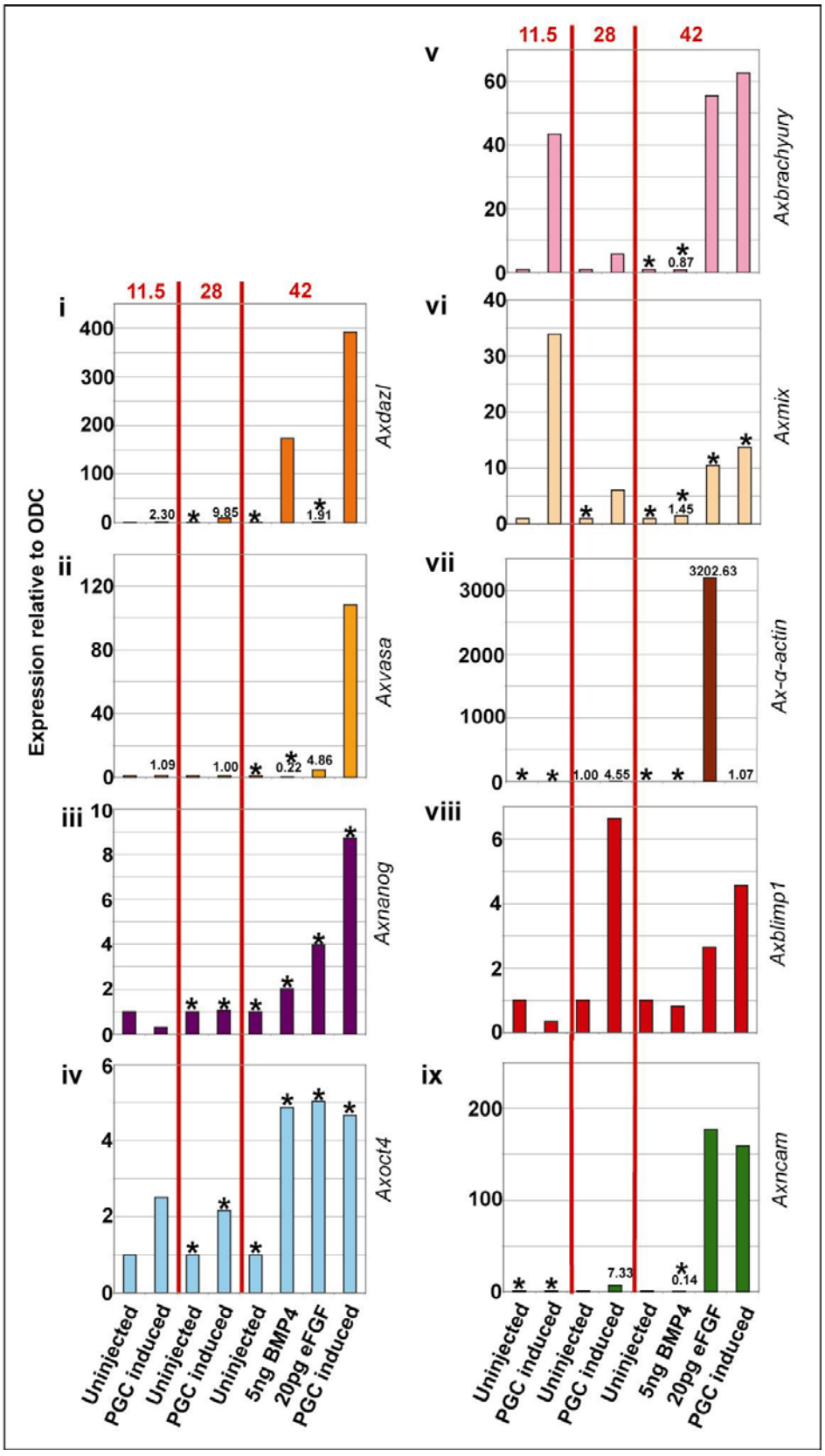
Expression relative to ODC
11.5
28
42
i
Axdazl
2.30
9.85
1.91
ii
Axvasa
1.09
1.00
0.22
4.86
iii
Axnanog
iv
Axoct4
v
Axbrachyury
0.87
vi
Axmix
1.45
vii
Ax-α-actin
3202.63
1.00
4.55
1.07
viii
Axblimp1
ix
Axncam
7.33
0.14
Uninjected
PGC induced
Uninjected
PGC induced
Uninjected
5ng BMP4
20pg eFGF
PGC induced

5.6 Conservation of the maternal inheritance of pluripotency factors

Similarly to axolotl, germ plasm was not identified in the oocytes of the gulf sturgeon, *Ascipenser oxyrhynchus* [Johnson *et al*, unpublished]. *Vasa* and *dazl* homologues, which are commonly localised to the germ plasm, are not localised in sturgeon oocytes suggesting the absence of germ plasm [Johnson *et al*, unpublished]. Thus, it was proposed that PGCs would be specified *via* epigenesis. It was considered that the maternal inheritance of pluripotency factors might be peculiar to organisms that specify their germ cells *via* epigenesis. Thus, a sturgeon *nanog* orthologue, *stnanog*, along with a sturgeon *oct4* orthologue, *stoct4,* were cloned from oocytes [J. Dixon, unpublished]. Following this, *in situ* hybridisations were carried out on sections of sturgeon ovary tissue to analyse the localisation of transcripts (**Figure 5.4**). Similar to observations in axolotl ovary tissue, non-localised expression was detected in the cytoplasm of stage I oocytes. This suggests that the maternal inheritance of pluripotency factors might be conserved amongst anamniotes that specify their PGCs *via* epigenesis.

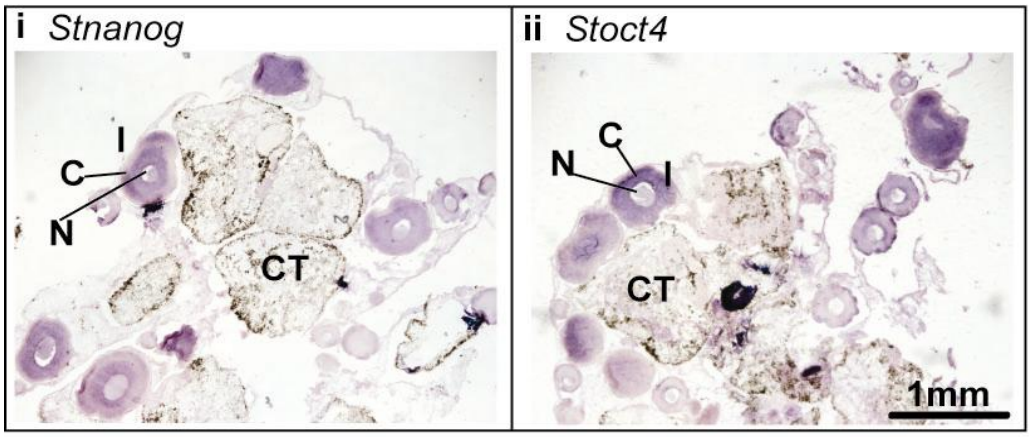

Figure 5.4 Spatial expression of *stnanog* and *stoct4* in ovary tissue
Panels show *in situ hybridisation*s on sections of sturgeon ovary tissue. *Stnanog* (i) and *stoct4* (ii) expression was detected in the cytoplasm of stage I oocytes. **N = nucleus; C = Cytoplasm; CT = Connective tissue, I = stage I oocyte.**

5.7 Discussion

How the germ line is segregated from somatic cells is a fundamental question in developmental biology. There are two known modes of PGC specification, preformation and epigenesis. A common feature of both appears to be the necessity to silence programs of somatic gene expression [Nakamura and Seydoux 2008]. Little is known about the molecular mechanisms governing axolotl PGC development, but given the similarities to murine PGC development it was considered that homologous molecules might be involved. Thus, the roles of *axblimp1*, *axoct4* and *axnanog* in PGC development were investigated.

Murine Blimp1 has been shown to have a critical role in PGC development [Ohinata *et al.* 2005; Vincent *et al.* 2005; Ancelin *et al.* 2006]. It is thought to mediate a program of epigenetic modifications in PGCs, which silences somatic gene expression and promotes a PGC-specific program of expression from the onset of PGC specification (E5.5) [Ancelin *et al.* 2006; Kurimoto *et al.* 2008]. *Axblimp1* expression was not detected in PGCs by *in situ* hybridisation (**Chapter 3**) and expression was not increased in PGC-induced caps at stage 11.5 (late-gastrula), the time when PGCs are believed to be specified. This data suggests that Axblimp1 expression is not required from the onset of PGC specification as in mice. However, it is possible that Axblimp1 has a role at a later stage of PGC development as expression was increased in stage 28 and stage 42 PGC induced caps. These increases may also be attributable to the induction of

mesodermal and neural tissues, in which *axblimp1* expression has been detected by *in situ hybridisation* (**Chapter 3**). Expression was also detected in differentiated germ cells i.e. small oocytes. The absence of *axblimp1* expression in PGCs would be consistent with previous observations that PGC precursor cells in axolotl may be multipotent until a relatively late stage in development [Bachvarova *et al.* 2004]. Bachvarova *et al*. (2004) identified cells co-expressing *axscl*, a blood stem cell marker, and *axdazl*, in an equivalent position to HSCs in *Xenopus* [Walmsley *et al.* 2005]. They suggested a common origin for blood and PGCs. The absence of *axblimp1* expression in PGCs is consistent with the hypothesis that the precursors of axolotl germ cells are multipotent as Blimp1 in murine PGCs is coincident with lineage restriction. In order to definitively rule out a role for Axblimp1 in PGC development it will be necessary to carry out overexpression assays and knock-down experiments. These experiments could be carried out in animal caps to avoid the potentially widespread defects, given the known expression pattern, of whole embryo experiments. For example, an Axblimp1 morpholino could be injected along with RNAs to induce PGCs, in order to measure the effect of an Axblimp1 knock-down on PGC induction directly.

Nanog and Oct4 also have roles in the maintenance of PGCs in mouse [Kehler *et al.* 2004; Chambers *et al.* 2007], thus *axnanog* and *axoct4* expression was also investigated in PGC-induced caps. The data suggests that there is not a conserved role for these molecules in

post-specification PGC maintenance, however, given their expression in the lateral-plate mesoderm, they may be required to maintain a pluripotent/multipotent PGC-precursor tissue. Notably, *axnanog* and *axoct4* expression was detected in differentiated germ cells i.e. small oocytes.

Axnanog is the first orthologue to be identified in an anamniote model organism. Many prominent lower vertebrate model organisms specify their germ cells *via* maternally inherited molecules [Houston and King 2000], germ plasm, as opposed to inductive signalling in mouse and axolotl [Sutasurja and Nieuwkoop 1974; McLaren 2003]. The proposed function of *Axnanog* (**Chapter 4**) is to coordinate the epigenetic events that are required to maintain germ line competent cells whilst also enabling somatic differentiation during embryonic development and I suggested that this function might not be required in organisms that specify their germ cells *via* preformation. Similar to axolotl, germ plasm was not identified in the oocytes of the gulf sturgeon, *Ascipenser oxyrhynchus* [Johnson *et al*, unpublished] and expression of *stnanog* and *stoct4* was detected in small oocytes. This supports the hypothesis that Nanog function is required in organisms that specify their PGCs *via* epigenesis. Interestingly, a *nanog* homologue has been identified in the chicken genome and chickens also specify their germ cells *via* germ plasm. Johnson *et al.* (2003) previously proposed that the specification of PGCs *via* germ plasm early in development might remove an evolutionary constraint, thus, allowing more rapid embryogenesis and

the evolution of novel mechanisms governing development. The removal of this evolutionary constraint might also allow organisms to bypass pluripotency and may be permissive for the loss of *nanog* from the genome. However, the presence of Nanog in the chicken genome suggests loss of *nanog* is not necessary to allow regulative specification of PGCs.

Interestingly, both *nanog* and *oct4* expression was detected in small oocytes in axolotl and sturgeon ovary tissue. The maternal inheritance of Nanog is not conserved in mammals. However, zygotic transcription commences at the two-cell stage in mouse embryos, whereas in anamniotes it does not commence until the blastula stage (MBT). Thus, early development in anamniotes is governed entirely by maternally inherited molecules. The maternal inheritance of Nanog in axolotl and sturgeon embryos may be essential for the early establishment of pluripotent gene expression in the absence of zygotic transcription.

The molecular mechanisms governing axolotl PGC development remain elusive. It is likely that as in other organisms there is a program of molecular events that prevent the PGCs from responding to somatic inducing signals and diverging from the germ line. Future investigations should eliminate the possibility that Blimp1 has a role in axolotl PGC development through functional assays and also examine the function of other candidate molecules. It will be interesting to uncover how divergent the axolotl mode of PGC specification is from mice, especially

given the striking similarities of other developmental processes. Discerning the molecular mechanisms governing PGC development in axolotl could help us to understand the evolution of these mechanisms in mammals.

5.7.1 Summary

1. Axblimp1 expression was not detected in PGCs (**Chapter 3**) and analysis of expression in PGC-induced caps suggested that it does not have a role in PGC specification, but did not rule out a later role in PGC maintenance. Functional analyses are required to eliminate the possibility that Axblimp1 has a role in PGC development.

2. Analysis of *axnanog* and *axoct4* expression in PGC-induced caps suggested that they do not have a role in PGC maintenance as in mouse. However, their expression may be required to maintain the pluripotent tissue from which PGCs are specified. This could be determined in animal cap assays as described in **Chapter 4**.

3. The maternal expression of Nanog is peculiar to the anamniotes in which it has been identified. I proposed that this maternal inheritance may be necessary in anamniotes in order to establish pluripotency as zygotic transcription does not commence until the mid-blastula transition, whereas, in mammals the onset of zygotic transcription is much earlier.

Chapter 6 Overall conclusions

- Axolotls are good model organisms for studying the evolution of developmental processes in amniotes as there are many similarities between the developmental mechanisms in axolotl and mouse. Additionally genes in axolotl are predicted to be 1:1 orthologs with those in humans.

- Cells with pluripotent properties (animal cap cells) were first identified in axolotl embryos. In this study, the cloning and characterisation of *axnanog*, the first *nanog* homologue to be identified in an anamniote model organism was described. *Axnanog* was coexpressed with *axoct4* in the undifferentiated tissues of blastula and gastrula stage embryos, suggesting that these molecules may have a conserved role in pluripotency/multipotency.

- Depletion of Axnanog through the use of antisense morpholino oligonucleotides disrupted gastrulation. Additionally, the expression of pluripotency genes and genes associated with early tissue specification was maintained in morphant embryos, whilst terminal differentiation markers were only expressed at a low level. There are two explanations for this phenotype, a migration defect or a developmental block. Further analyses are required to distinguish between these two possibilities. I proposed that a developmental block might have been caused

by misregulation of epigenetic regulators. Future analyses could consider this possibility.

- Preliminary knock-down data for Axoct4 revealed a similar phenotype to Axnanog morphant embryos, suggesting that these molecules may function in the same pathways during development to regulate pluripotency/multipotency.

- Interestingly, maternal *nanog* expression was detected in both axolotl and sturgeon oocytes. Maternal expression of *nanog* has not been detected in mammals, suggesting that this may be peculiar to anamniotes. I proposed that maternal expression may be necessary to establish pluripotency in anamniotes as zygotic transcription does not commence until MBT, whereas, in mammals the onset of zygotic transcription is much earlier.

- Little is known about PGC development in axolotls. Given that there are similarities between axolotl and mouse PGC specification it was considered that homologous molecules might have a role. The roles of Axoct4, Axnanog and Axblimp1 were investigated. The data suggested that neither Axoct4 nor Axnanog have a role in PGC maintenance but it is possible that their expression is required to maintain the tissue from which PGCs are specified. *Axblimp1* expression was not detected in PGCs by *in situ* hybridisation, but this might be attributable to

assay sensitivity. Analysis of expression in PGC-induced caps suggested that Axblimp1 does not have a role in PGC specification, as in mouse, but it did not rule out a role in PGC maintenance. Further functional analyses are required to definitively ascertain if Axblimp1 has a role in PGC development.

- Much remains to be discerned about both the mechanisms governing pluripotency/multipotency and those governing PGC development in axolotl. The investigations presented here will provide a good foundation for future analyses.

7. References

Aboim, A. N. (1945). Developpement embryonnair et postembryonair des gonades normales et agametiques de *Drosophila melanogaster*. Rev Suisse Zool **52**: 53-154.

Ahringer, J. (2000). NuRD and SIN3 histone deacetylase complexes in development. Trends Genet **16**(8): 351-6.

Amaya, E., T. J. Musci*, et al.* (1991). Expression of a dominant negative mutant of the FGF receptor disrupts mesoderm formation in Xenopus embryos. Cell **66**(2): 257-70.

Amit, M. and J. Itskovitz-Eldor (2006). Maintenance of human embryonic stem cells in animal serum- and feeder layer-free culture conditions. Methods Mol Biol **331**: 105-13.

Ancelin, K., U. C. Lange*, et al.* (2006). Blimp1 associates with Prmt5 and directs histone arginine methylation in mouse germ cells. Nat Cell Biol **8**(6): 623-30.

Arman, E., R. Haffner-Krausz*, et al.* (1998). Targeted disruption of fibroblast growth factor (FGF) receptor 2 suggests a role for FGF signaling in pregastrulation mammalian development. Proc Natl Acad Sci U S A **95**(9): 5082-7.

Ashe, H. L. and J. Briscoe (2006). The interpretation of morphogen gradients. Development **133**(3): 385-94.

Avilion, A. A., S. K. Nicolis*, et al.* (2003). Multipotent cell lineages in early mouse development depend on SOX2 function. Genes Dev **17**(1): 126-40.

Bachvarova, R. F., T. Masi*, et al.* (2004). Gene expression in the axolotl germ line: Axdazl, Axvh, Axoct-4, and Axkit. Dev Dyn **231**(4): 871-80.

Ballycuif, L., C. Goridis*, et al.* (1993). The Mouse Ncam Gene Displays a Biphasic Expression Pattern During Neural-Tube Development. Development **117**(2): 543-552.

Barthels, D., M. J. Santoni*, et al.* (1987). Isolation and nucleotide sequence of mouse NCAM cDNA that codes for a Mr 79,000 polypeptide without a membrane-spanning region. Embo J **6**(4): 907-14.

Barthels, D., G. Vopper*, et al.* (1988). NCAM-180, the large isoform of the neural cell adhesion molecule of the mouse, is encoded by an alternatively spliced transcript. Nucleic Acids Res **16**(10): 4217-25.

Baxendale, S., C. Davison*, et al.* (2004). The B-cell maturation factor Blimp-1 specifies vertebrate slow-twitch muscle fiber identity in response to Hedgehog signaling. Nat Genet **36**(1): 88-93.

Beck, F., T. Erler*, et al.* (1995). Expression of Cdx-2 in the mouse embryo and placenta: possible role in patterning of the extra-embryonic membranes. Dev Dyn **204**(3): 219-27.

Belting, H. G., G. Hauptmann*, et al.* (2001). spiel ohne grenzen/pou2 is required during establishment of the zebrafish midbrain-hindbrain boundary organizer. Development **128**(21): 4165-76.

Blaser, H., S. Eisenbeiss*, et al.* (2005). Transition from non-motile behaviour to directed migration during early PGC development in zebrafish. J Cell Sci **118**(Pt 17): 4027-38.

Bonfanti, L. (2006). PSA-NCAM in mammalian structural plasticity and neurogenesis. Progress in Neurobiology **80**(3): 129-164.

Bordzilovskaya, N. P., T. A. Dettlaff*, et al.* (1989). Developmental-stage series of axolotl embryos. Developmental Biology of the Axolotl. J. B. Armstrong and G. M. Malacinski, Oxford University Press, New York.

Boterenbrood, E. C. and P. D. Nieuwkoop (1973). Formation of Mesoderm in Urodelean Amphibians .5. Its Regional Induction by Endoderm. Wilhelm Roux Archiv Fur Entwicklungsmechanik Der Organismen **173**(4): 319-332.

Botquin, V., H. Hess*, et al.* (1998). New POU dimer configuration mediates antagonistic control of an osteopontin preimplantation enhancer by Oct-4 and Sox-2. Genes Dev **12**(13): 2073-90.

Boucaut, J. C., T. Darribere*, et al.* (1985). Evidence for the role of fibronectin in amphibian gastrulation. J Embryol Exp Morphol **89 Suppl**: 211-27.

Bounoure, L. (1939). L'origine des Cellules Reprodutrices et le Probleme de la Lignee Germinale. Paris, Gauthier-Villars

Bouwmeester, T. (2001). The Spemann-Mangold organizer: the control of fate specification and morphogenetic rearrangements during gastrulation in Xenopus. Int J Dev Biol **45**(1): 251-8.

Boyer, L. A., T. I. Lee*, et al.* (2005). Core transcriptional regulatory circuitry in human embryonic stem cells. Cell **122**(6): 947-956.

Brambrink, T., R. Foreman*, et al.* (2008). Sequential expression of pluripotency markers during direct reprogramming of mouse somatic cells. Cell Stem Cell **2**(2): 151-9.

Brons, I. G., L. E. Smithers*, et al.* (2007). Derivation of pluripotent epiblast stem cells from mammalian embryos. Nature **448**(7150): 191-5.

Brummendorf, T. and F. G. Rathjen (1994). Cell adhesion molecules. 1: immunoglobulin superfamily. Protein Profile **1**(9): 951-1058.

Brummendorf, T. and F. G. Rathjen (1995). Cell adhesion molecules 1: immunoglobulin superfamily. Protein Profile **2**(9): 963-1108.

Burgess, S., G. Reim*, et al.* (2002). The zebrafish spiel-ohne-grenzen (spg) gene encodes the POU domain protein Pou2 related to mammalian Oct4 and is essential for formation of the midbrain and hindbrain, and for pre-gastrula morphogenesis. Development **129**(4): 905-16.

Bylund, M., E. Andersson*, et al.* (2003). Vertebrate neurogenesis is counteracted by Sox1-3 activity. Nat Neurosci **6**(11): 1162-8.

Callery, E. M. (2006). There's more than one frog in the pond: a survey of the Amphibia and their contributions to developmental biology. Semin Cell Dev Biol **17**(1): 80-92.

Cao, Y., S. Knochel*, et al.* (2004). The POU factor Oct-25 regulates the Xvent-2B gene and counteracts terminal differentiation in Xenopus embryos. J Biol Chem **279**(42): 43735-43.

Cao, Y., D. Siegel*, et al.* (2006). Xenopus POU factors of subclass V inhibit activin/nodal signaling during gastrulation. Mech Dev **123**(8): 614-25.

Chambers, I. (2004). The molecular basis of pluripotency in mouse embryonic stem cells. Cloning Stem Cells **6**(4): 386-91.

Chambers, I., D. Colby*, et al.* (2003). Functional expression cloning of Nanog, a pluripotency sustaining factor in embryonic stem cells. Cell **113**(5): 643-55.

Chambers, I., J. Silva*, et al.* (2007). Nanog safeguards pluripotency and mediates germline development. Nature **450**(7173): 1230-4.

Chang, D. H., G. Cattoretti*, et al.* (2002). The dynamic expression pattern of B lymphocyte induced maturation protein-1 (Blimp-1) during mouse embryonic development. Mech Dev **117**(1-2): 305-9.

Chazaud, C., Y. Yamanaka*, et al.* (2006). Early lineage segregation between epiblast and primitive endoderm in mouse blastocysts through the Grb2-MAPK pathway. Dev Cell **10**(5): 615-24.

Chen, S. L., K. A. Loffler*, et al.* (2002). The coactivator-associated arginine methyltransferase is necessary for muscle differentiation: CARM1 coactivates myocyte enhancer factor-2. J Biol Chem **277**(6): 4324-33.

Chu, G. C., N. R. Dunn*, et al.* (2004). Differential requirements for Smad4 in TGF beta-dependent patterning of the early mouse embryo. Development **131**(15): 3501-3512.

Chung, Y., I. Klimanskaya*, et al.* (2006). Embryonic and extraembryonic stem cell lines derived from single mouse blastomeres. Nature **439**(7073): 216-9.

Ciemerych, M. A., D. Mesnard*, et al.* (2000). Animal and vegetal poles of the mouse egg predict the polarity of the embryonic axis, yet are nonessential for development. Development **127**(16): 3467-74.

Colas, J. F. and G. C. Schoenwolf (2001). Towards a cellular and molecular understanding of neurulation. Dev Dyn **221**(2): 117-45.

Conlon, F. L., S. G. Sedgwick*, et al.* (1996). Inhibition of Xbra transcription activation causes defects in mesodermal patterning and reveals autoregulation of Xbra in dorsal mesoderm. Development **122**(8): 2427-35.

Cremer, H., R. Lange*, et al.* (1994). Inactivation of the N-Cam Gene in Mice Results in Size-Reduction of the Olfactory-Bulb and Deficits in Spatial-Learning. Nature **367**(6462): 455-459.

D'Souza, A., M. Lee*, et al.* (2003). Molecular components of the endoderm specification pathway in Xenopus tropicalis. Dev Dyn **226**(1): 118-27.

Daheron, L., S. L. Opitz*, et al.* (2004). LIF/STAT3 signaling fails to maintain self-renewal of human embryonic stem cells. Stem Cells **22**(5): 770-8.

Dale, L., G. Howes*, et al.* (1992). Bone morphogenetic protein 4: a ventralizing factor in early Xenopus development. Development **115**(2): 573-85.

Darr, H., Y. Mayshar*, et al.* (2006). Overexpression of NANOG in human ES cells enables feeder-free growth while inducing primitive ectoderm features. Development **133**(6): 1193-1201.

Darribere, T. and J. E. Schwarzbauer (2000). Fibronectin matrix composition and organization can regulate cell migration during amphibian development. Mech Dev **92**(2): 239-50.

de Souza, F. S., V. Gawantka*, et al.* (1999). The zinc finger gene Xblimp1 controls anterior endomesodermal cell fate in Spemann's organizer. Embo J **18**(21): 6062-72.

Deppe, U., E. Schierenberg*, et al.* (1978). Cell lineages of the embryo of the nematode Caenorhabditis elegans. Proc Natl Acad Sci U S A **75**(1): 376-80.

Ecochard, V., C. Cayrol*, et al.* (1998). A novel Xenopus mix-like gene milk involved in the control of the endomesodermal fates. Development **125**(14): 2577-85.

Eddy, E. M. (1974). Fine structural observations on the form and distribution of nuage in germ cells of the rat. Anat Rec **178**(4): 731-57.

Eddy, E. M. (1975). Germ plasm and the differentiation of the germ cell line. Int Rev Cytol **43**: 229-80.

Edelman, G. M. and K. L. Crossin (1991). Cell adhesion molecules: implications for a molecular histology. Annu Rev Biochem **60**: 155-90.

Eisen, J. S. and J. C. Smith (2008). Controlling morpholino experiments: don't stop making antisense. Development **135**(10): 1735-43.

Evans, M. J. and M. H. Kaufman (1981). Establishment in culture of pluripotential cells from mouse embryos. Nature **292**(5819): 154-6.

Extravour, C. G. and M. Akam (2003). Mechanisms of germ cell specification across the metazoans: epigenesis and preformation. Development **130**: 5869-5884.

Fantes, J., N. K. Ragge*, et al.* (2003). Mutations in SOX2 cause anophthalmia. Nat Genet **33**(4): 461-3.

Fleming, T. P. (1987). A quantitative analysis of cell allocation to trophectoderm and inner cell mass in the mouse blastocyst. Dev Biol **119**(2): 520-31.

Fong, H., K. A. Hohenstein*, et al.* (2008). Regulation of Self-renewal and Pluripotency by Sox2 in Human Embryonic Stem Cells. Stem Cells.

Franz, J. K. and W. W. Franke (1986). Cloning of Cdna and Amino-Acid-Sequence of a Cytokeratin Expressed in Oocytes of Xenopus-Laevis. Proceedings of the National Academy of Sciences of the United States of America **83**(17): 6475-6479.

Fujikura, J., E. Yamato*, et al.* (2002). Differentiation of embryonic stem cells is induced by GATA factors. Genes Dev **16**(7): 784-9.

Gao, X., P. Tate*, et al.* (2008). ES cell pluripotency and germ-layer formation require the SWI/SNF chromatin remodeling component BAF250a. Proc Natl Acad Sci U S A **105**(18): 6656-61.

Gardner, R. L. and J. Rossant (1979). Investigation of the fate of 4-5 day post-coitum mouse inner cell mass cells by blastocyst injection. J Embryol Exp Morphol **52**: 141-52.

Gene-Tools. (2008). Retrieved July 2008.

Gilbert, S. F. (2000a). Early development and axis formation in amphibians. Developmental Biology, Sinauer Associates**:** 303-338.

Gilbert, S. F. (2000b). Early development in selected invertebrates. Developmental Biology, Sinauer Associates**:** 223-261.

Gilbert, S. F. (2000c). The saga of the germ line. Developmental Biology, Sinauer Associates**:** 585-620.

Goridis, C. and J. F. Brunet (1992). NCAM: structural diversity, function and regulation of expression. Semin Cell Biol **3**(3): 189-97.

Graham, V., J. Khudyakov*, et al.* (2003). SOX2 functions to maintain neural progenitor identity. Neuron **39**(5): 749-65.

Gu, L. H. and P. A. Coulombe (2007). Keratin finction in skin epithelia: a broadening palette with surprising shades. Current Opinion in Cell Biology **19**(1): 13-23.

Guo, W., A. P. Chan*, et al.* (2002). A human Mix-like homeobox gene MIXL shows functional similarity to Xenopus Mix.1. Blood **100**(1): 89-95.

Gyory, I., J. Wu*, et al.* (2004). PRDI-BF1 recruits the histone H3 methyltransferase G9a in transcriptional silencing. Nat Immunol **5**(3): 299-308.

Ha, A. S. and R. D. Riddle (2003). *cBlimp-1* expression in chick limb bud development. Gene Expr Patterns **3**(3): 297-300.

Hall, T. (1999). BioEdit: a user-friendly biological sequence alignment editor and analysis program for Windows 95/98/NT. Nucleic Acids Symposium Series **41**: 95-98.

Halpern, M. E., R. K. Ho*, et al.* (1993). Induction of muscle pioneers and floor plate is distinguished by the zebrafish no tail mutation. Cell **75**(1): 99-111.

Hansis, C., J. A. Grifo*, et al.* (2000). Oct-4 expression in inner cell mass and trophectoderm of human blastocysts. Mol Hum Reprod **6**(11): 999-1004.

Hart, A. H., L. Hartley*, et al.* (2002). Mixl1 is required for axial mesendoderm morphogenesis and patterning in the murine embryo. Development **129**(15): 3597-608.

Hashimoto, Y., H. Suzuki*, et al.* (2006). Bruno-like protein is localized to zebrafish germ plasm during the early cleavage stages. Gene Expr Patterns **6**(2): 201-5.

Hauptmann, G. and T. Gerster (1995). Pou-2--a zebrafish gene active during cleavage stages and in the early hindbrain. Mech Dev **51**(1): 127-38.

Hay, D. C., L. Sutherland*, et al.* (2004). Oct-4 knockdown induces similar patterns of endoderm and trophoblast differentiation markers in human and mouse embryonic stem cells. Stem Cells **22**(2): 225-35.

Heisenberg, C. P. and L. Solnica-Krezel (2008). Back and forth between cell fate specification and movement during vertebrate gastrulation. Curr Opin Genet Dev **18**(4): 311-6.

Hemmati-Brivanlou, A. and D. Melton (1997). Vertebrate neural induction. Annu Rev Neurosci **20**: 43-60.

Hemperly, J. J., G. M. Edelman*, et al.* (1986). cDNA clones of the neural cell adhesion molecule (N-CAM) lacking a membrane-spanning region consistent with evidence for membrane attachment via a phosphatidylinositol intermediate. Proc Natl Acad Sci U S A **83**(24): 9822-6.

Henry, G. L. and D. A. Melton (1998). Mixer, a homeobox gene required for endoderm development. Science **281**(5373): 91-6.

Herrmann, B. G. (1991). Expression pattern of the Brachyury gene in whole-mount TWis/TWis mutant embryos. Development **113**(3): 913-7.

Hinkley, C. S., J. F. Martin*, et al.* (1992). Sequential expression of multiple POU proteins during amphibian early development. Mol Cell Biol **12**(2): 638-49.

Hird, S. N., J. E. Paulsen*, et al.* (1996). Segregation of germ granules in living Caenorhabditis elegans embryos: cell-type-specific mechanisms for cytoplasmic localisation. Development **122**(4): 1303-12.

Houston, D. W. and M. L. King (2000). Germ plasm and molecular determinants of germ cell fate. Curr Top Dev Biol **50**: 155-81.

Howley, C. and R. K. Ho (2000). mRNA localization patterns in zebrafish oocytes. Mech Dev **92**(2): 305-9.

Hoyt, P. R., C. Bartholomew*, et al.* (1997). The Evi1 proto-oncogene is required at midgestation for neural, heart, and paraxial mesenchyme development. Mech Dev **65**(1-2): 55-70.

Huang, S. (2002). Histone methyltransferases, diet nutrients and tumour suppressors. Nat Rev Cancer **2**(6): 469-76.

Huang, S., G. Shao*, et al.* (1998). The PR domain of the Rb-binding zinc finger protein RIZ1 is a protein binding interface and is related to the SET domain functioning in chromatin-mediated gene expression. J Biol Chem **273**(26): 15933-9.

Humphrey, R. R. (1925a). The primordial germ cells of Hemidactylium and other Amphibia. J Morphol Physiol **41**: 1–43.

Humphrey, R. R. (1925b). The primordial germ cells of Hemidactyliumand other Amphibia. J Morph Physiol **41**: 1-43.

Hyslop, L., M. Stojkovic*, et al.* (2005). Downregulation of NANOG induces differentiation of human embryonic stem cells to extraembryonic lineages. Stem Cells **23**(8): 1035-43.

Ikenishi, K. and P. D. Nieuwkoop (1978). Location and ultrastructure of primordial germ cells (PGCs) in *Ambystoma mexicanum*. Dev Growth Differ **20**: 1-9.

Illmensee, K. and A. P. Mahowald (1974). Transplantation of posterior polar plasm in Drosophila. Induction of germ cells at the anterior pole of the egg. Proc Natl Acad Sci U S A **71**(4): 1016-20.

Isaacs, H. V., M. E. Pownall*, et al.* (1994). eFGF regulates Xbra expression during Xenopus gastrulation. Embo J **13**(19): 4469-81.

Ivanova, N., R. Dobrin*, et al.* (2006). Dissecting self-renewal in stem cells with RNA interference. Nature **442**(7102): 533-8.

Izumi, N., T. Era*, et al.* (2007). Dissecting the molecular hierarchy for mesendoderm differentiation through a combination of embryonic stem cell culture and RNA interference. Stem Cells **25**(7): 1664-74.

Jacobson, A. G. and J. D. Moury (1995). Tissue boundaries and cell behavior during neurulation. Dev Biol **171**(1): 98-110.

Jacobson, M. and U. Rutishauser (1986). Induction of neural cell adhesion molecule (NCAM) in Xenopus embryos. Dev Biol **116**(2): 524-31.

Jamrich, M., T. D. Sargent*, et al.* (1987). Cell-Type-Specific Expression of Epidermal Cytokeratin Genes During Gastrulation of Xenopus-Laevis. Genes & Development **1**(2): 124-132.

Jenner, R. A. (2006). Unburdening evo-devo: ancestral attractions, model organisms, and basal baloney. Dev Genes Evol **216**(7-8): 385-94.

Jenner, R. A. and M. A. Wills (2007). The choice of model organisms in evo-devo. Nat Rev Genet **8**(4): 311-9.

Jin, Z. and T. Xie (2006). Germline specification: small things have a big role. Curr Biol **16**(22): R966-7.

Johnson, A. D., R. F. Bachvarova*, et al.* (2001). Expression of axolotl DAZL RNA, a marker of germ plasm: widespread maternal RNA and onset of expression in germ cells approaching the gonad. Dev Biol **234**(2): 402-15.

Johnson, A. D., R. J. Cork*, et al.* (1990). H-ras(val12) induces cytoplasmic but not nuclear events of the cell cycle in small Xenopus oocytes. Cell Regul **1**(7): 543-54.

Johnson, A. D., B. Crother*, et al.* (2003a). Regulative germ cell specification in axolotl embryos: a primitive trait conserved in the mammalian lineage. Philosophical Transactions of the Royal Society of London Series B **358**: 1371-1379.

Johnson, A. D., B. Crother*, et al.* (2003b). Regulative germ cell specification in axolotl embryos: a primitive trait conserved in the mammalian lineage. Philos Trans R Soc Lond B Biol Sci **358**(1436): 1371-9.

Johnson, M. H. and J. M. McConnell (2004). Lineage allocation and cell polarity during mouse embryogenesis. Semin Cell Dev Biol **15**(5): 583-97.

Jonas, E., T. D. Sargent*, et al.* (1985). Epidermal Keratin Gene Expressed in Embryos of Xenopus-Laevis. Proceedings of the National Academy of Sciences of the United States of America **82**(16): 5413-5417.

Jones, C. M. and J. C. Smith (1998). Establishment of a BMP-4 morphogen gradient by long-range inhibition. Dev Biol **194**(1): 12-7.

Kaji, K., I. M. Caballero*, et al.* (2006). The NuRD component Mbd3 is required for pluripotency of embryonic stem cells. Nat Cell Biol **8**(3): 285-92.

Kaji, K., J. Nichols*, et al.* (2007). Mbd3, a component of the NuRD co-repressor complex, is required for development of pluripotent cells. Development **134**(6): 1123-32.

Kallies, A., J. Hasbold*, et al.* (2004). Plasma cell ontogeny defined by quantitative changes in blimp-1 expression. J Exp Med **200**(8): 967-77.

Kallies, A., E. D. Hawkins*, et al.* (2006). Transcriptional repressor Blimp-1 is essential for T cell homeostasis and self-tolerance. Nat Immunol **7**(5): 466-74.

Kallies, A. and S. L. Nutt (2007). Terminal differentiation of lymphocytes depends on Blimp-1. Curr Opin Immunol **19**(2): 156-62.

Kehler, J., E. Tolkunova*, et al.* (2004). Oct4 is required for primordial germ cell survival. Embo Reports **5**(11): 1078-1083.

Keller, A. D. and T. Maniatis (1991). Identification and characterization of a novel repressor of beta-interferon gene expression. Genes Dev **5**(5): 868-79.

Kintner, C. R. and D. A. Melton (1987). Expression of Xenopus N-Cam Rna in Ectoderm Is an Early Response to Neural Induction. Development **99**(3): 311-325.

Kishi, M., K. Mizuseki*, et al.* (2000). Requirement of Sox2-mediated signaling for differentiation of early Xenopus neuroectoderm. Development **127**(4): 791-800.

Kloc, M., S. Bilinski*, et al.* (2001). RNA localization and germ cell determination in Xenopus. Int Rev Cytol **203**: 63-91.

Knaut, H., F. Pelegri*, et al.* (2000). Zebrafish vasa RNA but not its protein is a component of the germ plasm and segregates asymmetrically before germline specification. J Cell Biol **149**(4): 875-88.

Kofron, M., C. Wylie*, et al.* (2004). The role of Mixer in patterning the early Xenopus embryo. Development **131**(10): 2431-41.

Kopp, J. L., B. D. Ormsbee*, et al.* (2008). Small increases in the level of sox2 trigger the differentiation of mouse embryonic stem cells. Stem Cells **26**(4): 903-11.

Koprunner, M., C. Thisse*, et al.* (2001). A zebrafish nanos-related gene is essential for the development of primordial germ cells. Genes Dev **15**(21): 2877-85.

Kosaka, K., K. Kawakami*, et al.* (2007). Spatiotemporal localization of germ plasm RNAs during zebrafish oogenesis. Mech Dev **124**(4): 279-89.

Koutsourakis, M., A. Langeveld*, et al.* (1999). The transcription factor GATA6 is essential for early extraembryonic development. Development **126**(9): 723-32.

Krebs, H. A. (1975). The August Krogh Principle: "For many problems there is an animal on which it can be most conveniently studied". J Exp Zool **194**(1): 221-6.

Krieg, C., T. Cole*, et al.* (1978). The cellular anatomy of embryos of the nematode Caenorhabditis elegans. Analysis and reconstruction of serial section electron micrographs. Dev Biol **65**(1): 193-215.

Kuo, T. C. and K. L. Calame (2004). B lymphocyte-induced maturation protein (Blimp)-1, IFN regulatory factor (IRF)-1, and IRF-2 can bind to the same regulatory sites. J Immunol **173**(9): 5556-63.

Kurimoto, K., Y. Yabuta*, et al.* (2008). Complex genome-wide transcription dynamics orchestrated by Blimp1 for the specification of the germ cell lineage in mice. Genes Dev **22**(12): 1617-35.

Latinkic, B. V. and J. C. Smith (1999). Goosecoid and mix.1 repress Brachyury expression and are required for head formation in Xenopus. Development **126**(8): 1769-79.

Lavial, F., H. Acloque*, et al.* (2007). The Oct4 homologue PouV and Nanog regulate pluripotency in chicken embryonic stem cells. Development **134**(19): 3549-63.

Lawson, K. A. and W. J. Hage (1994). Clonal analysis of the origin of primordial germ cells in the mouse. Ciba Found Symp **182**: 68-84; discussion 84-91.

Lee, M. A., J. Heasman*, et al.* (2001). Timing of endogenous activin-like signals and regional specification of the Xenopus embryo. Development **128**(15): 2939-52.

Lee, Y. H., S. A. Coonrod*, et al.* (2005). Regulation of coactivator complex assembly and function by protein arginine methylation and demethylimination. Proc Natl Acad Sci U S A **102**(10): 3611-6.

Lemaire, P., S. Darras*, et al.* (1998). A role for the vegetally expressed Xenopus gene Mix.1 in endoderm formation and in the restriction of mesoderm to the marginal zone. Development **125**(13): 2371-80.

Levi, G., K. L. Crossin*, et al.* (1987). Expression sequences and distribution of two primary cell adhesion molecules during embryonic development of Xenopus laevis. J Cell Biol **105**(5): 2359-72.

Li, J., G. Pan*, et al.* (2007). A dominant-negative form of mouse SOX2 induces trophectoderm differentiation and progressive polyploidy in mouse embryonic stem cells. J Biol Chem **282**(27): 19481-92.

Liang, J., M. Wan*, et al.* (2008). Nanog and Oct4 associate with unique transcriptional repression complexes in embryonic stem cells. Nat Cell Biol.

Livak, K. J. and T. D. Schmittgen (2001). Analysis of relative gene expression data using real-time quantitative PCR and the 2(-Delta Delta C(T)) Method. Methods **25**(4): 402-8.

Loh, Y. H., J. H. Ng*, et al.* (2008). Molecular framework underlying pluripotency. Cell Cycle **7**(7): 885-91.

Loh, Y. H., Q. Wu*, et al.* (2006). The Oct4 and Nanog transcription network regulates pluripotency in mouse embryonic stem cells. Nature Genetics **38**(4): 431-440.

Lunde, K., H. G. Belting*, et al.* (2004). Zebrafish pou5f1/pou2, homolog of mammalian Oct4, functions in the endoderm specification cascade. Curr Biol **14**(1): 48-55.

Magin, T. M., P. Vijayaraj*, et al.* (2007). Structural and regulatory functions of keratins. Experimental Cell Research **313**(10): 2021-2032.

Mahowald, A. P. (2001). Assembly of the Drosophila germ plasm. Int Rev Cytol **203**: 187-213.

Masi, T., M. Drum*, et al.* (2000). Expression of the cardiac actin gene in axolotl embryos. Int J Dev Biol **44**(5): 479-84.

Masui, S., Y. Nakatake*, et al.* (2007). Pluripotency governed by Sox2 via regulation of Oct3/4 expression in mouse embryonic stem cells. Nat Cell Biol **9**(6): 625-35.

McLaren, A. (1999). Signaling for germ cells. Genes Dev **13**(4): 373-376.

McLaren, A. (2003). Primordial germ cells in the mouse. Developmental Biology **262**: 1-15.

McLaren, A. and G. Durcova-Hills (2001). Germ cells and pluripotent stem cells in the mouse. Reproduction Fertility and Development **13**(7-8): 661-664.

Mead, P. E., Y. Zhou*, et al.* (1998). Cloning of Mix-related homeodomain proteins using fast retrieval of gel shift activities, (FROGS), a technique for the isolation of DNA-binding proteins. Proc Natl Acad Sci U S A **95**(19): 11251-6.

Mello, C. C., B. W. Draper*, et al.* (1992). The pie-1 and mex-1 genes and maternal control of blastomere identity in early C. elegans embryos. Cell **70**(1): 163-76.

Mello, C. C., C. Schubert*, et al.* (1996). The PIE-1 protein and germline specification in C. elegans embryos. Nature **382**(6593): 710-2.

Mishima, Y., A. J. Giraldez*, et al.* (2006). Differential regulation of germline mRNAs in soma and germ cells by zebrafish miR-430. Curr Biol **16**(21): 2135-42.

Mitsui, K., Y. Tokuzawa*, et al.* (2003). The homeoprotein Nanog is required for maintenance of pluripotency in mouse epiblast and ES cells. Cell **113**(5): 631-42.

Miyatani, S., J. A. Winkles*, et al.* (1986). Stage-Specific Keratins in Xenopus-Laevis Embryos and Tadpoles the Xk-81 Gene Family. Journal of Cell Biology **103**(5): 1957-1966.

Mizuno, T., M. Kawasaki*, et al.* (2001). Molecular diversity in zebrafish NCAM family: Three members with different VASE usage and distinct localization. Molecular and Cellular Neuroscience **18**(1): 119-130.

Mizuseki, K., M. Kishi*, et al.* (1998). Xenopus Zic-related-1 and Sox-2, two factors induced by chordin, have distinct activities in the initiation of neural induction. Development **125**(4): 579-87.

Morrisey, E. E., Z. Tang*, et al.* (1998). GATA6 regulates HNF4 and is required for differentiation of visceral endoderm in the mouse embryo. Genes Dev **12**(22): 3579-90.

Morrison, G. M. and J. M. Brickman (2006). Conserved roles for Oct4 homologues in maintaining multipotency during early vertebrate development. Development **133**(10): 2011-2022.

Motono, M., T. Ohashi*, et al.* (2008). Analysis of chicken primordial germ cells. Cytotechnology **57**(2): 199-205.

Moury, J. D. and A. G. Jacobson (1989). Neural fold formation at newly created boundaries between neural plate and epidermis in the axolotl. Dev Biol **133**(1): 44-57.

Moury, J. D. and A. G. Jacobson (1990). The origins of neural crest cells in the axolotl. Dev Biol **141**(2): 243-53.

Nakamura, A. and G. Seydoux (2008). Less is more: specification of the germline by transcriptional repression. Development **135**(23): 3817-27.

Newport, J. and M. Kirschner (1982). A major developmental transition in early Xenopus embryos: I. characterization and timing of cellular changes at the midblastula stage. Cell **30**(3): 675-86.

Nichols, J., B. Zevnik*, et al.* (1998). Formation of pluripotent stem cells in the mammalian embryo depends on the POU transcription factor Oct4. Cell **95**(3): 379-91.

Nieuwkoop, P. D. (1947). Experimental investigations on the origin and determination of the germ cells and on the development of the lateral plates and germ ridges in the urodeles. Arch Neer Zool **8**: 1–205.

Nieuwkoop, P. D. (1969). The Formation of the Mesoderm in Urodelean Amphibians I. Induction by the Endoderm. Wilhelm Roux Archiv Fur Entwicklungsmechanik Der Organismen **162**(1): 341-373.

Nieuwkoop, P. D. (2006). What are the key advantages and disadvantages of urodele species compared to anurans as a model system for experimental analysis of early development? Int J Dev Biol **40**: 617-9.

Nishimoto, M., A. Fukushima*, et al.* (1999). The gene for the embryonic stem cell coactivator UTF1 carries a regulatory element which selectively interacts with a complex composed of Oct-3/4 and Sox-2. Mol Cell Biol **19**(8): 5453-65.

Niwa, H. (2007). How is pluripotency determined and maintained? Development **134**(4): 635-46.

Niwa, H., J. Miyazaki*, et al.* (2000). Quantitative expression of Oct-3/4 defines differentiation, dedifferentiation or self-renewal of ES cells. Nat Genet **24**(4): 372-6.

Niwa, H., Y. Toyooka*, et al.* (2005). Interaction between Oct3/4 and Cdx2 determines trophectoderm differentiation. Cell **123**(5): 917-29.

Ohinata, Y., B. Payer*, et al.* (2005). Blimp1 is a critical determinant of the germ cell lineage in mice. Nature **436**(7048): 207-13.

Okada, M., I. A. Kleinman*, et al.* (1974). Restoration of fertility in sterilized Drosophila eggs by transplantation of polar cytoplasm. Dev Biol **37**(1): 43-54.

Okamoto, K., H. Okazawa*, et al.* (1990). A novel octamer binding transcription factor is differentially expressed in mouse embryonic cells. Cell **60**(3): 461-72.

Okamura, D., Y. Tokitake*, et al.* (2008). Requirement of Oct3/4 function for germ cell specification. Dev Biol **317**(2): 576-84.

Okuda, Y., H. Yoda*, et al.* (2006). Comparative genomic and expression analysis of group B1 sox genes in zebrafish indicates their diversification during vertebrate evolution. Dev Dyn **235**(3): 811-25.

Olsen, L. C., R. Aasland*, et al.* (1997). A vasa-like gene in zebrafish identifies putative primordial germ cells. Mech Dev **66**(1-2): 95-105.

Onichtchouk, D., A. Glinka*, et al.* (1998). Requirement for Xvent-1 and Xvent-2 gene function in dorsoventral patterning of Xenopus mesoderm. Development **125**(8): 1447-56.

Palmieri, S. L., W. Peter*, et al.* (1994). Oct-4 transcription factor is differentially expressed in the mouse embryo during establishment of the first two extraembryonic cell lineages involved in implantation. Dev Biol **166**(1): 259-67.

Pan, G. and J. A. Thomson (2007). Nanog and transcriptional networks in embryonic stem cell pluripotency. Cell Res **17**(1): 42-9.

Peale, F. V., Jr., L. Sugden*, et al.* (1998). Characterization of CMIX, a chicken homeobox gene related to the Xenopus gene mix.1. Mech Dev **75**(1-2): 167-70.

Pearce, J. J. and M. J. Evans (1999). Mml, a mouse Mix-like gene expressed in the primitive streak. Mech Dev **87**(1-2): 189-92.

Pedersen, R. A., K. Wu*, et al.* (1986). Origin of the inner cell mass in mouse embryos: cell lineage analysis by microinjection. Dev Biol **117**(2): 581-95.

Pesce, M. and H. R. Schöler (2001). Oct-4: gatekeeper in the beginnings of mammalian development. Stem Cells **19**(4): 271-8.

Pesce, M., X. Wang*, et al.* (1998). Differential expression of the Oct-4 transcription factor during mouse germ cell differentiation. Mech Dev **71**(1-2): 89-98.

Ragge, N. K., B. Lorenz*, et al.* (2005). SOX2 anophthalmia syndrome. Am J Med Genet A **135**(1): 1-7; discussion 8.

Rajasekhar, V. K. and M. Begemann (2007). Concise review: roles of polycomb group proteins in development and disease: a stem cell perspective. Stem Cells **25**(10): 2498-510.

Ralston, A. and J. Rossant (2008). Cdx2 acts downstream of cell polarization to cell-autonomously promote trophectoderm fate in the early mouse embryo. Dev Biol **313**(2): 614-29.

Reim, G. and M. Brand (2002). Spiel-ohne-grenzen/pou2 mediates regional competence to respond to Fgf8 during zebrafish early neural development. Development **129**(4): 917-33.

Reim, G. and M. Brand (2006). Maternal control of vertebrate dorsoventral axis formation and epiboly by the POU domain protein Spg/Pou2/Oct4. Development **133**(14): 2757-70.

Reim, G., T. Mizoguchi*, et al.* (2004). The POU domain protein spg (pou2/Oct4) is essential for endoderm formation in cooperation with the HMG domain protein casanova. Dev Cell **6**(1): 91-101.

Ren, B., K. J. Chee*, et al.* (1999). PRDI-BF1/Blimp-1 repression is mediated by corepressors of the Groucho family of proteins. Genes Dev **13**(1): 125-37.

Robb, L., L. Hartley*, et al.* (2000). Cloning, expression analysis, and chromosomal localization of murine and human homologues of a Xenopus mix gene. Dev Dyn **219**(4): 497-504.

Robertson, E. J., I. Charatsi*, et al.* (2007). Blimp1 regulates development of the posterior forelimb, caudal pharyngeal arches, heart and sensory vibrissae in mice. Development **134**(24): 4335-45.

Rosner, M. H., M. A. Vigano*, et al.* (1990). A POU-domain transcription factor in early stem cells and germ cells of the mammalian embryo. Nature **345**(6277): 686-92.

Roy, S. and T. Ng (2004). Blimp-1 specifies neural crest and sensory neuron progenitors in the zebrafish embryo. Curr Biol **14**(19): 1772-7.

Saiki, R. K., S. Scharf*, et al.* (1985). Enzymatic amplification of beta-globin genomic sequences and restriction site analysis for diagnosis of sickle cell anemia. Science **230**(4732): 1350-4.

Saint-Jeannet, J. P., F. Foulquier*, et al.* (1989a). Expression of N-Cam Precedes Neural Induction in Pleurodeles-Waltlii Urodele Amphibian. Development (Cambridge) **106**(4): 675-684.

Saint-Jeannet, J. P., F. Foulquier*, et al.* (1989b). Expression of N-CAM precedes neural induction in Pleurodeles waltl (urodele, amphibian). Development **106**(4): 675-83.

Saitou, M., S. C. Barton*, et al.* (2002). A molecular programme for the specification of germ cell fate in mice. Nature **418**: 293-300.

Santoni, M. J., D. Barthels*, et al.* (1989). Differential exon usage involving an unusual splicing mechanism generates at least eight types of NCAM cDNA in mouse brain. Embo J **8**(2): 385-92.

Schoenwolf, G. C. and J. L. Smith (1990). Mechanisms of neurulation: traditional viewpoint and recent advances. Development **109**(2): 243-70.

Schoenwolf, G. C. and J. L. Smith (2000). Mechanisms of neurulation. Methods Mol Biol **136**: 125-34.

Schöler, H. R., A. K. Hatzopoulos*, et al.* (1989). A family of octamer-specific proteins present during mouse embryogenesis: evidence for germline-specific expression of an Oct factor. Embo J **8**(9): 2543-50.

Schulte-Merker, S., M. Hammerschmidt*, et al.* (1994). Expression of zebrafish goosecoid and no tail gene products in wild-type and mutant no tail embryos. Development **120**(4): 843-52.

Seydoux, G., C. C. Mello*, et al.* (1996). Repression of gene expression in the embryonic germ lineage of C. elegans. Nature **382**(6593): 713-6.

Seydoux, G. and S. Strome (1999). Launching the germline in Caenorhabditis elegans: regulation of gene expression in early germ cells. Development **126**(15): 3275-83.

Shaffer, A. L., M. Shapiro-Shelef*, et al.* (2004). XBP1, downstream of Blimp-1, expands the secretory apparatus and other organelles, and increases protein synthesis in plasma cell differentiation. Immunity **21**(1): 81-93.

Shapiro-Shelef, M., K. I. Lin*, et al.* (2003). Blimp-1 is required for the formation of immunoglobulin secreting plasma cells and pre-plasma memory B cells. Immunity **19**(4): 607-20.

Shin, T. H. and C. C. Mello (2003). Chromatin regulation during C. elegans germline development. Curr Opin Genet Dev **13**(5): 455-62.

Shook, D. R. and R. Keller (2008a). Epithelial type, ingression, blastopore architecture and the evolution of chordate mesoderm morphogenesis. J Exp Zoolog B Mol Dev Evol **310**(1): 85-110.

Shook, D. R. and R. Keller (2008b). Morphogenic machines evolve more rapidly than the signals that pattern them: lessons from amphibians. J Exp Zoolog B Mol Dev Evol **310**(1): 111-35.

Shook, D. R., C. Majer*, et al.* (2002). Urodeles remove mesoderm from the superficial layer by subduction through a bilateral primitive streak. Dev Biol **248**(2): 220-39.
Small, S. J., G. E. Shull*, et al.* (1987). Identification of a cDNA clone that contains the complete coding sequence for a 140-kD rat NCAM polypeptide. J Cell Biol **105**(5): 2335-45.
Smith, A. (2005). The battlefield of pluripotency. Cell **123**(5): 757-60.
Smith, A. G., J. Nichols*, et al.* (1992). Differentiation inhibiting activity (DIA/LIF) and mouse development. Dev Biol **151**(2): 339-51.
Smith, J. C., B. M. Price*, et al.* (1991). Expression of a Xenopus homolog of Brachyury (T) is an immediate-early response to mesoderm induction. Cell **67**(1): 79-87.
Smith, J. J., S. Putta*, et al.* (2009). Genic regions of a large salamander genome contain long introns and novel genes. BMC Genomics **10**: 19.
Soullier, S., P. Jay*, et al.* (1999). Diversification pattern of the HMG and SOX family members during evolution. J Mol Evol **48**(5): 517-27.
Spemann, H. and H. Mangold (2001). Induction of embryonic primordia by implantation of organizers from a different species. 1923. Int J Dev Biol **45**(1): 13-38.
Stein, S., T. Roeser*, et al.* (1998). CMIX, a paired-type homeobox gene expressed before and during formation of the avian primitive streak. Mech Dev **75**(1-2): 163-5.
Stern, C. D. (2006). Neural induction: 10 years on since the 'default model'. Curr Opin Cell Biol **18**(6): 692-7.
Streit, A., S. Sockanathan*, et al.* (1997). Preventing the loss of competence for neural induction: HGF/SF, L5 and Sox-2. Development **124**(6): 1191-202.
Streit, A. and C. D. Stern (1999). Establishment and maintenance of the border of the neural plate in the chick: involvement of FGF and BMP activity. Mech Dev **82**(1-2): 51-66.
Strome, S. and R. Lehmann (2007). Germ versus soma decisions: lessons from flies and worms. Science **316**(5823): 392-3.
Strome, S. and W. B. Wood (1982). Immunofluorescence visualization of germ-line-specific cytoplasmic granules in embryos, larvae, and adults of Caenorhabditis elegans. Proc Natl Acad Sci U S A **79**(5): 1558-62.
Strumpf, D., C. A. Mao*, et al.* (2005). Cdx2 is required for correct cell fate specification and differentiation of trophectoderm in the mouse blastocyst. Development **132**(9): 2093-102.
Suda, Y., M. Suzuki*, et al.* (1987). Mouse embryonic stem cells exhibit indefinite proliferative potential. J Cell Physiol **133**(1): 197-201.
Sun, X., E. N. Meyers*, et al.* (1999). Targeted disruption of Fgf8 causes failure of cell migration in the gastrulating mouse embryo. Genes Dev **13**(14): 1834-46.
Surani, M. A., K. Hayashi*, et al.* (2007). Genetic and epigenetic regulators of pluripotency. Cell **128**(4): 747-62.
Sutasurja, L. A. and P. D. Nieuwkoop (1974). Induction of Primordial Germ-Cells in Urodeles. Wilhelm Roux Archiv Fur Entwicklungsmechanik Der Organismen **175**(3): 199-220.
Swiers, G. (2008). A single mix gene in the axolotl investigating mesendoderm and blood specification, University of Nottingham.
Tada, M., E. S. Casey*, et al.* (1998). Bix1, a direct target of Xenopus T-box genes, causes formation of ventral mesoderm and endoderm. Development **125**(20): 3997-4006.
Takahashi, K., K. Tanabe*, et al.* (2007). Induction of pluripotent stem cells from adult human fibroblasts by defined factors. Cell **131**(5): 861-72.

Takahashi, K. and S. Yamanaka (2006). Induction of pluripotent stem cells from mouse embryonic and adult fibroblast cultures by defined factors. Cell **126**(4): 663-76.

Takeda, H., T. Matsuzaki*, et al.* (1994). A novel POU domain gene, zebrafish pou2: expression and roles of two alternatively spliced twin products in early development. Genes Dev **8**(1): 45-59.

Tarkowski, A. K. (1959). Experiments on the development of isolated blastomers of mouse eggs. Nature **184**: 1286-7.

Technau, U. (2001). Brachyury, the blastopore and the evolution of the mesoderm. Bioessays **23**(9): 788-94.

Tenenhaus, C., K. Subramaniam*, et al.* (2001). PIE-1 is a bifunctional protein that regulates maternal and zygotic gene expression in the embryonic germ line of Caenorhabditis elegans. Genes Dev **15**(8): 1031-40.

Tesar, P. J., J. G. Chenoweth*, et al.* (2007). New cell lines from mouse epiblast share defining features with human embryonic stem cells. Nature **448**(7150): 196-9.

Thompson, J. D., D. G. Higgins*, et al.* (1994). CLUSTAL W: improving the sensitivity of progressive multiple sequence alignment through sequence weighting, position-specific gap penalties and weight matrix choice. Nucleic Acids Res **22**(22): 4673-80.

Togashi, S. and M. Okada (1986). Effects of UV-irradiation at various wavelengths on sterilising *Drosophila melanogaster*. Dev Growth Differ **25**: 133-141.

Tolkunova, E., F. Cavaleri*, et al.* (2006). The caudal-related protein cdx2 promotes trophoblast differentiation of mouse embryonic stem cells. Stem Cells **24**(1): 139-44.

Torres-Padilla, M. E., D. E. Parfitt*, et al.* (2007). Histone arginine methylation regulates pluripotency in the early mouse embryo. Nature **445**(7124): 214-8.

Tremblay, K. D., N. R. Dunn*, et al.* (2001). Mouse embryos lacking Smad1 signals display defects in extra- embryonic tissues and germ cell formation. Development **128**(18): 3609-3621.

Tsunekawa, N., M. Naito*, et al.* (2000). Isolation of chicken vasa homolog gene and tracing the origin of primordial germ cells. Development **127**(12): 2741-2750.

Tsunoda, Y. and A. McLaren (1983). Effect of various procedures on the viability of mouse embryos containing half the normal number of blastomeres. J Reprod Fertil **69**(1): 315-22.

Tunyaplin, C., M. A. Shapiro*, et al.* (2000). Characterization of the B lymphocyte-induced maturation protein-1 (Blimp-1) gene, mRNA isoforms and basal promoter. Nucleic Acids Res **28**(24): 4846-55.

Turner, C. A., Jr., D. H. Mack*, et al.* (1994). Blimp-1, a novel zinc finger-containing protein that can drive the maturation of B lymphocytes into immunoglobulin-secreting cells. Cell **77**(2): 297-306.

Vincent, S. D., N. R. Dunn*, et al.* (2005). The zinc finger transcriptional repressor Blimp1/Prdm1 is dispensable for early axis formation but is required for specification of primordial germ cells in the mouse. Development **132**(6): 1315-25.

Walmsley, M., A. Ciau-Uitz*, et al.* (2005). Tracking and programming early hematopoietic cells in Xenopus embryos. Methods Mol Med **105**: 123-36.

Wang, J., S. Rao*, et al.* (2006). A protein interaction network for pluripotency of embryonic stem cells. Nature **444**(7117): 364-8.

Wang, S. H., M. S. Tsai*, et al.* (2003). A novel NK-type homeobox gene, ENK (early embryo specific NK), preferentially expressed in embryonic stem cells. Gene Expr Patterns **3**(1): 99-103.

Watanabe, Y., H. Kobayashi*, et al.* (2001). New epidermal keratin genes from Xenopus laevis: hormonal and regional regulation of their expression during anuran skin metamorphosis. Biochimica Et Biophysica Acta-Gene Structure and Expression **1517**(3): 339-350.

Watson, C. M. and P. P. L. Tam (2001). Cell lineage determination in the Mouse. Cell Structure and Function **26**: 123-129.

Wegner, M. and C. C. Stolt (2005). From stem cells to neurons and glia: a Soxist's view of neural development. Trends Neurosci **28**(11): 583-8.

Weidinger, G., J. Stebler*, et al.* (2003). dead end, a novel vertebrate germ plasm component, is required for zebrafish primordial germ cell migration and survival. Curr Biol **13**(16): 1429-34.

Wernig, M., A. Meissner*, et al.* (2007). In vitro reprogramming of fibroblasts into a pluripotent ES-cell-like state. Nature **448**(7151): 318-24.

Whitfield, T., J. Heasman*, et al.* (1993). XLPOU-60, a Xenopus POU-domain mRNA, is oocyte-specific from very early stages of oogenesis, and localised to presumptive mesoderm and ectoderm in the blastula. Dev Biol **155**(2): 361-70.

Willey, S., A. Ayuso-Sacido*, et al.* (2006). Acceleration of mesoderm development and expansion of hematopoietic progenitors in differentiating ES cells by the mouse Mix-like homeodomain transcription factor. Blood **107**(8): 3122-30.

Wilm, T. P. and L. Solnica-Krezel (2005). Essential roles of a zebrafish prdm1/blimp1 homolog in embryo patterning and organogenesis. Development **132**(2): 393-404.

Winkles, J. A., T. D. Sargent*, et al.* (1985). Developmentally Regulated Cytokeratin Gene in Xenopus-Laevis. Molecular and Cellular Biology **5**(10): 2575-2581.

Wolf, N., J. Priess*, et al.* (1983). Segregation of germline granules in early embryos of Caenorhabditis elegans: an electron microscopic analysis. J Embryol Exp Morphol **73**: 297-306.

Wylie, C. (1999). Germ Cells. Cell **96**: 165-174.

Wylie, C. C., S. Holwill*, et al.* (1985). Germ plasm and germ cell determination in Xenopus laevis as studied by cell transplantation analysis. Cold Spring Harb Symp Quant Biol **50**: 37-43.

Xu, C., M. S. Inokuma*, et al.* (2001). Feeder-free growth of undifferentiated human embryonic stem cells. Nat Biotechnol **19**(10): 971-4.

Yamaguchi, S., H. Kimura*, et al.* (2005). Nanog expression in mouse germ cell development. Gene Expr Patterns **5**(5): 639-46.

Yeom, Y. I., G. Fuhrmann*, et al.* (1996). Germline regulatory element of Oct-4 specific for the totipotent cycle of embryonal cells. Development **122**(3): 881-94.

Ying, Q. L., J. Nichols*, et al.* (2003). BMP induction of Id proteins suppresses differentiation and sustains embryonic stem cell self-renewal in collaboration with STAT3. Cell **115**(3): 281-92.

Yoon, C., K. Kawakami*, et al.* (1997). Zebrafish vasa homologue RNA is localized to the cleavage planes of 2- and 4-cell-stage embryos and is expressed in the primordial germ cells. Development **124**(16): 3157-65.

Yu, J., C. Angelin-Duclos*, et al.* (2000). Transcriptional repression by blimp-1 (PRDI-BF1) involves recruitment of histone deacetylase. Mol Cell Biol **20**(7): 2592-603.

Yuan, H., N. Corbi*, et al.* (1995). Developmental-specific activity of the FGF-4 enhancer requires the synergistic action of Sox2 and Oct-3. Genes Dev **9**(21): 2635-45.

Zaehres, H., M. W. Lensch*, et al.* (2005). High-efficiency RNA interference in human embryonic stem cells. Stem Cells **23**(3): 299-305.

Zernicka-Goetz, M. (1998). Fertile offspring derived from mammalian eggs lacking either animal or vegetal poles. Development **125**(23): 4803-8.

Zernicka-Goetz, M. (2006). The first cell-fate decisions in the mouse embryo: destiny is a matter of both chance and choice. Curr Opin Genet Dev **16**(4): 406-12.

Zhang, Y., H. H. Ng*, et al.* (1999). Analysis of the NuRD subunits reveals a histone deacetylase core complex and a connection with DNA methylation. Genes Dev **13**(15): 1924-35.

Zhao, S., J. Nichols*, et al.* (2004). SoxB transcription factors specify neuroectodermal lineage choice in ES cells. Mol Cell Neurosci **27**(3): 332-42.

Zust, B. and K. E. Dixon (1975). The effect of u.v. irradiation of the vegetal pole of Xenopus laevis eggs on the presumptive primordial germ cells. J Embryol Exp Morphol **34**(1): 209-20.

8. Appendices

8.1 Nucleotide Sequences

Full nucleotide sequences obtained during the study are shown below. Regions highlighted in blue represent the fragments used as ISH probes. *Axnos1* sequence was obtained by screening a stage 10.5 (mid-gastrula) cDNA library with a fragment obtained previously by degenerate PCR. *Axpumilo* sequences were both obtained by screening the same library with a fragment of the *Xenopus pumilio* homologue (*Xpum*: AB045628). Further *axpumilio2* sequence was obtained by 5' RACE. Regions highlighted in red are ORFs.

Axcarm1

```
TCGATTATCGGGGACGCGAACGGTGAGATCNAGCGGCACGCCGAGCAGCAGGCCCTGCGGCTGGAGGTCCGGGGGACGCCCGAAGCGGCGCTCATCGCTC 100
TCTACAGCCACGAAGATGTGTGCGTATTTAAGTGTTCGGTGTCCCGTGAAACTGAGTGCAGTCGAGTCGGCAAGCAGTCTTTTATTGTCACATTGGGCTG 200
CAATAGTGTCCTCATACAATTTGCAACGCCCAATGATTTTTGCTCTTTTTATAATATCCTCAAGAACTGCCGGGGCCACAACTCTGAGCGGTCCGTCTTC 300
AGTGAGCGGACGGAGGAGTCGTCAGCTGTTCAGTATTTCCAGTTCTATGGGTATCTATCACAGCAACAGAACATGATGCAGGATTATGTACGGACAGGGA 400
CGTACCAGAGGGCTATCCTGCAGAACCATGCAGATTTTAAAGATAAAGTTGTATTAGATGTTGGGTGTGGCTCCGGAATCCTGTCCTTTTTTGCAGCACA 500
GGCCGGAGCCAGAAAAGTCTATGCAGTGGAGGCCAGTACAATGGCGCAACATGCTGAGCTTTTAGTAAAAAGCAATAACCTCACCGACCGGATTCTGGTA 600
ATCCCAGGGAAGGTAGAGGAGATCTCGCTCCCGGAGCAGGTGGACATAATCATCTCGGAGCCCATGGGCTACATGCTCTTTAATGAGCGCATGCTGGAGA 700
GTTACTTGCACGCCAAGAAGTTCTTAAGGCCTAATGGTAACATGTTCCCCACTATTGGCGATGTTCATCTGGCTCCCTTCACTGACGAGCAGCTCTACAT 800
GGAGCAGTTTACGAAGGCCAACTTCTGGTATCAGCCGTCCTTCCACGGAGTGGATTTATCTGTTCTTAGAGGTGCTGCAGTGGATGAATATTTCAAGCAG 900
CCTGTTGTGGATACCTTTGATATCCGGATTTTAATGGCAAAGTCCGTTAAATATACAGTGAATTTCCTGGATGCCAAGGAATGTGATTTGCACAGGATAG 1000
AGATACCCTTCAAGTTTCACATGTTGCACTCTGGTTTGGTGCATGGCCTGGCGTTCTGGTTTGACGTGGCTTTCATTGGTTCAATAATGACGGTCTGGCT 1100
CTCCACTGCACCCACAGAGCCGTTGACACACTGGTACCAAGTACGCTGCCTACTCCAGTCACCACTATTTACAAAAGCAGGTGACACTCTCTCGGGGACT 1200
GTCCTCCTTATAGCTAACAAAAGACAAAGTTACGACATCAGTATTGTAGCCCAGGTGGATCAGACTGGTTCCAAGTCAAGCAATCTCCTCGACTTGAAAA 1300
ACCCCTTTTTCAGGATGCCTACTGCTTATGACCTCAGTGGAGTAATGGGCGGCGGTTCCACCATTGGACACAACAATCTGATTCCTTTAGGATCTGCTGG 1400
TGGCCAGGGCGGAGGCAATTCAAGCACCCACTACCCCGTCAACAGCCAGTTCACAATGGGCGGACCCGCGATCTCTATGGCATCACCAATGTCCATCACC 1500
ACCAACACAATGCACTACGGGAGC 1524
```

Axncam

```
ATGCTGCATACTCAGGATCTCATCTGGACTTGGCTTTTGCTGGGAACCGCAGTCTGTATTCAGGTGAACGTTGTGCCAAACCAGGTAGACGTCGATGTGG 100
GAGAGTCCAAGTTCTTCTCATGCCAAGTAACGGGTGGGGAAGCCAAAGATATATTCTGGTTTGCCCCAAGTGGAGAGAAGATTGATTCAAATCAACAGGA 200
GCTATCAGTTATACGAAATGATGAGGTGTCATCCACGCTTTCTATCTACAATGTTGACATCGATGACGCCGGTATCTACAAATGTGTTGCCACGACCGAA 300
GGGGAGGGAGAAGTGGAAGCTACTGTTAATGTGCAAATTTACCAAAAAATGATTTTCAAGAATGCACCTTCACCCCAAGAATTTACAGAAGGAGAAGATG 400
CGGTTGTCATTTGTGATGTCAGCAGCGTACAGACGCCTTCGATAATGTGGAAGCACAAAAACCGAGATGTTGTCCTTAAAAAAGACGTCCGATTTGTTGT 500
CTTGACCAACAACTACTTGCAGATCCGAGGAATTAAGAAAACAGACGAAGGGGAGTACCGCTGTGAGGGGAGGATCCTGGCACGTGGGGAGATCGCCTTC 600
AGGGATATCCAAGTGGTTGTGAATGTTGCCCCCGTTGTCCGGGCTCTACAGAGTACTGTCAATGCTACAGCAAACCTTGGGGAATCCGCTATCTTGGCAT 700
GTGCTGCTGAAGGATTTCCTGACCCAGAGATAAGTTGGACAAAGGAAGGTGAAATGATTGAAGAAGACAGTGACAAATACAAGTTCACCGAAGATGGCTC 800
CCAGATGACCATCTTCAAGGTGGACAAGAGCGATGAAGGGGATTATACTTGCATTGCAGAGAATAAGGCCGGCGAGCAAGAAGCATCTATTCTCCTGAAA 900
GTCTACGCAAAGCCCAAGATCACATATGTGGAGAACAAAACAGCCATGGAACTGGAGGAACAGATCACTCTGACGTGCGAGGCCACAGGCGACCCCACAC 1000
CAAGCATCACCTGGAGAATGGCGACAAGGAACATCAGCAGCGAAGAAAAGACTCTGGATGGACGTATCGTGGTGAGCAGTCACGCCAGGGTCTCGTCTCT 1100
CACGTTGAACGACATTCAGTACACCGATGCGGGGGAGTACTTCTGCATTGCGAGCAACACCATTGGACAGGACTCTCAGGCCATGTACCTCGAAGTGCAG 1200
TATGCCCCTAAGTTGCAAGGCCCAATTGCCGTTTACACCTGGGAAGGGAACGCAGTCAATATCACCTGTGAGGTCTTCGCTTACCCCAGCGCCGTCATTT 1300
CTTGGTTCCGAGATGGGCAGGCCCTGCCAAGCTCCAACTACAGCAACATCAAGATATACAGCACCCCATCTGCAAGCTTCTTGGAGGTTGTTCCAGATTC 1400
TGAAAATGATTTTGGCAACTACAACTGCACCGCCATCAACCGCATTGGCCAGGATTCTTCCGAGTTTATCCTAGTTCAAGCAGACACTCCATCCTCTCCT 1500
TCCATTCTGAAGTTGGACCCTTACTCCAGCAGTGCCAAGATTGAGTTTGACGAGCCTGATGCCACTGGTGGAGTGCCCATCCTGAAGTACCGTGCCGAGT 1600
GGAAAGCGGTCACTGATGAGGAGTGGAGCTCTAGAATGTATGATGCCAAGGAAGCGAGCATCGAAAATGCAGTCACCATTGTAGGCCTGAAACCGGAGAC 1700
ATTTTATGCAGTGCGACTATCCGCCATCAACGGCAAAGGCTTGGGAGAGTACAGCTCGATATCAAAGTTCCAAACTCAGCCCGTCCAAGGGGAACCCAGT 1800
GCTCCAAAGCTGGATGGACAGATGGGAGAGGACGGAAACTCCATAAAAGTGAACCTAATCAAGCAAGATGATGGAGGATCCCCAATCAGGCACTATCTGG 1900
TTACGTACCGAGCAAAAAATGCTCTTGAATGGAAACCAGAAATTAAAGTTCCTTCTGGTAGCAACCACGTCATGCTCAAAGCTCTAGACTGGAATGCAGA 2000
ATACGAAGTCTTTGTGATAGCCGAAAACCAGCAAGGCAAATCGAAACCGGCCAGCTTCTCCTTCAGGACTCTCGCCCAGCCCACTGCCATTCCAGCAGGT 2100
CCAAGCCATGGTTCCGGGCTGGGCACTGGTGCCATCGTGGGTATCCTGATCATCGTGTTTGTCATCCTCCTGGTCGTGGTTGACGTCACCTGCTACTTCC 2200
TGAACAAGTGTGGCCTGTTGATGTGCATCGCCGTGAACCTGTGCGGCAAATCCGGCCCAGGAGCAAAGGGCAAAGACATTGAAGAGGGGAAAGCCGCCTC 2300
CTCGAAAGACGAATCTAAGGAGCCCATTGTGGAAGTGAGGACGGAAGAAGAGAGGACCCCAAACCACGACGGAGGCAACCAGACCGAACCCAATGAAACC 2400
ACTCCGTTAACAGAACCTGAGAAGGCCCCTGTAGAAGAAAACTCCAAGCCCGAAGATACGGAAGCCAAGACAACTGCGCCCGAAGTCAAGACGATCCCGA 2500
ACAATGCCCCACAGACAAACGAGAATGAGAGCAAGGCA 2538
```

Axblimp1

```
ATGAAAATGGACATGGAGGACGCCGACATGACCCAGTGGACGGAGGCGGGGTTTGAGGAGAAGTGCACCTACATTGTGAACGATCACGCCAGGGACCCCT 100
TGGCCGATGCCGGTTCGGCCTCGCAGGCCGAAGCGTCCCTGCCCAGGAACCTGACCTTCAAGTACTCTGACAACTACAAGGAGGTCATTGGGGTTGTCAG 200
CAAAGAGTATATCCCAAAAGGAACCCGGTTCGGTCCCCTGGTTGGTGAGACCTACACGCCCGACACCGTTCCAAAGGATGCCAACAGAAAGTACTTTTGG 300
CGGATTTACTCCGGTGCTGACTTCGACCATTTCATTGACGGCTTCAATGAAGATAAGAGCAACTGGATGCGCTACGTCAACCCTGCGCACTCGGTGCAGG 400
AGCAGAGCCTGGCTGCTTGCCAGAATGGCATGGACATCTACTTCTACACCATCAAGCCCATTCCCGCCAACCAGGAGCTACTTGTCTGGTACTGTCGGGA 500
CTTTGCAGATAGGCTGAACTACCCTTCCTCGGGAGAACTCACGATGGTGACTCCGAAACAGACCAGCATCAACCCAAAGCAACAGCACACTGAAAAGGAG 600
GTGCTTCACCACAAAAGTGCCCCGAAAAAAGAACACAGCATGAAGGAGATTCTTAAAACTTCTGTAAGCCAATCCAAAGGCAAGGACTTCTACCTGAACC 700
GCATTTCACCAATCACGCCAGAGAAGGACTTGGGTGACTTGAGGAAAAACTGCAGCCCGGAGAGGCCGTTCTTTCCCCGGGTGGTATACCCAATCCGGCC 800
TCACATTCCAGAAGATTATTTGAAGGTGTCTTTAGCGTACGGGATGGACAGGCCGAATTATCTCTCGCACTCACCAATGCCATCGTCCACGACGCCCAGT 900
CCTTCTGCACGGAGCAGCCCAGACCAAAGTTACAAAAGTTCCAGCCCGCAAAGCAGCCCAGGTGCCACAGTGTCCCCCCTCATGACTTCTTTACAAGAAC 1000
AGCGGGAGTCTTACCCATACCTGAATGGACCGTGCAGCACAGAAGGTCTGGGATCGTATCCTGGCTACGCCCCGCACAATAGCCACCTCTCTTCGGCTTT 1100
CCTATCTTCCTACAACCACCATTACCAAAAGTTCTTGCTACCTCCTTTCAACATGGGCTGCCCCAGCCTGAGCACCTTGAACAATATTAACAGCCTCAAC 1200
AATTTCAGCCTCTTCCCTAAAATGTACCCGCTTTGCAACAACTTGCTCAGTGGGGGAAGCCTCTCTCACCACATGCTCAACCAGGTGGCTCTTCCATCAT 1300
CTCTGCCCCACGAAAGTGGGCGCCGCATGCTCCACCCTGAGCAACCCCGGGACTTTCTCATTCCAGCACCCAACAGTGCCTTCTCCATCACCGGGGCGGC 1400
TGCTAGTATGAAGGACAAGCCAAGCACTCCCACCAGCGGCTCTCCGACTGCTGCCACGGCAGCCGCTTCCGAACACTTAATGCATCCGAAAGCTACCTCA 1500
GCTGCGCTGGCCGCCAGCAACGAAGAAGCAATGAATCTTATTAAAAATAAGAGGAACATGACTGGTTACAAAACGCTTCCATATCCGCTCAAGAAGCAGA 1600
ACGGGAAGATTAAGTACGAGTGCAACATTTGCTCAAAGACATTTGGCCAGCTGTCAAACTTGAAGGTTCACCTGCGAGTACACAGCGGGGAGAGGCCGTT 1700
CAAATGTCAGACGTGCAACAAAGGATTCACGCAGCTGGCCCATCTGCAGAAGCACTACCTTGTACACACGGGAGAAAAGCCACACGAATGCCAGGTCTGC 1800
CATAAA 1806
```

8.2 Intron sequences

Full intron sequences obtained are shown below in blue. Flanking exon sequence is shown in black. Gaps in the sequence are indicated by dashes.

Axnanog intron 1

```
CGCAAATGAGGGTGCCAGGATACCAGGCCTACACGGAACTGAACCAACCGTGTGCTGTGGCGGCGAACTACGCGCCAGCATTCCAGGGGAACCTGCAGGC 100
CGCAGAAGAGGGGCGCCCGGTCCCGGCAGgTAAACAACCTTGAAATCCAGCGGGGCATATCACGCGGCCATCGCCAGCTAGAGGGGAGGGGATGGGGGGG 200
CTGTGTATGCCACGCAGAAGCGGAGTATTCCATGCCACTAGCCCTCATTTATTTTAGAATGCCAGCATTACCTGCGCGGATAGCTCGGCGGGTGGAGCGC 300
GTGTTGTAAAGGCCTATTTCTACGGCCAGATAGACACCTGCCTTACTTTGATTACTTTGAAAGATACCCCCACTCTAGGGCGAGAGGTTCCCAGTCGTCA 400
GGAACCCGACACATCATAGAAGTCTCTCCGTTTTGCGGGAAATGTGCATTGAAAAGGTGCATTCTGGCATCATGTTCCCGCACCCCGTCCCGCAACACGA 500
ACTCGTGGCCTAACCTGGGTCTGTATTCTGGGCAGTTTCCTGTGTAATTAAACAGCGCACCTTTTTATCAACGTCAATTTTAGGCCATTTGCATTATACC 600
TCTGCAGGGAAGTAGTTTCGGGGCGACGCGCAGGCTGGTTGTAATAGCTGGTGTTACTTTTGTAACTGTGCTCCGGGGCACTTGGTTCGCGTGCCCACCT 700
GACTGTCTTCACCCCTGCACACTCCAATCATGGCTCCTCATCGGCATTTCCTCCTGATCTACCCTCCCCTCCATACACAGCAGCGGTTCCTGTTTTGTCC 800
CCTCATTCCTCANCATGTCCCTCGGCTGCCCTCCCTTCTCAGTCCGCAGTGGTGCCTTCTGCACAGCAGTTCTGCCTGCCCTGCCTGTGCGTCACTGCTT 900
TGCA--------------------GTCACTGCTTTGCAATGCATTGCGTATTAGCAGCACAGACACTTGGTGGGTGGCACCGTGCCAGGGGGTCCAAACG 980
CAACAGTGTAAAATATTATCTGGGAATGGGGAGAGCAAAGGGGTCGCTCGATCAGCCTCTCGAGAATTGGATTCCATAAGATAAAAACGGGGGGGCAGGG 1080
GGAGAGGCGGTCGCGCAGCGGGCTCCGTTGAAAGGGTCTTGTAGACTGGTGTGCTCGAAAAACAAAAACGTGCTTGCTTCTAAATTGTGCTGGTTGGAGG 1180
CAAACCATGGCACATTTCCTAACACGTACAGCAGAGGGCAGCAAAGGCGTGCGCACTTGCGCTCACCACGCATTCAAGCCCCAATTTCAATGAGCAACAC 1280
AATCGTGTTATTCCACAATTGCGACAGAGGTTGGAAAAGGCTACTTTGCGTTATGTCGTTTGTTATTATATACTATATTGCATTACATTTGATTTAGTAT 1380
CCTAGGTTGCATGGTTTAAGTAGTGTATTTAATATTAACGGATAGAGCATATGTGATATTCTCAACGATGGTTATTTTGATCAACTTGGCAGGTCGGTGC 1480
GGTGAAGCGAATGTGCCAGTATTCAAATGCATGCAAGTTACACGCCCGGTGGCAGGGGCATTAACCCACTGAGGCGGCGCTCCCTCCAATCGTGCACCAG 1580
TAGACCATTCAAAACAAGGCACGGTTTCCACTCTGTGTGTAATGTGTCTGATTCCGTTTGTTGGCTGGTGGCCCCATTTGCCCGCATACTCTTTCCAGCT 1680
GATTTCACGCGTGCCATGTCTTCGTTTTGTTTCAgTCCTGCCGTCTTCCCCCGACTCAGCCACCAGCCCAAAGGTGGATCCGTTCGCCCAGTGTGCCCCG 1780
```

Axnanog intron 2

```
CAATGCAGGCGCAGCAGCTGGCGGCGGATCTCAACCTCACATACAAGCAGGtACAGGCCTAAAGAGAGGGGCAGAGTGTGGGGGGTGATACTTCAGAAAA 100
CAACGTGGGAAGATAGTTTAATTTTTCAATCCATCTCTTGGTAgGTGAAGAACTGGTTCCAGAACCGAAGGATGAAGCACAAACTGTCCCTGAA 194
```

Axoct4 introns

ATGGCTGGGCATTTGGGACAGGAGATTGGGCGGGCTGCCTATGGGTTCGGTGCACAGGCCTTGCACCTGGGGGCCGGGGGCCTCGAGGCGGGCGGGCCGG 100
GCTTCCTGTCCGAGAGCTATGGGCCCTACGCCGGCTTCAAGGCGCTGGAGTATGCCCATGGCGGGGCGGAAGGAGAGGGCCGACCGGGGGCCCATGGGCT 200
GGCACGGGCCTGGTACCCCTTCTCGGAGGCCTGGGGCCCTGTGTATGGGCAGAGCGGTGCCGGCGCAGGGTTCGAGAGCAGCCGGGTGGAGGTCAAGGTG 300
GAGAGGCCCGACAAGGAGGCTGGCTACGGGCAGCAGCACCAGCAGGCCTGGGCTGGCTACTTCGTGCCCCAGCTGGCAGTGCCCGCCAGGTCGCCTGCGT 400
CCGTGGCCAGCGGAGGGCAAGTACCGGCCGCACCTGCCAGCCCGTCCGATGACAGCCCGCACAGCAGCACCGCCAGCAGCAGCAGCGCCAGCCCGGACCT 500
GGGGGCTGGGGGCGCCCCGCGGGACCTGGACAGCGGAGACGAGGAAGGGGGGACGTCGGCGGACCTTGAACAGTTTGCCAAGGAGCTGAAGCAGAAGCGC 600
ATCACGCTGGGCTTTACGCAGGCGGATGTAGGGCTGGCGCTCGGGGCGCTGTACgGTGAGTGTCCTGGCCTATGCCTGAAGTACCCACAGTTGCACACCA 700
AGGCTTCTAGTTTGCCATCACCTGATGGCCCATCTCCACACCTTCCCGAGGGACTGGCCACACTGCCTTCGGTTGGCATCACTGCGTGGGTCCTCCGATG 800
GGTGGGCTGTAGGGGTACTGGAGCCCACTTGTTTGTCACCCACTCTTAAGTGCCTCTACTCTTGTGCCTTGACCCaGGGAAGATGTTCAGCCAGACGACG 900
ATCTGCCGGTTCGAGGCCCTGCAACTGAGCTTCAAGAACATGTGTAAACTGAGACCCCTGCTCCAGCGCTGGCTGGTCGAGGCCGACACCAACGAGAACC 1000
TGCAGGaGGTAAAGGGCTTCCGGGGAAGGGTACTTGCGGCATGATGGACCACCCTAATGCTGGGAACTCTGTCCGCACCTGTGTGGGAACCGTCATGTGC 1100
ACCTAGGTTTGGGGGGGGGGGATCTCCATCACTTGCTTTTCTGACTGCATATTTTTCTAGGTTTGGGGGGGGGCACCTATAGGATGCAGGGACTTCAGCC 1200
TTCCCTGACCGAGCCTTACGCACGCTTGGCCTCTGTCTTGCTTGGCCTCTGTCTTGACCGTCTCTTCTTGCATCACCCACTTcAGCTCTGCAACCTGGAG 1300
AATGCCCTGCAACAAGCCCGGAAGAGGAAAAGAACCAGCATCGAGAACAGCGTCAAGGACAACCTGGAGGCCTTCTTCCTGAAGTGTCCGAAGCCCACCC 1400
ATCAGGAGATCGCCCACATCTCCGAGGACCTCAATCTGGAGAAGGACgTAAGTGGCCTATAATTCCAACAGCGCTCACCCCACCTAACCTGCTCCTCGAG 1500
ACACGGTCTAGCCCAGAGCTCACGTTCTACCATTTGGATAACTTGCCACCAAGTGTGTCTGGCACCTGGTACACCTGTTGGGCAGGTCTTTCCCACTAGC 1600
CTCTAACTCTCCTCTCCTGCAGCGTCATACGCAGCAGAGCCAAACCGCAGGGCAGGTGGGCACCACACAGAACCATCATCATGGCCTTCTGTTGCTGATT 1700
GGGGGGGGGGGGGGTAACAGGGTAAAAAGCCCACTCTTGGTGGGCTTGCTTTTGGGTTGGATACATAAGTGTGTTGGTAAAACGGGTCGATGATAGTTTG 1800
GGAGGGGATTGGGCAAACAGACGTAGGTTTGTCAAGGGGCAGTGTTGGGGCAAACTAGGTCCTGAGTCTTTCCTAGAGGTTGGTTACTCTATGGTAACTT 1900
GTTGTGGATACCCCCAAAAAGGAGCTGTTGCTTCCAGGCCAGAGTGTGCTTCTAGTTTACACCTGGTGCATGCCTGGTCTTGCCACCGCCAACTCCAGTT 2000
TATGCCCTCGCCACCCACCTGGGATTCTCATCACTCCACACATGAAACCCGCAACCAAATTAATTATCCTAGGTGCCCTCAACCTTGGGTACAATGACCT 2100
CTCTGACCTGAAAGCCTCTGTACTAGCTCTAGAAGACTCTCGGCTAATGCAACTATTGACATGGTCTCGCATCATGGTCCCGCATCAGTCTCACATCATG 2200
GTCCCCATCAGTCCCACATCATGGTCCGATCACTTCTACCTGAACCTCTCTATTGCCACTCCTGCCGCGGCCCAGACTTTAGTTTTGGTTAGGAATACCT 2300
GCAAATAGACGCACATGGTTCTAAAACAACTCTCCTGGCATCACTTAATACTACACTCTTGCCAACAAAATTCCCTCAAGACATAGCCAACCACTGCCAT 2400
GATTGCCTACGCCGCACCATGCCCCATATCACTGCCAAGACACCCAAACCTCATCTACTCTATCAAGCACGATTTTCTTAAGGGCTACTTTTCCCTATGG 2500
AGGCAAAGGGTGCTCAACACCTATACAAAAAGCACCCAACCGCAAGCCCGATCCCTGGCTCTTTGACCGGAGTAAAACGTTGTCCATGTACCCTGTACCA 2600
GTGATAGCCCGTGAGTAACTGAAGGAAGGCCTTTGTCTCCCCCGCAgGTGGTCCGCGTCTGGTTCTGCAACAGGCGACAGAAGGGGAAGCGCAGCATTTG 2700
CCGGGAGGAGTATGATGGCTTCCAGCAGTACCCAGGGATGCAGCCGGG 2748

An alignment of *axoct4* intron boudaries with splice-blocking morpholinos

Exon sequences are shown in black, intron sequences are shown in blue and morpholino sequences are shown in red. Panels **A**, **B**, and **C** show *axoct4* intron boundaries and morpholino designs. Suitable sites for morpholino design were not identified at the intron-exon boundary of *axoct4* intron 4. Note. PCR designed to clone *axoct4* intron 1 from genomic DNA only produced products lacking an intron suggesting there may not be an intron at this position in *axoct4.* Morpholinos would be synthesised antisense to the sequences shown.

A. Oct4 Intron 2

```
Exon-Intron Boundary CGCTGGGCTTTACGCAGGCGGATGTAGGGCTGGCGCTCGGGGCGCTGTACGGTGAGTGTCCTGGCCTATGCCTGAAGTACCCACAGTTGCACACCAAGGC 100
                    ---------------------------------------------GCTGTACGGTGAGTGTCCTGGCCTA------------------------------ 25

Intron-Exon Boundary CACTTGTTTGTCACCCACTCTTAAGTGCCTCTACTCTTGTGCCTTGACCCAGGGAAGATGTTCAGCCAGACGACGATCTGCCGGTTCGAGGCCCTGCAAC 100
                    --------------------------------TACTCTTGTGCCTTGACCCAGGGAA---------------------------------------- 25
```

B. Oct4 Intron 3

```
Exon-Intron Boundary CCTGCTCCAGCGCTGGCTGGTCGAGGCCGACACCAACGAGAACCTGCAGGAGGTAAAGGGCTTCCGGGGAAGGGTACTTGCGGCATGATGGACCACCCTA 100
                    ---------------------------------------------GCAGGAGGTAAAGGGCTTCCGGGGA------------------------------ 25

Intron-Exon Boundary CTGTCTTGCTTGGCCTCTGTCTTGACCGTCTCTTCTTGCATCACCCACTTCAGCTCTGCAACCTGGAGAATGCCCTGCAACAAGCCCGGAAGAGGAAAAG 100
                    --------------------------------TTCTTGCATCACCCACTTCAGCTCT---------------------------------------- 25
```

C. Oct4 Intron 4

```
Exon-Intron Boundary CCCATCAGGAGATCGCCCACATCTCCGAGGACCTCAATCTGGAGAAGGACGTAAGTGGCCTATAATTCCAACAGCGCTCACCCCACCTAACCTGCTCCTC 100
                    ---------------------------------------------AAGGACGTAAGTGGCCTATAATTCC------------------------------ 25

Intron-Exon Boundary ACCAGTGATAGCCCGTGAGTAACTGAAGGAAGGCCTTTGTCTCCCCCGCAGGTGGTCCGCGTCTGGTTCTGCAACAGGCGACAGAAGGGGAAGCGCAGCA 100
```

Axblimp1 intron 4

Partial sequence is shown the full intron was 5 kb.

```
ACATCTACTTCTACACCATCAAGCCCATTCCCGCCAACCAGGAGCTACTTGTCTGGTACTGTCGGGACTTTGCAGATAGGCTGAACTACCCTTCCTCGGG 100
AGAACTCACGATGGTGACTCCGAgTAAGTACTTTTGGAAGAAATTGAATCTTGCAATGCTCACGCGAGGATTTATTGGTATGCAGTACAGTCACGTAGAC 200
GCCTCGCCAGTATTCTGATTGGAGAGACCGTGCCAGACAGTTTTAGTCCGGTCTAAAGCAGTGGTCTGGCTCTCCAGATGCTTCAGACTACCCCATCCGC 300
TTTATCCAGCATAGTCAATGGCGAGAGGTTATGGGAGTCTTAGTCGGAAGCATCTGGCAAGCTGCCGTCTCATGGACGTCTAGACAACAAGGGCACGCGG 400
TAGCAGCCAATGAAGATACACTTTTGAGGCCTTAATAAACATCGATGTAGGGATCTGTAGAATGAACAATGGTGGCCAGATTTGGGGGGACTTCAAACGG 500
CAAGGCCCTCTAAAACTGATCCTAAAACTGTATCCGTATTTAAGGCAGGTAGGAGACTGCATGTATTGCACAAACGGAAAAGAATTTACACCCCAAATCA 600
TTAATTGGCCGGGGACAAGGAACTCAAATTAAGGCTACCACAAAATAGGCCAAGTGTACAGTGTTAAGTTACAATACCCTGCACCAAAGATATTGCTCTG 700
ACTGACTGTTGGAATGAGGGGTACTGATTGTTTTCAGTGTTGTATGTGTGAAGTGATTGCACAAAAAAAGTGATGGCTGGACCTGTTTGTGCCAATTCTG 800
GCAATTGCATCCGTGCCCTTTACCTCTCTGGAGTTACTGGTATCGAACCAATCTCTATAAAATG----------~~~ATCCTTGCTGA 875
CCGCCCCCATTGGAATGCGGACACACCCAGATTAGGTGCTGTTTAGGTCATGTTGTCAGATCGCCGCCTTCCCAATAGTTGCCCATGTATTTTTGTTTTG 975
TTTTTAGTTGGATTATTGGCAATTAATAAAGTGCTTCATGCCGGATGCCCCCAGCTTCCAAGCGCTTGATGCAAGGCTGTTTTCCAATTGACAGTCATTG 1075
GTGGGTGGCAGATGGGGAGAATGCCCCCCATCTCCCCAGGCCTCCCAGGTTTGCCACTCGAGGCCGAGTTCCCAACCCTGCCGAGTCTGTGTACCCATCG 1175
CCTGTCACCACGGAATTGAGTTTGGCGGGGTATATATAACCTTGCCATTACCTGAGGGTAAGAGGTGTTGTAAGCATTATTGCATTCAATTTCTATTGTC 1275
CCAAAGGAGTCCTCGGGGACCTTTTTAATGAGGAAAAACTGAACCCCCAAATAGAGTGGTAAACTACCATGACCGCAAGTGATAACAAGTAATTCAGCTT 1375
TGTTGTATTAGCGGATCTAATGCTGCCACATGTGTAATTGGGTCGTGAGTCGCAGGTTGTAGTTCTTATTCCAGTGGGCGTGTCTTTACCTGTGTCTGTT 1475
GCTTCATCTTTATGTAACCGTGGAAGAGAAACGCGTGACTAACCATTGCCTGGTATCTCCTCCATTTCAgAACAGACCAGCATCAACCCAAAGCAACAGC 1575
ACACTGAAAAGGAGGTGCTTCACCACAAAAGTGCCCCGAAAAAAGAACACAGCATGAAGG 1635
```

Axblimp1 intron 5

Partial sequence is shown the full intron was 4 kb

```
TGACTGGTTACAAAACGCTTCCATATCCGCTCAAGAAGCAGAACGGGAAGATTAAGTACGAGTGCAACATTTGCTCAAAGACATTTGGCCAGCTGTCAAA 100
CTTGAAGgTAAGCGAGCCCCCTTTTCTGTATTTACTTGACAAGCAATTCTTCTTACTGCGAGCCAGAATGTAATTGACGATCCCTCCCACCTTCTCCCCG 200
GCTATCCTGTCCGGGCACTTACTTACACTCCCGGCTGCCATAAATGAATTTAAGGGGCTGCCTTCAGTTGGCAGTGAGCCATATAAGTGGGCATACCCTT 300
TCCTCCAAAGCCCCTTCCAAGCACCCACGGATCGGTGCTTTTGTCTGCATTGAGTTAGTGCCCACCCATTCCTACAGGACACCCTGTGTTGAGGGGTTTA 400
GGGAGACACCTGCATCTCAGCCGTGTAGTGGG~~~~~~~~~~~~~~~~~~~~~~~~~ACCTGGTAGCGCGTGCACATTTCAAGAGGCATGCAGGTTTGCC 475
TTAAAGTGCTCTTCAGATCTGACGGTAACGGCACAGCTCTGCTGGCGCAGCTTATCCAAACATGTCTGCGGAGCTGTG~TGGGCGAGCGTAGGCGACCAA 574
ATCCTGGGTCCATTATTTG~TTTGGAGTATTTTTACTGCCCAATCTGTTATGCCGGGAGCATGACGTGTTTTTAGGGTGCAAATATGGCTGAAATGGTCA 673
TCTTGAAATCGTATTGTACACAATCGACTCTAATTGGAAGATGCAACCTGTCGCATCGTTATGACCCCCCCCCAGTGGCCCGATTTTTGCGTGTGTCCAA 773
TGTTGCCTAACAACCCTAGCCAAGAGGGAAGTCTGCGCAGAGTCTGCAACGCCCTTGGAGCACTTTACTTCATTTCCATTGTGCAACCGGTTGCTCTGCG 873
CCGTTTTGTGGTGGTTGATATCTGACGGCACCAGATCGTACACGCTGCAAAGTTTCTGGCCTCTGCAAACCCTTTCTAAACTAGCACCATGTGTACATCT 973
GACCCAGACATGCGCATTCTCAATATCCGCCCCTTTCATATATTTTGAAGTGTCAATTATTTGAATTGAAACGGTCTCTTATTTGTTGGAGCTGTGAGAT 1073
GGCCTTGTTGTTTTTGAACCTGCAGCAGCCATGTTGTTTTCTTCCAgGTTCACCTGCGAGTACACAGCGGGGAGAGGCCGTTCAAATGTCAGACGTGCAA 1173
CAAAGGATTCACGCAGCTGGCCCATCTGCAGAAGCACTACCTTGTA 1219
```

8.3 *Axnanog* splice products

Sequence of splice variants generated by targeting of *axnanog* splice-blocking morpholino (targeted to the intron-exon boundary of intron 1) and their translations are shown below. Exons are shown in alternating colours (Black and Green). Stars indicate stop codons, the first one in each sequence is highlighted in red and the homeodomain and the short region of conservation upstream of the homeodomain are highlighted in blue.

Intron insertion (indicated by orange type)

```
ATGCCCGCCCACTGCATGACCCCGCAAATGAGGGTGCCAGGATACCAGGCCTACCCGGAACTGAACCAACCGTGTGCTGTGGCGGCGAACTACGCGCCAG 100
 M  P  A  H  C  M  T  P  Q  M  R  V  P  G  Y  Q  A  Y  P  E  L  N  Q  P  C  A  V  A  A  N  Y  A  P
CATTCCAGGGGAACCTGCAGGCCGCAGAAGAGGGGCGCCCGGTCCCGGCAGGTCGGTGCGGTGAAGCGAATGTGCCAGTATTCAAATGCATGCAAGTTAC 200
A  F  Q  G  N  L  Q  A  A  E  E  G  R  P  V  P  A  G  R  C  G  E  A  N  V  P  V  F  K  C  M  Q  V  T
ACGCCCGGTGGCAGGGGCATTAACCCACTGAGGCGGCGCTCCCTCCAATCGTGCACCAGTAGACCATTCAAAACAAGGCACGGTTTCCACTCTGTGTGTA 300
  R  P  V  A  G  A  L  T  H  *  G  G  A  P  S  N  R  A  P  V  D  H  S  K  Q  G  T  V  S  T  L  C  V
ATGTGTCTGATTCCGTTTGTTGGCTGGTGGCCCCATTTGCCCGCATACTCTTTCCAGCTGATTTCNCGCGTGCCATGTCTTCGTTTTGTTTCAGTCCTGC 400
 M  C  L  I  P  F  V  G  W  W  P  H  L  P  A  Y  S  F  Q  L  I  X  R  V  P  C  L  R  F  V  S  V  L
CGTCTTCCCCCGACTCAGCCACCAGCCCAAAGGTGGATCCGTTCGCCCAGTGTGCCCCGGATGTAGCGGTGGGAGGTGAGACGAAGGCCCAGGCGAGAAA 500
P  S  S  P  D  S  A  T  S  P  K  V  D  P  F  A  Q  C  A  P  D  V  A  V  G  G  E  T  K  A  Q  A  R  K
GCGCACGTGCTTCAGTCAGGAACAGCTCGTGGCCCTGCACCGAATGTTCCAGAAGCAGCATTACATGAACCCAATGCAGGCGCAGCAGCTGGCGGCGGAT 600
  R  T  C  F  S  Q  E  Q  L  V  A  L  H  R  M  F  Q  K  Q  H  Y  M  N  P  M  Q  A  Q  Q  L  A  A  D
CTCAACCTCACATACAAGCAGGTGAAGAACTGGTTCCAGAACCGAAGGATGAAGCACAAACTGTCCCTGAAGGACTCAGTGTGGCTGGACAAGAGGTGCT 700
 L  N  L  T  Y  K  Q  V  K  N  W  F  Q  N  R  R  M  K  H  K  L  S  L  K  D  S  V  W  L  D  K  R  C
GGCAACCACAGGCGAGCTCAATCCTAACACCGGCTCAGCCGCAGTCCACGGGGTGCCCGGAAAGCTCCTCCCACTTGCCTCAGAGATACACAGTGCACCA 800
W  Q  P  Q  A  S  S  I  L  T  P  A  Q  P  Q  S  T  G  C  P  E  S  S  S  H  L  P  Q  R  Y  T  V  H  H
TAGTGCACTTGCCCAGCGAGTCACCAGTCACCCCTACCAGAAGTACAGTGGGATTCAGAACCCTCACCAGAAAGTGCTGTCAGAAGACGCAGCAACAGTG 900
  S  A  L  A  Q  R  V  T  S  H  P  Y  Q  K  Y  S  G  I  Q  N  P  H  Q  K  V  L  S  E  D  A  A  T  V
CAGCACAGGGAGGCCGCCCCGCAGTGCATGGGGCCACAGCAGTACATGAACAGGCACCAAAATTACCCAACCATTGAGTACGCCGGAGCAAGACCAGTAG 1000
 Q  H  R  E  A  A  P  Q  C  M  G  P  Q  Q  Y  M  N  R  H  Q  N  Y  P  T  I  E  Y  A  G  A  R  P  V
AAGGGTACAACCTTAAGACTCCTCTGCAGTACCCTTCGATGGCACCATACCCCAACTACTACTACCAGCAGCCACCGCCCTACATTCATCAGCAGGGCCG 1100
E  G  Y  N  L  K  T  P  L  Q  Y  P  S  M  A  P  Y  P  N  Y  Y  Y  Q  Q  P  P  P  Y  I  H  Q  Q  G  R
GCCCGATATCAGATTTCAGAGCACGCAGGGCATGTGA 1137
  P  D  I  R  F  Q  S  T  Q  G  M  *
```

Deletion of exon 2*

```
ATGCCCGCCCACTGCATGACCCCGCAAATGAGGGTGCCAGGATACCAGGCCTACCCGGAACTGAACCAACCGTGTGCTGTGGCGGCGAACTACGCGCCAG 100
 M  P  A  H  C  M  T  P  Q  M  R  V  P  G  Y  Q  A  Y  P  E  L  N  Q  P  C  A  V  A  A  N  Y  A  P
CATTCCAGGGGAACCTGCAGGCCGCAGAAGAGGGGCGCCCGGTCCCGGCAGGTGAAGAACTGGTTCCAGAACCGAAGGATGAAGCACAAACTGTCCCTGA 200
A  F  Q  G  N  L  Q  A  A  E  E  G  R  P  V  P  A  G  E  E  L  V  P  E  P  K  D  E  A  Q  T  V  P  E
AGGACTCAGTGTGGCTGGACAAGAGGTGCTGGCAACCACAGGCGAGCTCAATCCTAACACCGGCTCAGCCGCAGTCCACGGGGTGCCCGGAAAGCTCCTC 300
  G  L  S  V  A  G  Q  E  V  L  A  T  T  G  E  L  N  P  N  T  G  S  A  A  V  H  G  V  P  G  K  L  L
CCACTTGCCTCAGAGATACACAGTGCACCATAGTGCACTTGCCCAGCGAGTCACCAGTCACCCCTACCAGAAGTACAGTGGGATTCAGAACCCTCACCAG 400
 P  L  A  S  E  I  H  S  A  P  *  C  T  C  P  A  S  H  Q  S  P  L  P  E  V  Q  W  D  S  E  P  S  P
AAAGTGCTGTCGGAAGACGCAGCAACAGTGCAGCACAGGGAGGCCGCCCCGCAGTGCATGGGGCCACAGCAGTACATGAACAGGCACCAAAATTACCCAA 500
E  S  A  V  G  R  R  S  N  S  A  A  Q  G  G  R  P  A  V  H  G  A  T  A  V  H  E  Q  A  P  K  L  P  N
CCATTGAGTACGCCGAAGCAAGACCAGTAGAAGGGTACAACCTTAAGACTCCTCTGCAGTACCCTTCGATGGCACCATACCCCAACTACTACTACCAGCA 600
  H  *  V  R  R  S  K  T  S  R  R  V  Q  P  *  D  S  S  A  V  P  F  D  G  T  I  P  Q  L  L  L  P  A
GCCACCGCCCTACATTCATCAGCAGGGCCGGCCCGATATCAGATTTCAGAGCACGCAGGGCATG 664
 A  T  A  L  H  S  S  A  G  P  A  R  Y  Q  I  S  E  H  A  G  H
```

Deletion of exons 2* and 3

```
ATGCCCGCCCACTGCATGACCCCGCAAATGAGGGTGCCAGGATACCAGGCCTACCCGGAACTGAACCAACCGTGTGCTGTGGCGGCGAACTACGCGCCAG 100
 M  P  A  H  C  M  T  P  Q  M  R  V  P  G  Y  Q  A  Y  P  E  L  N  Q  P  C  A  V  A  A  N  Y  A  P
CATTCCAGGGGAACCTGCAGGCCGCAGAAGAGGGGCGCCCGGTCCCGGCAGGCTCAGCCGCAGTCCACGGGGTGCCCGGAAAGCTCCTCCCACTTGCCTC 200
A  F  Q  G  N  L  Q  A  A  E  E  G  R  P  V  P  A  G  S  A  A  V  H  G  V  P  G  K  L  L  P  L  A  S
AGAGATACACAGTGCACCATAGTGCACTTGCCCAGCGAGTCACCAGTCACCCCTACCAGAAGTACAGTGGGATTCAGAACCCTCACCAGAAAGTGCTGTC 300
  E  I  H  S  A  P  *  C  T  C  P  A  S  H  Q  S  P  L  P  E  V  Q  W  D  S  E  P  S  P  E  S  A  V
AGAAGACGCAGCAACAGTGCAGCACAGGGAGGCCGCCCCGCAGTGCATGGGGCCACAGCAGTACATGAACAGGCACCAAAATTACCCAACCATTGAGTAC 400
 R  R  R  S  N  S  A  A  Q  G  G  R  P  A  V  H  G  A  T  A  V  H  E  Q  A  P  K  L  P  N  H  *  V
GCCGGAGCAAGACCAGTAGAAGGGTACAACCTTAAGACTCCTCTGCAGTACCCTTCGATGGCACCATACCCCAACTACTACTACCAGCAGCCACCGCCCT 500
R  R  S  K  T  S  R  R  V  Q  P  *  D  S  S  A  V  P  F  D  G  T  I  P  Q  L  L  L  P  A  A  T  A  L
ACATTCATCAGCAGGGCCGGCCCNATATCAGATTTCAGAGCACGCAGGGCATGTGA 556
  H  S  S  A  G  P  A  X  Y  Q  I  S  E  H  A  G  H  V
```

*Exon 2 contains the majority of the homeodomain and the short region of conservation upstream of the homeodomain. The remaining portion of the homeodomain is in exon 3